

**Reduction of Atmospheric Transboundary  
Fluxes of Heavy Metals in Europe:  
Scientific Support for European Environmental  
Protection Conventions**

(Universität Lüneburg, Fachbereich Umweltwissenschaften,  
Fachgebiet Umweltchemie, Habilitationsschrift, 2002)

**Autor:**

***G. Petersen***



**Reduction of Atmospheric Transboundary  
Fluxes of Heavy Metals in Europe:  
Scientific Support for European Environmental  
Protection Conventions**

(Universität Lüneburg, Fachbereich Umweltwissenschaften,  
Fachgebiet Umweltchemie, Habilitationsschrift, 2002)

**Author:**

***G. Petersen***

*(Institute for Coastal Research)*

Die Berichte der GKSS werden kostenlos abgegeben.  
The delivery of the GKSS reports is free of charge.

*Anforderungen/Requests:*

GKSS-Forschungszentrum Geesthacht GmbH  
Bibliothek/Library  
Postfach 11 60  
D-21494 Geesthacht  
Germany  
Fax.: (49) 04152/871717

Als Manuskript vervielfältigt.  
Für diesen Bericht behalten wir uns alle Rechte vor.

ISSN 0344-9629

GKSS-Forschungszentrum Geesthacht GmbH · Telefon (04152)87-0  
Max-Planck-Straße · D-21502 Geesthacht/Postfach 11 60 · D-21494 Geesthacht

GKSS 2003/2

## Reduction of Atmospheric Transboundary Fluxes of Heavy Metals in Europe: Scientific Support for European Environmental Protection Conventions

*(Universität Lüneburg, Fachbereich Umweltwissenschaften, Fachgebiet Umweltchemie, Habilitationsschrift, 2002)*

Gerhard Petersen

*242 pages with 18 figures and 5 tables*

### Abstract

This study summarizes more than 15 years of scientific support for the United Nations-Economic Commission Europe (UN-ECE) Convention on Long Range Transboundary Air Pollution (LRTAP) and other European environmental protection conventions such as the Commission for the Protection of the Marine Environment of the North-East Atlantic (OSPAR) and the Baltic Marine Environment Protection Commission (HELCOM) by means of development and application of numerical simulation models for the atmospheric long-range transport of heavy metals. The work is mainly based on results and conclusions described in the nine papers of the appendix but some more recent investigations which have not yet been published in the scientific literature are also presented.

An introductory overview and synthesis of current knowledge and understanding pertaining to all major aspects of heavy metals in the atmosphere is presented from a viewpoint that numerical modelling of their atmospheric processes is necessary and feasible to support the conventions mentioned above. The models discussed in this study have capabilities to quantify transboundary fluxes of lead, cadmium and mercury as the priority metals of concern and have a potential to identify sources as well as to predict the impact of emission reductions on the load of terrestrial and aquatic ecosystems in Europe. Advantages and limitations of relatively simple Lagrangian models are outlined within the context of issues currently facing the environmental scientific and policy making communities. However, a focus of this study is a comprehensive model system for atmospheric mercury species using a fully three-dimensional Eulerian reference frame and incorporating a state-of-science mercury chemistry scheme, which has been adopted by various scientific institutions for their modelling purposes. The model system, which has an established record of published investigations including the development and testing of the mercury chemistry scheme and comparison of model results against field observation in Europe, has been selected to be one of the reference models within the upcoming Air Quality Directive of the European Union and is currently participating into an international model intercomparison study in the framework of the UN-ECE LRTAP convention.

Overall, the present development level of the advanced models and their components presented in this study is such, that they can provide key information needed to quantify the relationship between anthropogenic emissions and deposition fluxes of heavy metals to remote ecosystems in Europe and that their application within the environmental protection conventions mentioned above is fully justified. The model will be extended and developed further with respect to air pollutants of future relevance (e.g. particulate matter, persistent organic pollutants) according to advancements in the knowledge of their atmospheric processes to ensure that the model maintains its capabilities to address effectively the scientific and political questions that may arise over the next decade.

# Reduzierung der grenzüberschreitenden atmosphärischen Transporte von Schwermetallen in Europa: wissenschaftliche Unterstützung für europäische Umweltschutzkonventionen

## Zusammenfassung

In dieser Arbeit wird die wissenschaftliche Unterstützung beschrieben, die während der vergangenen 15 Jahre auf dem Gebiet der Entwicklung und Anwendung von numerischen Simulationsmodellen zum großräumigen atmosphärischen Transport von Schwermetallen für die Wirtschaftskommission der Vereinten Nationen für Europa (United Nations-Economic Commission Europe UN-ECE) über weiträumige, grenzüberschreitende Luftverschmutzung (LRTAP) sowie anderer europäischer Umweltschutzkonventionen wie die Kommission zum Schutz der marinen Umwelt des Nordost-Atlantiks (OSPAR) und der Ostsee (HELCOM) durchgeführt wurde. Die Arbeit basiert hauptsächlich auf den Ergebnissen und Schlussfolgerungen der 9 Publikationen im Anhang. Darüber hinaus werden neuere Forschungsergebnisse diskutiert, die noch nicht in der wissenschaftlichen Literatur veröffentlicht sind.

Einleitend wird der Stand des Wissens über atmosphärische Prozesse von Schwermetallen unter der Annahme dargestellt, dass diese Prozesse in einer für Zwecke der zuvor genannten Umweltschutzkonventionen geeigneten Weise in Modellen parameterisiert werden können. Mit diesen Modellen können grenzüberschreitende Flüsse der drei prioritären Schwermetalle Blei, Cadmium und Quecksilber quantifiziert werden sowie Aussagen über die Herkunft der gemessenen Schwermetallkonzentrationen gemacht werden und die Auswirkung von Emissionsminderungen auf terrestrische und aquatische Ökosysteme in Europa prognostisch abgeschätzt werden. Relativ einfache Lagrange-Modelle werden im Kontext mit aktuellen umweltwissenschaftlichen und umweltpolitischen Fragen diskutiert. Schwerpunkt dieser Arbeit ist ein komplexes dreidimensionales Eulersches Modellsystem zum atmosphärischen Transport und chemischen Transformationen von Quecksilberspezies. Dieses Modellsystem repräsentiert weltweit den aktuellen Stand der Wissenschaft und ist in seinen Kernstücken von anderen Umweltforschungsinstituten übernommen worden. Es ist als eines der drei Referenzmodelle für die derzeit erstellte 'EU Air Quality Directive' für Quecksilber ausgewählt worden und nimmt an einem internationalen Modellvergleich im Rahmen der UN-ECE Konvention teil.

Der derzeitige Entwicklungsstand der in dieser Arbeit vorgestellten Modellsysteme erlaubt deren weiteren Einsatz für umweltpolitische Zwecke im Rahmen der obengenannten Konventionen. Dabei werden sowohl die Quantifizierung der grenzüberschreitenden atmosphärischen Schwermetalltransporte und deren Bewertung hinsichtlich ihrer Auswirkungen auf terrestrische und aquatische Ökosysteme als auch die Erweiterung der Modelle bezüglich umweltrelevanter Stoffe der Zukunft (Feinstaub, persistente organische Verbindungen) von besonderer Bedeutung sein.

## PREFACE

A main purpose of the present work is to demonstrate the need for advanced numerical simulation models for the quantification of long-range atmospheric transboundary fluxes of heavy metals and their impacts on sensitive ecosystems in Europe. The work therefore deals with the identification of the transport of heavy metals from European anthropogenic sources in connection with physico-chemical transformations and deposition estimates with emphasis on source receptor relationships in the framework of the UN-ECE Convention and other European environmental protection agreements.

This work is based on the results and conclusions presented in the following papers, referred to by bold Roman numerals in the text:

**I.** G. Petersen, A. Iverfeldt, J. Munthe (1995):

Atmospheric Mercury Species over Central and Northern Europe. Model Calculations and Comparison with Observations from the Nordic Air and Precipitation Network for 1987 and 1988.

ATMOSPHERIC ENVIRONMENT, Vol 29, No.1, pp. 47-67.

**II.** G. Petersen, J. Munthe, R. Bloxam (1996):

Numerical Modelling of Regional Transport, Chemical Transformations and Deposition Fluxes of Airborne Mercury Species.

In: W. Baeyens, R. Ebinghaus and O. Vasiliev (eds.): Regional and Global Mercury Cycles: Sources, Fluxes and Mass Balances .NATO-Advanced Science Institute Series, Partnership Sub-Series 2: Environment - Vol. 21, pp. 191-217.

Kluwer Academic Publishers, 3300 AA Dordrecht, the Netherlands.

ISBN 0-7923-4314-X

**III.** G. Petersen, J. Munthe, R. Bloxam, A. Vinod Kumar (1998):

A Comprehensive Eulerian Modelling Framework for Airborne Mercury Species: Development and Testing of the Tropospheric Chemistry Module (TCM).

ATMOSPHERIC ENVIRONMENT - Special Issue on Atmospheric Transport, Chemistry, and Deposition of Mercury (edited by S. E. Lindberg, G. Petersen and G. Keeler), Vol. 32, No. 5, pp. 829-843.

**IV.** G. Petersen (1998):

Numerical Simulation Models for Airborne Heavy Metals in Europe: A Review.

In: I. Linkov and R. Wilson (eds. ): Air Pollution in the Ural Mountains. Environmental, Health and Policy Aspects. NATO-Advanced Science Institute Series, Partnership Sub-Series 2: Environment - Vol. 40, pp. 81 -97.

Kluwer Academic Publishers, 3300 AA Dordrecht, the Netherlands.

ISBN 0-7923-4967-9

- V.** G. Petersen (1999):  
Airborne Heavy Metals over Europe: Emissions, Long-range Transport and Deposition Fluxes to Natural Ecosystems.  
In : I. Linkov and W. R. Schell (eds): Contaminated Forests, NATO SCIENCE Series, 2. Environmental Security, Vol. 58, pp. 123-132.  
Kluwer Academic Publishers, 3300 AA Dordrecht, the Netherlands.  
ISBN 0-7923-5739-6
- VI.** B. Schneider, D. Ceburnis, R. Marks, J. Munthe, G. Petersen, M. Sofiev (2000):  
Atmospheric Pb and Cd input into the Baltic Sea: A new estimate based on measurements.  
MARINE CHEMISTRY 71, pp. 297-307.
- VII.** M. Sofiev, G. Petersen, O. Krüger, B. Schneider, M. Hongisto, K. Jylhä (2001):  
Model Simulations of the Atmospheric Trace Metal Concentrations and Depositions over the Baltic Sea.  
ATMOSPHERIC ENVIRONMENT Vol. 35. No.8, pp. 1395-1409.
- VIII.** G. Petersen, R. Bloxam, S. Wong, J. Munthe, O. Krüger, S. R. Schmolke, A. Vinod Kumar (2001):  
A Comprehensive Eulerian Modelling Framework for Airborne Mercury Species: Model Development and Applications in Europe.  
ATMOSPHERIC ENVIRONMENT - Special ELOISE Issue, Vol. 35. No. 17, pp. 3063-3074.
- IX.** J. Munthe, K. Kindbom, O. Krüger, G. Petersen, J. Pacyna, A. Iverfeldt (2001):  
Examining Source-Receptor Relationships for Mercury in Scandinavia - Modelled and Empirical Evidence.  
WATER, AIR, AND SOIL POLLUTION: Focus 1: pp. 299-310.

## TABLE OF CONTENTS

<b>1. INTRODUCTION</b>	<b>13</b>
<b>EINLEITUNG</b>	<b>17</b>
<b>2. HEAVY METALS IN THE ATMOSPHERE</b>	<b>21</b>
<b>3. CURRENT STATE OF ATMOSPHERIC CHEMISTRY/TRANSPORT MODELS</b>	<b>25</b>
<b>4. A COMPREHENSIVE EULERIAN MODELLING FRAMEWORK FOR AIRBORNE HEAVY METALS</b>	<b>29</b>
<b>4.1 Approaches to the ADOM model for heavy metals</b>	<b>30</b>
<b>4.2 The tropospheric chemistry module for mercury</b>	<b>32</b>
<b>4.3 Evaluation of model performance</b>	<b>42</b>
4.3.1 Applications of the model to episodes of high mercury concentrations in Central Europe	42
4.3.2 Applications of the model to episodes of low mercury concentrations in Northern Europe	46
<b>4.4 Atmospheric input of heavy metals to the Baltic Sea</b>	<b>50</b>
<b>5. SUMMARY AND CONCLUSIONS</b>	<b>57</b>
<b>6. ACKNOWLEDGEMENTS</b>	<b>61</b>
<b>7. REFERENCES</b>	<b>63</b>
<b>8. LIST OF SYMBOLS, UNITS AND ACRONYMS</b>	<b>73</b>
<b>9. LIST OF FIGURES</b>	<b>77</b>
<b>10. LIST OF TABLES</b>	<b>79</b>
APPENDIX: REPRINTS OF PAPERS	81



## 1. INTRODUCTION

The United Nations-Economic Commission Europe (UN-ECE) Convention on Long Range Transboundary Air Pollution (LRTAP) and other European environmental protection conventions such as the Commission for the Protection of the Marine Environment of the North-East Atlantic (OSPAR) and the Baltic Marine Environment Protection Commission (HELCOM) provide frameworks for international action to reduce the impact of air pollution in Europe and its marginal seas. The work under these conventions has established a sound process for negotiating concrete measures to control emissions of air pollutants through legally binding protocols. In this process, the main objective of the Co-operative Programme for Monitoring and Evaluation of the Long-Range Transmission of Air Pollutants in Europe (EMEP) program is to regularly provide with qualified scientific information to support the review and further extension of the international protocols negotiated with the conventions mentioned above.

The main task of EMEP, whose organisational structure is schematically depicted in FIGURE 1, has been to provide the UN-ECE LRTAP, OSPAR, HELCOM and governments in Europe with regular information on past and predicted emissions, concentrations and/or depositions of air

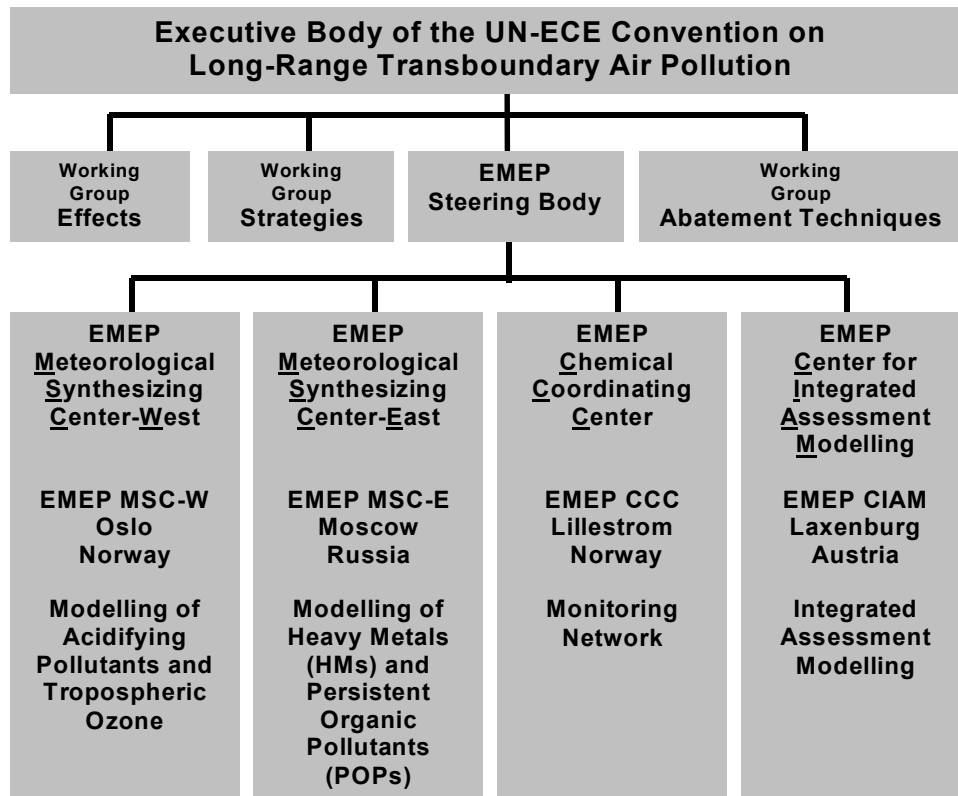


FIGURE 1. Organisational structure of the co-operative programme for monitoring and evaluation of the long range transmission of air pollutants in Europe (EMEP).

pollutants in Europe and, in particular, on the quantity and significance of their long-range transboundary transport. As the work of the conventions has advanced, the requirements on the information provided by EMEP have also evolved. On the seventh phase of the programme, EMEP has been requested to focus further in the evaluation of international abatement strategies and review the success or failure of the existing protocols. To satisfy these needs, the work of EMEP has been formulated in five thematic areas:

- Acid deposition and eutrophication
- Photochemical oxidants
- Heavy metals
- Persistent organic pollutants
- Aerosols

This study focuses on the third of these areas heavy metals, for which the Executive Body of the UN-ECE Convention adopted the „Protocol on Heavy Metals“ on 24 June 1998 in Aarhus (Denmark). It targets three particularly harmful metals: cadmium, lead and mercury. According to one of the basic obligations, Parties will have to reduce their emissions for these three metals below their levels in 1990 (or an alternative year between 1985 and 1995). The protocol aims to cut emissions from industrial sources (iron and steel industry, non-ferrous metal industry) combustion processes (power generation, road transport) and waste incineration. It lays down stringent limit values for emissions from stationery sources and suggests best available techniques (BAT) for these sources, such as special filters or scrubbers for combustion sources or mercury-free processes. The Protocol requires Parties to phase out leaded petrol. It also introduces measures to lower heavy metal emissions from other products, such as mercury in batteries, and proposes the introduction of management measures for other mercury containing products, such as electrical switches and thermostats, fluorescent lamps, dental amalgam, pesticides and paint.

The main task of EMEP within the Heavy Metals Protocol is the above mentioned assessment of the quantity and significance of their long-range transboundary transport in Europe by means of monitoring networks and numerical simulation models. The overall objective of the work described in the subsequent chapters is to give EMEP scientific support in fulfilling its tasks concerning modelling the long-range transport of the priority metals lead, cadmium and mercury over Europe. The support was initiated by the German Federal Environmental Agency (Umweltbundesamt) and is partly embedded into a formal co-operation agreement between the GKSS Research Center Geesthacht and the EMEP institution responsible for heavy metals modelling, namely the EMEP Meteorological Synthesizing Center East (MSC-E) (see FIGURE 1).

The work on which the scientific support is based, was carried out over the last 15 years and is still ongoing with a broad network of scientists from European countries, Canada and the United States that contribute with the systematic collection, analysis and reporting of emission inventories, measurements from monitoring networks inside and outside the EMEP area and results from modelling studies. Special emphasis is placed on the development and application of

advanced numerical simulation models that incorporate detailed physical and chemical processes of heavy metals in the atmosphere.

This study consists of three parts and an appendix. The first part (chapter 2) briefly reviews the current state-of knowledge on the three heavy metals of concern with respect to atmospheric levels and species together with emissions and removal processes.

In the second part (chapters 3 and 4) regional cycles and budgets are introduced in the context of results, which have not yet been published in the scientific literature and are hence not included in the annex, are presented:

- A state-of-the-science chemistry and transport model for mercury species is discussed in the framework of an international model intercomparison study initiated by the UN-ECE Convention and organised by EMEP MSC-E.
- The performance of a comprehensive model system for mercury species is evaluated by comparing model results against field observations in Europe
- Model derived estimates of the atmospheric input of mercury to the Baltic Sea in support of HELCOM.

The third part (chapter 5) presents conclusions and a summary of major achievements with respect to introduction of models for the UN-ECE Convention, PARCOM and HELCOM and some suggestions for further model improvements and extensions are provided.

The appendix contains the reprints from publications in books and peer reviewed journals, on which this study is based.



## 1. EINLEITUNG

Mit der Konvention der Wirtschaftskommission der Vereinten Nationen (United Nations – Economic Commission Europe UN-ECE) über weiträumige, grenzüberschreitende Luftverschmutzung (Long-Range Transboundary Air Pollution LRTAP) sowie anderer Umweltschutzkonventionen wie die Kommissionen zum Schutz der marinen Umwelt des Nord-Ost Atlantiks (OSPAR) und der Ostsee (HELCOM) wurden internationale Vereinbarungen zur Reduzierung der Luftverschmutzung über Europa und seinen Randmeeren geschaffen. Die im Rahmen dieser Konventionen ausgehandelten rechtlich verbindlichen Protokolle beinhalten konkrete Ziele zur Emissionsminderung von Luftschadstoffen auf der Grundlage von regulärer und kontinuierlicher wissenschaftlicher Unterstützung durch das ‚Kooperative Programm zur Erfassung und Bewertung des grossräumigen Transports von Luftschadstoffen über Europa‘ (EMEP).

Die für die UN-ECE LRTAP, OSPAR und HELCOM hauptsächlich zu erbringenden Leistungen von EMEP, dessen Organisationsstruktur in Abbildung 1 schematisch dargestellt ist, umfassen die Bereitstellung von früheren und zukünftigen Emissionsdaten sowie der Konzentrations- und

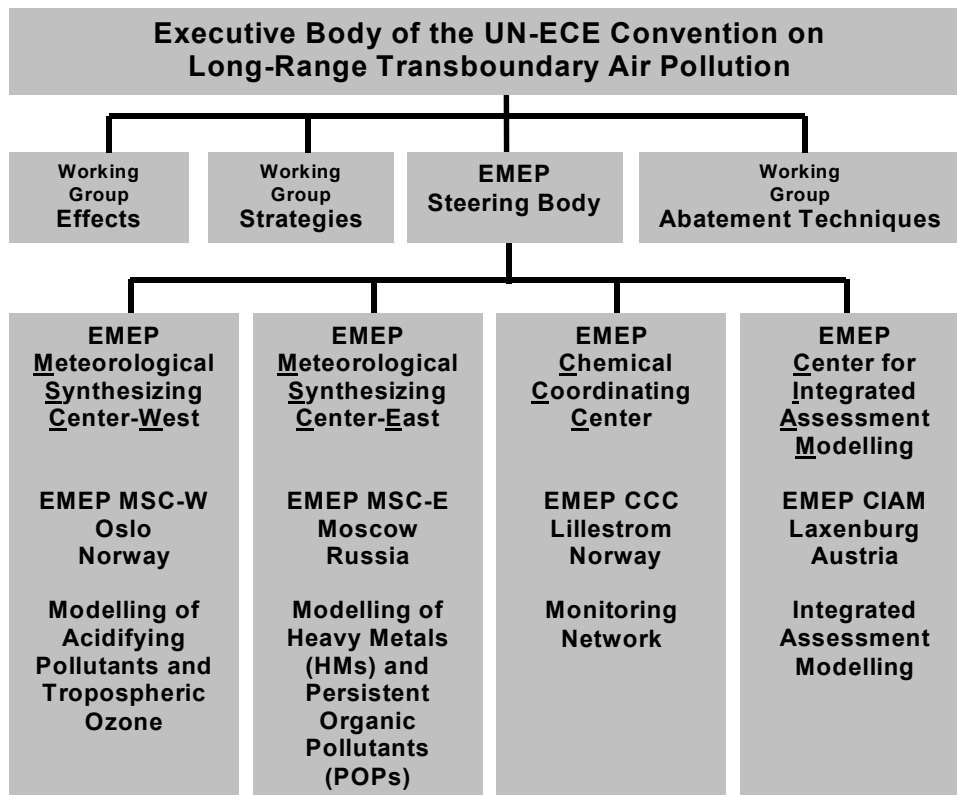


ABBILDUNG 1. Organigramm des Kooperativen Programms zur Erfassung und Bewertung des grossräumigen Transports von Luftschadstoffen in Europa (EMEP).

Depositionsfeldern von Luftschadstoffen über Europa mit besonderem Augenmerk auf die Quantifizierung von deren weiträumigen, grenzüberschreitenden Transporten. Im Zuge der von den Arbeitsprogrammen der Konventionen erzielten Fortschritte sind auch deren Anforderungen an EMEP erhöht worden und im Rahmen der derzeit laufenden siebenten Phase des Programms ist EMEP aufgefordert worden, sich zusätzlich auf die Bewertung von internationalen Emissionsminderungsstrategien hinsichtlich ihres Erfolges oder Misserfolges mit folgender thematischer Gliederung zu konzentrieren:

- Saure Deposition und Eutrophierung
- Photochemische Oxidantien
- Schwermetalle
- Persistente Organische Verbindungen
- Aerosole

Die vorliegende Arbeit ist auf das Themenfeld Schwermetalle konzentriert, für die das ‚Executive Body‘ der UN-ECE Konvention am 24. Juni in Aarhus, Dänemark, ein ‚Schwermetall-Protokoll‘ geschaffen hat, in welchem Blei, Cadmium und Quecksilber als die drei prioritären Schwermetalle genannt sind und in welchem sich die Teilnehmerländer grundsätzlich verpflichten, die Emissionen der zuvor genannten Metalle auf einen Stand von unterhalb der Emissionen des Jahres 1990 (oder eines alternativen Jahres zwischen 1985 und 1995) zu reduzieren. Das Protokoll zielt auf eine Minderung der Emissionen aus Industrieanlagen (Eisen- und Stahlindustrie, Verhüttung von Nichteisenmetallen), Verbrennungsprozesse (Kraftwerke, Strassenverkehr) und Müllverbrennung durch Einführung von stringenten Grenzwerten für Emissionen aus stationären Quellen. Dabei wird die Einführung der besten verfügbaren Technologien wie spezielle Filter und Reinigungsanlagen für Verbrennungsprozesse, die Nutzung quecksilberfreier Produktionsprozesse und die Herstellung quecksilberfreier Produkte (z.B. elektrische Schalter, Thermostate, Leuchtstoffröhren, Amalgam-Zahnfüllungen, Pestizide, Farbe) sowie die ausschliessliche Verwendung von bleifreiem Benzin im Strassenverkehr dringend empfohlen.

Die Hauptaufgabe von EMEP im Rahmen des Schwermetall-Protokolls besteht in der Quantifizierung der grenzüberschreitenden atmosphärischen Transporte von Schwermetallen durch ein europaweites Messnetz und durch die Entwicklung und Anwendung von numerischen Simulationsmodellen. In der vorliegenden Arbeit wird die wissenschaftliche Unterstützung beschrieben, die EMEP bei seinen Modellierungs-Aktivitäten zum Transport und Deposition der drei prioritären Schwermetalle Blei, Cadmium und Quecksilber zuteil wurde. Die Unterstützung wurde durch das Umweltbundesamt als der für die deutschen Belange bei der UN-ECE LRTAP zuständigen Fachbehörde initiiert und ist Gegenstand eines Kooperationsvertrages zwischen dem GKSS Forschungszentrum und dem EMEP Meteorologischen Syntheszentrum Ost, welches die Modellierung der Schwermetalltransporte im Auftrage der UN-ECE LRTAP durchführt (siehe Abbildung 1). Schwerpunkt der Unterstützung ist die Entwicklung und Anwendung von Simulationsmodellen mit detaillierten, dem aktuellen Stand der Wissenschaft entsprechenden

Parameterisierungen der physikalischen und chemischen Prozesse von Schwermetallen in der Atmosphäre.

Die vorliegende Arbeit besteht aus einem dreiteiligen Überbau und einem Anhang mit Sonderdrucken aus Fachzeitschriften und Büchern. Im ersten Teil des Überbaus (Kapitel 2) wird der aktuelle Stand des Wissens über die drei zuvor genannten prioritären Schwermetalle bezüglich ihrer physiko-chemischen Prozesse in der Atmosphäre zusammengefasst. Der zweite Teil (Kapitel 3 und 4) beinhaltet eine Beschreibung der historischen Entwicklung und des aktuellen Standes von numerischen Simulationsmodellen zum atmosphärischen Transport von Schwermetallen. Das für Schwermetalle modifizierte komplexe Euler'sche Modellsystem Acid Deposition and Oxidants Model (ADOM) bildet das Kernstück dieser Arbeit und wird im Überbau im Hinblick auf folgende neuere, bisher nicht veröffentlichten Modellanwendungen beschrieben:

- Entwicklung und Test eines den Stand der Wissenschaft repräsentierenden Chemie-Moduls für Quecksilberspezies im Rahmen eines internationalen Modellvergleichs, der von der UN-ECE intiiert wurde und vom EMEP MSC-E organisiert wird.
- Evaluation des Modellsystems mit Hilfe von europäischen Feldmessungen.
- Abschätzung der atmosphärischen Quecksilbereinträge in die Ostsee für HELCOM

Der dritte Teil (Kapitel 5) enthält Schlussfolgerungen aus der vorliegenden Arbeit. Die Ergebnisse bezüglich der Anwendung von numerischen Simulationsmodellen für die UN-ECE Konvention, PARCOM und HELCOM sowie Vorschläge für weitere Modellverbesserungen werden zusammenfassend dargestellt.

Der Anhang besteht aus 10 Sonderdrucken aus Büchern und Zeitschriften mit detaillierten Beschreibungen von Modellentwicklungen und –anwendungen zur wissenschaftlichen Unterstützung der zuvor genannten Umweltschutzkonventionen.



## 2. HEAVY METALS IN THE ATMOSPHERE

It is increasingly evident that human activities have modified the global atmospheric cycles of the heavy metals. In many instances, the emissions from anthropogenic sources exceed the contributions from natural sources by severalfold. Such massive redistribution caused by mankind has apparently overwhelmed the natural reservoirs and mass fluxes for some of the heavy metals in many ecosystems. In view of the close linkage of the metal cycles to biological processes, there is growing evidence which shows a general elevation of heavy metal burdens in many marine and land biota.

In absolute terms, the mass flux of heavy metals from the atmosphere into soils, forests and lakes in Europe is rather low compared to the flux of acidifying substances such as sulfur and nitrogen oxides [Georgii et al., 1983]. Nevertheless, heavy metals are mobile in the environment, sometimes bioaccumulate in fauna and flora, and can lead to a variety of soil, forest, aquatic and public health impacts [Nriagu, 1990]. The atmospheric deposition of heavy metals is also a major source of these substances in European marginal seas such as the North Sea and the Baltic Sea [VI; VII; Petersen, 1992b; Petersen and Krüger, 1993; Krüger, 1996; Bartnicki et al., 1998]. Circumstantial evidence and model calculations suggest that much of the deposition of heavy metals in rural areas of Europe is due to the transport of metals from distant (greater than 100 km) sources [Schroeder and Lane, 1988; Duce et al., 1991; Ryaboshapko et al., 1999].

It has been found that several heavy metals, including lead, cadmium and a part of atmospheric mercury species are associated with the fine particulate matter size ranges in the ambient air. This is important not only from a health viewpoint since fine particles (aerodynamic diameter  $< 2.5 \mu\text{m}$ ) are respirable, but also because fine particles tend to persist in the atmosphere where they can undergo chemical reaction and be transported from their sources over long distances to pristine areas in the environment. This study is focusing on the three metals mentioned above, which have been defined by the UN-ECE LRTAP Convention, OSPAR and HELCOM to be the priority metals of concern. Special attention is being given to mercury occurring in the atmosphere in various chemical forms with typical concentration ranges in Central and Northern Europe summarised in TABLE 1. Unlike other heavy metals, mercury exists in ambient air predominantly in gaseous elemental form with an estimated global atmospheric residence time of about one year making it subject to long-range transport over spatial scales from about 100 km to continental and global. Hence, mercury is a pollutant of concern in remote areas far away from anthropogenic sources, such as polar regions, coastal seas and remote inland lakes in North America and Scandinavia. Sources of mercury are ubiquitous. According to the U.S. Environmental Protection Agency [EPA, 1996] the type of mercury emissions is defined as either

- anthropogenic mercury emissions: the mobilization or release of geologically bound mercury by human activities, with mass transfer of mercury to the atmosphere.
- natural mercury emissions: the mobilization or release of geologically bound mercury by natural processes, with mass transfer of mercury to the atmosphere

or

- re-emitted mercury: the mass transfer of mercury to the atmosphere by biologic and geologic processes drawing on a pool of mercury that was deposited to the earth's surface after initial mobilization by either anthropogenic or natural activities.

TABLE 1: Mercury species in ambient air in Central and Northern Europe.  
(typical concentration ranges and Henry's law coefficients)

species	concentration range [ng m <sup>-3</sup> ]	Henry's law coefficient [-]	reference
Hg <sup>0</sup>	1-4	0.3	Ebinghaus et al., 1995 Schmolke et al., 1999
HgCl <sub>2</sub>	0.005-0.050	3x10 <sup>-8</sup>	Munthe, 2001 Pirrone, 1998
MeHg	0.0005-0.010	0.3 (CH <sub>3</sub> ) <sub>2</sub> Hg 2x10 <sup>-5</sup> CH <sub>3</sub> HgCl	Munthe, 2001
Hg(part.)	0.010-0.100		Pirrone, 1998 Munthe, 2001

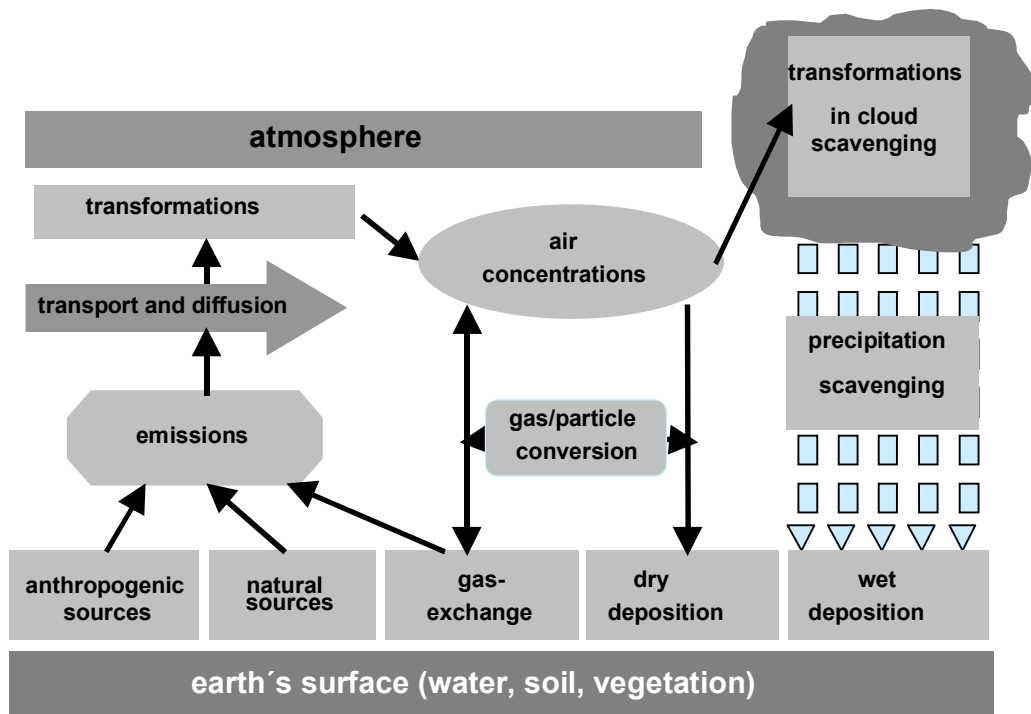


FIGURE 2. Conceptual framework of the atmospheric emissions-to-deposition cycle for heavy metals. (Adopted from Schroeder and Munthe (1998)).

Anthropogenic emissions of mercury (and other heavy metals) can be further divided into area and point sources. Anthropogenic area sources are typically small and numerous and usually cannot be readily located geographically. Point sources are those anthropogenic sources that are associated with a fixed geographic location.

Determinations of heavy metals in the atmosphere have, for the most part, been concerned with regions of high population density and with emissions from specific sources. However, a considerable amount of attention also has been recently focused on determining heavy metals in rural and remote areas in order to estimate the regional and global effects of man's activities. A review of the processes by which airborne heavy metals are transported from the main emission areas in Europe and become subject to deposition and absorption into terrestrial and aquatic ecosystems is given in [V] and references cited therein. Additionally, a broad overview and synthesis of current knowledge and understanding pertaining to all major aspects of mercury in the atmosphere is presented in Schroeder and Munthe (1998).

This study will build on the conceptual framework of atmospheric pathways and processes schematically depicted in FIGURE 2 and described in detail in [V].



### 3. CURRENT STATE OF ATMOSPHERIC CHEMISTRY/TRANSPORT MODELS

Atmospheric phenomena such as increasing green house gas concentrations, stratospheric ozone depletion, acid deposition, increasing tropospheric ozone concentrations and higher levels of toxic trace substances such as persistent organic pollutants and heavy metals have been the focus of large national research programmes. Over the next 10-20 years, many difficult decisions will have to be made by policy makers world-wide to deal with these and other problems and the atmospheric science community must continue its efforts to lay a firm scientific foundation on which these policy decisions can be based. However, the complexity of physical and chemical atmospheric processes makes results from comprehensive air pollutants measurement programmes difficult to interpret without a clear conceptual model of the workings of the atmosphere. A single measurement campaign gives investigators only a snapshot of prevailing atmospheric conditions at a particular time and location, while most issues involving human-induced environmental impacts are concerned with the temporal change of these conditions over local, regional and global or near-global areas. Further, measurements alone cannot be used directly by policy-makers to form balanced and cost-effective strategies for dealing with these problems: an understanding of individual processes within the atmosphere does not automatically imply an understanding of the system as a whole. Only with detailed numerical models, based on best available conceptual and technological formulations, can a thorough understanding of individual processes and the atmospheric system as a whole be obtained.

A variety of modelling techniques have been developed for exploration of atmospheric processes of heavy metals. These include relative simple mass balance models that examine the pooling and exchange of heavy metals between various environmental compartments as well as complex deterministic atmospheric dispersion models attempting to simulate the transport and deposition of heavy metals over domains of hundreds to thousands of kilometers, while detailed chemical transformation models incorporate the most sophisticated treatment of atmospheric mercury chemical processes. An extensive review of models for the long-range transport of heavy metals over Europe and hence of particular relevance for potential application within the UN-ECE protocol on heavy metals, but also for OSPAR and HELCOM is given in [IV] and references cited therein.

The review presented in [IV] and other background documents for EMEP preparatory workshops for the UN-ECE Heavy Metals Protocol [Petersen, 1993; Petersen and Iverfeldt, 1994] comprises model developments until 1996. A typical example for model applications in the framework of the OSPAR and HELCOM Conventions in the time period from 1989 to 1995 for mercury is described in detail in [II]. Also, this model system has been used to assess the atmospheric input of heavy metals to the North Sea and the Baltic Sea for purposes of UBA policy issues concerning the protection of these sea areas from pollution from land-based sources [Petersen, 1991; Petersen, 1992a, 1992b; Petersen and Krüger, 1993] and to calculate annual concentration and deposition pattern of acidifying pollutants and heavy metals in Europe in support of the scientific advisory board „Global Environmental Changes“ of the German Federal Government [Krüger and Petersen, 1993]. Moreover, the mercury model system has been used to examine the source-receptor relationship for mercury in Scandinavia and in particular the effects of mercury emission reductions in Central Europe on the mercury deposition fluxes in Sweden [IX]. The transport and deposition of heavy metals in the studies mentioned above have been analyzed through Lagrangian approaches. These types of models, which have also been extensively used to

calculate transboundary fluxes of acidifying pollutants [Iversen, 1993; Tuovinen et al., 1994] and photo-chemical oxidants in Europe [Simpson et al. 1998], are variants of the so-called trajectory models formulated under assumptions of simplified turbulent diffusion, no convergent or divergent flows and no wind shear. In these models, parcels of air containing emissions from each source are advected with the mean wind, with a parcels location computed at equal time intervals.

A Lagrangian approach does offer advantages relative to a Eulerian approach (which is the main topic of discussion in this work). In particular, the Lagrangian approach avoids many of the computational complexities associated with the simultaneous solution of many differential equations; this generally results in requiring significantly less computational resources and can facilitate an understanding of problems that do not require interactive non-linear processes. However, with the Lagrangian approach, only first-order chemical reactions can be treated rigorously. For higher order reactions (which is the case for the majority of atmospheric chemical reactions of mercury species), a simple superposition of Lagrangian parcels is not strictly valid. Hence, for direct modelling of the complex non-linear chemistry of the atmosphere and to obtain three dimensional air pollutant distributions which are desirable from the standpoint of policy applications of the UN-ECE Protocols and the other agreements mentioned above, the Eulerian modelling approach seems to offer the most appropriate basis for current and future atmospheric chemistry and transport models.

Besides basic differences in their mathematical formulation, the distinction between Lagrangian and Eulerian models lies mainly in their treatment of gas- and aqueous phase chemistry, and cloud and precipitation scavenging processes. Lagrangian models typically use highly parameterized formulations for chemical transformation, usually with both gas and aqueous phase reactions lumped into one overall transformation rate. Further, Lagrangian models either ignore cloud and precipitation scavenging processes or use highly parameterized treatments (e. g. scavenging coefficients). On the other hand, Eulerian models employ extensive gas- and aqueous phase chemical mechanisms and explicitly track numerous pollutants concentrations. Also, Eulerian models include a more detailed numerical formulation for physical and chemical processes occurring within and below precipitating clouds. Typically, these models contain modules designed to calculate explicitly the chemical interactions that move gas-phase material into and among the various aqueous phases within clouds, as well as calculate the aqueous-phase chemical transformations that occur within cloud and precipitation droplets.

Since 1996, in view of the upcoming UN-ECE heavy metals protocol and other environmental protection agreements such as the U.S/Canada Great Lakes Water Quality Agreement (GLWQA), an intensified scientific and political interest in comprehensive Eulerian model developments to derive estimates of ambient concentrations and dry and wet deposition fluxes of heavy metals over Europe [Bartnicki, 1998; Pirrone, 1998; Ryaboshapko et al., 1999; Lee et al., 2001] and North America [Pai et al., 1997, Pai et al., 1999, Bullock, 2000; Seigneur et al., 2001] has been observed. These models are typical of the state-of-science models over the past several years and their main features show a couple of similarities. This is not surprising since these models were all developed in similar time periods and were all focused on the simulation of continental scale transport and deposition of heavy metals. Since these types of continental-scale models have been under intense development for several years, they are more comprehensive in many respects than current global-scale models [Bergan et al., 1999; Shia et al., 1999, Seigneur et al., 2001], particularly in their treatment of gas- and aqueous-phase chemistry. However, the next generation

of global-scale models will likely be more comprehensive than even the most sophisticated of the current continental-scale models.

A relatively long-term effort beginning in the early 1990s and involving a large team of atmospheric scientists is the Models-3 Community Multiscale Air Quality (CMAQ) system of the U.S. EPA [Dennis et al., 1996; U.S. EPA, 1999]. Models-3 represents the next generation of urban and regional scale air quality models in terms of a flexible software system, that provides a user-interface for CMAQ air quality modelling applications and tools for analysis, management of model input/output, and visualization of data. The Models-3 framework relies on two modelling systems to provide the meteorological and emissions data needed for air quality modelling. With this data, the Models-3 CMAQ Modelling system can be used for air quality simulation of tropospheric ozone, acid deposition, visibility and particulate matter ( $PM_{2.5}$  and  $PM_{10}$ ). The model framework is designed as an open system where alternative models such as the heavy metals version of ADOM described in the next chapter can be used to generate the data.



#### 4. A COMPREHENSIVE EULERIAN MODELLING FRAMEWORK FOR AIRBORNE HEAVY METALS

The methodology and basic structure of current Eulerian atmospheric chemistry and transport models are a decade old and were based on computer architectures and numerical schemes that were leading-edge at that time. Many of the models have been improved and enhanced, especially during the early to mid 1990s, and more than a single version of most models exists. Representative examples for these model developments are the chemical transport models RADM [Chang et al., 1987] and ADOM [Venkatram et al., 1988] and their recent updates, extensions and modifications which are still representative and state-of-science models for continental scale applications for acid rain and photochemical oxidants studies in North America [Binkowski et al., 1991; Karamchandani and Venkatram, 1992; Venkatram et al., 1994] and Europe [Stern et al., 1990; Memmesheimer et al., 1995; Ebel et al., 1997]. A detailed comparison of the features and applications of the basic version of these models (and others) is contained in Seigneur and Saxena, 1990) and is not repeated here. In order to test the performance of RADM and ADOM, and to establish its usefulness as a tool for making acid rain policy decisions, a comprehensive two-year field study, called the Eulerian Model Evaluation and Field Study (EMEFS) was undertaken providing a unique data base for model evaluation [NTIS, 1991]. One finding of EMEFS was that RADM and ADOM type models can realistically simulate the transport and deposition of sulphur and other compounds related to acid rain and that future efforts should include adapting the models for other air quality issues, such as particulate matter and air toxics. In this context the basic version of ADOM has been fundamentally restructured in this work to

- address current understanding of atmospheric processes of heavy metals
- utilize an up-to-date understanding of the complex physico-chemical transformations of atmospheric mercury species
- handle cloud physics and precipitation chemistry more effectively.

This model, which has an established record of published investigations [II, III, VII, VIII], represents the state-of-science in continental scale heavy metals modelling over the past several years. It exists in two basic versions: one for metals associated with airborne particles assumed to be chemically inert such as lead and cadmium, the other for a variety of mercury species in gaseous and particulate form including their chemical transformation reactions.

In the following paragraphs, the main features of the comprehensive model system for heavy metals using the Eulerian reference frame of the ADOM model are summarized. A number of key processes incorporated into the chemistry module of the mercury version are discussed in the context of an international inter-comparison study of mercury chemistry schemes. Comparisons of model results with field observations additional to those presented in [VII] and [VIII] are presented. Finally, model results concerning the atmospheric input of lead and cadmium into the Baltic Sea are evaluated against previous estimates based on model calculations and extrapolations from measurements at coastal sites and atmospheric fluxes of mercury species into the Baltic Sea are estimated using the latest mercury version of the ADOM model.

#### 4.1 Approaches to the ADOM model for heavy metals

The starting point for the heavy metals version of ADOM was the existing Eulerian modelling framework that included the governing processes relevant to long range transport of atmospheric pollutants. These processes include transport by three dimensional flows over a domain with horizontal scales of a few thousand kilometers and vertical scales of a few kilometers, transformation by gas- and aqueous phase chemistry, scavenging by cloud processes and interactions of gaseous and particulate species with the ground.

FIGURE 3 shows schematically the various components of the ADOM model modified for transport, transformations and deposition of heavy metals. Two different versions of the model exist: a European 76 by 76 grid domain (FIGURE 4a) and a North American 33 by 33 grid domain (FIGURE 4b) version with a grid cell size of approximately 55x55 km<sup>2</sup> and 127x127 km<sup>2</sup>, respectively. The vertical grid, with 12 unevenly spaced levels between 0 and 10 km, is identical for both versions and is designed to resolve the higher concentration gradients in the boundary layer.

The basic model time step is one hour. Horizontal and vertical wind fields along with the eddy diffusivity, temperature, humidity, surface precipitation, and information about the distribution of clouds make up the meteorological input data set. The data set is derived diagnostically using the weather prediction model HIRLAM for Europe and the Canadian Meteorological Center's model for a North American version of the model. Other than meteorological data, the input and data requirements for ADOM are emissions, initial and boundary conditions, geophysical data and fields of other air pollutants relevant for chemical reactions with mercury species such as ozone and elemental black carbon (soot).

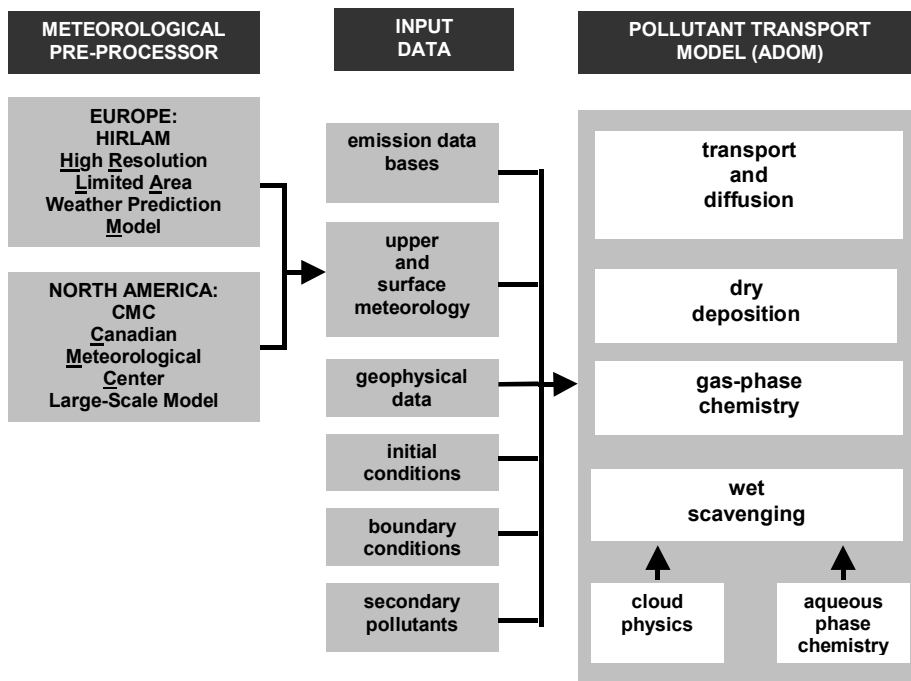


FIGURE 3. The ADOM model system for heavy metals.

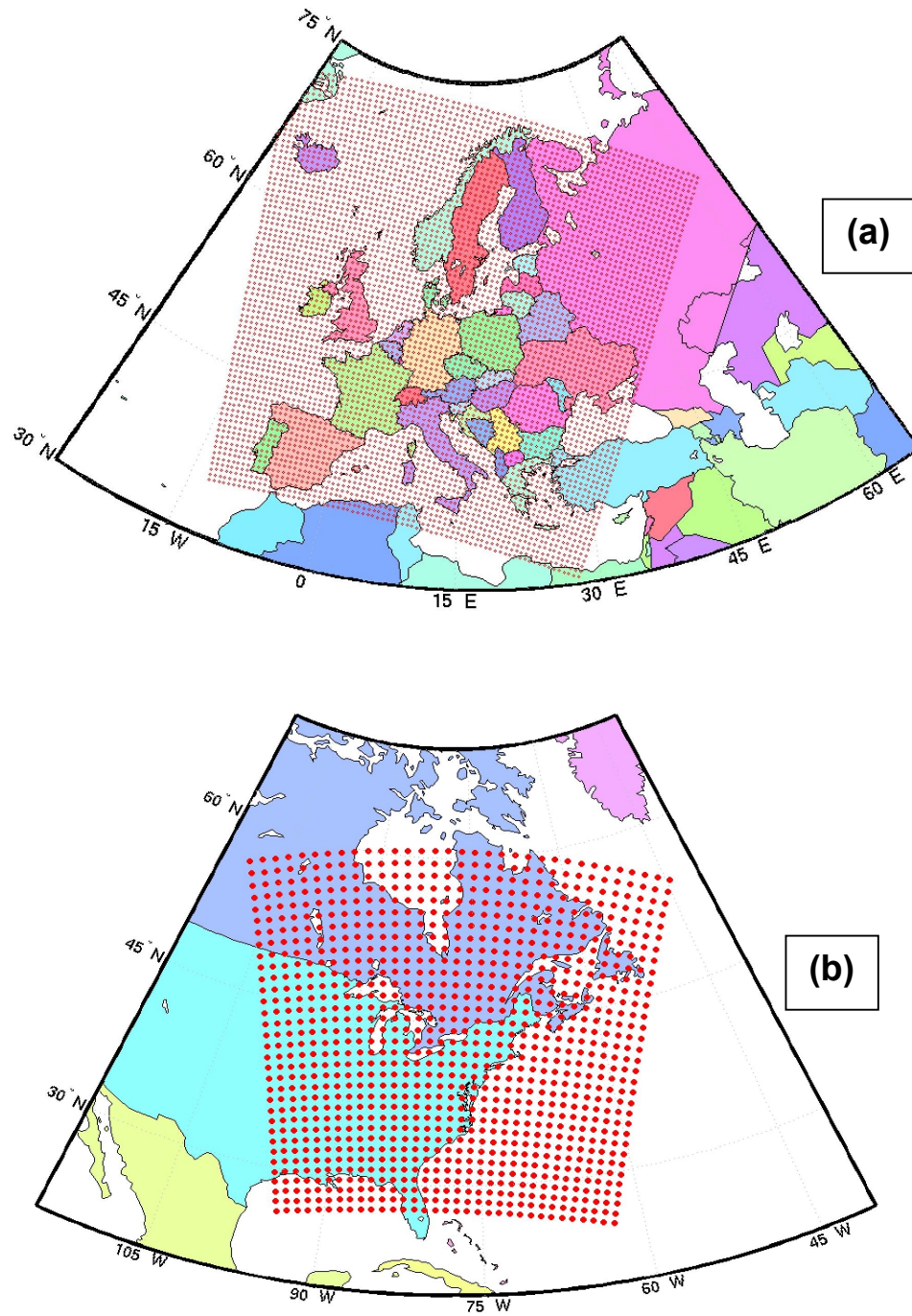


FIGURE 4. The ADOM model domain for

- |                   |   |
|-------------------|---|
| (a) Europe        | (76 by 76 grid cells, 55x55 km <sup>2</sup> grid cell size)   |
| (b) North America | (33 by 33 grid cells, 127x127 km <sup>2</sup> grid cell size) |

European emission data for lead, cadmium and mercury were derived from the UBA/TNO inventory for toxic substances in Europe [Berdowski et al., 1997]. These inventories were compiled for the reference year 1990, which results in uncertainties connected with emission trends between 1990 and 1998. For mercury, an emission update for 1995 including mercury speciation and emission heights for various source categories has become available now [Pacyna et al., 2001] and comparative model runs using the inventories for 1990 and 1995 are now underway [Petersen et al., 2002].

Wet scavenging involves modules for handling cloud physics and aqueous phase chemistry. Clouds are classified as stratus (layer clouds) or cumulus (convective clouds) according to the diagnostic output from the weather prediction model. Observations of the fractional coverage and the vertical extent of clouds are combined with output from the diagnostic model to yield the input fields used in this module.

A detailed description of the entire ADOM modelling framework can be found in ERT (1984). The development and testing of the cloud physics and mercury chemistry module considered to be the core part of the ADOM model system for heavy metals is discussed in the subsequent chapter.

## 4.2 The tropospheric chemistry module for mercury

In the framework of restructuring the ADOM model system for heavy metals a stand-alone version of the cloud mixing, scavenging, chemistry and wet deposition model components referred to as the Tropospheric Chemistry Module (TCM) has been developed and tested [II, III]. This module schematically depicted in FIGURE 5 can be used to test the sensitivity of heavy metals wet deposition to various assumptions about the chemical reactions illustrated in FIGURE 6 including the rate constants and the scavenging of mercury species by water droplets. The sensitivity of the model to various cloud parameters such as the cloud depth, vertical temperature and moisture profiles, the lifetime of cumulus clouds, cloud fractional coverage and the precipitation rate can also be examined.

Besides initial tests described in [II, III] the TCM took part in an international model intercomparison study for mercury chemistry modules [Ryaboshapko et al., 2001]. The study was organised by the EMEP MSC-E in the framework of the UN-ECE Heavy Metals Protocol involving four other advanced chemistry modules, namely the

- Single volume version of the Community Multi-Scale Air Quality Model (CMAQ) of the U.S. Environmental Protection Agency (U.S.A.)
- Mercury chemistry module of the Atmospheric Environment Research/Electric Power Research Institute (AER/EPRI) (U.S.A.)
- Chemistry of Atmospheric Mercury (CAM) process model of the Swedish Environmental Research Institute (IVL) (Sweden)
- Chemical module of MSC-E Heavy Metal Model (MSCE-HM) of the EMEP Meteorological Synthesizing Centre-East (Russia)

The objective of the intercomparison was a comparative evaluation of the chemistry module performances by running them in a cloud environment with identical initial vertical concentration profiles of elemental mercury ( $\text{Hg}^0$ ), mercury chloride ( $\text{HgCl}_2$ ) and particulate mercury

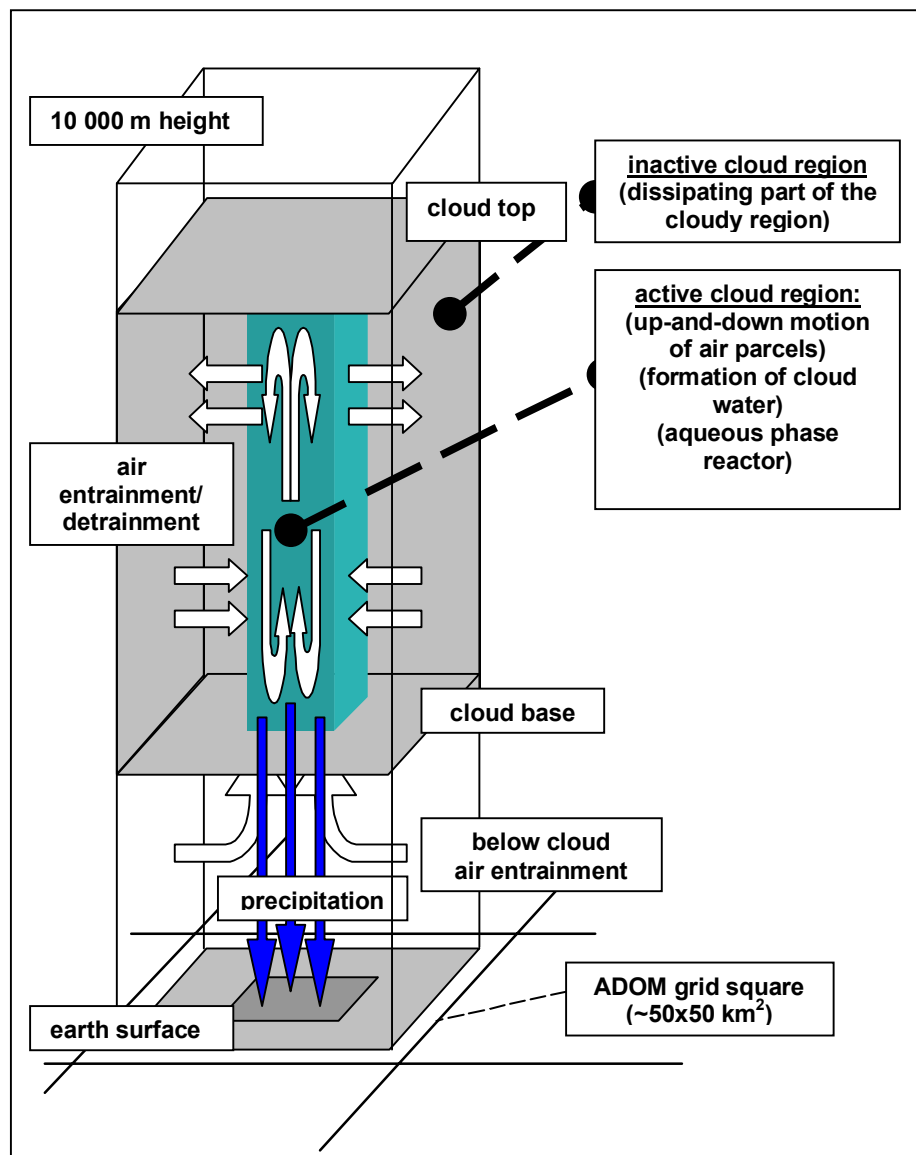


FIGURE 5: Schematic view of the Tropospheric Chemistry Module (TCM) for cumulus clouds.

(Hg(part.)) and other trace constituents affecting the mercury chemistry such as soot, ozone and sulfur dioxide. The TCM has been run over the agreed time period of 48 hours using the closest possible approximation to the common input parameters for the cloud environment, i.e. a non-precipitating cumulus cloud with a cloud base and top height of about 400 m and 4700 m, respectively. The input vertical profiles of temperature, pressure and relative humidity have been adjusted to generate a cloud with an average liquid water content of  $0.5 \text{ g m}^{-3}$ . The initial mercury concentration profiles in the cloud region and above are identical with the concentrations from the input parameter list, whereas the below-cloud initial concentrations are two orders of magnitude lower to avoid any substantial mercury inflow into the cloud from the below-cloud region.

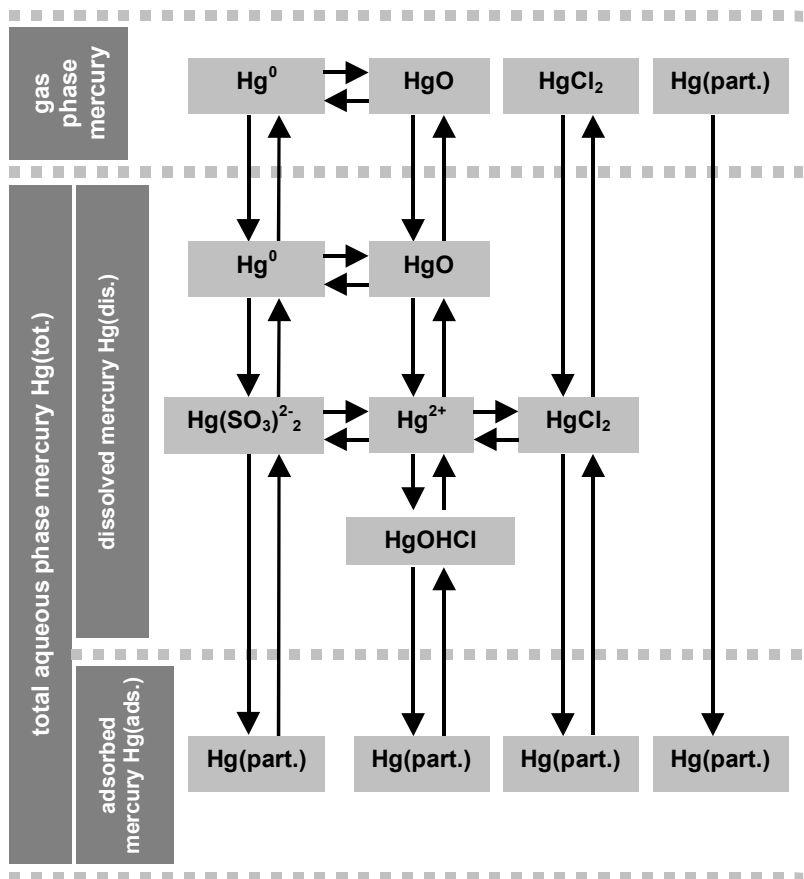


FIGURE 6. The mercury chemistry scheme used with the Tropospheric Chemistry Module (TCM).

Since the TCM is a system which incorporates atmospheric mercury chemistry together with cloud mixing, the results are affected by cloud formation and dissipation processes and by vertical up-and-down motion of air parcels resulting in pronounced vertical  $\text{Hg}^0$ ,  $\text{HgCl}_2$  and  $\text{Hg}(\text{part.})$  concentration profiles after cloud evaporation at the end of each time step (FIGURES 7a-7c). These profiles are generated over the entire troposphere assuming a soot concentration in air of  $0.5 \mu\text{g m}^{-3}$  including the regions below and above cloud base and cloud top, respectively. For all three species, changes in vertical profiles in the cloud area are due to vertical mixing together with aqueous phase chemistry, scavenging and back evaporation of the aqueous species at the end of each time step. Due to vertical redistribution after cloud dissipation below cloud concentrations of all three species are adjusting with time to cloud area concentrations, i. e. initial below cloud concentrations are increasing with time until they have reached the concentration level in the cloud and then closely follow in-cloud concentration changes.

FIGURE 7a shows a relative small  $\text{Hg}^0$  depletion in the cloudy area caused by mass transfer of this species into the aqueous phase. The  $\text{HgCl}_2$  depletion in FIGURE 7b is far more pronounced since this species is readily scavenged and subsequently adsorbed on soot particles. At the end of each time step, adsorbed  $\text{HgCl}_2$  is evaporated back to  $\text{Hg}(\text{part.})$  in air and hence contributing to the increase of  $\text{Hg}(\text{part.})$  concentration as a function of time (FIGURE 7c).

Concentration profiles generated by the TCM for a no-soot scenario are depicted in FIGURE 8a, 8b and 8c. A comparison of profiles in FIGURE 7a and 8a reveals their similarities. Due to its low water solubility changes in  $\text{Hg}^0$  concentrations are mainly determined by mass transfer processes into the aqueous phase and only to a minor extent by subsequent adsorption on soot particles. In the absence of soot  $\text{HgCl}_2$  depletion is considerably smaller (FIGURE 8b), because mass transfer of  $\text{HgCl}_2$  from the gas phase into the aqueous phase is slowed down if a subsequent adsorption on soot particles is missing. This also effects the time evolution of  $\text{Hg}(\text{part.})$ , i.e. a smaller amount of adsorbed  $\text{HgCl}_2$  is evaporated back thus changing the  $\text{Hg}(\text{part.})$  build up into a slight  $\text{Hg}(\text{part.})$  depletion.

FIGURES 9 and 10 show time dependent average gas-phase and aqueous-phase concentrations for the  $0.5 \mu\text{g m}^{-3}$  soot and the no-soot scenario, respectively, in the cloudy area after chemistry has taken place but before cloud dissipation and vertical redistribution of mercury species. It should be noted, that concentrations of all species undergo a spin-up period of about 6 hours according to the adjustments in the cloudy area as illustrated in FIGURES 8 and 9.

The low solubility of  $\text{Hg}^0$  causes the majority of  $\text{Hg}^0$  to be present in the gas phase in both the  $0.5 \mu\text{g m}^{-3}$  soot and the no-soot scenario (FIGURES 9a and 9b). However,  $\text{HgCl}_2$  and  $\text{Hg}(\text{part.})$  gas phase concentrations behave significantly different in both scenarios: In case of the  $0.5 \mu\text{g m}^{-3}$  soot scenario  $\text{Hg}(\text{part.})$  concentrations are slightly increasing with time after the spin-up period, whereas  $\text{HgCl}_2$  shows the opposite trend (FIGURE 9a). This can be explained by an increasing ratio of adsorbed and dissolved species in the aqueous phase as a function of time and hence, after back evaporation at the end of the cloud life cycle, an increasing ratio of  $\text{Hg}(\text{part.})$  and  $\text{HgCl}_2$  gas phase concentrations. At the end of the 48 hours simulation the  $\text{Hg}(\text{part.})$  concentrations are a factor of about 8 higher than  $\text{HgCl}_2$  concentrations. If no soot is involved (FIGURE 9b) less aqueous Hg is present in the adsorbed phase resulting in less back evaporation of  $\text{Hg}(\text{part.})$  and, at the end of the simulation period, in  $\text{HgCl}_2$  concentrations slightly higher than  $\text{Hg}(\text{part.})$  (FIGURE 9b)

The  $\text{Hg}(\text{dis.})_{\text{aq}}$  and the  $\text{Hg}(\text{ad.})_{\text{aq}}$  lines in FIGURES 10a and 10b represent the sum of all dissolved and adsorbed species, respectively, in the aqueous phase and the  $\text{Hg}(\text{tot.})_{\text{aq}}$  line is the sum of  $\text{Hg}(\text{dis.})_{\text{aq}}$  and  $\text{Hg}(\text{ad.})_{\text{aq}}$  (see FIGURE 5). For both scenarios the curves for  $\text{Hg}(\text{dis.})_{\text{aq}}$  and  $\text{Hg}(\text{ad.})_{\text{aq}}$  show a shape very similar to  $\text{HgCl}_2$  and  $\text{Hg}(\text{part.})$  gas phase concentrations in FIGURES 9a and 9b. because the mercury species in the cloud are not depleted by precipitation after aqueous phase chemistry has taken place and no gas phase species are added the beginning of the next time step. Hence, the cloud is governed by back evaporation i.e. most of the aqueous species are converted back to gaseous  $\text{HgCl}_2$  and  $\text{Hg}(\text{part.})$  at the end of each time step reaching almost steady state conditions at the end of the simulation period with  $\text{Hg}(\text{tot.})_{\text{aq}}$  concentrations of about  $110 \text{ ng l}^{-1}$  for both scenarios. In case of the  $0.5 \mu\text{g m}^{-3}$  soot scenario about 95% of the aqueous species are associated with particles at the end of the simulation period, whereas for the no-soot scenario the major fraction (about 54%) is in the dissolved phase, but a relative large  $\text{Hg}(\text{ad.})_{\text{aq}}$  fraction of about 46% is also present due to a certain amount of initial  $\text{Hg}(\text{part.})$  in air, which is chemically inert and therefore just scavenged and evaporated back during the simulation period.

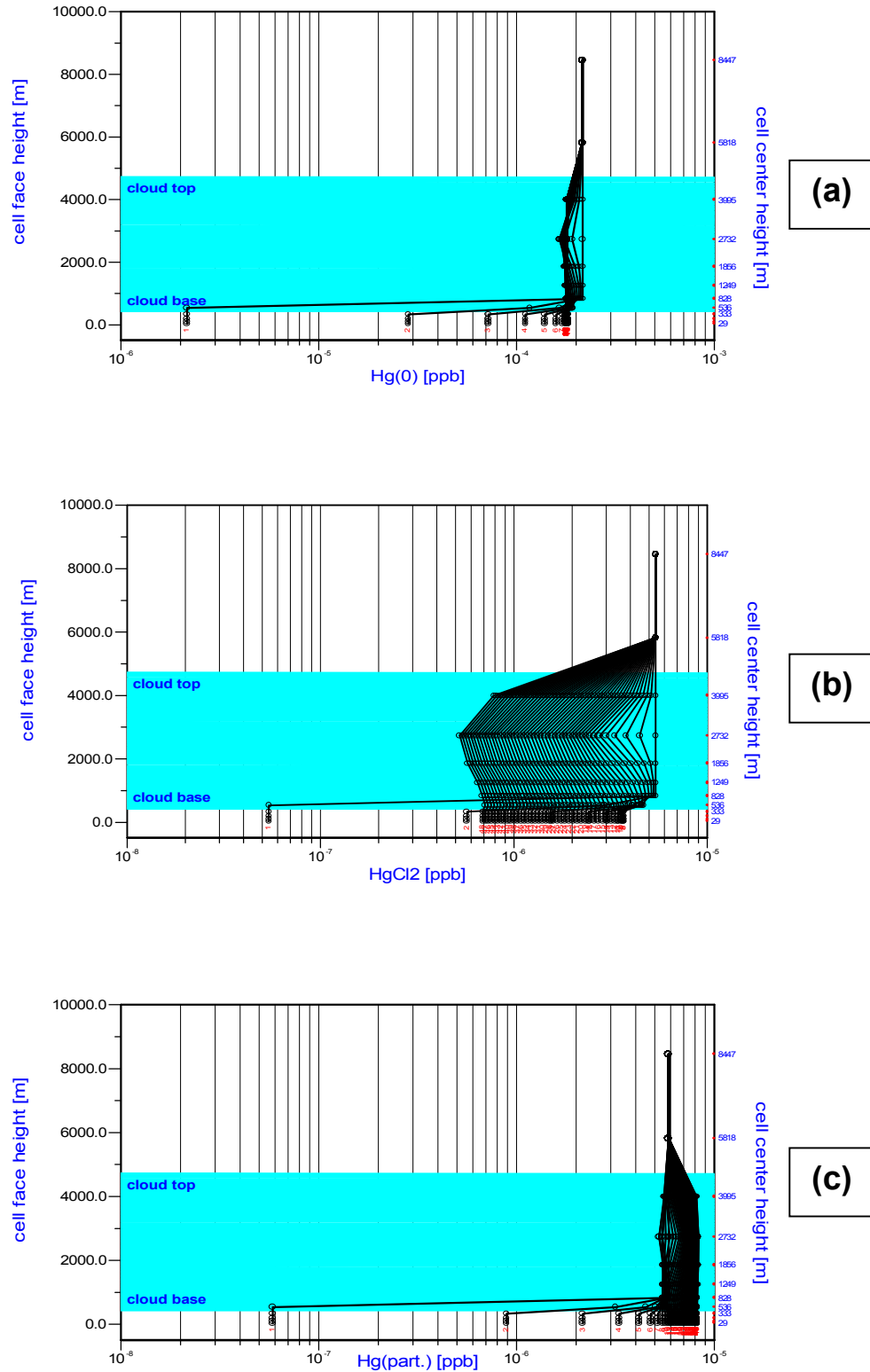


FIGURE 7. 48 hour time evolution of (a)  $\text{Hg}^0$  (b)  $\text{HgCl}_2$  (c)  $\text{Hg}(\text{part.})$  concentration profiles at the end of each 1 hour time step after cloud evaporation.  
( $0.5 \mu\text{g m}^{-3} \text{soot}$ )

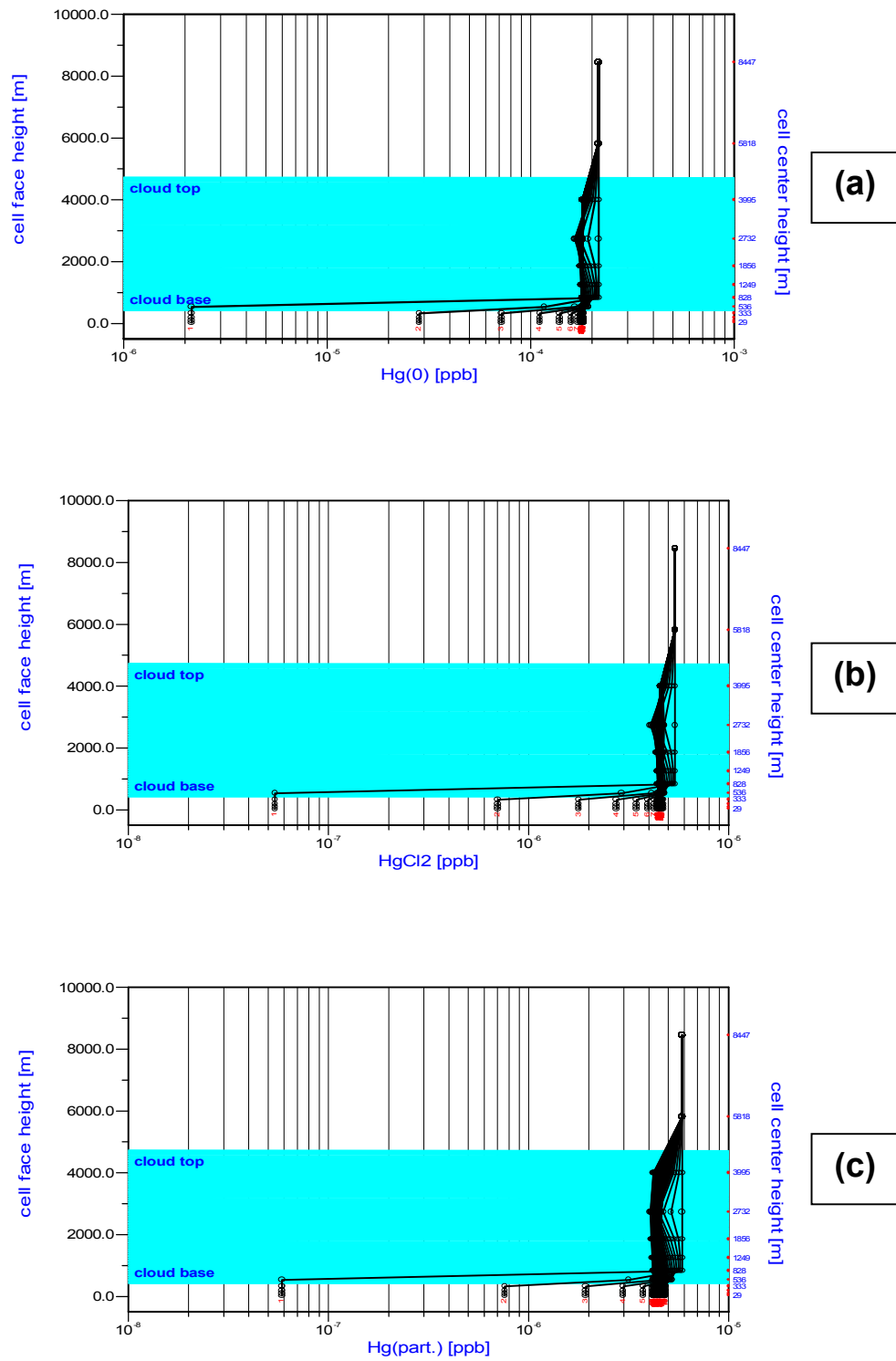


FIGURE 8. 48 hour time evolution of (a)  $\text{Hg}^0$  (b)  $\text{HgCl}_2$  (c)  $\text{Hg}(\text{part.})$  concentration profiles at the end of each 1 hour time step after cloud evaporation. (no soot)

TABLE 2. Input parameters for the intercomparison study of atmospheric mercury chemistry schemes.

	$\text{Hg}^0$ [ng m <sup>-3</sup> ]	$\text{HgCl}_2$ [ng m <sup>-3</sup> ]	$\text{Hg}(\text{part.})$ [ng m <sup>-3</sup> ]	soot [ $\mu\text{g m}^{-3}$ ]	precip. rate [mm (48 h) <sup>-1</sup> ]
<b>case 1</b>	1.600	0.000	0.000	0.0	0.00
<b>case 2</b>	1.600	0.000	0.000	0.5	0.00
<b>case 3</b>	1.600	0.000	0.040	0.0	0.00
<b>case 4</b>	1.600	0.005	0.000	0.5	0.00
<b>case 5</b>	1.600	0.005	0.040	0.5	0.00
<b>case 6</b>	1.600	0.005	0.040	0.5	3.50
<b>case 7</b>	1.600	0.005	0.040	0.5	7.00
<b>case 8</b>	1.600	0.005	0.040	0.5	10.50

Additional runs have been performed to compare TCM results against field observations using data from simultaneous measurements of mercury species in ambient air and in precipitation at a site at the GKSS Research Center Geesthacht. These data form the basis for eight different cases defined in TABLE 2. Results in terms of  $\text{Hg}(\text{tot.})_{\text{aq}}$  concentrations as a function of time and soot concentrations are summarized in FIGURES 11a and 11b. To demonstrate the impact of TCM depletion by precipitation in more detail,  $\text{Hg}(\text{tot.})_{\text{aq}}$  concentrations in these two figures have been generated without spin up during the first six hours as mentioned above and as shown in FIGURES 7-8.

FIGURE 11a illustrates the impact of  $\text{HgCl}_2$  and  $\text{Hg}(\text{part.})$  concentrations on  $\text{Hg}(\text{tot.})_{\text{aq}}$  at a constant  $\text{Hg}^0$  level of 1.6 ng m<sup>-3</sup>. As expected,  $\text{Hg}(\text{tot.})_{\text{aq}}$  shows minimum values for both with and without soot when  $\text{HgCl}_2$  and  $\text{Hg}(\text{part.})$  are set to zero (case 1 and 2). Adding 0.04 ng m<sup>-3</sup>  $\text{Hg}(\text{part.})$  results in an about fourfold increase of  $\text{Hg}(\text{tot.})_{\text{aq}}$  (case 3), whereas additional 0.005 ng m<sup>-3</sup>  $\text{HgCl}_2$  only contributes to about 10-15% to  $\text{Hg}(\text{tot.})_{\text{aq}}$  (case 4). The input data of case 5 represent the observed average Hg concentrations in air but with the precipitation rate set to zero yielding a  $\text{Hg}(\text{tot.})_{\text{aq}}$  concentration of about 80 ng l<sup>-1</sup> (FIGURE 11a and 11b). If the TCM is depleted with the observed average precipitation rate of 3.5 mm during 48 hours,  $\text{Hg}(\text{tot.})_{\text{aq}}$  is decreasing to about 30 ng l<sup>-1</sup> (case 6 in FIGURE 11b). The observed precipitation rate represents an average value during a ten days sampling period, and is therefore most probably underestimated for events of heavier rainfalls during a 48 hour period. Increasing the precipitation by factors of 2 and 3 (case 7 and 8, respectively) gives  $\text{Hg}(\text{tot.})_{\text{aq}}$  concentrations of about 10 ng l<sup>-1</sup> or less. If one allows for potential uncertainties in the observed precipitation rate during the 48 hours of simulation, agreement with the observed average  $\text{Hg}(\text{tot.})_{\text{aq}}$  concentration of 7.2 ng l<sup>-1</sup> is fairly good and the TCM has demonstrated its capabilities to reproduce observed field data in terms of concentrations in precipitation as a function of both cloud mixing and mercury chemistry reasonably well.

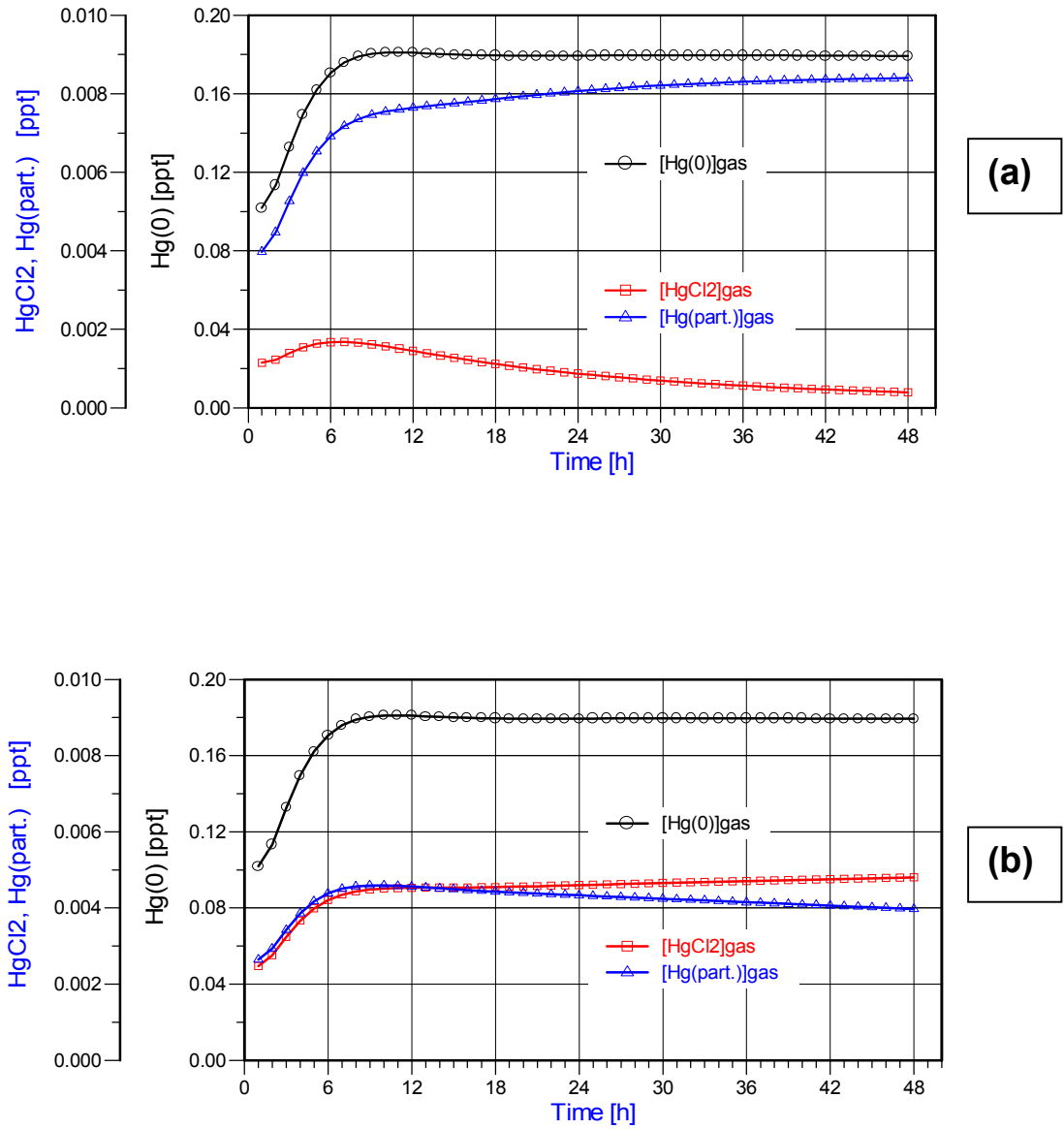


FIGURE 9. 48 hour time evolution of  
 (a) average gas phase concentration in the cloud area after aqueous phase chemistry ( $0.5 \mu\text{g m}^{-3}$  soot)  
 (b) average gas phase concentration in the cloud area after aqueous phase chemistry (no soot)

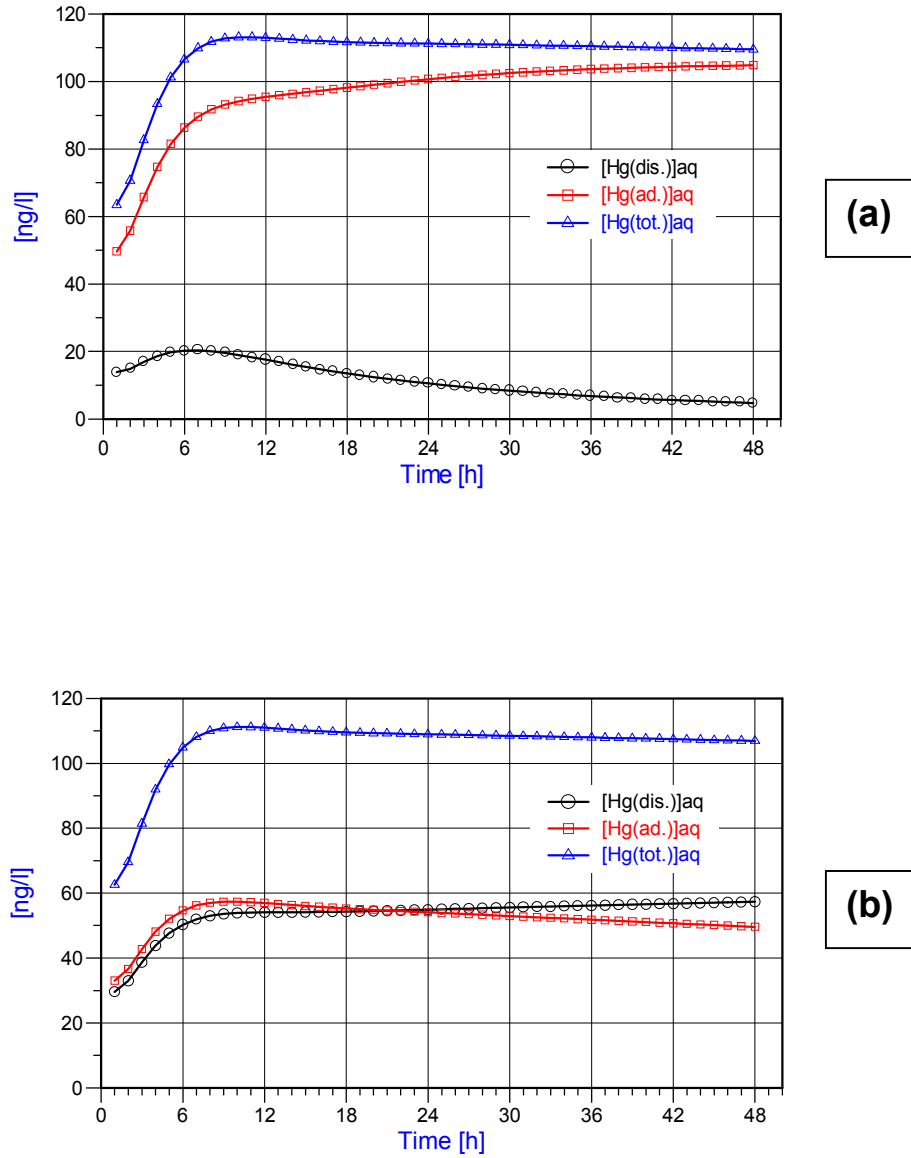


FIGURE 10. 48 hour time evolution of  
 (a) average aqueous phase concentration in the cloud area after aqueous phase chemistry ( $0.5 \mu\text{g m}^{-3}$  soot)  
 (b) average aqueous phase concentration in the cloud area after aqueous phase chemistry (no soot)

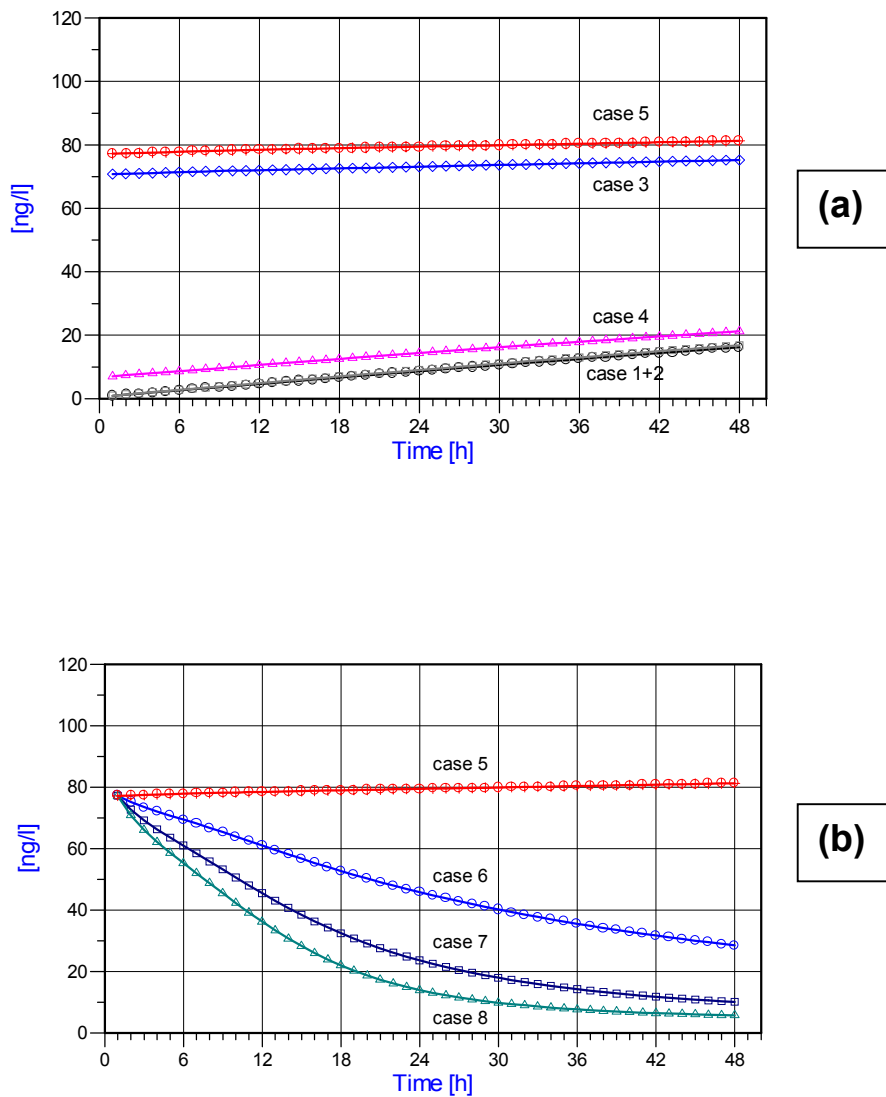


FIGURE 11. 48 hour time evolution of  
 (a) average aqueous phase concentration in the cloud area after aqueous phase chemistry for 5 cases defined in TABLE 2.  
 (b) average aqueous phase concentration in the cloud area after aqueous phase chemistry for 4 cases defined in TABLE 2.

### 4.3 Evaluation of model performance

Model evaluation is a key consideration when developing new and advanced comprehensive models. Since the ADOM for heavy metals, in particular the mercury version, was intended to be applied to simulations with policy implications, thorough validation and verification of the model and its components (such as the TCM discussed in the previous chapter) is a requirement. A model developed or utilized without continual comparison against actual data is less than worthless: it is dangerous. Such a model is nothing more than a collection of mathematical formulae, no matter how elegant its formulation or how efficient its coding. Only with the close integration of state-of-science models and state-of-science experimental measurements can real progress be made towards the solution of the complex problems that are currently faced, i. e. the continual interplay between conceptual understanding and experimental evidence.

#### 4.3.1 Applications of the model to episodes of high mercury concentrations in Central Europe

High quality monitoring data for mercury air concentrations and deposition in Europe are still limited, although several recent investigations have improved the database [Ebinghaus et al., 1995, Lee et al., 1998; Munthe, 2001; Pirrone et al. 2000; Berg et al., 1996; Berg et al., 1997, Berg and Hjellbrekke, 1998; Schmolke et al., 1999]. Fortunately, a few studies of air concentrations measured simultaneously in Germany and in Sweden are available now for evaluation of model performance. These data, although restricted to four sites (FIGURE 12) and

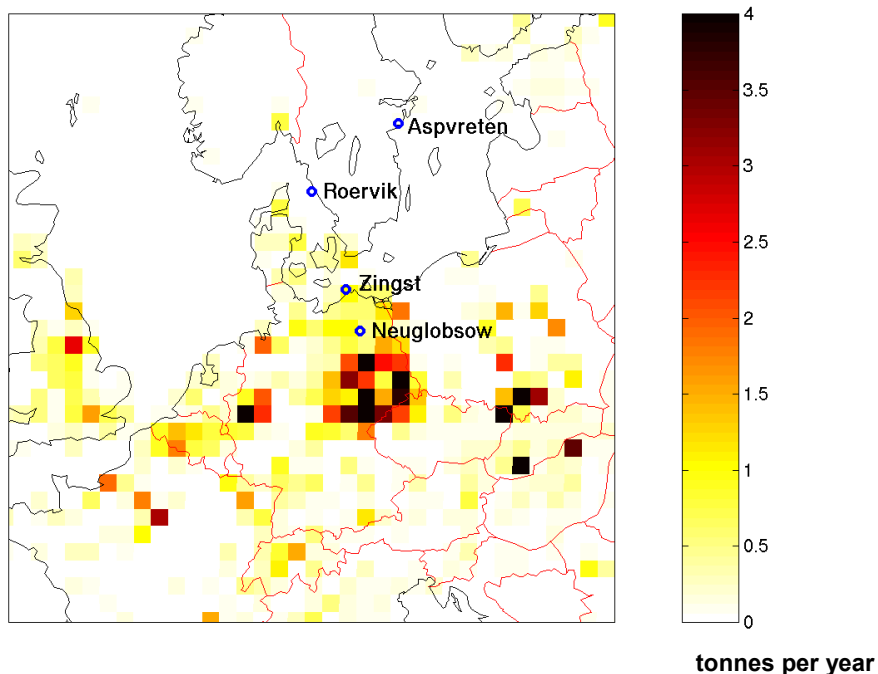


FIGURE 12. Location of sites involved in the evaluation of the model performance and mercury emissions in individual grid cells.

to a few 1-2 months measurement periods provide an opportunity for comparison with model predicted concentrations. A detailed description and a full documentation of the comparison of model results against observations is provided in [Schmolke and Petersen, 2002], and in the final report of the project “Mercury Species over Europe” funded by the EC [Munthe, 2001], respectively. This chapter is restricted to some illustrative examples concerning episodes of high mercury concentrations in Europe.

FIGURE 13 shows hourly averages (Neuglobsow, Zingst and Aspvreten) and three or one day averages (Roervik) of TGM observations together with model predicted hourly  $\text{Hg}^0$  concentrations for November/December 1998. Measurements at Zingst cover the entire two months, whereas the other three sites are limited to a two weeks period of measurements. One should note the episodic nature of the observed and model predicted values at the two German sites spanning more than a threefold range of concentrations from 1.5 to approximately  $5 \text{ ng m}^{-3}$ . The lower end of the range is representative of hemispheric background concentrations of about  $1.5 \text{ ng m}^{-3}$  [Ebinghaus et al., 1995; Lee et al. 1998], whereas the concentrations at the upper end of the range are most probably due to long-range transport from anthropogenic sources in Central Europe. Of particular interest are November 25 and December 4-5 of 1998 when the model predictions show coinciding peaks at all four sites ranging from about 2.5 to  $5.5 \text{ ng m}^{-3}$ . Observed levels are on a similar elevated level, except Aspvreten on November 25. This day has been examined with reference to 72 hours back trajectories, which have been derived from the horizontal wind field at the third ADOM vertical level at approximately 250 meters height. These trajectories describe the route taken during the previous three days by the air masses arriving at the four sites (FIGURE 14). Originating in Romania and the Ukraine air masses move along the trajectories into the main emission areas in southern Poland and eastern Germany, where they change their directions and move northwards arriving at the four sites. The good agreement between observed and model predicted peak concentrations during episodes when trajectories exhibit the above described travel pattern is an indication that the model has capabilities to simulate atmospheric transport over distances of several hundred kilometers and that the emission inventory used with the model is based on realistic emission estimates for central Europe in 1998.

Another example for coinciding peaks of observed and model predicted mercury concentrations is depicted in FIGURE 15. The elevated levels during March 26 of 1997 are quite well reproduced by the model at all 4 sites. Maximum concentrations have been observed and calculated around noon of March 26 at Neuglobsow, Zingst and Roervik with second smaller peaks predicted by the model (and observed at Neuglobsow and Roervik as well) in the evening. The Aspvreten maximum is occurring a couple of hours later and the slight evening peak is missing at this site. These phenomena are supported by the routes of the trajectories on March 26 (FIGURE 16): During the first half of the day air masses start over Poland and adjacent areas, traverse East Germany picking up high emission rates and eventually arrive at the four sites. In the afternoon trajectories arriving at all sites except Aspvreten are changing their routes significantly: They originate over the Western Atlantic and subsequently pass over emission areas in Britain and West Germany. Evidently, the routes of these trajectories cause the smaller concentration peaks mentioned above.

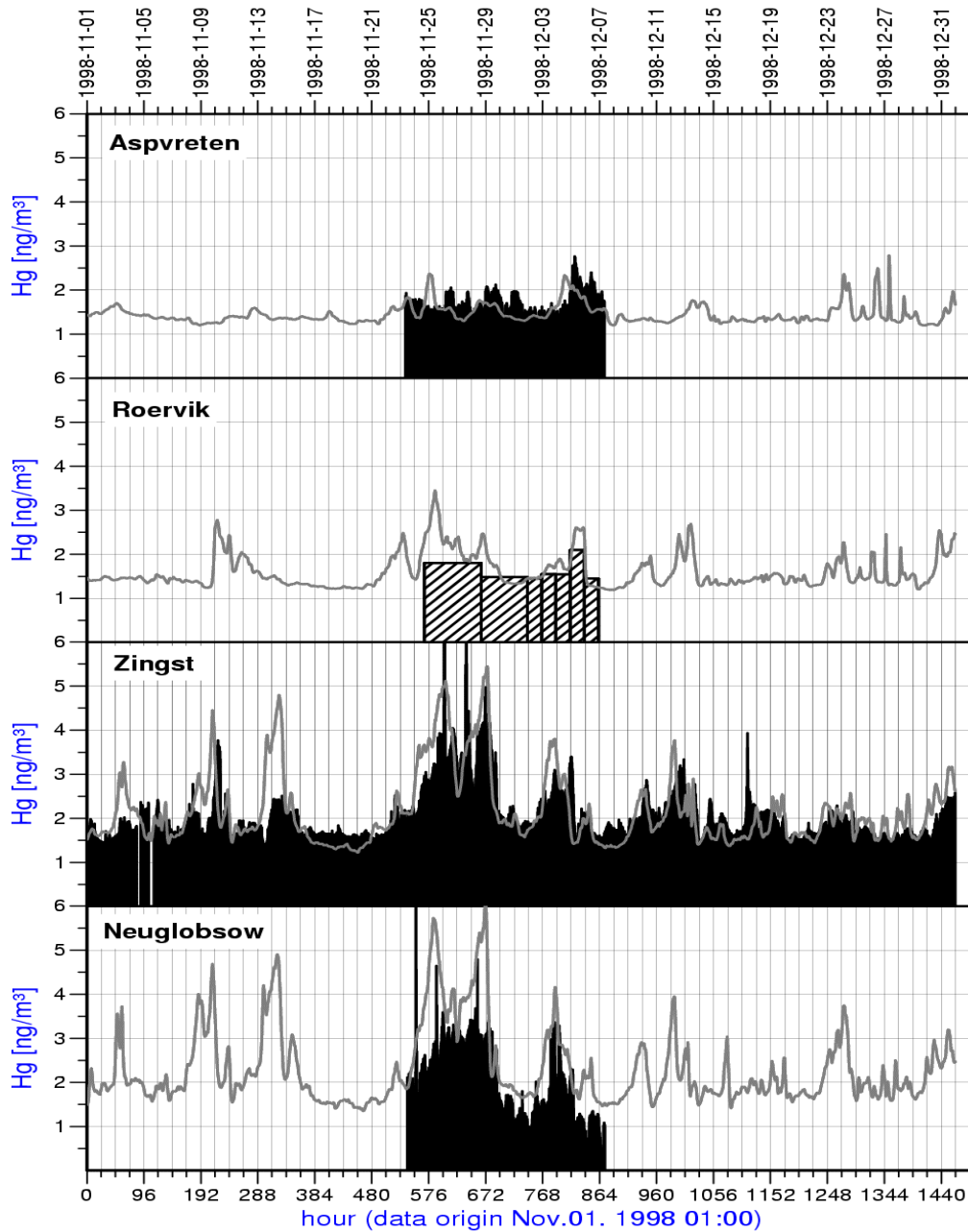


FIGURE 13: Time series of hourly averages of observed TGM concentrations (black area) and model predicted  $\text{Hg}^0$  concentrations in air (grey line) at two Swedish sites (Aspvreten, Roervik) and two German sites (Zingst, Neuglobsow), November/December 1998. (The observations at Roervik are daily and multi-day averages)

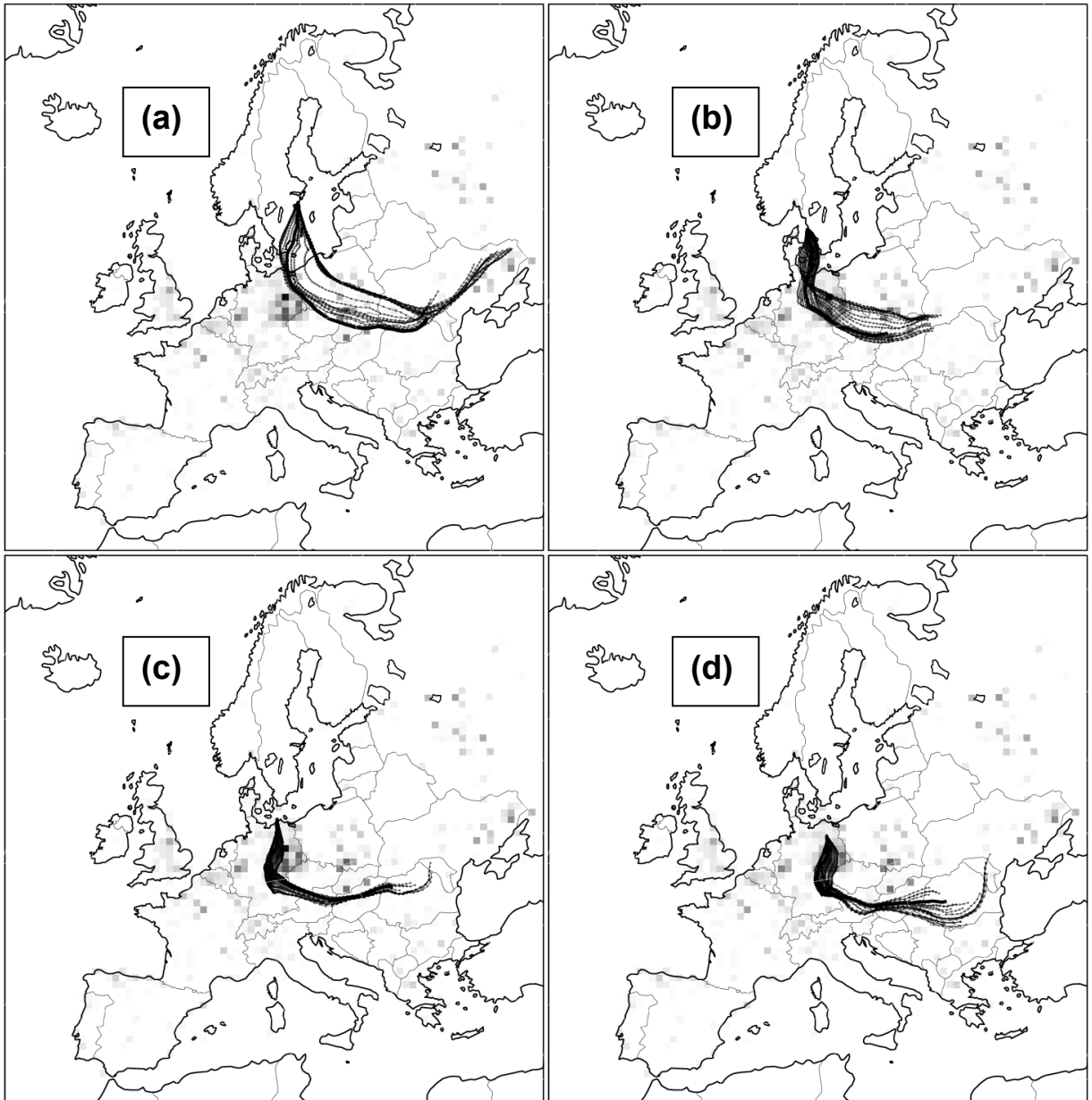


FIGURE 14: 72 hours backward trajectories November 25, 1998 for  
(a) Aspvreten  
(b) Roervik  
(c) Zingst  
(d) Neuglobsow

#### 4.3.2 Applications of the model to episodes of low mercury concentrations in Northern Europe

In terms of comparing measurements made at the two Swedish sites with model output there is evidence that the model has a tendency to underestimate observations probably due to missing natural and re-emission processes in the model at present. Both observed and model predicted time series are characterized by low temporal variability except the high concentration episode described in the previous section and except some low concentration episodes typically occurring over a time period of 12 hours or less.

Of particular interest in FIGURE 15 are the four events of observed low concentration at the northern most site Aspvreten on 22, 23, 24 and 28 of March 1997, which are not reproduced by the model. The trajectories in FIGURE 17 are either originating from Finland and Northern Russia or they are pointing towards ice-covered regions of the Arctic Ocean as a potential source of mercury depleted air masses during that time of the year. Indeed, mercury depletion phenomenon have been observed during the three months period following polar sunrise in March [Schroeder et al., 1998; Schroeder and Barrie, 1998, Lu et al., 2001] and the observed episodic minimum concentrations in the Aspvreten time series may be an indication for transport of air masses from polar regions. However, the database is too scarce to draw any firm conclusions and more work in terms of using a model approach that can take into account the global cycling of mercury is required to identify this phenomenon with more confidence [Seigneur et al., 2001]. Because of the coarse resolution necessarily used in global simulations, such simulations cannot be used to assess the mercury deposition fluxes in specific regions such as the Baltic Sea which are discussed in the next chapter. On the other hand, these regional simulations must rely on boundary conditions that may influence the model results. It is necessary therefore to develop a multiscale modelling approach, that consists of the existing regional scale ADOM model for mercury and a global chemical transport model, which provides the time dependent boundary concentrations for the ADOM model.

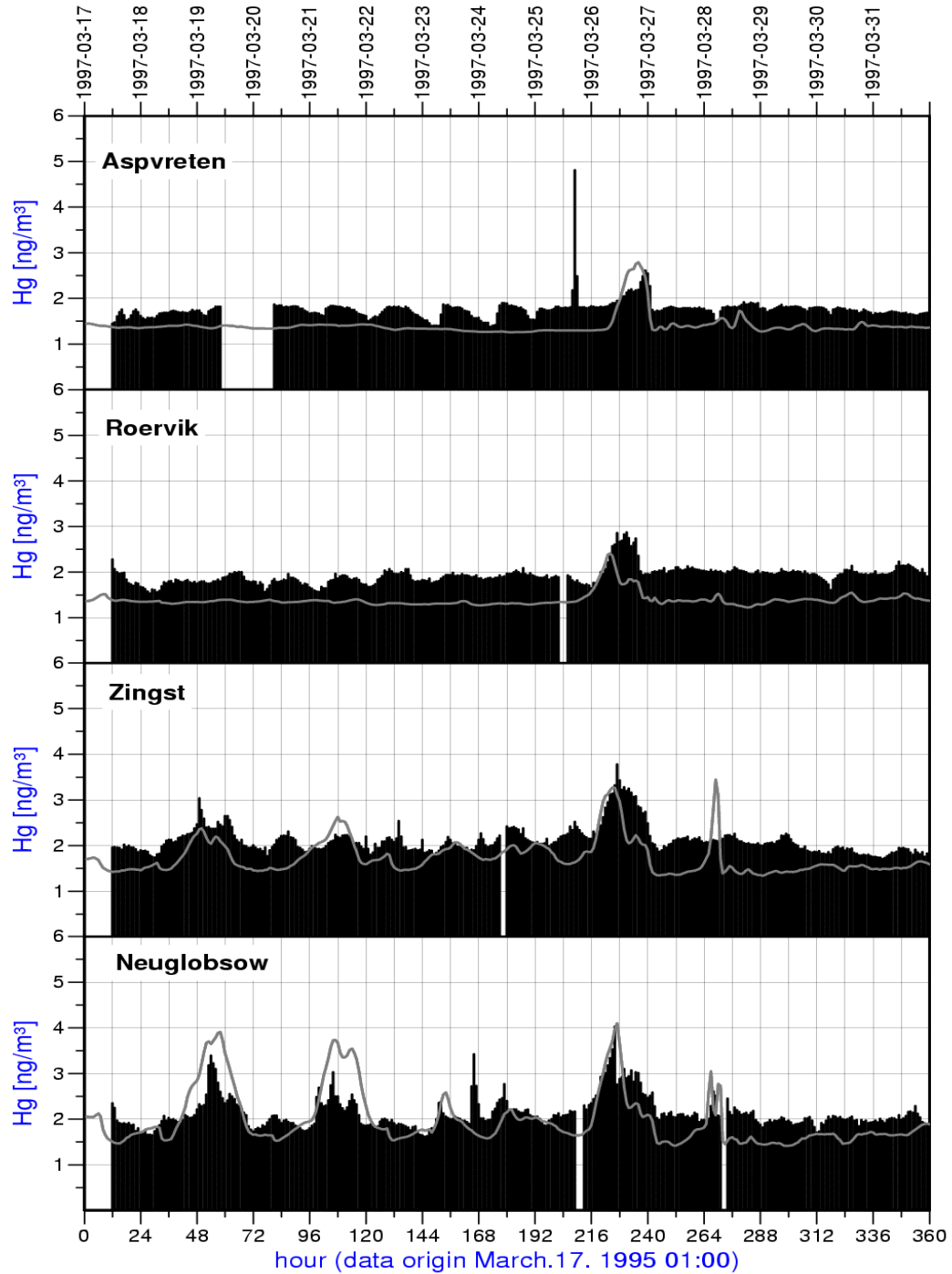


FIGURE 15: Time series of hourly averages of observed TGM concentrations (black area) and model predicted  $\text{Hg}^0$  concentrations in air (grey line) at two Swedish sites (Aspvreten, Roervik) and two German sites (Zingst, Neuglobsow), March, 1997.

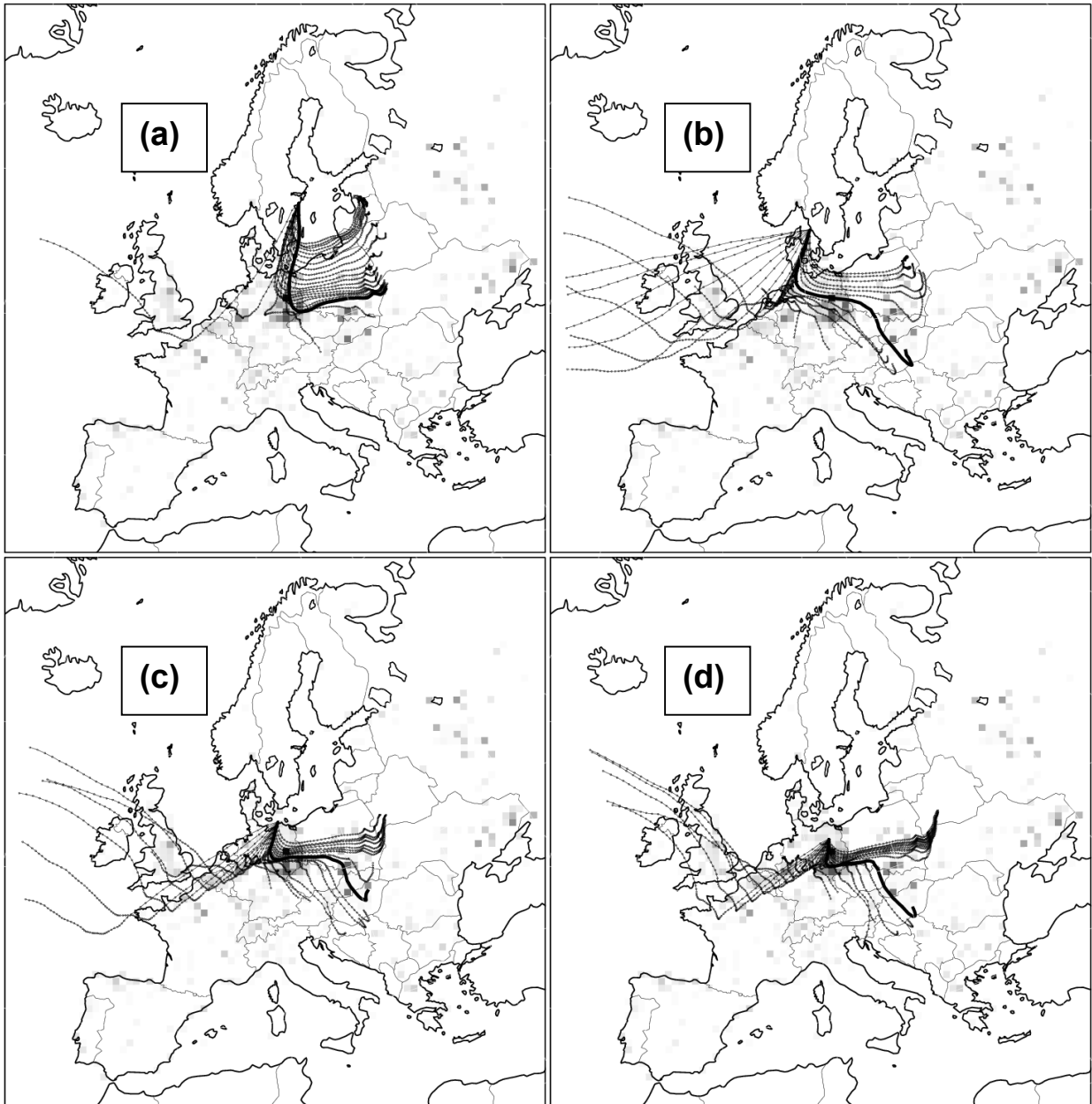


FIGURE 16: 72 hours backward trajectories March 26, 1997 for  
(a) Aspvreten  
(b) Roervik  
(c) Zingst  
(d) Neuglobsow

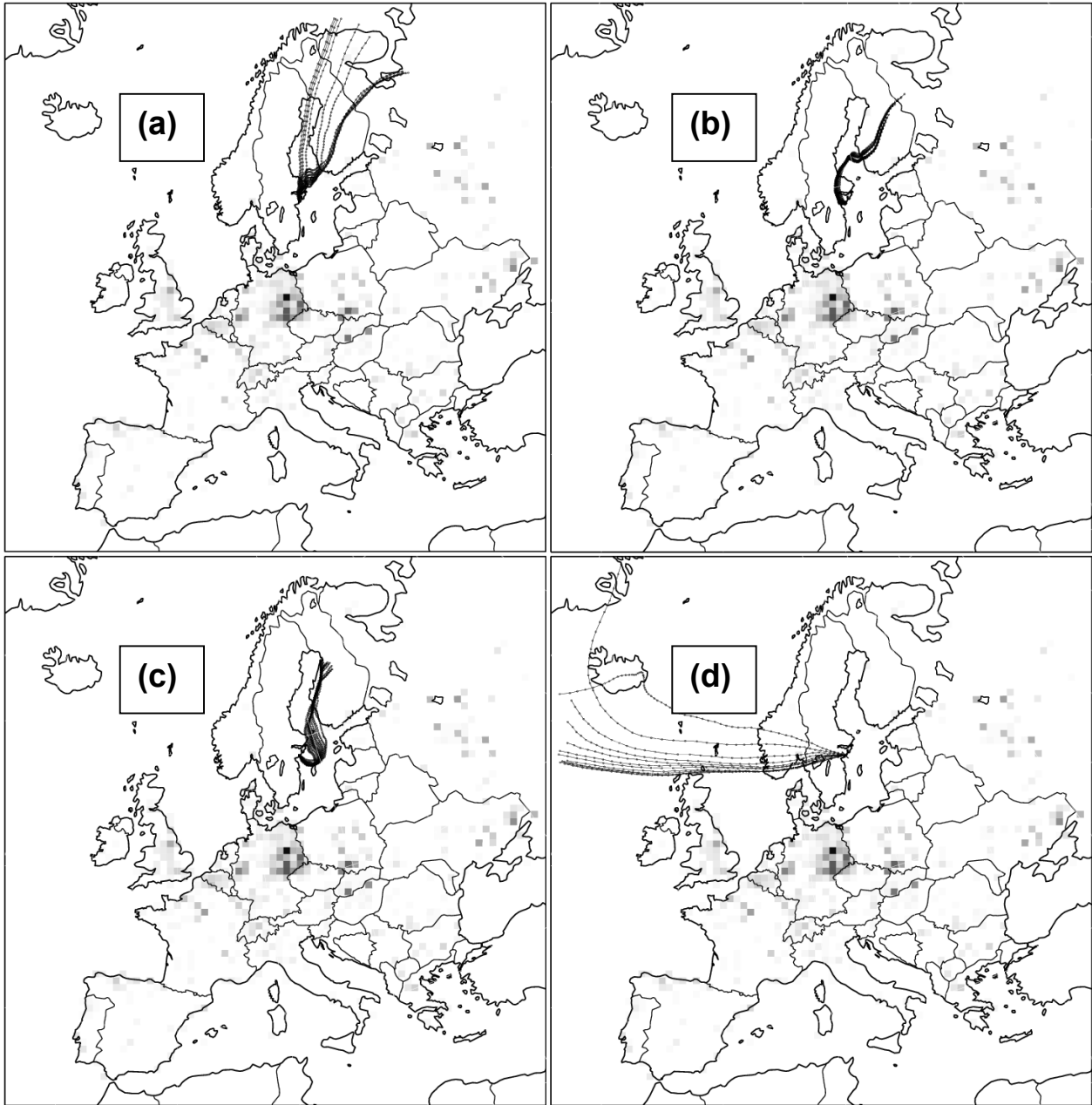


FIGURE 17: 72 hours backward trajectories Aspveten

(a) March 22 1997

(b) March 23 1997

(c) March 24 1997

(d) March 28 1997

#### 4.4 Atmospheric Input of Heavy Metals to the Baltic Sea

Concern over the quality of marine waters and biota has highlighted the numerous geochemical pathways for the transfer of terrestrial and anthropogenically derived heavy metals from their sources to the marine environment. Traditionally these pathways have been assumed to be riverine, but there is much evidence that atmospheric inputs contribute significantly to marine areas [Duce et al., 1991] and may be comparable to those of riverine inputs for the Baltic Sea as an almost totally enclosed water body [HELCOM, 1996; HELCOM, 1998].

Despite the fact that the metals in question exist almost solely in particulate form (with the exception of mercury) there are still massive problems in making reliable estimates of atmospheric input. These problems include uncertainties in both wet and dry deposition flux contributions to the overall atmospheric input due substantially to inadequate knowledge of pollutant concentration fields over the sea area, together with a poorly defined precipitation field, and in quantification of the dry deposition velocity for particulate material to the sea surface.

Estimates of atmospheric input of heavy metals to the Baltic Sea are either based on extrapolations from measurements made on the edges of the surrounding landmasses or on applications of numerical simulation models. Most recent results for lead and cadmium achieved in the framework of the EU MAST III Baltic Sea System Study (BASYS) do suggest that the atmospheric input for both metals has significantly decreased during the past 10-15 years but that the atmospheric input still exceeds the riverine input by about 50% [VI]. Compared to extrapolated measurements model results show a tendency for underprediction of annual inputs, which may be due to inaccurate emission data bases used with the model calculations [VII].

Recent progress in understanding physico-chemical processes of atmospheric mercury and the availability of European emission data bases for different mercury species has permitted to investigate mercury input to the Baltic Sea by means of the comprehensive Eulerian model ADOM described in the previous chapters. Model runs were performed for two episodes i.e. for a BASYS summer network study during June-August 1997 and for a winter network study during February-March 1998. Typical results in terms of monthly average concentrations and deposition fluxes inside and around the Baltic Sea receptor area used with the model are depicted in FIGURE 18. The area within the irregular frame consists of grid cells which cover the Baltic Sea and for which sea area weighted average concentrations and deposition fluxes have been calculated for two scenarios:

1. Using the UBA-TNO inventory for anthropogenic mercury emissions in Europe compiled for the reference year 1990 [Berdowski et al., 1997].
2. Cutting off the European anthropogenic emissions and calculating deposition fluxes to the Baltic Sea caused by global mercury background concentrations by using a typical European background concentration of  $1.5 \text{ ng m}^{-3}$  for  $\text{Hg}^0$  as a boundary condition for the model runs.

TABLE 3 and 4 summarize the results in terms of deposition fluxes of individual mercury species and the total input rates for both episodes and both scenarios. Deposition fluxes and hence input rates to the Baltic Sea are higher in winter due to more intense transport from the main emission areas and from the western inflow boundary of the model domain as well as lower mixing layer

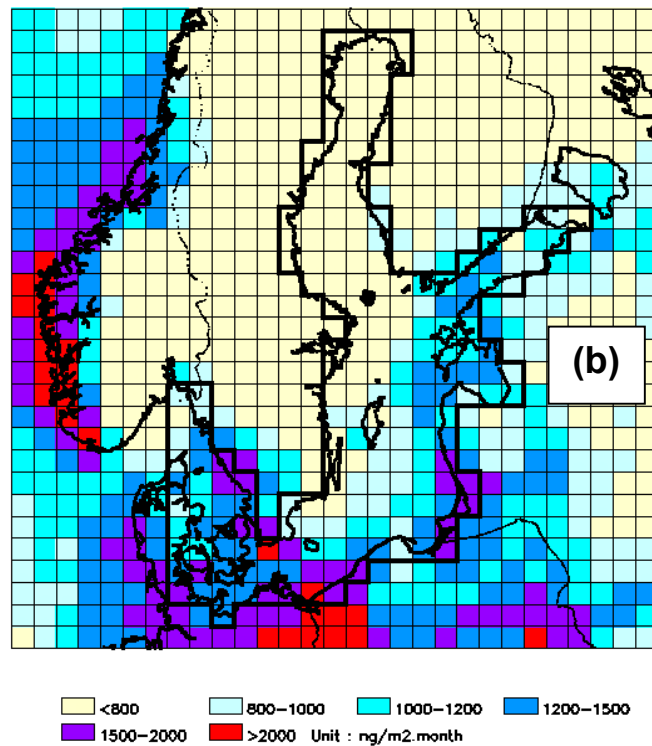
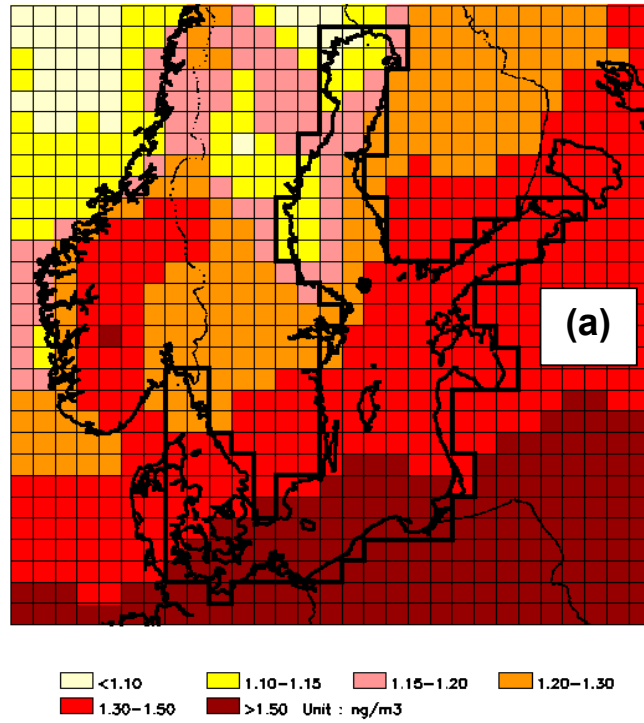


FIGURE 18. Model predicted  
 (a) monthly average concentrations of elemental mercury ( $\text{Hg}^0$ ) in air  
 (b) monthly total deposition flux (dry + wet) of mercury.  
 Baltic Sea-February 1998

TABLE 3. Model predicted deposition fluxes of mercury species to the Baltic Sea.

## Daily dry and wet deposition fluxes with anthropogenic emissions in Europe

	summer network study 1997		winter network study 1998	
	ng m <sup>-2</sup> d <sup>-1</sup>	kg d <sup>-1</sup>	ng m <sup>-2</sup> d <sup>-1</sup>	kg d <sup>-1</sup>
dry Hg <sup>0</sup>	0.00	0.00	0.00	0.00
dry HgCl <sub>2</sub>	1.16	0.48	1.05	0.43
dry Hg(part.)	1.78	0.74	0.41	0.17
dry HgO	1.82	0.76	1.39	0.58
dry total	4.76	1.98	2.85	1.18
wet Hg (diss.)	4.24	1.76	7.05	2.92
wet Hg (part.)	7.82	3.24	15.80	6.54
wet total	12.06	5.00	22.85	9.46
dry + wet total	16.82	6.98	25.70	10.64

Daily dry and wet deposition fluxes without anthropogenic emissions in Europe  
(contribution from global background)

	summer network study 1997		winter network study 1998	
	ng m <sup>-2</sup> d <sup>-1</sup>	kg d <sup>-1</sup>	ng m <sup>-2</sup> d <sup>-1</sup>	kg d <sup>-1</sup>
dry Hg <sup>0</sup>	0.00	0.00	0.00	0.00
dry HgCl <sub>2</sub>	0.07	0.03	0.00	0.00
dry Hg(part.)	0.10	0.04	0.36	0.15
dry HgO	1.07	0.44	0.90	0.37
dry total	1.24	0.51	1.26	0.52
wet Hg (diss.)	1.85	0.77	3.45	1.43
wet Hg (part.)	4.61	1.91	5.13	2.13
wet total	6.46	2.68	8.58	3.56
dry + wet total	7.60	3.19	9.84	4.08

TABLE 4. Model predicted atmospheric input rates of mercury to the Baltic Sea.

Monthly and annual input rates with anthropogenic emissions in Europe		
	summer network study 1997	winter network study 1998
extrapolated monthly input rates	212 kg / month	324 kg / month
extrapolated annual input rate (average of 1997 and 1998)	<b>3216 kg / year</b>	
Monthly and annual input rates without anthropogenic emissions in Europe (contribution from global background)		
	summer network study 1997	winter network study 1998
extrapolated monthly input rates	97 kg / month (46%)	124 kg / month (38%)
extrapolated annual input rate (average of 1997 and 1998)	<b>1326 kg / year (41%)</b>	

heights and more precipitation. In all cases wet deposition is the main contributor to the total input. The reason for the relatively low dry deposition is twofold: Firstly, there is no experimental evidence for dry deposition of  $\text{Hg}^0$  over sea surfaces and is hence assumed to be zero in the model and secondly, the dry deposition of the other species is minor over the sea, because they are already effectively dry deposited over land close to the land-based sources of those species.

An interesting feature in TABLE 4 is the relative high contribution from global mercury background concentrations to the total input to the Baltic Sea in the range of 38-46%. Conversely, current anthropogenic emissions in Europe only account for about 60% of atmospheric mercury load of the Baltic Sea with a decreasing portion towards the northern parts of that sea area, since the density of anthropogenic emissions is greater around the southern Baltic Sea. This indicates that emission reductions of land-based mercury sources in Europe, which is the main target of the UN-ECE CLRTAP Convention and HELCOM, would only have a

TABLE 5: Estimates of annual atmospheric mercury input rates to the Baltic Sea.

<b>annual input rate</b> [tonnes per year]	<b>reference year(s)</b>	<b>method</b>	<b>reference</b>
<b>6</b>	1980	extrapolation from observations at coastal sites	GESAMP, 1989
<b>11.3</b>	1980	extrapolation from observations at coastal sites	Lithner et al., 1990
<b>6-13</b>	1987-1988	model calculation	Petersen et al., 1995 [I]
<b>5.5</b>	1994-1996	model calculation	Bartnicki et al., 1998
<b>5</b>	1997-1998	model calculation	Ilyin et al., 2000
<b>3.2</b>	1997-1998	model calculation	this study

limited effect on the atmospheric load of the Baltic Sea particularly its the northern parts. Knowledge of global or at least hemispherical emissions and their effects on boundary conditions (i. e. upwind time dependent vertical concentration profiles) is of similar importance. Since measurements, particularly aloft, are scarce, uncertainties are believed to be associated with the boundary conditions mentioned above and a multiscale modelling approach consisting of a global and a continental scale model is needed to reduce those uncertainties.

In TABLE 5 estimates of integrated mercury loading to the Baltic Sea from other investigators are compared with results from this study. Overall, annual input rates span more than a fourfold range from about 3 to 13 tonnes per year most probably due to uncertainties in the estimated input rates and to changes in European mercury emissions during the last two decades. The discrepancy in the two 1980 estimates based on extrapolated measurements at coastal sites is rather large and may be attributed to both uncertainties in the quality of measurement data at that time and to insufficient extrapolation methods. The model predicted results in TABLE 5 show some evidence of decreasing inputs after the political changes of the 1990s in Central and Eastern Europe, which brought a sharp decline of industrial activities, followed by significant restructuring of the economy and industry. The resulting mercury emission reductions from 730 tonnes per year in the late 80s [Axenfeld et al., 1991] to 460 tonnes per year in the early 90s [Berdowski et al., 1997] are clearly reflected in the corresponding input rates of Petersen et al., 1995 and of this study. The relative wide range of the 1987-1988 estimate was caused by a

certain range of speciation percentages of emissions, which had to be assumed in the model since knowledge of mercury speciation was more limited at that time. The results from model simulations performed by Bartnicki et al., 1998, and by Ilyin et al., 2001, are similar, which is not surprising since they are based on the same model approach. Comparing these results with the result of this study, the difference is rather large and requires resolution. The anthropogenic emission inventory and the chemistry schemes used in the models is either identical or very similar and cannot account for the differences. However, the different results are explicable by the treatment of natural emissions and reemissions, which are implemented into the model approach of Bartnicki and Ilyin in a simple and uncertain way. In this study, these processes are not incorporated in the current version of the model since surface/atmosphere exchange terms for mercury over land and seawater are not well characterized for Central and Northern Europe and this requires more work so that models can be parameterized with more confidence.



## 5. SUMMARY AND CONCLUSIONS

The main objective of activities described in this work was to develop and test numerical simulation models with capabilities to quantify atmospheric transboundary fluxes of heavy metals over Europe in order to provide scientific support for European environmental protection conventions by either

- applying models to assess long-range transport of heavy metals over Europe with subsequent deposition into aquatic and terrestrial ecosystems

or

- transferring advanced models or parts of them to institutions directly involved in the scientific work of the conventions (e.g. the EMEP Meteorological Synthesizing Centers in the framework of the UN-ECE Protocol on Heavy Metals and the Arctic Monitoring and Assessment Programme AMAP) for direct use or for implementation into their existing operational models.

Examples for both model applications and model transfers discussed in the previous chapters and in some of the ten annex papers are:

- Lagrangian model applications for the European marine environment protection conventions OSPAR (North Sea, North East Atlantic) and HELCOM (Baltic Sea) to assess the atmospheric input of mercury [Petersen, 1992b] and of lead, cadmium zinc and arsenic [Petersen and Krueger, 1993] into the Convention Waters.
- Lagrangian model applications for the Scientific Council “Global Environmental Changes” of the German Federal Government to calculate concentration and deposition patterns of acidifying pollutants and heavy metals over Europe [Krueger and Petersen, 1993].
- Eulerian model applications for the EU E&C and ELOISE Study MOE to calculate concentration and deposition patterns of mercury species over Europe [Munthe, 2001, **III**, **VIII**].
- Eulerian model applications for the EU MAST III Regional Seas Study BASYS to simulate atmospheric deposition fluxes of lead, cadmium and zinc into the Baltic Sea ecosystem by one-way nesting with the mesoscale model HILATAR of the Finnish Meteorological Institute (FMI) [**VII**] and by comparing model results with measurement based estimates of the Baltic Sea Research Institute Warnemünde (IOW) [**VI**].
- Selection of the mercury version of the Eulerian model as one of the reference models in the upcoming EU Air Quality Directive for mercury [European Commission, 2001].
- Transfer of relative simple mercury chemistry schemes adequate for Lagrangian models to the US-EPA [Bullock et al., 1997] and AMAP [Bartnicki et al., 1998]
- Transfer of complex state-of-science mercury chemistry schemes adequate for comprehensive Eulerian models to the EMEP MSC-E for use in their operational model [Ryaboshapko et al.,

1999], the Meteorological Service of Canada [MSC] for use in their global mercury model [Dastoor and Larocque, 2002] and the Danish National Environmental Research Institute (NERI) for their mercury model of the Northern hemisphere [Christensen, 2001].

- Participation into international model intercomparison studies for lead [Sofiev et al., 1996], cadmium [Gusev et al., 1998] and mercury [Ryaboshapko et al., 2001] initiated by the UN-ECE Convention and organised by the EMEP Meteorological Synthesizing Centre East.

These model developments and applications comprise both relatively simple Lagrangian and comprehensive Eulerian approaches with an established record of published investigations, which are either listed in the annex or mentioned in the reference list. This study is focusing on the most recent heavy metals version of the Eulerian model system ADOM with the Tropospheric Chemistry Module (TCM) as its major component, which is considered to be a state-of-the-science model over the past several years. The evaluation of the model performance led to four main issues provided below:

1. In general, the model system has capabilities to describe the atmospheric pathways of transport, transformations and deposition of heavy metals from their way from emissions to deposition over spatial scales from about hundred kilometer to continental with a basic time step of one hour. These capabilities can be used (and are used now) for making future predictions of heavy metals deposition patterns as well as for optimizing control measures and for estimating how a specific region is affected by heavy metals emissions in other areas.
2. Sensitivity studies conducted with the Tropospheric Chemistry Module (TCM) allowed for gaining scientific insights into mercury transport, chemical transformations and deposition processes which cannot be obtained through field measurements or experiments in the laboratory. TCM predictions of mercury concentrations in rainwater compare satisfactorily with observations thus indicating that the TCM is based on an adequate parameterization of atmospheric mercury processes.
3. Modelled hourly average concentrations of elemental mercury in air were shown to compare satisfactorily with observations from stations in Germany and Sweden. Coinciding peaks of observed and calculated concentrations at the two German stations indicate, that the emission data base used with the model calculations is based on realistic estimates of emission peaks in the main source areas of Central Europe. However, the model tends to underestimate observations at the two Swedish stations, most probably due to exclusions of processes e.g. air-soil and air-water exchange that may influence the atmospheric concentration level of mercury. These processes have not been explicitly treated in the model due to significant gaps in our current understanding and knowledge.
4. Results from measurements and model simulations to quantify the cumulative deposition of heavy metals to the Baltic Sea do suggest that the atmospheric input has significantly decreased during the last 10-15 years, but the atmosphere is still the dominating pathway for the heavy metals loading of the Baltic Sea. Model simulations for mercury performed in this study show a contribution from global background concentrations in the order of 40% of the total atmospheric input. This indicates that emission reductions in Europe would only have a limited effect on the reduction of the total mercury load of the Baltic Sea, and global scale models are clearly needed to quantify the contribution from global background concentrations

more accurately. The results from this study are believed to be the best estimates currently available when only emissions from European land based sources are taken into account but as already indicated above, contributions from natural emissions and re-emissions are still missing and have to be implemented into the model when better knowledge on these processes becomes available.

Overall, the present development level of the ADOM model for heavy metals is such, that it can provide key information needed to quantify the relationship between anthropogenic emissions and deposition fluxes of heavy metals to remote ecosystems and that its application within environmental protection conventions mentioned above is fully justified. The model will be extended and developed further according to advancements in the knowledge of atmospheric processes of heavy metals and persistent organic pollutants (POPs) to ensure that it maintains its capabilities to address effectively the scientific and political questions that may arise over the next decade. Some suggestions for model improvements and extensions are provided below, but certainly not limited to:

- Emission data bases: Emissions are always a potential source of uncertainty in the modelling of atmospheric pollution, but in case of mercury the uncertainties in the total amount and spatial and temporal distribution of emissions are further complicated by the importance of mercury speciation that arises from the vastly different removal rates for the principal emitted species  $\text{Hg}^0$ ,  $\text{HgCl}_2$  and  $\text{Hg}(\text{part.})$ . Because  $\text{HgCl}_2$  and  $\text{Hg}(\text{part.})$  are deposited so efficiently, knowledge of the effective emission heights of these species is also important, as the dry deposition pattern for a surface source is greater in magnitude and shorter in distance than that of an elevated source, which may be decoupled from surface removal processes during stable nocturnal conditions.
- Up and downscale links to global scale models: New links with other areas of modelling, including scale and media, are envisioned. It is planned that information from ADOM applications and from global and hemispheric modelling applications will be bridged. Because ADOM and in particular the mercury version offers the state of science to simulate atmospheric processes of mercury species as realistic as possible, ADOM output can be used to benchmark or examine the parametric basis of process formulation in global and hemispheric models. From a downscale perspective, global model output can be used to improve or enhance the initial and boundary concentrations in ADOM simulations.
- Ecosystem modelling: Efforts to combine environmental modelling techniques to encompass an entire ecosystem is needed to address heavy metals and POPs cycle modelling, which includes pathways through the atmosphere, water bodies and soil. With this ecosystem approach, air quality issues can be studied in combination with other aspects of environmental health such as adverse indirect human exposure from bioaccumulation through the food chain.

Maintaining the extended model system to use emerging computing capabilities and transferring that capabilities to the scientific community and environmental decision makers will continue to be the focus of the efforts described in this study.



## 6. ACKNOWLEDGEMENTS

This work was performed during my ongoing lecturing at the University of Lüneburg, Department of Environmental Sciences. Special thanks to the Dean of the Department Prof. Dr. Wolfgang Ruck and his predecessor Prof. Dr. Werner Härdtle, who have initiated this work.

Also, this work summarizes more than 15 years of activities in air pollution modelling at the GKSS Research Center Geesthacht at the former Institute of Physics and at its successor, the Institute for Coastal Research / System Analysis and Modelling. I wish to acknowledge two of the directors of these Institutes, Prof. Dr. Hartmut Grassl (1984-1988) and Prof. Dr. Hans von Storch (since 1996), respectively, for providing me with the opportunity for continuous work in this field and for all their encouragement and support.

I want to express my gratitude to various scientific institutions on national and international level for their long-lasting fruitful co-operation, e.g. the German Federal Environmental Agency (UBA), the Swedish Institute for Environmental Research (IVL), the Norwegian Institute for Air Research (NILU), the Ontario Ministry of the Environment (OME), the Meteorological Service of Canada (MSC) and the EMEP Meteorological Synthesizing Centers East and West, just to name a few.

This research was supported through various grants and contracts from the European Commission, the Nordic Council of Ministers (NMR), the German Federal Environmental Agency (UBA) and in the framework of the German/Canadian Agreement on Co-operation in Science and Technology.

I am deeply indebted to my late parents for their fostering and education, especially to my mother during her last and difficult times.



## 7. REFERENCES

- Axenfeld F., Münch J. and Pacyna J. (1991)  
 Europäische Test-Emissionsdatenbasis von Quecksilberkomponenten für Modellrechnungen.  
 Umweltforschungsplan des Bundesministers für Umwelt, Naturschutz Reaktorsicherheit-  
 Luftreinhaltung- 10402726.
- Bartnicki J., Barrett K., Tsyro S., Erdmann L., Gusev A., Dutchak S., Pekar M., Lükeville A. and  
 Krognos T. (1998)  
 Atmospheric supply of nitrogen, lead, cadmium, mercury and lindane to the Baltic Sea.  
 EMEP Centres Joint Note for HELCOM. EMEP MSC-W Note 3/98.
- Bartnicki J. (1998)  
 Heavy Metals Eulerian Transport Model HMET. Model description and results.  
 Norwegian Meteorological Institute (DNMI), Oslo, Norway, Research Report No. 65.
- Berdowski J., Baas J., Bloos J.J., Visschedijk A.J.H., Zandveld P.Y.J. and Bousardt, F.L.M.  
 (1997)  
 The European atmospheric emission inventory of heavy metals and persistent organic  
 pollutants.  
 UBA/TNO, June 1997, CD-ROM.
- Berg T., Hjellbrekke A.G. and Skelmoen J. E. (1996)  
 Heavy metals and POPs within the ECE region  
 Norwegian Institute for Air Research, Postboks 100, N-2007 Kjeller, Norway.  
 EMEP CCC Report 8/96.
- Berg T., Hjellbrekke A.G. and Ritter N. (1997)  
 Heavy metals and POPs within the ECE region. Additional data.  
 Norwegian Institute for Air Research, Postboks 100, N-2007 Kjeller, Norway.  
 EMEP CCC Report 9/97.
- Berg T. and Hjellbrekke A.G. (1998)  
 Heavy metals and POPs within the ECE region. Supplementary data for 19989-1996.  
 Norwegian Institute for Air Research, Postboks 100, N-2007 Kjeller, Norway.  
 EMEP CCC Report 7/98.
- Bergan T., Gallardo L. and Rodhe H. (1999)  
 Mercury in the global troposphere: a three-dimensional study.  
*Atmospheric Environment* **33**, 1575-1585.
- Binkowski F.S., Chang J.S., McHenry J.N., Reynolds S.D. and Cohn R. D. (1991)  
 Estimation of the annual contribution of US sulfur emissions to Canadian acidic deposition  
 and vice versa.  
 In: Air Pollution Modelling and its Application VIII, Edited by H. van Dop and D.G. Steyn,  
 Plenum Press, New York, 1991.

- Bullock O. R., Benjey, W. G. and Keating M. H. (1997)  
 The modelling of regional scale atmospheric mercury transport and deposition using RELMAP.  
 In: Atmospheric Deposition of Contaminants to the Great Lakes and Coastal Water, edited by J. E. Baker, 323-347, Society of Environmental Toxicology and Chemistry, Pensacola, Fla.
- Bullock O. R. (2000)  
 Modelling assessment of transport and deposition patterns of anthropogenic mercury air emissions in the United States and Canada.  
*Science of the Total Environment* **259**, 145-157.
- Chang J.S., Brost R.A., Isaksen I.S.A., Madronich S., Middleton P., Stockwell P. R. and Walcek C. J. (1987)  
 A three-dimensional Eulerian acid deposition model: physical concepts and formulation.  
*Journal of Geophysical Research* **92**, 14,681-14,700.
- Christensen J. (2001)  
 Modelling of mercury with the Danish Eulerian hemispheric model.  
 Proceedings of the EUROTRAC-2 Mercury and POP (MEPOP) Workshop, Roskilde, Denmark, September 10-12, 2001.
- Dastoor A. P. and Larocque Y. (2002)  
 Development of a comprehensive multi-scale global atmospheric mercury model.  
 Submitted to *Atmospheric Environment*.
- Dennis R. L., Byun D. W., Novak J. H., Galluppi K. L., Coats C. J. and Vouk M. A. (1996)  
 The next generation of integrated air quality modeling: EPA's Models-3.  
*Atmospheric Environment* **30**, 1925-1938.
- Duce R. A., Liss P. S., Merrill J. T., Buat-Menard P., Hicks B. B., Miller J.M., Prospero J. M., Arimoto R., Church T. M., Ellis W., Galloway J. M., Hansen L., Jickels T. D., Knap A. H., Reinhardt K.-H., Schneider B., Soudine A., Tokos J. J., Tsunogai S., Wollast R. and Zhou M. (1991)  
 The input of atmospheric trace species to the world ocean.  
*Global Biogeochemical Cycles* **5**, 193-253.
- Ebel A., Elbern H., Feldmann H., Jacobs H.J., Kessler C., Memmesheimer M., Oberreuter A. and Piekorz G. (1997)  
 Air Pollution Studies with the EURAD model system (3): EURAD –European Air Pollution Dispersion Model System.  
 Mitteilungen aus dem Institut für Geophysik und Meteorologie, A. Ebel, M. Kerschgens, F. M. Neubauer, eds., Nr. 120, Cologne.

- Ebinghaus R., Kock H. H., Jennings S.G., McCartin P. and Orren M.J. (1995)  
Measurements of atmospheric mercury concentrations in northwestern and central Europe-  
Comparison of experimental data and model results.  
*Atmospheric Environment* **29**, 3333-3344.
- EPA (1996)  
Mercury study report to congress: SAB review draft.  
Document No. EPA-452/R-96-001, U.S. Environmental Protection Agency, Research  
Triangle Park, NC 27711.
- EPA (1999)  
Science algorithms of the EPA Models-3 Community Multiscale Air Quality (CMAQ)  
Modelling System  
Document No. EPA/600/R-99/030, U.S. Environmental Protection Agency, Research  
Triangle Park, NC 27711.
- ERT (1984)  
ADOM/TADAP Model Development Program, Vols. 1-8.  
ERT No. P-B980-535, July 1984. Environmental Research and Technology Inc., Newbury  
Park, California 91230.
- European Commission (2001)  
Ambient Air Pollution by Mercury (Hg) – Position Paper.  
Position paper in preparation of the Air Quality Directive for mercury of the European  
Commission. Prepared by the Working Group on Mercury, October 2001.  
Office for the Official Publications of the European Communities, L-2985 Luxembourg.  
(<http://europa.eu.int/comm/environment/air/background.htm>)
- Georgii, H. W., Perseke C. and Rohbock E. (1983)  
Wet and dry deposition of acidic and heavy metal components in the Federal Republic of  
Germany.  
In: Acid Deposition (edited by S. Beilke and A. Elshout), 142-148, D. Reidel, Dordrecht, the  
Netherlands.
- GESAMP (1989)  
The atmospheric input of trace species to the world ocean.  
IMO/FAO/UNESCO/WMO/IAEA/UN/UNEP.  
World Meteorological Organisation Reports and Studies 38.
- Gusev A., Ilyin I., Petersen G., van Pul A. and Syrakov D. (1998)  
Long-range transport model intercomparison study for cadmium. Prepared by Meteorological  
Synthesizing Centre-East/EMEP in co-operation with advisory expert group.  
EMEP Meteorological Synthesizing Center-East, EMEP/MSC-E Report 6/99.
- HELCOM (1996)  
Third periodic assessment of the marine environment of the Baltic Sea.  
Baltic Sea Environment Proceedings No. 64B.

HELCOM (1998)

The third Baltic Sea pollution load compilation (PLC-3).  
Baltic Sea Environment Proceedings No. 70.

Ilyin I., Ryaboshapko A., Travnikov O., Berg T., Hjellbrekke A. G. and Larsen R. (2000)  
Heavy Metal Transboundary Air Pollution in Europe: Monitoring and Modelling Results for 1997 and 1998.  
EMEP Meteorological Synthesizing Center-East, EMEP Chemical Co-ordinating Centre.  
EMEP Report 3/2000.

Ilyin I., Ryaboshapko A., Afinogenova O., Berg T. and Hjellbrekke A. G. (2001)  
Evaluation of Transboundary Transport of Heavy Metals in 1999. Trend Analysis.  
EMEP Meteorological Synthesizing Center-East, EMEP Chemical Co-ordinating Centre.  
EMEP Report 3/2001.

Iversen T. (1993)

Modelled and measured transboundary acidifying air pollution in Europe – verification and trends.  
*Atmospheric Environment* **27A**, 889-920.

Karamchandani P. and Venkatram A. (1992)

The role of non-precipitating clouds in producing ambient sulfate during summer: Results from simulations with the Acid Deposition and Oxidants Model (ADOM).  
*Atmospheric Environment* **26A**, 1041-1052.

Krüger O. and Petersen G. (1993)

Europaweite Deposition von Schwefel-und Stickstoffverbindungen und Schwermetallen im EMEP-Gitter.  
Im Auftrage des Wissenschaftlichen Beirates der Bundesregierung Globale Umweltveränderungen  
Externer Bericht GKSS 93/E/105 (in German).

Krüger O. (1996)

Atmospheric deposition of heavy metals to North European marginal seas: scenarios and trend for lead.  
*GeoJournal* **39.2**, 117-131.

Lee D. S., Dollard G. J. and Pepler S. (1998)

Gas-phase mercury in the atmosphere of the United Kingdom.  
*Atmospheric Environment* **32**, 855-864.

Lee D. S., Nemetz E., Fowler D. and Kingdon R.B. (2001)

Modelling atmospheric mercury transport and deposition across Europe and the UK.  
*Atmospheric Environment* **35**, 5455-5466.

- Lithner G. H., Borg H., Grimas H., Göthberg G., Neumann G. and Wradhe H. (1990)  
Estimating the load of metals to the Baltic Sea.  
In: Royal Swedish Academy of Science, HELCOM (eds.): Current Status of the Baltic Sea.  
*Ambio Special Report 7*, 7-9.
- Lu J. Y., Schroeder W. H., Barrie L. A., Steffen A., Welch H. E., Martin K., Lyle L., Hunt R. V.,  
Boila G. and Richter A. (2001)  
Magnification of atmospheric mercury deposition to polar regions in springtime: the link to  
tropospheric ozone depletion chemistry.  
*Geophysical Research Letters* **28** NO 17, 3219-3222.
- Memmesheimer M., Hass H., Tipke J. and Ebel A. (1995)  
Modelling of episodic emission data for Europe with the EURAD emission model (EEM).  
In: Regional Photochemical Measurement and Modelling Studies, A.J. Ranzeri, P.A.  
Solomon (eds), Vol 2, pp. 495-499, Air & Waste Management Association, Pittsburgh.
- Munthe J. (2001)  
Mercury Species over Europe. Relative Importance of Depositional Methylmercury Fluxes to  
Various Ecosystems (MOE).  
Contract ENV4-CT97-0595 of the European Commission, Directorate General XII Science,  
Research and Development, Environment and Climate Programme 1994-1998. Final Report.
- Nriagu J. (1990)  
A silent epidemic of environmental metal poisoning?  
*Environmental Pollution* **50**, 139-161.
- NTIS (1991)  
The EMEFS Model Evaluation: An Interim Report  
National Technical Information Service, U.S. Department of Commerce, 5285 Port Royal  
Road, Springfield, VA 22161.
- Pacyna E.G., Pacyna J.M. and Pirrone N. (2001)  
European emissions of atmospheric mercury from anthropogenic sources in 1995.  
*Atmospheric Environment* **35**, 2987-2996.
- Pai P., Karamchandani P. and Seigneur C. (1997)  
Simulation of the regional atmospheric transport and fate of mercury using a comprehensive  
Eulerian model.  
*Atmospheric Environment* **31**, 2717-2732.
- Pai P., Karamchandani P., Seigneur C. and Allan M.A. (1999)  
Sensitivity of simulated atmospheric mercury concentrations and deposition to model input  
parameters.  
*Journal of Geophysical Research* **104**, 13855-13868.

Petersen G. (1991)

Atmospheric Input of Mercury to the North Sea.  
Working Document for the Ninth Meeting of the Working Group on the Atmospheric Input of Pollutants to Convention Waters (PARCOM-ATMOS 9/13/1).  
Paris Commission for the Prevention of Pollution of the North Sea from Land-based Sources.

Petersen G. (1992a)

Atmospheric Input of Mercury to the Baltic Sea.  
Working Document for the Ninth Meeting of the Group of Experts on Airborne Pollution of the Baltic Sea Area (HELCOM-EGAP 9/2/5).  
Helsinki Commission - Baltic Marine Environment Protection Commission.

Petersen G. (1992b)

Belastung von Nord- und Ostsee durch ökologisch gefährliche Stoffe am Beispiel atmosphärischer Quecksilberverbindungen.  
Umweltforschungsplan des Bundesministeriums für Umwelt, Naturschutz und Reaktorsicherheit -Luftreinhalteung-104 02 726 (in German).

Petersen G., Krüger O. (1993)

Untersuchung und Bewertung des Schadstoffeintrags über die Atmosphäre im Rahmen von PARCOM (Nordsee) und HELCOM (Ostsee). Teilvorhaben: Modellierung des grossräumigen Transports von Spurenmetallen.  
Umweltforschungsplan des Bundesministeriums für Umwelt, Naturschutz und Reaktorsicherheit -Luftreinhalteung -104 02 583 (in German).

Petersen G. (1993)

Modelling the Atmospheric Transport and Deposition of Heavy Metals - A Review of Results from Models Applied in Europe.  
J. M. Pacyna, E. Voldner, G. J. Keeler, G. Evans (eds.): Proceedings of the The First Workshop on Emissions and Modelling of Atmospheric Transport of Persistent Organic Pollutants and Heavy Metals. EMEP/CCC-Report 7/93, pp. 261-279. Norwegian Institute for Air Research, P. O. Box 64, N-2001 Lillestrom, Norway, October 1993.

Petersen G. and Iverfeldt A. (1994)

Numerical Modelling of Atmospheric Transport and Deposition of Heavy Metals - A Review of Results from Models Applied in Europe.  
Background Document of the EMEP Workshop on European Monitoring, Modelling and Assessment of Heavy Metals and Persistent Organic Pollutants. Rijksinstituut voor Volksgezondheid en Milieuhygiene, P. O. Box 1, NL-3720 BA Bilthoven, the Netherlands, pp. 23-31.

Petersen G., Iverfeldt A. and Munthe J. (1995)

Atmospheric mercury species over central and northern Europe. Model calculations and comparison with observations from the Nordic air and precipitation network for 1987 and 1988.  
*Atmospheric Environment* **29**, 47-67.

- Petersen G., Schmolke S.R. and Pacyna J.M. (2002)  
Response of mercury concentrations in air to emission reduction in Europe: a model study.  
Submitted to *Atmospheric Environment*.
- Pirrone N. (1998)  
Modelling the dynamics of atmospheric mercury over the Mediterranean Sea: The MAMCS project.  
*Journal of Aerosol Science* **29**, 1155-1156.
- Pirrone N., Hedgecock I.M., and Forlano L. (2000)  
Role of the ambient aerosol in the atmospheric processing of semi-volatile contaminants: A parameterized numerical model (GASPAR).  
*Journal of Geophysical Research* **105**, D8, 9773-9790.
- Ryaboshapko A., Ilyin I., Gusev A. and Afinogenova O. (1998)  
Mercury in the atmosphere of Europe: Concentrations, deposition patterns, transboundary fluxes.  
EMEP Meteorological Synthesizing Center-East, EMEP/MSC-E Report 7/98.
- Ryaboshapko A., Ilyin I., Gusev A., Afinogenova O., Berg T. and Hjellbrekke (1999)  
Monitoring and modelling of lead, cadmium and mercury transboundary transport in the atmosphere of Europe.  
Joint Report of EMEP Centers MSC-E and CCC.  
MSC-E Report 1/99.
- Ryaboshapko A., Ilyin I., Bullock R., Ebinghaus R., Lohman K., Munthe J., Petersen G., Seigneur C. and Wängberg I. (2001)  
Intercomparison Study of Numerical Models for Long-Range Transport of Mercury. Stage I. Comparison of chemical modules for mercury transformations in a cloud/fog environment.  
EMEP Meteorological Synthesizing Center-East, EMEP/MSC-E Technical Report 2/2001.
- Schmolke S. R., Schroeder W. H., Kock H. H., Schneeberger D., Munthe J. and Ebinghaus R. (1999)  
Simultaneous measurements of total gaseous mercury at four sites on a 800 km transect: distribution and short-time variability of total gaseous mercury over Central Europe.  
*Atmospheric Environment* **33**, 1725-1733.
- Schmolke S.R. and Petersen G. (2002)  
A comprehensive Eulerian modelling framework for airborne mercury species: model validation using observed data in Central and Northern Europe.  
Submitted to *Atmospheric Environment*.
- Schroeder W.H. and Lane D. A. (1988)  
The fate of toxic airborne pollutants.  
*Environmental Science and Technology* **22**, 240-246.

- Schroeder W.H. and Munthe J. (1998)  
Atmospheric mercury - an overview.  
*Atmospheric Environment* **32**, 809-822.
- Schroeder W.H. and Barrie L.A. (1998)  
Is mercury input to Polar ecosystems enhanced by springtime ozone depletion chemistry?,  
*IGACTivities Newsletter* of the International Global Atmospheric Chemistry Project, Issue  
No. 14, September 1998.
- Schroeder W.H., Anlauf K.G., Barrie L.A., Lu J.Y., Steffen A., Schneeberger D.R. and Berg T.  
(1998)  
Arctic springtime depletion of mercury.  
*NATURE* **394**, 331-332.
- Seigneur C. and Saxena P. (1990)  
Status of sub-regional and mesoscale models, Vol. 1: air quality models.  
Electric Power Research Institute, EPRI EN-6649.
- Seigneur C., Karamchandani P., Lohman K. and Vijayaraghavan K. (2001)  
Multiscale modeling of the atmospheric fate and transport of mercury.  
*Journal of Geophysical Research* **106**, NO. D21, 27795-27809.
- Shia, R.L., Seigneur C., Pai P., Ko M. and Sze N.D. (1999)  
Global simulation of atmospheric mercury concentrations and deposition fluxes.  
*Journal of Geophysical Research* **104**, 23747-23760.
- Simpson D., Altenstedt J. and Hjellbrekke A.G. (1998)  
The Lagrangian oxidant model: Status and multi-annual evaluation.  
In: EMEP MSC-W Report 2/98, Part I Transboundary photooxidant air pollution in Europe.  
Calculations of tropospheric ozone and comparison with observations.  
Norwegian Meteorological Institute, Oslo, Norway.
- Sofiev M., Maslyayev A. and Gusev A. (1996)  
Heavy metal model intercomparison. Methodology and results for Pb in 1990.  
EMEP Meteorological Synthesizing Center-East, EMEP/MSC-E Report 2/96.
- Stern R., Scherer B. and Schubert S. (1990)  
Modelling of photochemical oxidant formation in North-Western Europe with special  
emphasis on the non-linearity issue in the SO<sub>x</sub>/NO<sub>x</sub>/VOC system.  
EMEP Workshop on Progress in of Transport Modelling of Nitrogen Compounds, Potsdam,  
Germany, October 1990.
- Tuovinen J.P., Barrett K. and Styve H. (1994)  
Transboundary Acidifying Pollution in Europe: Calculated fields and budgets 1985-93.  
EMEP MSC-W Report 1/94. Norwegian Meteorological Institute, Oslo, Norway.

Venkatram A., Karamchandani P.K. and Misra P.K. (1988)  
Testing a comprehensive acid deposition model.  
*Atmospheric Environment* **22**, 737-747.

Venkatram A., Karamchandani P.K., Pai P. and Goldstein R. (1994)  
The development and application of a simplified ozone modelling system (SOMS).  
*Atmospheric Environment* **28**, 3665-3678.



## 8. LIST OF SYMBOLS, UNITS AND ACRONYMS

ADOM	Acid Deposition and Oxidants Model
AER	Atmospheric and Environmental Research Inc., San Ramon, CA, U.S.A.
AMAP	Arctic Monitoring and Assessment Programme
BASYS	Baltic Sea System Study
BAT	Best Available Technology
CAM	Chemistry of Atmospheric Mercury
CCC	Chemical Co-ordinating Centre of EMEP
CMAQ	Community Multi-Scale Air Quality Model
CMC	Canadian Meteorological Center
CIAM	Centre for Integrated Assessment Modelling of EMEP
DNMI	Det Norske Meteorologiske Institutt (The Norwegian Meteorological Institute)
EC	European Commission
E&C	Environment and Climate
ECE	Economic Commission for Europe
EEM	EURAD Emission Model
ELOISE	European Land Ocean Interaction Studies
EMEFS	Eulerian Model Evaluation and Field Study
EMEP	Co-operative Programme for Monitoring and Evaluation of the long-range Transmission of Air Pollutants in Europe
EPRI	Electric Power Research Institute
ERT	Environmental Research and Technology
EU	European Union
EURAD	European Air Pollution Dispersion Model System

EUROTRAC	The Eureka Project on the Transport and Chemical Transformation of Environmentally Relevant Trace Constituents in the Troposphere over Europe
FAO	Food and Agricultural Organisation
FMI	Finnish Meteorological Institute
GASPAR	Gas-Particle Partitioning Model
GESAMP	Joint Group of Experts on the Scientific Aspects of Marine Pollution
GLWQA	U.S./Canada Great Lakes Water Quality Agreement
HELCOM	Baltic Marine Environment Protection Commission (Helsinki Commission)
Hg <sup>0</sup>	elemental mercury
HgCl <sub>2</sub>	mercury chloride
Hg(part.)	mercury associated with particles
HgO	mercury oxide
Hg(dis.) <sub>aq</sub>	dissolved mercury species in the aqueous phase
Hg(ads.) <sub>aq</sub>	mercury species in the aqueous phase adsorbed on particles
Hg(tot.) <sub>aq</sub>	total mercury species in the aqueous phase (Hg(dis.) <sub>aq</sub> + Hg(ads.) <sub>aq</sub> )
HILATAR	High Resolution Limited Area Transport And Removal Model
HIRLAM	High Resolution Limited Area Weather Prediction Model
HMET	Heavy Metals Model
IAEA	International Atomic Energy Organisation
IGAC	International Global Atmospheric Chemistry
IOW	Institut für Ostseeforschung Warnemünde
IVL	Institutet för Vatten- och Luftvårdsforskning (Swedish Environmental Research Institute)
LRTAP	Long Range Transboundary Air Pollution
MAMCS	Mediterranean Atmospheric Mercury Cycling Study

MAST	Marine Science and Technology
MeHg	methyl mercury
MEPOP	Mercury and Persistent Organic Pollutants (EUROTRAC-2 subproject)
MSC	Meteorological Service of Canada
MSC-E	Meteorological Synthesizing Centre-East of EMEP
MSC-W	Meteorological Synthesizing Centre-West of EMEP
NERI	National Environmental Research Institute (Denmark)
NILU	Norsk Institutt for Luftforskning (Norwegian Institute for Air Research).
NMR	Nordisk Minister Rat
NTIS	National Technical Information Service
OSPAR	The Convention for the Protection of the Marine Environment of the North-East Atlantic (Oslo-Paris-Commission)
PM <sub>2.5</sub>	Particulate matter less than 2.5 µm in diameter
PM <sub>10</sub>	Particulate matter less than 10 µm in diameter
POPs	Persistent organic pollutants
RADM	Regional Acid Deposition Model
RELMAP	Regional Lagrangian Model of Air Pollution
RGM	Reactive Gaseous Mercury
SOMS	Simplified Ozone Modelling System
TADAP	Transport and Deposition of Acidifying Pollutants
TCM	Tropospheric Chemistry Module
TGM	Total Gaseous Mercury
TNO	Togepaste Naturwetenschapplike Ondersuchungen (The Netherlands Institute for Applied Research)
UBA	Umweltbundesamt (German Federal Environmental Agency)

UN-ECE United Nations - Economic Commission for Europe

US-EPA United States Environmental Protection Agency

WMO World Meteorological Organisation

## 9. LIST OF FIGURES

- FIGURE 1. Organisational Structure of the co-operative programme for monitoring and evaluation of the long range transmission of air pollutants in Europe (EMEP).
- FIGURE 2. Conceptual framework of the atmospheric emissions-to-deposition cycle for heavy metals. (adopted from Schroeder and Munthe (1998)).
- FIGURE 3. The ADOM model system for heavy metals.
- FIGURE 4. The ADOM model domain for (a) Europe and (b) North America.
- FIGURE 5. Schematic view of the Tropospheric Chemistry Module (TCM) for cumulus clouds.
- FIGURE 6. The mercury chemistry scheme used with the Tropospheric Chemistry Module (TCM)
- FIGURE 7. 48 hour time evolution of (a)  $\text{Hg}^0$  (b)  $\text{HgCl}_2$  (c)  $\text{Hg}(\text{part.})$  concentration profiles at the end of each 1 hour time step after cloud evaporation. ( $0.5 \mu\text{g m}^{-3}$  soot)
- FIGURE 8. 48 hour time evolution of (a)  $\text{Hg}^0$  (b)  $\text{HgCl}_2$  (c)  $\text{Hg}(\text{part.})$  concentration profiles at the end of each 1 hour time step after cloud evaporation. (no soot)
- FIGURE 9. 48 hour time evolution of  
 (a) average gas phase concentration in the cloud area after aqueous phase chemistry ( $0.5 \mu\text{g m}^{-3}$  soot)  
 (b) average gas phase concentration in the cloud area after aqueous phase chemistry (no soot)
- FIGURE 10. 48 hour time evolution of  
 (a) average aqueous phase concentration in the cloud area after aqueous phase chemistry ( $0.5 \mu\text{g m}^{-3}$  soot)  
 (b) average aqueous phase concentration in the cloud area after aqueous phase chemistry (no soot)
- FIGURE 11. 48 hour time evolution of  
 (a) average aqueous phase concentration in the cloud area after aqueous phase chemistry for 5 cases defined in TABLE 2.  
 (b) average aqueous phase concentration in the cloud area after aqueous phase chemistry for 4 cases defined in TABLE 2.
- FIGURE 12. Location of sites involved in the evaluation of model performance and mercury emissions in individual grid cells.

- FIGURE 13. time series of hourly averages of observed TGM concentrations (black area) and model predicted  $\text{Hg}^0$  concentrations (grey line) in air at two Swedish sites (Aspvreten, Roervik) and two German sites (Zingst, Neuglobsow). November/December, 1998  
(The observations at Roervik are multi-day and daily averages)
- FIGURE 14. 72 hours backward trajectories November 25, 1998 for  
(a) Aspvreten  
(b) Roervik  
(c) Zingst  
(d) Neuglobsow
- FIGURE 15. Time series of hourly averages of observed TGM concentrations (black area) and model predicted  $\text{Hg}^0$  concentrations (grey line) in air at two Swedish sites (Aspvreten, Roervik) and two German sites (Zingst, Neuglobsow). March, 1997.
- FIGURE 16. 72 hours backward trajectories March 26, 1997 for  
(a) Aspvreten  
(b) Roervik  
(c) Zingst  
(d) Neuglobsow
- FIGURE 17. 72 hours backward trajectories Aspvreten  
(a) Aspvreten  
(b) Roervik  
(c) Zingst  
(d) Neuglobsow
- FIGURE 18. Model predicted  
(a) Monthly average concentrations of elemental mercury ( $\text{Hg}^0$ ) in air  
(b) Monthly total deposition flux (dry+wet) of mercury  
Baltic Sea-February 1998.

## 10. LIST OF TABLES

TABLE 1. Mercury species in ambient air in Central and Northern Europe.  
(typical concentration ranges and Henry's law coefficient)

TABLE 2. Input parameters for the intercomparison study of atmospheric mercury chemistry schemes.

TABLE 3. Model predicted deposition fluxes of mercury species to the Baltic Sea.

TABLE 4. Model predicted atmospheric input rates of mercury species to the Baltic Sea.

TABLE 5. Estimates of annual atmospheric mercury input rates to the Baltic Sea.



## **APPENDIX**

This study is based on the following ten papers presented in chronological order of their publication and referred to by bold Roman numerals in the text.



# Paper I





1352-2310(94)00223-1

## ATMOSPHERIC MERCURY SPECIES OVER CENTRAL AND NORTHERN EUROPE. MODEL CALCULATIONS AND COMPARISON WITH OBSERVATIONS FROM THE NORDIC AIR AND PRECIPITATION NETWORK FOR 1987 AND 1988

G. PETERSEN,\* Å. IVERFELDT† and J. MUNTHER†

\* GKSS Research Centre, Institute of Physics, Max-Planck-Str. 1, D-21502 Geesthacht, Germany;

† Swedish Environmental Research Institute (IVL), P.O. Box 47086, S-402 58 Göteborg, Sweden

(First received 1 September 1993 and in final form 20 July 1994)

**Abstract**—A chemical scheme based upon current knowledge of physicochemical forms and transformation reactions of atmospheric mercury has been implemented into a regional pollutant dispersion model for Europe. Existing databases for anthropogenic mercury emissions in Europe have been updated for 1987 and 1988 using new information on source data from eastern European countries including the former German Democratic Republic. Concentrations of total gaseous and particle associated mercury in air and mercury in precipitation calculated by the model are compared with observed values at Roervik in southwestern Sweden, Aspveten, south of Stockholm and other locations of the Nordic network, on a daily basis. The results show that the model is capable of simulating long-range transport of mercury from Central Europe to Scandinavia including discrete events with peak concentrations in air and precipitation in the range of  $10 \text{ ng m}^{-3}$  and  $100 \text{ ng l}^{-1}$ , respectively. Coinciding observed and calculated peak concentrations indicate that exceptionally high mercury emissions, most probably from chlor-alkali industry and lignite coal combustion in East Germany and Czechoslovakia, must have occurred in 1987 and 1988.

**Key word index:** Mercury species, atmospheric mercury chemistry, transport models, monitoring, atmospheric deposition, North Sea input, Baltic Sea input.

### 1. INTRODUCTION

Mercury exists in the atmosphere in different physical and chemical forms, whose properties and interactions with their surroundings determine its transport and transformations, as well as its removal mechanisms such as wet and dry deposition to the earth's surface (Schroeder, 1982; Lindqvist and Rodhe, 1985; Schroeder *et al.*, 1991). It is now generally accepted that more than 90% of atmospheric mercury is in the vapor phase while the remainder is associated with particulate matter (Brosset, 1982; Ferrara *et al.*, 1982; Iverfeldt, 1991a). The chemical speciation of mercury in the atmosphere is still under discussion, although there is evidence for the total predominance of elemental mercury (Brosset, 1987; Schroeder and Jackson, 1987; Iverfeldt, 1991a). Recent data indicate that, besides elemental mercury, methylmercury species are present in ambient air in minor quantities (Bloom and Fitzgerald, 1988). In the emissions from high-temperature combustion facilities without flue gas cleaning systems, divalent inorganic mercury compounds in gaseous or particulate form have been identified

(Bergström, 1986; Lindqvist and Schager, 1990), but far from sources these species are at very low or currently undetectable levels (Brosset and Iverfeldt, 1989; Brosset and Lord, 1991).

Measurements have shown that vapor-phase mercury in ambient air is present in the atmospheric boundary layer over Scandinavia at concentrations of typically  $2\text{--}4 \text{ ng m}^{-3}$  with a weak south-to-north decreasing gradient throughout the year, but more pronounced during winter. Due perhaps to local factors and gas-to-particle conversion processes, observations of particulate-phase mercury in air do not indicate such clear gradients. The observed yearly average concentration levels of  $0.05\text{--}0.06 \text{ ng m}^{-3}$  suggest substantial contributions to the total mercury deposition fluxes, as particulate mercury would be effectively dry deposited and removed by in-cloud and below-cloud scavenging. In precipitation, mercury occurs primarily in the oxidized state, and a large part of the mercury content is associated with particles. The range of regional average precipitation concentrations observed in Scandinavia is  $20\text{--}40 \text{ ng l}^{-1}$ , but during episodic events considerably higher values, up

to  $100 \text{ ng } \ell^{-1}$ , can occur. The south-to-north gradient of mercury concentrations in precipitation is more pronounced most likely due to the impact of aqueous-phase redox reactions and adsorption processes (Iverfeldt, 1991a).

The anthropogenic influence on mercury concentrations in the lower troposphere over Scandinavia shows up in several ways. Firstly, a strong correlation of mercury with sulfate and soot carbon is found at the southern stations of the Nordic network, indicating a connection of the atmospheric mercury load in Scandinavia to Central European anthropogenic activities, such as combustion of fossil fuels and waste incineration. In addition, a wind trajectory classification has demonstrated increased mercury concentrations in the southern trajectory sectors with incoming air masses from the main industrial areas in Central Europe. According to recent European emission surveys for mercury, the dominating sources in 1987 and 1988 were chlor-alkali factories in East Germany and coal combustion units without flue gas cleaning systems in East Germany and Czechoslovakia, together accounting for nearly 40% of the total anthropogenic mercury emissions in Europe. These emissions are assumed to be made up of elemental mercury and divalent inorganic mercury compounds in the gaseous phase as well as a minor part of particle-associated mercury. This degree of speciation is considered to be the first approach and the uncertainties involved are hard to estimate because of a lack of reliable environmental measurement data on this subject.

In order to investigate in more detail the effects of the European sources of the above-mentioned three mercury species on the atmospheric mercury input to the North Sea and the Baltic Sea, a regional dispersion model has been developed and applied within the framework of a research project of the German Federal Environmental Agency (Petersen, 1992a, b). The results indicate a significant effect of the presence of gas-phase divalent inorganic mercury compounds on the deposition pattern in Central Europe and the southern parts of the two seas, but for this species it is not possible to evaluate the model performance because of a total lack of validated measurement data.

This paper focusses on model applications to species which have been definitely observed over Scandinavia, i.e. elemental mercury in the gaseous phase and particulate-phase mercury. Model runs are performed using kinetic data from laboratory studies (Munthe *et al.*, 1991; Munthe, 1992) and with field data from the Nordic air and precipitation network (Lindqvist *et al.*, 1991; Iverfeldt, 1991a). An outline of the network design is given together with a presentation of the monitoring data. The development and application of the model is described with special emphasis on the formulation of the chemical scheme employed in the calculations and on a comparison of model results with observed data, respectively.

## 2. MODEL DESCRIPTION

### 2.1. Outline

The long-period model for sulfur used under the European Monitoring and Evaluation Programme (EMEP) (Eliassen and Saltbones, 1983) has been modified for transport, chemical transformations and deposition of mercury species. The model is a one-layer column trajectory model. Columns of air in the atmospheric boundary layer are followed along specified 96 h trajectories picking up emissions of mercury species from the underlying grid. The mass balance equations are integrated along each trajectory, taking into account emissions, chemical transformations, dry and wet depositions and the meteorological input data. The transport equation for the concentration  $q$  to be solved along each trajectory can be written as

$$\frac{dq}{dt} = -\left(\frac{v_d}{h} + W\frac{P}{h}\right)q + (1-\alpha)\frac{Q}{h} \quad (1)$$

where the operator  $d/dt$  is the total (Lagrangian) time derivative,  $Q$  is the mercury emission per unit area and time,  $v_d$  is the dry deposition velocity,  $W$  is the scavenging ratio, and  $P$  is the 6 hourly rainfall amount. The mixing height  $h$  is the height of the air column containing the bulk of the polluted air.  $\alpha$  represents additional dry deposition in an emission grid square, i.e. a fraction of the emission is deposited locally inside the same grid square as emitted.

The model grid is shown in Fig. 1. Trajectories are calculated within the entire grid to the arrival points contained within the irregular subgrid. Equation (1) is integrated along the trajectories to give instantaneous concentration fields of mercury species when the trajectories arrive at 00, 06, 12 and 18 GMT. Deposition fluxes of gaseous and particulate-phase mercury species are derived from their concentration fields by applying dry and wet removal parameters which are described in more detail in Section 2.4.

The meteorological data needed are summarized in Table 1. Most of the data are taken from the output of the Norwegian Numerical Weather Prediction (NWP) model (Gronas and Hellevik, 1982; Nordeng, 1986). The calculation of the 96 h backward trajectories to any point in the grid is based upon the  $u$  and  $v$  components of wind speed provided by the NWP model. Six-hourly precipitation amounts are analyzed from observations over continental regions. Over sea areas, estimates from the NWP model are used. The mixing height is derived at 12:00 GMT each day from radiosonde data. The 850 mb vertical velocity derived from the NWP model is then used to calculate the changes in the mixing height as the air column is subject to convergence or divergence. After 24 h the resulting calculated mixing height is compared with the new radiosonde observation and, if appropriate, an exchange of air takes place with the free troposphere. The amount of air exchanged is determined by the difference between these two heights.

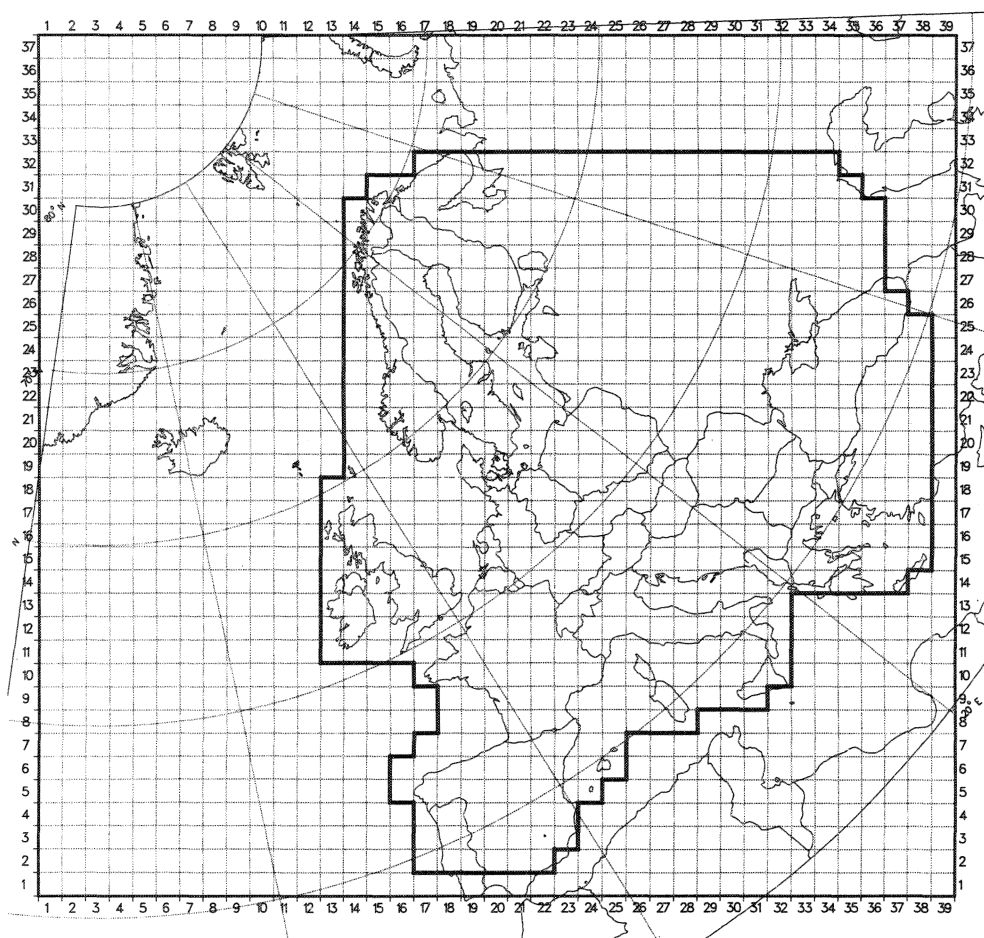


Fig. 1. The EMEP/MSC-W grid (large area) and the area for which concentrations are calculated (irregular subarea).

Table 1. Meteorological data used in the mercury model (adopted from Iversen *et al.*, 1991)

	Physical parameter	Level	Period between input	Purpose	Source
$v$	Advection wind	$\sigma = 0.925$ $z \approx 750$ m	6 h	Horizontal transport, trajectories	NWP model
$H_M$	Height of mixed layer	Above ground	24 h (12 GMT)	Initial dilution of emissions	Analysed observations
$P$	Grid element average precipitation	Ground	6 h accumulated	Wet deposition	Ocean: NWP m. Land: An. Obs.
$w$	Vertical velocity	$\sigma = 0.85$ $z \approx 1500$ m	6 h	Free troposphere exchange	NWP model
$p_s$	Ground surface pressure	$\sigma = 1$ (ground)	6 h	Air density at ground surface	NWP model
$T_2$	Temperature in ground air	$z = 2$ m	6 h	Aerodynamic resistance to dry deposition	NWP model
$\tau$	Turbulent stress	Surface layer	6 h	Aerodynamic resistance to dry deposition	NWP model
$H_d$	Turbulent heat flux density	Surface layer	6 h	Aerodynamic resistance to dry deposition	NWP model

## 2.2. Emissions

The databases for anthropogenic mercury emissions in Europe employed in the model calculations have been compiled for 1987 and 1988 (Axenfeld *et al.*, 1991). In this work, the emission rates and their spatial distribution in the model grid (Fig. 2) are based upon location and capacity of their dominating source

categories such as combustion of fossil fuels in power plants, non-ferrous metal smelters, waste incinerators, chlor-alkali factories and other industrial installations. The emission rates in each grid square are speciated with respect to elemental mercury ( $\text{Hg}^0$ ), divalent inorganic mercury ( $\text{Hg(II)(g)}$ ) and particulate mercury  $\text{Hg(part.)}$  using estimated sector speciation percentages shown in Table 2. For modelling pur-

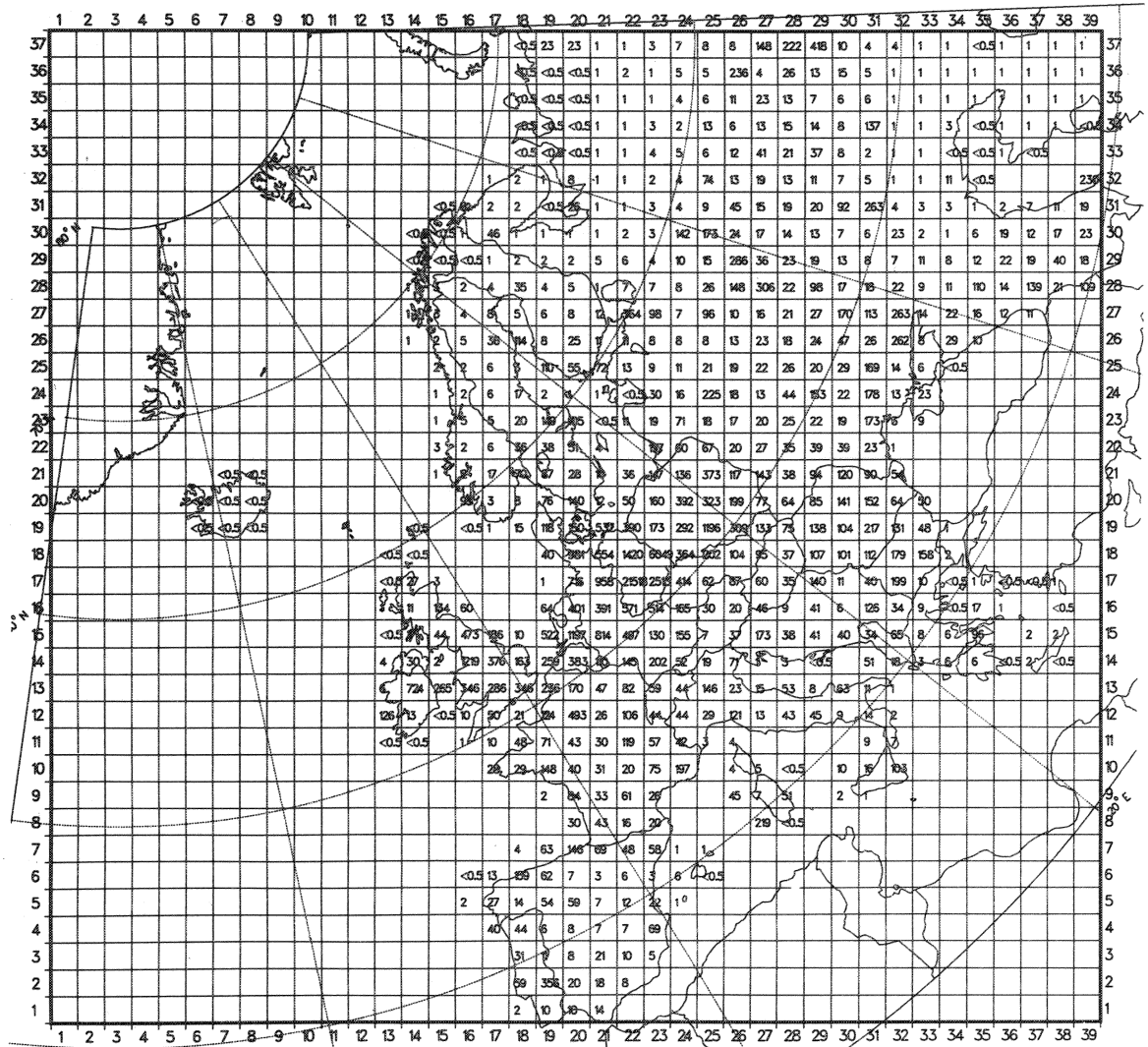


Fig. 2. 1987 and 1988 emissions of total anthropogenic mercury in each grid square of the EMEP/MSC-W grid for model calculations (Units: 10 tonnes per annum as Hg).

Table 2. Sector speciation percentages for anthropogenic mercury emissions in Europe (Axenfeld *et al.*, 1991)

	Elemental mercury in the gas phase $\text{Hg}^0$	Divalent inorganic mercury compounds $\text{Hg(II)(g)}$	Particulate mercury $\text{Hg(part.)}$
Combustion of fossil fuels	50%	30%	20%
Nonferrous metal smelting	85%	10%	5%
Chlor-alkali factories	70%	30%	
Waste incinerators	20%	60%	20%

Table 3. Average of 1987 and 1988 emissions of anthropogenic mercury species in Europe employed in the model calculations (Axenfeld *et al.*, 1991). Unit: tonnes per annum

	Number of point sources	Hg <sup>0</sup>	Hg(II)(g)	Hg(part.)	Total
Albania	1	0.417	0.250	0.167	0.834
Austria	13	0.626	0.276	0.180	1.083
Belgium	21	5.281	2.244	1.371	8.895
Bulgaria	14	4.726	2.375	1.564	8.665
CSSR	31	7.830	4.474	2.673	14.977
Denmark	21	2.098	1.911	0.771	4.780
Finland	33	3.064	0.754	0.324	4.142
France	59	15.329	9.058	5.489	29.876
German Dem. R.	23	203.076	99.104	28.326	330.506
Germany Fed. R.	225	37.612	20.560	6.806	64.977
Great Britain	127	21.083	13.841	5.644	40.568
Greece	6	1.070	0.622	0.414	2.106
Hungary	31	1.423	0.810	0.516	2.749
Iceland	1	0.001	0.000	0.000	0.001
Ireland	6	4.400	2.633	1.755	8.789
Italy	62	8.197	3.741	1.175	13.113
Yugoslavia	24	3.993	1.924	1.263	7.180
Luxemburg	2	0.034	0.019	0.013	0.066
Netherlands	39	3.020	3.857	1.388	8.265
Norway	9	1.423	0.466	0.171	2.060
Poland	42	23.344	13.084	8.318	44.746
Portugal	4	3.459	1.638	0.397	5.494
Romania	35	8.070	4.752	3.164	15.986
Spain	13	6.848	2.798	1.108	10.755
Sweden	34	5.561	1.391	0.550	7.501
Switzerland	2	0.125	0.062	0.041	0.228
Soviet Union	50	45.046	25.612	17.017	87.675
Total	928	417.156	218.256	90.606	726.017

poses, this speciation provides a possibility of separate treatment of mercury emitted in three different physicochemical forms and hence an assessment of the potential importance of these species for the mercury deposition pattern in Europe.

The anthropogenic emissions of mercury species in the European countries together with the national totals are shown in Table 3. In 1987 and 1988 the emissions in the German Democratic Republic accounted for more than 40% of the European total and were hence substantially larger than in each of the other countries. According to Hellwig and Neske (1990), this was due to both burning of lignite coal, most intensively used in East Germany's power plants without flue gas desulfurization equipment, and high losses of mercury from the chlor-alkali factories heavily concentrated in the Halle/Leipzig/Bitterfeld area until 1990.

In Europe, large uncertainties are associated with inventories of natural emissions of mercury with respect to their magnitude and their geographical and seasonal variation. In a few cases, reasonably reliable data on degassing rates of mercury from terrestrial and aquatic systems are available from flux measurements over soil and lake surfaces in Sweden (Xiao *et al.*, 1990) and vertical concentration gradients over a cinnabar deposit in Italy (Ferrara *et al.*, 1991). However, the available data sets are too scarce for any firm

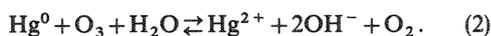
conclusions concerning the importance of natural emissions for the temporal and spatial variability of mercury deposition fluxes in Central and Northern Europe. For simplicity, natural emissions are represented in the model as a part of a Hg<sup>0</sup> background concentration of 2 ng m<sup>-3</sup>, constant in space and time. Compared to concentrations of anthropogenic origin, a relatively low variability of natural tropospheric background concentrations can be expected in the main emission areas of Central Europe, suggesting that a more detailed treatment of natural emissions is probably not required in this part of the model domain.

### 2.3. Atmospheric chemistry of mercury

The chemical scheme in the model is mainly based on results obtained during recent years in various research programmes in Sweden (Iverfeldt and Lindqvist, 1986; Lindqvist *et al.*, 1991; Munthe *et al.*, 1991; Munthe and McElroy, 1992; Munthe, 1992) and Canada (Schroeder and Jackson, 1987; Schroeder *et al.*, 1991). The results indicate that gas-phase chemistry of elemental mercury is probably of minor importance. Further, there is no evidence so far that mercury associated with particles and gaseous divalent inorganic mercury compounds undergo physical or chemical transformation during transport and diffusion through the atmosphere. Hence, in the present

model, chemical processes of  $\text{Hg}^0$  are restricted to the aqueous phase and it is assumed that partitioning between gas and particulate phase and chemical reactions are negligible for  $\text{Hg}(\text{part.})$  and  $\text{Hg}(\text{II})(\text{g})$ .

In the case of elemental mercury, investigations of redox processes that are relevant to atmospheric conditions have shown that, in the presence of liquid water, ozone is a major oxidant for this species:

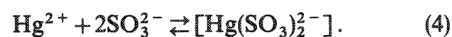


The rate of the reaction can be described by the following equation:

$$\frac{d[\text{Hg}^{2+}]}{dt} = k_1 [\text{Hg}^0]_{\text{aq}} [\text{O}_3]_{\text{aq}} \quad (3)$$

with a second-order rate constant  $k_1 = 4.7 \times 10^7 \text{ (M}^{-1} \text{s}^{-1})$  (Munthe, 1992).

It has also been shown, that sulfite is capable of reducing  $\text{Hg}^{2+}$  to  $\text{Hg}^0$  in aqueous solutions (Munthe *et al.*, 1991). As a first step, the proposed mechanism involves the complexation of  $\text{Hg}^{2+}$  by sulfite ions:



As the complexation reaction is very fast, it is assumed that it occurs spontaneously. Subsequently, the complex decomposes to produce  $\text{Hg}^+$  which in turn is rapidly reduced to  $\text{Hg}^0$ . In the present model, the decomposition has been treated as a first-order reaction:

$$\frac{d[\text{Hg}(\text{SO}_3)_2^{2-}]}{dt} = -k_2 [\text{Hg}(\text{SO}_3)_2^{2-}] \quad (5)$$

with a maximum value of the rate constant  $k_2 = 4 \times 10^{-4} \text{ (s}^{-1})$  (Munthe *et al.*, 1991).

In the atmospheric environment, it is assumed that  $\text{Hg}^{2+}$  is completely complexed, as a large excess of sulfite ions with respect to  $\text{Hg}^{2+}$  can be expected in atmospheric water droplets. Hence, the reduction rate of divalent mercury can be expressed as

$$\frac{d[\text{Hg}(\text{II})]}{dt} = -k_2 [\text{Hg}(\text{II})] \quad (6)$$

where  $[\text{Hg}(\text{II})]$  denotes the total dissolved concentration in the water droplets.

As the reductive processes occur simultaneously with the oxidation of elemental mercury by ozone, steady-state concentrations of  $\text{Hg}(\text{II})$  are built up in the water droplets depending on the reaction rates in equations (3) and (6). If those equations are assumed to represent the dominant reactions, the steady-state concentration of dissolved oxidized mercury in atmospheric water droplets can be calculated as a function of the rate constants  $k_1$  and  $k_2$ , ozone concentration in the aqueous phase and elemental mercury concentration in ambient air:

$$[\text{Hg}(\text{II})]_{\text{aq}} = \frac{k_1}{k_2 H_{\text{Hg}}} [\text{O}_3]_{\text{aq}} [\text{Hg}^0]_{\text{gas}} \quad (7)$$

implying net zero flux of  $\text{Hg}^0$  across the air/water interface for steady-state conditions and hence

$$[\text{Hg}^0]_{\text{gas}} = H_{\text{Hg}} [\text{Hg}^0]_{\text{aq}} \quad (8)$$

where  $H_{\text{Hg}}$  is the Henry's law constant for  $\text{Hg}^0$ .

The reduction of  $\text{Hg}(\text{II})$  to  $\text{Hg}^0$  by sulfite is assumed to occur independently of the  $\text{SO}_2$  concentration in air. This is equivalent to ignoring complexes other than  $\text{Hg}(\text{SO}_3)_2^{2-}$ . In reality, other complexes such as  $\text{HgCl}_2$  are probably as important as the sulfite complex. However, due to the predominance of particulate mercury in precipitation, this simplification will probably not affect the model results at the present degree of detail.

Analysis of mercury in precipitation in polluted areas has shown that a significant fraction of the total concentration is present in the particulate phase (Ferrara *et al.*, 1986; Ahmed and Stoeppler, 1987; Iverfeldt, 1991a). There is evidence that divalent aqueous Hg is adsorbed on soot particles, so that the total Hg concentration in the water droplets exceeds the steady-state value of  $\text{Hg}(\text{II})$  (Iverfeldt, 1991a; Brosset and Lord, 1991; Lindqvist *et al.*, 1991). The adsorption can be described by a mechanism which is known as the Langmuir isotherm:

$$\frac{[\text{Hg}(\text{II})]_{\text{ad}}}{F} = [\text{Hg}(\text{II})]_{\text{aq}} K_{\text{ad}} \quad (9)$$

where  $F$  is the total soot particle surface area per unit volume of water and  $K_{\text{ad}}$  represents the adsorption equilibrium constant.

Assuming a mean radius  $r$  for the soot particles and substituting  $F$  by the soot particle concentration in the water droplets  $[c_{\text{soot}}]_{\text{aq}}$ , it can be shown (Petersen, 1992a) that the concentration of mercury adsorbed on soot particles with the density  $\rho$  is given by

$$[\text{Hg}(\text{II})]_{\text{ad}} = [\text{Hg}(\text{II})]_{\text{aq}} K_{\text{ad}} \cdot \frac{3}{\rho} [c_{\text{soot}}]_{\text{aq}} \frac{1}{r} \quad (10)$$

where  $[c_{\text{soot}}]_{\text{aq}}$  is assumed to be  $500,000 [c_{\text{soot}}]_{\text{gas}}$ .

Expressing the constant values of equation (10) as a model-specific adsorption equilibrium constant  $K_3$ :

$$K_3 = K_{\text{ad}} \frac{3}{\rho} \quad (11)$$

leads to

$$[\text{Hg}(\text{II})]_{\text{ad}} = [\text{Hg}(\text{II})]_{\text{aq}} [c_{\text{soot}}]_{\text{aq}} \frac{1}{r} K_3. \quad (12)$$

The total concentration of elemental mercury oxidized by ozone in the aqueous phase  $[\text{Hg}(\text{II})]_{\text{tot}}$  is the sum of the dissolved and the adsorbed fraction:

$$[\text{Hg}(\text{II})]_{\text{tot}} = [\text{Hg}(\text{II})]_{\text{aq}} + [\text{Hg}(\text{II})]_{\text{ad}}. \quad (13)$$

By substituting equations (7) and (12) into equation (13) one obtains an equation for the total concentration of elemental mercury oxidized by ozone in the aqueous phase as a function of the concentration of

elemental mercury in ambient air:

$$[\text{Hg(II)}]_{\text{tot}} = \frac{k_1}{k_2} \cdot \frac{1}{H_{\text{Hg}}} [\text{O}_3]_{\text{aq}} \left( 1 + K_3 \frac{[c_{\text{soot}}]_{\text{aq}}}{r} \right) [\text{Hg}^0]_{\text{gas}} \quad (14)$$

#### 2.4. Wet and dry deposition

The wet deposition rate in equation (1) is parametrized in terms of the precipitation rate  $P$ , the height of the mixing layer  $h$  and a scavenging ratio  $W$ , which is a proportionality factor relating pollutant concentrations in precipitation to the respective concentrations in air. For elemental mercury the scavenging ratio is given by

$$W(\text{Hg}^0) = \frac{[\text{Hg(II)}]_{\text{tot}}}{[\text{Hg}^0]_{\text{gas}}} \quad (15)$$

Here, a negligibly small fraction of dissolved  $\text{Hg}^0$  is assumed, since this species most probably accounts for a 1% or less of the total mercury in precipitation.

By rearranging equation (14) the scavenging ratio of  $\text{Hg}^0$  can be expressed in terms of ozone and soot carbon concentration, three rate constants and Henry's law coefficient of  $\text{Hg}^0$ :

$$W(\text{Hg}^0) = \frac{[\text{Hg(II)}]_{\text{tot}}}{[\text{Hg}^0]_{\text{gas}}} = \frac{k_1}{k_2} \cdot \frac{1}{H_{\text{Hg}}} [\text{O}_3]_{\text{aq}} \left( 1 + K_3 \frac{[c_{\text{soot}}]_{\text{aq}}}{r} \right) \quad (16)$$

From equation (16) it is easy to see that

$$[\text{Hg(II)}]_{\text{tot}} \frac{H_{\text{Hg}}}{[\text{Hg}^0]_{\text{gas}}} \frac{H_{\text{O}_3}}{[\text{O}_3]_{\text{gas}}} = K_3 \cdot \frac{k_1}{k_2} \frac{[c_{\text{soot}}]_{\text{aq}}}{r} + \frac{k_1}{k_2} \quad (17)$$

In equation (17),  $[\text{O}_3]_{\text{aq}}$  is substituted by the ozone concentration in ambient air  $[\text{O}_3]_{\text{gas}}$  and Henry's law coefficient of ozone  $H_{\text{O}_3}$ , since an equilibrium distribution between the air and water phase due to relatively slow chemical degradation of ozone in water droplets can be assumed.

Equation (17) is represented by the dashed line in the coordinate system depicted in Fig. 3. If the relatively well-established reduction rate constant  $k_2$  (cf. Section 2.3) is prescribed, an oxidation rate constant  $k_1$  and the adsorption rate constant  $K_3$  can be determined from the dashed line's slope  $K_3 \cdot k_1/k_2$  and the y-axis intercept at  $k_1/k_2$ . The line is derived from linear regression of ozone, soot carbon and mercury concentrations in ambient air and in precipitation simultaneously measured at two sites in Sweden and Germany (Petersen, 1992a). It is evident, however, that  $k_1$  derived from the regression analyses is overestimated because the regression is based on measured total mercury concentration in precipitation  $[\text{Hg}_{\text{tot}}]_{\text{aq}}$ ,

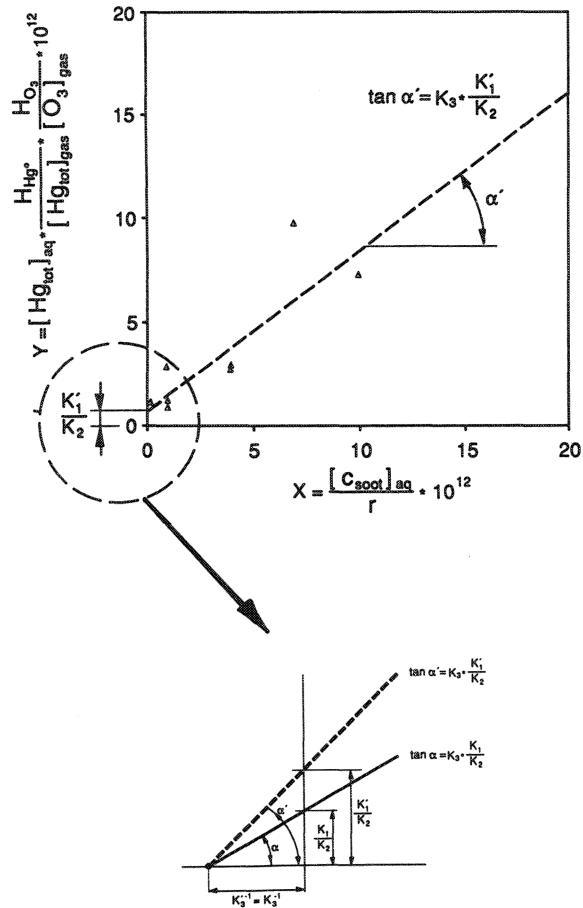


Fig. 3. Determination of rate constants by linear regression of field measurements.

which includes a certain amount of directly scavenged  $\text{Hg}(\text{part.})$ . Subtracting this  $\text{Hg}(\text{part.})$  fraction from  $[\text{Hg}_{\text{tot}}]_{\text{aq}}$  leads to a clockwise rotation of the regression line (lower part of Fig. 3) and hence to the smaller oxidation rate constant  $k_1$  from laboratory studies (cf. Section 2.3).

In Table 4 the rate constants  $k_1$ ,  $k_2$  and  $K_3$  determined by laboratory studies and regression analyses are summarized together with an identification of the values used with the calculation of the scavenging ratio of  $\text{Hg}^0$ . For these calculations a mean soot particle radius of  $0.5 \mu\text{m}$  has been assumed. For Henry's law coefficient of  $\text{Hg}^0$  the value of 0.29 at  $10^\circ\text{C}$  is used (Sanemasa, 1975).

Besides the above-mentioned constant values, input data of 6-hourly ozone and soot carbon concentrations for each grid element are required to calculate time and space-dependent scavenging ratios over the entire model domain. For ozone, these data are taken from the output of the EMEP MSC-W ozone model (Simpson, 1991, 1992) and from observed data of the OECD-OXIDATE project (Grennfelt *et al.*, 1987). The soot carbon concentrations are derived from

Table 4. Rate constants for redox reactions and equilibrium constants for adsorption processes of Hg in the aqueous phase

			Reference
<i>Oxidation</i>			
$k_1$	$1.2 \times 10^8$	( $M^{-1} s^{-1}$ )†	Regression analysis (Petersen, 1992a)
$*k_1$	$4.7 \times 10^7$	( $M^{-1} s^{-1}$ )†	Laboratory study (Munthe, 1992)
<i>Reduction</i>			
$*k_2$	$4 \times 10^{-4}$	( $s^{-1}$ )	Laboratory study (Munthe <i>et al.</i> , 1991)
<i>Adsorption</i>			
$*K_3 = K_3$	$5 \times 10^{-6}$	( $m^4 g^{-1}$ )	Regression analysis (Petersen, 1992a)

\* Rate constants employed in the model calculations.  
 † M denotes moles per liter.

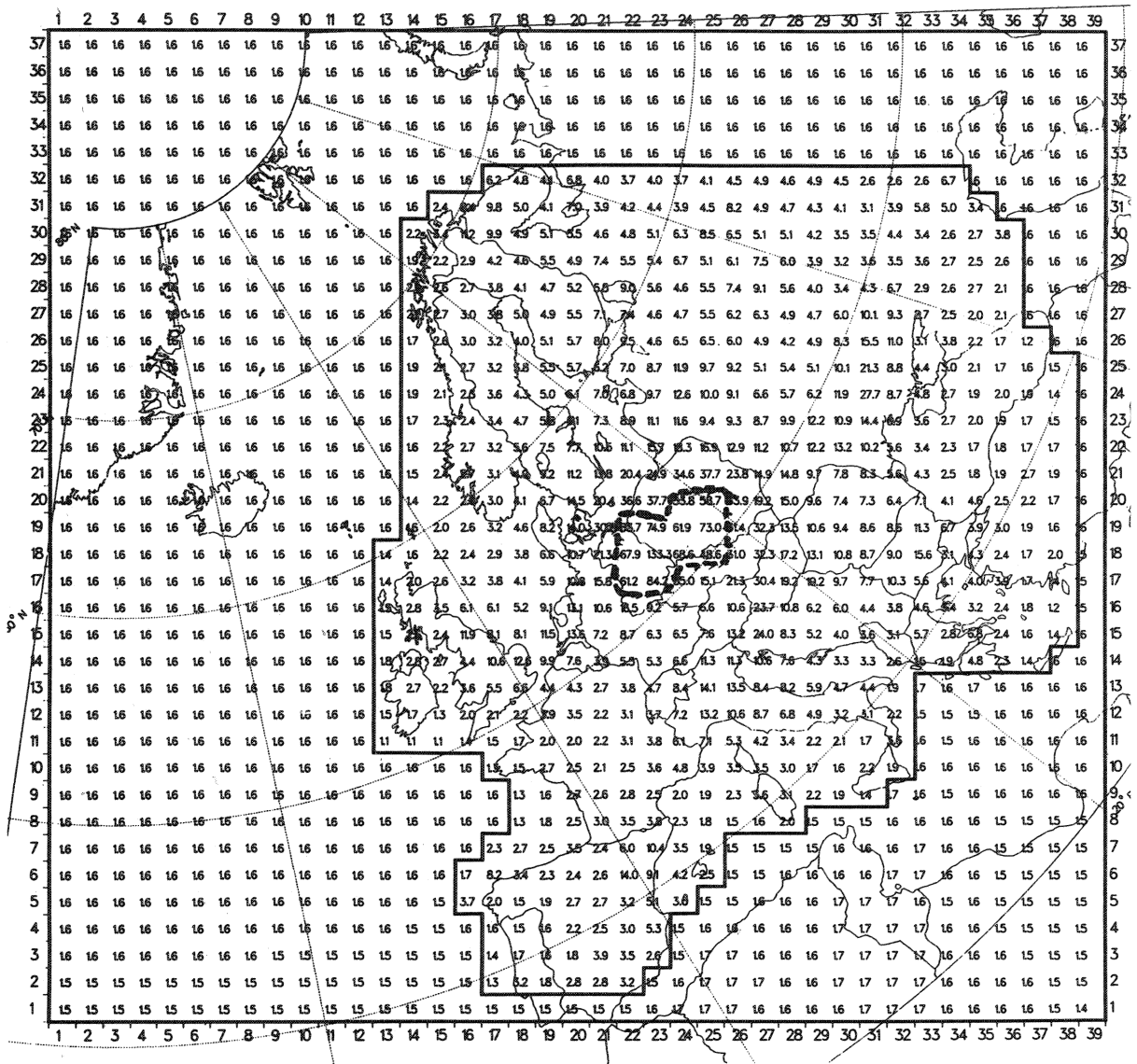


Fig. 4.  $Hg^0$  scavenging ratio  $10^{-3}$ —calculated monthly means for January 1988.

calculations of sulfur dioxide concentrations performed with the EMEP model for acidifying components (Iversen *et al.*, 1991) assuming constant soot carbon/SO<sub>2</sub> ratios for different regions of the European continent (Penner *et al.*, 1993). Over the North Atlantic, a constant soot carbon background concentration of 0.2 µg m<sup>-3</sup> has been applied (Andreae *et al.*, 1984; Cachier *et al.*, 1990).

Figure 4 shows an example for the spatial distribution of monthly mean values of Hg<sup>0</sup> scavenging ratios calculated with the output of the "preprocessor" models for ozone and soot carbon. Mainly due to the high atmospheric soot carbon load in Poland and Eastern Germany, scavenging ratios clearly peak in the area circled by the dashed line, whereas values over northern Scandinavia and the North Atlantic are two orders of magnitude lower. The spatial pattern depicted in Fig. 4 leads to a substantial south-to-north decrease of mercury concentrations in precipitation from Central Europe to Scandinavia. This is in qualitative agreement with observed data in that area (Iverfeldt, 1991a). Full details are given in Section 3.2, where modelled Hg concentrations in precipitation are compared with observations from the Nordic network.

For mercury associated with particles (Hg(part.)) and for gaseous inorganic mercury compounds Hg(II)(g), scavenging ratios are assumed to be constant in space and time. For Hg(part.), a scavenging ratio of  $5 \times 10^5$  has been adopted from a long-range transport model for lead (Petersen *et al.*, 1989), as field measurements have shown a similar size distribution for lead and mercury in particulate form (Graßl *et al.*, 1989). The gaseous nitric acid scavenging ratio of  $1.6 \times 10^6$ , used with the EMEP model for acidifying pollutants (Iversen *et al.*, 1991), has been applied for Hg(II)(g), since the water solubility of the two species is comparably high.

Dry deposition rates of Hg<sup>0</sup> should be negligibly small since the substance is almost insoluble. Therefore, the dry deposition velocity of Hg<sup>0</sup> is zero in the model, although recent studies indicate that there are measurable deposition rates of vapor-phase Hg to forest surfaces (Iverfeldt, 1991b; Lindberg *et al.*, 1991). Dry deposition velocities of 0.2 cm s<sup>-1</sup> for Hg(part.) and 4 cm s<sup>-1</sup> for Hg(II)(g) at 1 m height have been adopted from the above-mentioned models for lead and for nitric acid, respectively. For Hg(II)(g), the dry deposition velocity at 1 m height is corrected to a 50 m height value, which is considered to be representative for the average concentration in the well-mixed layer assumed by the model. This correction is done by applying the similarity theory for the constant flux layer which is about 50 m thick (Iversen *et al.*, 1991).

The model assumes instantaneous vertical mixing of pollutants in an air column passing over an emission grid square. Hence, during the first phase of dispersion, ground level concentrations would be underestimated and dry deposition rates would be too small if not corrected by the local deposition factor  $\alpha$  (cf.

Section 2.1). In a more recent investigation on incorporating a new parametrization of deposition processes into the EMEP model for acidifying pollutants, a local deposition factor of 0.1 has been found to be representative for sulfur dioxide (Krüger, 1993). Based on this result and a dry deposition velocity of 0.8 cm s<sup>-1</sup> for SO<sub>2</sub>, values of 0.5 and 0.025 can be applied for Hg(II)(g) and Hg(part.), if local deposition factors are assumed to be directly proportional to average dry deposition velocities.

### 3. MODELLING RESULTS

The model has been run for two full years, 1987 and 1988. The general objective of the model simulations was to quantify the atmospheric long-range transport of mercury from the main emission areas in Europe to Scandinavia and the adjacent North Sea and Baltic Sea. A focus of the study was to confirm one of the most important results from the Nordic network for atmospheric mercury, i.e. a relatively weak south-to-north gradient of mercury concentrations in ambient air and a more pronounced one in precipitation over Scandinavia, indicating a substantial impact from Central European anthropogenic mercury sources through long-range transport. To this end, four sites in Eastern Germany and four stations of the Nordic network forming a longitudinal corridor extending from the high emission region of Halle/Leipzig/Bitterfeld in Germany to Överbygd in northern Norway (see Fig. 5) were selected for an interpretative analysis of comparable field observations and model simulations. The data set of atmospheric mercury measurements performed at the German sites is still much smaller than that from the Nordic network and can hence only be used for a crude evaluation of the model performance. However, the measurements at the Scandinavian sites are most suitable for comparison with model results, since they represent the longest continuous time series reported to date of atmospheric mercury concentration data in Europe. An extensive treatment of the data generated within the Nordic network can be found in Iverfeldt (1991a).

In Sections 3.1 and 3.2 comparisons between measured and modelled mercury in ambient air and precipitation, respectively, are discussed together with model-predicted variability in monthly means of concentrations over Europe. Section 3.3 focusses on wet and dry deposition fluxes of mercury in Central and Northern Europe and on assessment of the atmospheric loading of mercury to the North Sea and the Baltic Sea. Section 4 provides a brief summary and conclusion.

#### 3.1. Mercury in air

Table 5 compares modelled and observed annual means of gaseous and particulate mercury concentrations in air at the eight locations depicted in Fig. 5. For gaseous mercury in air, a comparison of calculated

Table 5. Comparison of modelled vs observed mean mercury concentrations in air for 1988

	Gaseous mercury in air ( $\text{ng m}^{-3}$ )		Particulate mercury in air ( $\text{ng m}^{-3}$ )	
	Modelled $\text{Hg}^0$	Observed $\text{Hg}_T$	Modelled	Observed
Halle/Leipzig/Bitterfeld	10.1		0.279	
Neuglobsow	4.9		0.208	
Langenbrügge*	4.1	4.2	0.111	
Kap Arkona	3.6		0.107	
Rörvik	2.5	2.8	0.025	0.06
Aspvreten	2.5		0.019	
Vindeln	2.1	2.5	0.005	0.05
Överbygd	2.1	2.6	0.002	

\* Observations 1992.  $\text{Hg}^0$  denotes elemental mercury,  $\text{Hg}_T$  denotes total gaseous mercury.

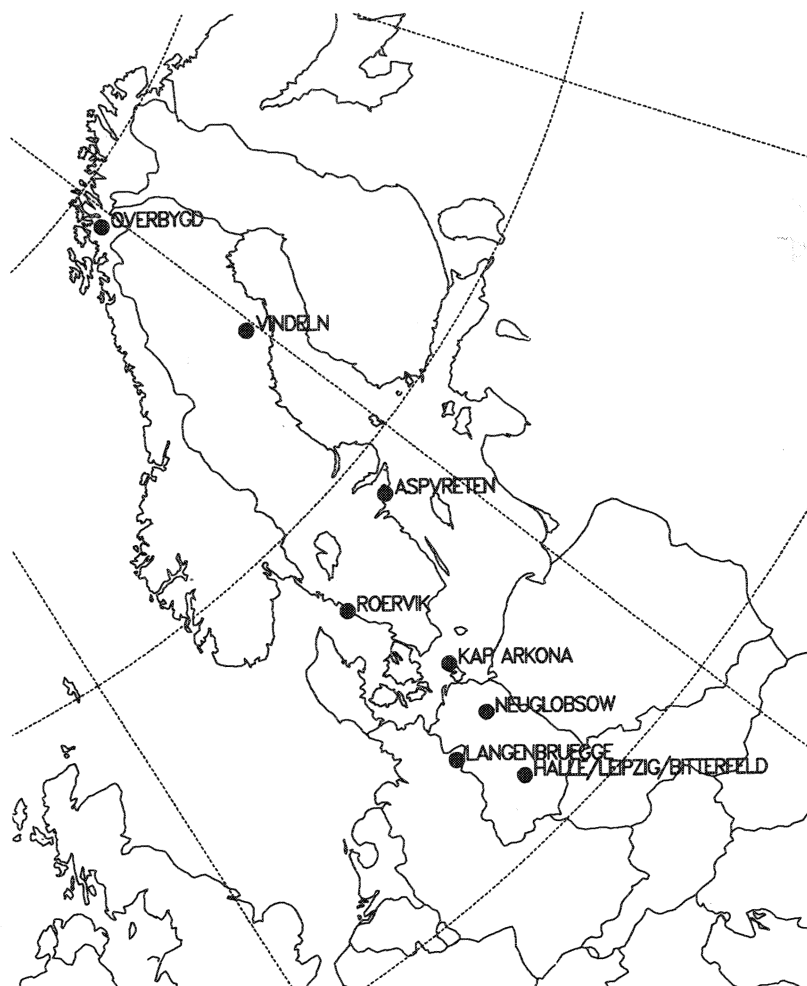


Fig. 5. Map showing location of sites involved in the evaluation of the model performance.

elemental mercury ( $\text{Hg}^0$ ) and observed total gaseous mercury ( $\text{Hg}_T$ ) is justifiable, because of the predominating elemental form at least at the Scandinavian locations far from source areas. Generally, the model predicts gaseous mercury concentrations reasonably

well at all measurement sites. The modelled results for particulate mercury show a significant south-to-north decrease due to effective dry and wet deposition of  $\text{Hg}(\text{part.})$ . The observed annual  $\text{Hg}(\text{part.})$  levels at Rörvik and Vindeln do not show a tendency to go to

lower values from south to north, possibly due to gas-to-particle conversion processes and/or local emissions of Hg(part.), which have not been taken into account by the model. However, the limited data material does not allow to draw any firm conclusions at present and a larger data set is needed to evaluate the model performance for mercury associated with airborne particles.

In Fig. 6, the 1987 results for the Swedish site of Rörvik are illustrated in more detail. This graph depicts measured and model predicted values obtained for the 24 h average concentration of Hg<sub>T</sub> and Hg<sup>0</sup>, respectively, and soot carbon as a function of time. One should note the episodic nature of the observed and calculated values for mercury, which span more than a fivefold range of concentrations, from 2 to approximately 12 ng m<sup>-3</sup>. The lower end of the range is representative of hemispheric background concentrations of mercury in air (Lindqvist and Rodhe, 1985), while the concentrations at the upper end of the range are frequently associated with high soot carbon concentrations, thus suggesting that these coinciding peaks are most probably due to long-range transport from anthropogenic sources in Central Europe. Of particular interest is the latter part of the month of March 1987, when high mercury concentrations ranging from 8 to 10 ng m<sup>-3</sup> have been observed. At two days, namely March 17 and March 24, model predicted concentrations are on the same elevated level as the observed values. These two days have been examined with reference to 96 h back trajectories, which describe the route taken during the previous 4 d period by the air masses arriving at Rörvik (Fig. 7).

The trajectories, originating in eastern Poland and in the Atlantic coast region of France, respectively, moved into the main mercury emission area of East Germany, where they changed their direction and headed northwards passing over the Baltic Sea before arriving at Rörvik. The good agreement between high observed and model predicted peak concentrations during episodes when trajectories exhibit the above described travel pattern, is an indication, that the emission inventory used with the model is based on realistic mercury emission estimates for Eastern Germany in 1987 and 1988.

The atmospheric mercury load over Central and Northern Europe is characterized by considerable temporal variability. As an example, for a winter maximum and a summer minimum, monthly averages of calculated concentrations of Hg<sup>0</sup> and Hg(part.) across the entire model domain for January and June 1988 are shown in Figs 8 and 9. The most interesting feature of comparing Figs 8a and 9a with Figs 8b and 9b, respectively, is the clear difference in spatial distribution of both species, which has to be ascribed to the difference in meteorological conditions during these two months. Due to lower mixing heights, concentrations in the mixed layer are generally higher during winter months. In January 1988, mean concentrations of Hg<sup>0</sup> in the main source areas of Central Europe are in the range 12–16 ng m<sup>-3</sup> and the concentration pattern of Hg<sup>0</sup> is substantially elongated towards Northern Europe, i.e. in the direction of the mean wind during that month (Fig. 8a). As can be seen from Fig. 9a, this elongation is less pronounced for Hg(part.), since this species has a significantly shorter

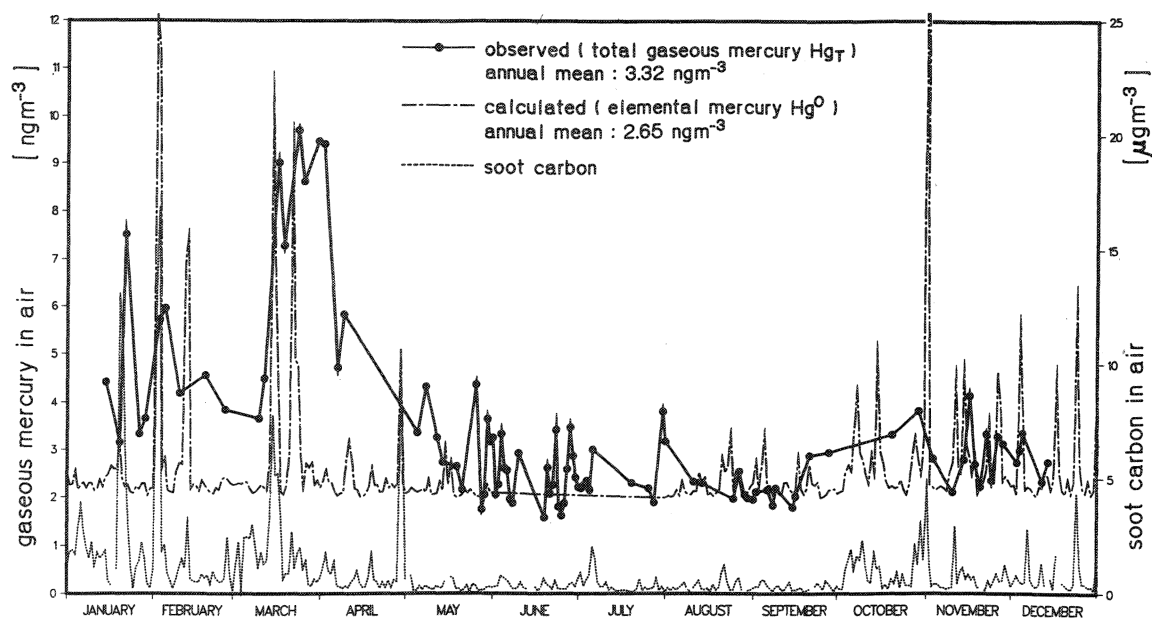


Fig. 6. Time series of daily average mercury and soot carbon concentrations in air at Rörvik for 1987 [soot carbon is derived from observed SO<sub>2</sub> according to Penner *et al.* (1993)].

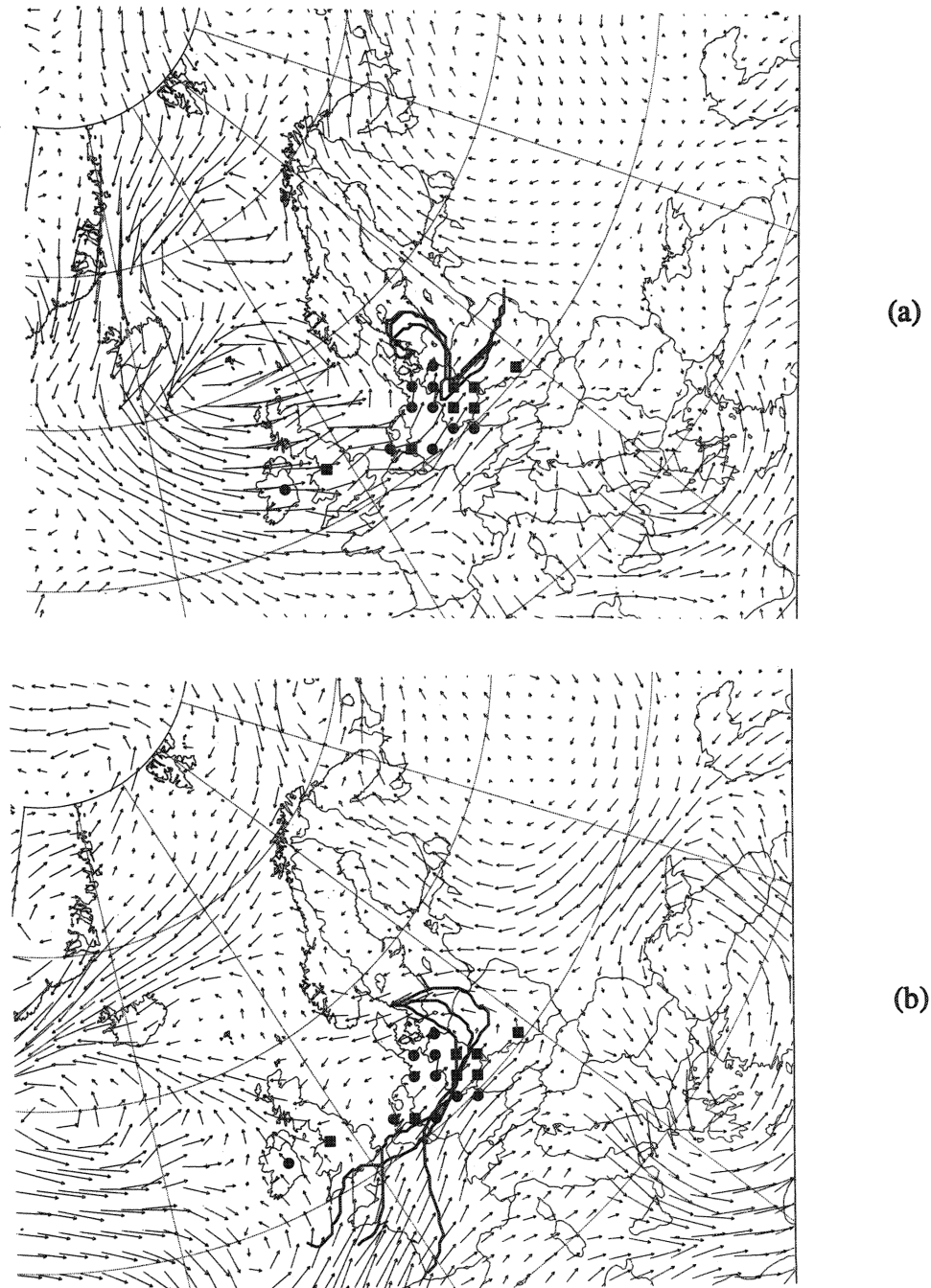


Fig. 7. 925 hPa-trajectories at 6:00, 12:00 and 18:00 GMT at Rörvik. 925 hPa-windfield at 12:00 GMT: (a) 17 March 1987; (b) 24 March 1987.

atmospheric life time mainly due to its effective dry deposition in the vicinity of the sources. The concentration patterns depicted in Figs 8b and 9b represent a typical summer minimum. The increased height of the mixing layer and a stable high pressure system over Central Europe during most of June 1988 lead to decreased levels in concentration in the main source

areas and to a very minor impact of those areas on concentration levels over Scandinavia.

### 3.2. Mercury in precipitation

According to Section 2.4 all three mercury species taken into account by the present model, i.e.  $\text{Hg}^0$ ,  $\text{Hg}(\text{part.})$  and  $\text{Hg}(\text{II})(\text{g})$  are contributing to the levels

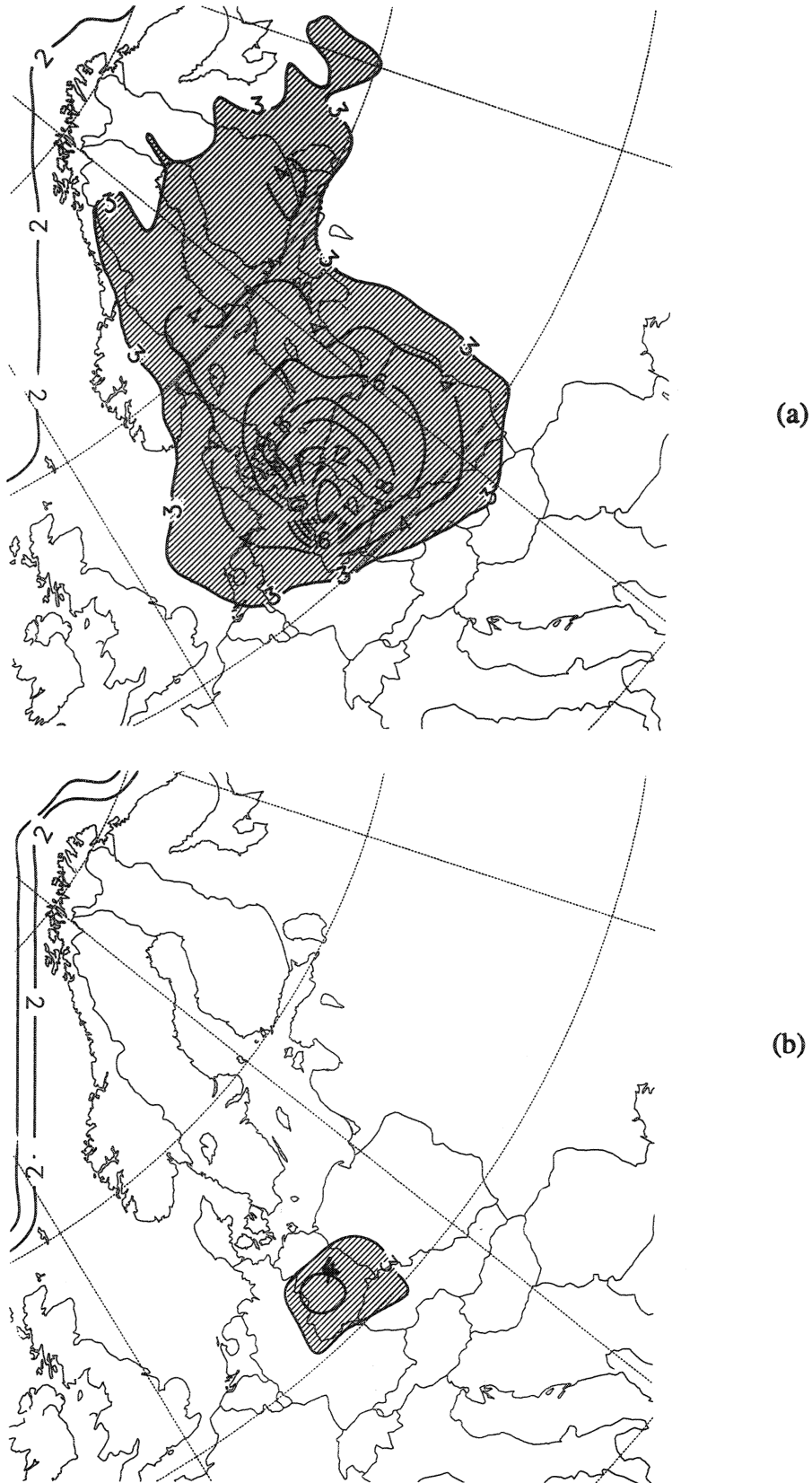


Fig. 8. Calculated monthly average of elemental mercury concentrations in air (Units: ngm<sup>-3</sup>):  
(a) January 1988; (b) June 1988.

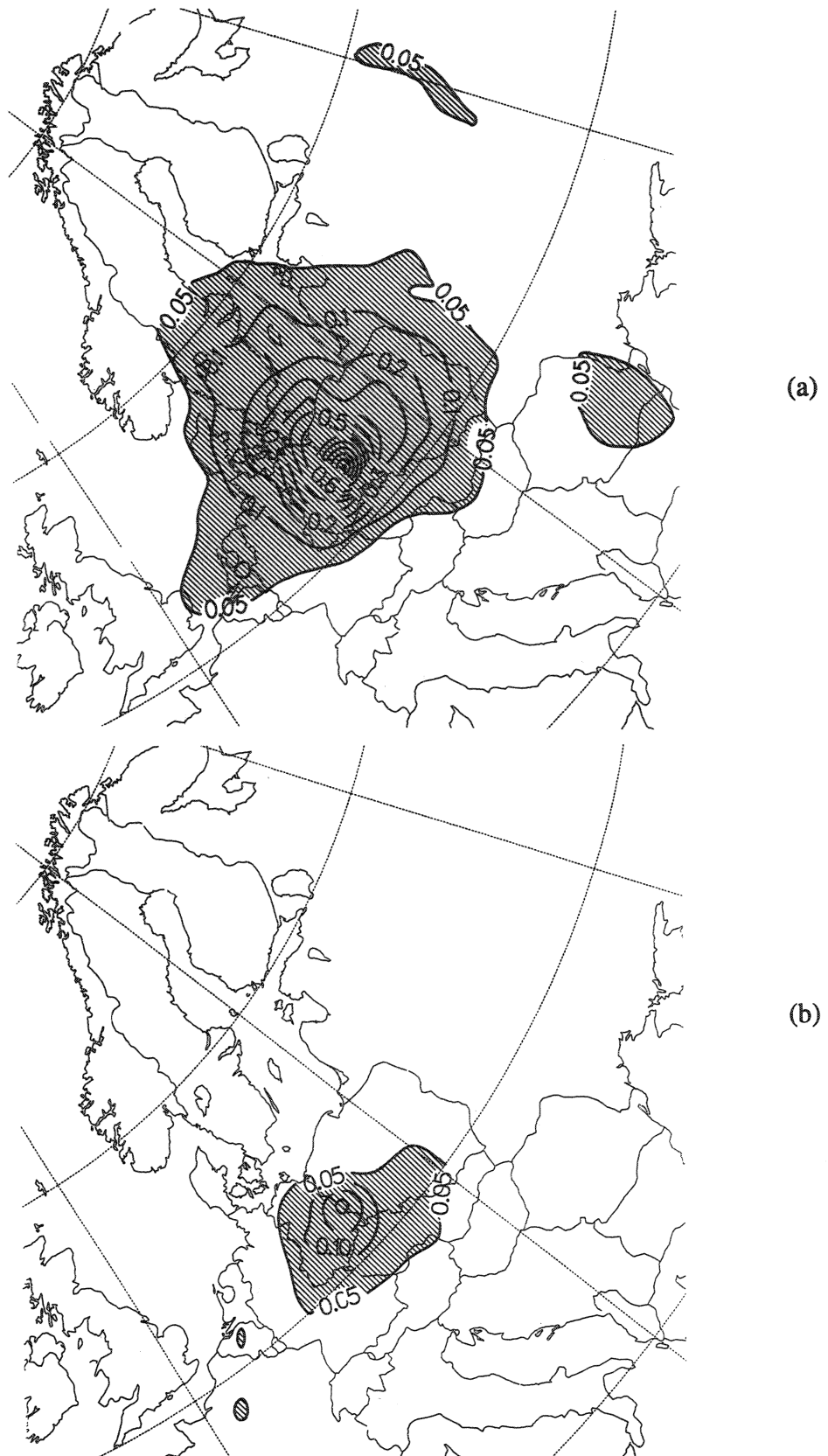


Fig. 9. Calculated monthly average of particulate mercury concentrations in air (Units:  $\text{ng m}^{-3}$ ):  
(a) January 1988; (b) June 1988.

of mercury in precipitation. However, the subsequent comparison between model predictions and field observations does not consider a possible Hg(II)(g) fraction in precipitation directly scavenged from the air, since at the measurement sites this species is present in ambient air at very low or undetectable levels (Brosset and Iverfeldt, 1989; Brosset and Lord, 1991). Concerning the physicochemical composition of mercury in precipitation the model is based on the following assumptions.

1. Total mercury concentration in precipitation (Hg-tot) consists of a dissolved fraction and of a fraction associated with particles.
2. The dissolved fraction is determined by redox processes of Hg<sup>0</sup> in the aqueous phase, i.e. the oxidation of Hg<sup>0</sup> by ozone and reduction of Hg(II)(g) by sulfite occurring simultaneously and hence building up a steady-state concentration of dissolved oxidized mercury, or according to the terminology used within the Swedish Hg research program, "reactive" mercury (Hg-IIa). This subsequently used terminology is operationally defined. It is based on the different ability of aqueous Hg compounds to be reduced to elemental mercury.
3. The fraction in association with particles is the sum of
  - (a) oxidized mercury which has been adsorbed on soot particles and
  - (b) particulate-phase mercury in air which has been scavenged by cloud droplets or rainwater.

In the model, the fractions of items 2 and 3a are calculated by equations (7) and (12), respectively. Item 3b is calculated from concentrations of Hg(part.) in air by applying a scavenging ratio of 500,000 (cf. Section 2.4).

In Table 6 average levels of observed and model predicted concentrations of reactive and total mercury in precipitation at various stations of the Nordic network and at one German station are compared. With the exception of the Aspvreten station where all precipitation events were collected and analyzed, the

average concentration values are based on a representative number ( $\geq 2$  per month) of collected events (Iverfeldt, 1991a). A clear south-to-north decrease of the calculated values is present, especially for Hg-tot but also for Hg-IIa. The observations show the same trend even though the picture is not yet complete due to missing values at various German stations. The model results are in agreement with observations within a factor of about 2, but with a tendency to overpredict Hg-IIa and underpredict Hg-tot concentrations. Results from the Aspvreten station are remarkable in that they show a very good agreement between model predicted and observed Hg-tot concentration. In this context it is especially valuable for model evaluation that the Aspvreten annual average for 1988 data is based on a large number of precipitation collections, namely more than 80 daily samples.

Figures 10 and 11 illustrate the January and June 1988 averages of calculated mercury concentration in precipitation originating from Hg<sup>0</sup> and Hg(part.), respectively, across the entire model domain. In general, Figs 10b and 11b show some qualitative similarities indicating that Hg<sup>0</sup> and Hg(part.) are accounting for approximately the same percentage of total mercury concentration in precipitation during June. However, there are some interesting differences in January concerning the maxima and the south-to-north decrease of the Hg<sup>0</sup>- and Hg(part.) fraction in precipitation (Figs 10a and 11a). For both species the maxima are located in the same area, but for Hg<sup>0</sup> clearly higher maximum values and much steeper gradients exist due to high soot carbon concentrations and hence high scavenging ratios of Hg<sup>0</sup> over Poland and Eastern Germany, suggesting that atmospheric soot carbon is a key constituent for the pattern of mercury concentration in precipitation over Central Europe.

### 3.3. Mercury deposition fluxes

The model calculates dry and wet deposition fluxes from concentrations of particle associated mercury in air and a dry deposition velocity and from total

Table 6. Comparison of modelled vs observed mean mercury concentrations in precipitation for 1988

	Reactive mercury in precipitation Hg-IIa (ng l <sup>-3</sup> )		Total mercury in precipitation Hg-tot (ng l <sup>-3</sup> )	
	Modelled	Observed	Modelled	Observed
Halle/Leipzig/Bitterfeld	9.2		330.5	
Neuglobsow	6.6		233.9	
Langenbrügge*	4.3		65.8	52.0
Kap Arkona	4.0		61.6	
Rörvik	2.3	1.9	17.4	35.0
Aspvreten	3.3	2.4	16.5	18.4
Vindeln	1.9	1.4	7.0	11.2
Överbygd	2.3	1.0	3.9	9.2

\* Observations 1992.

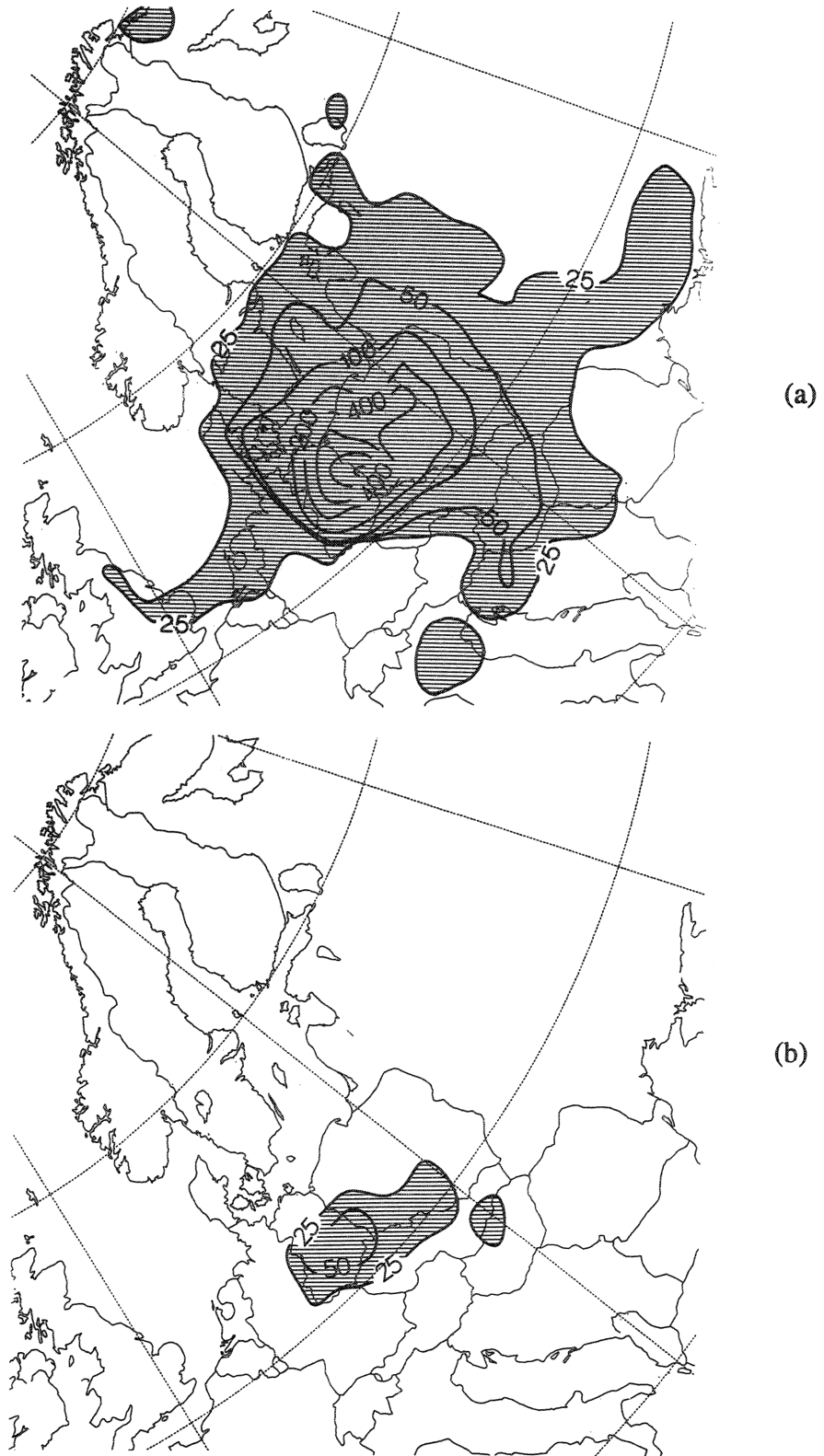


Fig. 10. Calculated monthly average of mercury concentrations in precipitation originating from elemental mercury (Units:  $\text{ng l}^{-1}$ ): (a) January 1988; (b) June 1988.

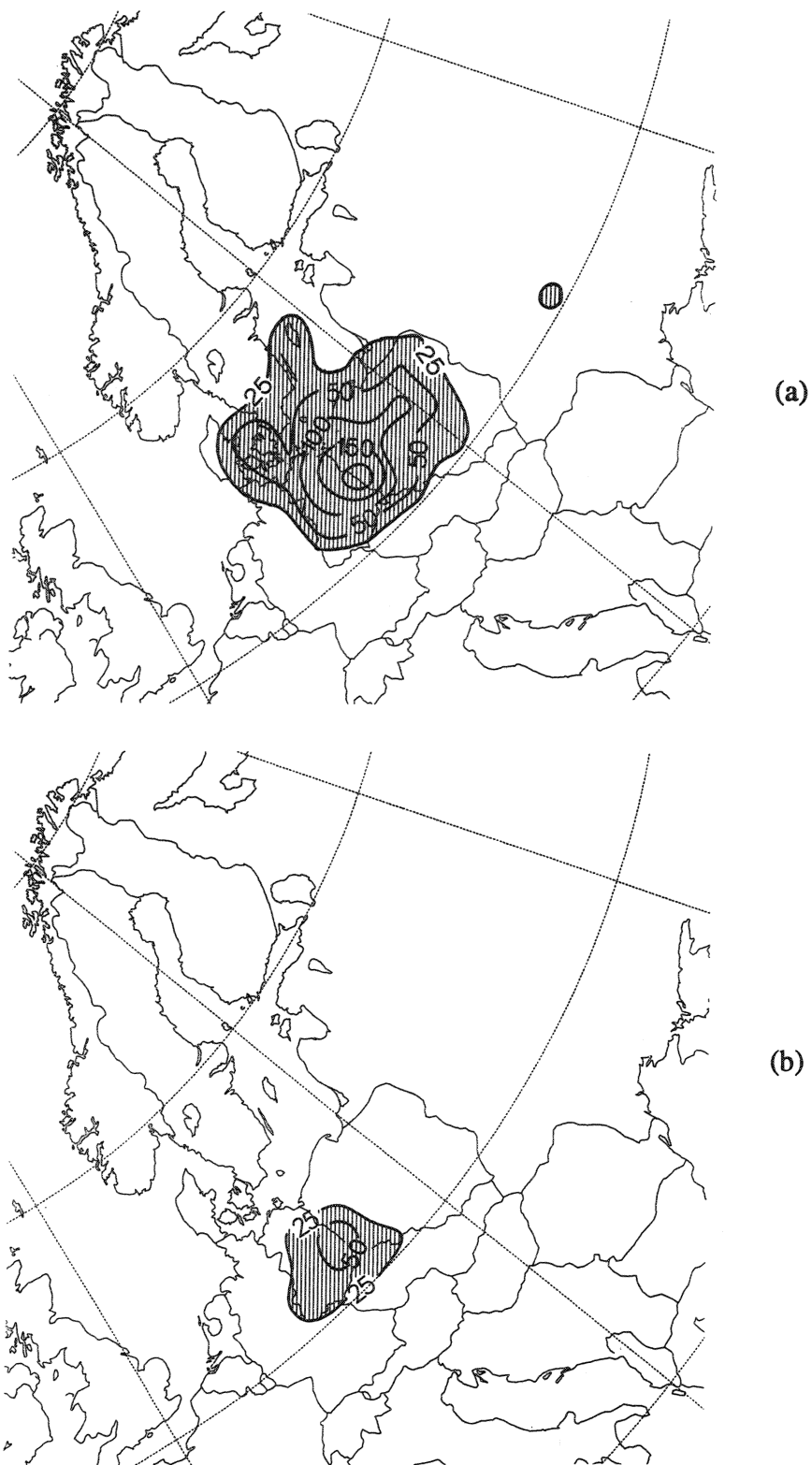


Fig. 11. Calculated monthly average of mercury concentrations in precipitation originating from particulate mercury (Units:  $\text{ng l}^{-1}$ ): (a) January 1988; (b) June 1988.

Table 7. Comparison of modelled vs observed mercury deposition fluxes for 1988

	Dry deposition of particulate mercury ( $\mu\text{g m}^{-2} \text{a}^{-1}$ )		Wet deposition of mercury ( $\mu\text{g m}^{-2} \text{a}^{-1}$ )	
	Modelled	Observed	Modelled	Observed
Halle/Leipzig/Bitterfeld	17.5		114.3	
Neuglobsow	13.1		94.5	
Langenbrügge	7.0		38.8	
Kap Arkona	6.8		46.1	
Rörvik	1.4		15.4	27.0
Aspvreten	1.2		10.2	10.1
Vindeln	0.3		4.9	7.3
Överbygd	0.1		2.1	5.0

mercury concentration in precipitation and the precipitation amount, respectively. In Table 7, model predicted annual dry and wet deposition fluxes are given together with estimated wet fluxes from measured annual averages of concentrations and precipitation amount. Due to the scarcity of observations, comparisons can be made for wet fluxes at the Nordic network stations only (Iverfeldt, 1991a). The agreement of these data is similar to that for Hg-tot in Table 6 indicating that the model predicts precipitation amounts reasonably well at these sites. The somewhat higher observed wet deposition value at Rörvik was first thought to be due to an overrepresentation of elevated concentration values, since the average concentration and the annual rainfall was used in the calculation (Iverfeldt, 1991a). However, even if the values are weighted by the actual observed rainfall amount at each event, a very similar value is derived.

The emission databases for  $\text{Hg}^0$ ,  $\text{Hg}(\text{part.})$  and  $\text{Hg}(\text{II})(\text{g})$  have been used to calculate the atmospheric input of mercury to the North Sea and the Baltic Sea. The model runs are based on two different scenarios:

1. Mercury in the European atmospheric environment is restricted to species which have been definitely observed at the various stations of the Nordic network, i.e.  $\text{Hg}^0$  and  $\text{Hg}(\text{part.})$ .
2. Scenario 1 plus emissions of  $\text{HgCl}_2$ . Implementing the emission inventory for this species gives about 100% higher wet deposition fluxes over Southern Scandinavia and the southern parts of the North Sea and the Baltic, whereas  $\text{HgCl}_2$  deposition in the northern parts of these areas is negligibly small. However, evaluation of the model performance is not possible for this scenario because of a total lack of  $\text{HgCl}_2$  measurements in air and because of the fact that a possible contribution from  $\text{HgCl}_2$  to the total mercury in precipitation is not discernible from other oxidized mercury species.

Figure 12 illustrates the potential exposure of the North Sea and the Baltic to the above defined emission scenarios. Comparison between the lower full lines (scenario 1) and the upper chain-dashed lines

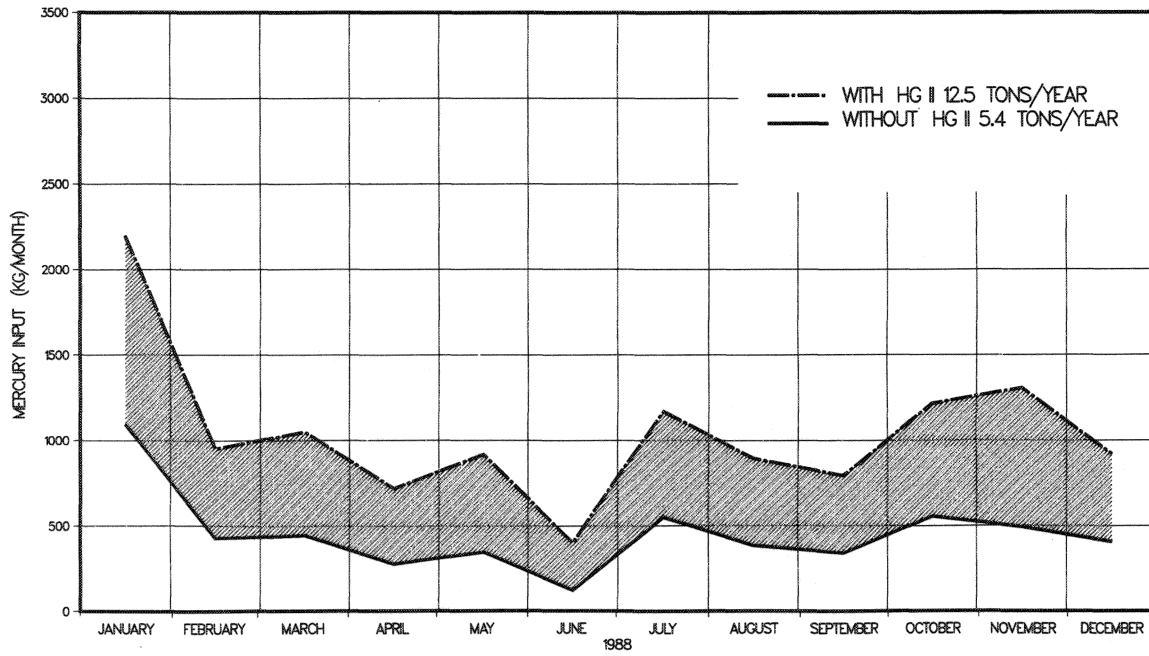
(scenario 2) reveals the substantial influence of  $\text{HgCl}_2$  emissions on the atmospheric mercury input to the two sea areas. According to the present state-of-science, however, results from scenario 1 have to be considered as a more realistic estimate. To improve the reliability of results derived from scenario 2 suitable atmospheric measurements for mercury species identification would be necessary to confirm the existence of  $\text{HgCl}_2$  in the main source areas of Central Europe.

#### 4. SUMMARY AND CONCLUSIONS

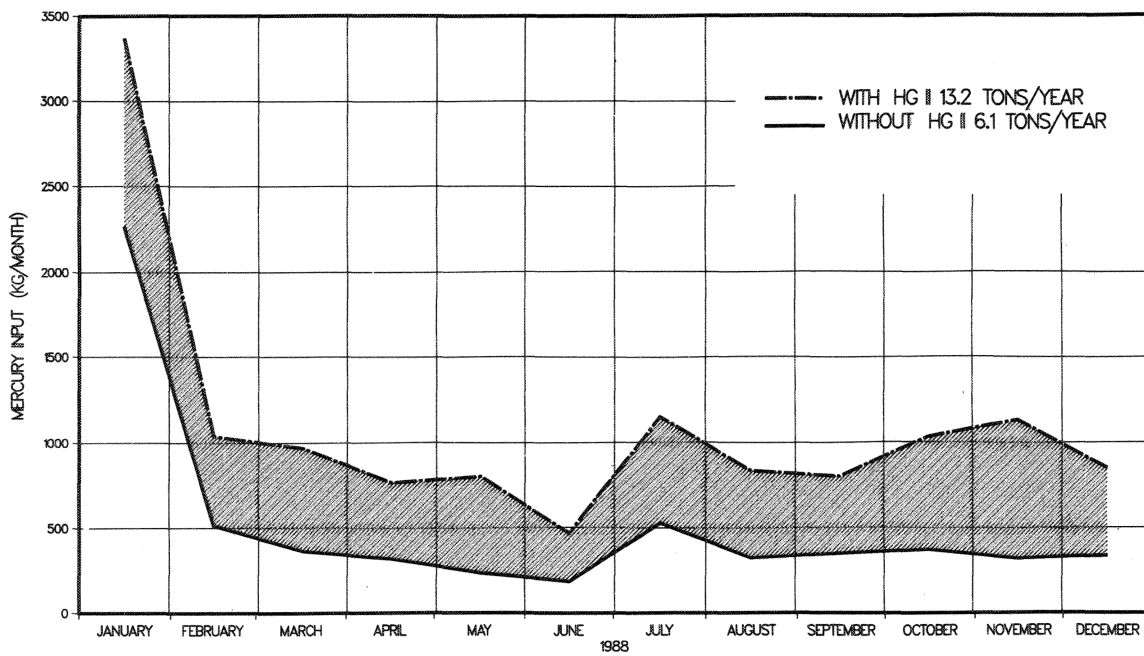
A numerical model for atmospheric long-range transport, chemical transformations and deposition of three mercury species, namely elemental mercury in the vapor phase ( $\text{Hg}^0$ ), mercury associated with particles ( $\text{Hg}(\text{part.})$ ) and divalent inorganic mercury compounds  $\text{Hg}(\text{II})(\text{g})$  was presented. Model results for  $\text{Hg}^0$  and  $\text{Hg}(\text{part.})$  were compared with 1987 and 1988 observations from various stations of the Nordic air and precipitation network and estimates of atmospheric mercury input to the North Sea and the Baltic Sea based on two different emission scenarios were given. The evaluation of the model performance led to three main issues:

(1) In general, modelled annual average concentrations of  $\text{Hg}^0$  in air were shown to compare satisfactorily with observations from all stations of the Nordic network and one station in Germany. Coinciding peaks in calculated and observed daily average concentrations at one station in southern Sweden indicate, that the emission database for  $\text{Hg}^0$  used with the model calculations is based on realistic estimates of emission peaks in the main source areas of Central Europe. However, the scarcity of  $\text{Hg}(\text{part.})$  measurements and uncertainties in the quality of these data are such that no firm conclusion can be drawn from the comparison of observed and calculated  $\text{Hg}(\text{part.})$  concentrations at present.

(2) Modelled annual average concentrations of mercury in precipitation both dissolved or "reactive" mercury ( $\text{Hg-IIa}$ ) and total mercury ( $\text{Hg-tot}$ ) agreed



North Sea



Baltic Sea

Fig. 12. Time series of monthly atmospheric input of mercury to the North Sea and Baltic Sea for 1988.

within a factor of about 2 with observed values, thus indicating that the model is capable of reproducing the observed south-to-north gradients in concentration of Hg-tot and Hg-IIa. At the Aspveten station in Central Sweden, modelled Hg-tot concentrations were shown to compare well with observations even on a daily basis. These results together with a good correlation between elevated levels in calculated Hg-tot and soot carbon concentrations do suggest that the chemical scheme in the model is based on an adequate parametrization of aqueous-phase chemistry, i.e. redox reactions of Hg<sup>0</sup> and adsorption of oxidized Hg on soot particles.

(3) The lower end of the range of model predicted atmospheric input of mercury to the North Sea and Baltic Sea is considered to be reliable since it is based on species which have definitely been observed in the adjacent Scandinavian countries and for which the model is sufficiently validated. The additional HgCl<sub>2</sub> emission input in the model was shown to lead to an increase in mercury deposition to both of the sea areas of about 100%, but the existence of this species far from sources and hence the upper end of the estimated range is subject to considerable uncertainty at present.

Overall, measurements from the Nordic air and precipitation network are quite well reproduced by the model, despite their relatively wide geographical separation. Measurements at German stations, which are presently underway, will provide better spatial coverage and will improve the reliability of model predictions. Further evaluation of the model requires the availability of accurate measurements, especially for Hg(II)(g) but also for Hg(part.) preferably in the main source areas of Central Europe.

Finally, further progress in understanding the atmospheric mercury cycle would emphasize the need for comprehensive Eulerian regional and mesoscale grid models which are comprised of a series of modules with a more detailed description of emissions, transport, gaseous and aqueous chemistry, cloud mixing and scavenging, and dry and wet deposition of mercury species at different vertical levels in the entire troposphere.

*Acknowledgements*—The authors wish to acknowledge the financial support for this work which was provided by the German Umweltbundesamt, research contract no. 104 02 726. Thanks are due to Dr W. H. Schroeder, Environment Canada, Atmospheric Environment Service and to Dr R.-D. Wilken, Dr R. Ebinghaus and their group at the GKSS Institute of Chemistry for supplying data for model development and evaluation and to Dr B. Schneider, Institut für Meereskunde an der Universität Kiel, Germany, for reviewing the chemical scheme used in the model.

#### REFERENCES

- Ahmed R., May K. and Stoepler M. (1987) Ultratrace analysis of mercury and methylmercury (MM) in rainwater using cold vapour atomic absorption spectroscopy. *Fresenius Z. analyt. Chem.* **326**, 510–516.
- Andreae M. O., Andreae T. W., Ferek R. J. and Raemdonck H. (1984) Long range transport of soot carbon in the marine atmosphere. *Sci. total Envir.* **36**, 73–80.
- Axenfeld F., Münch J. and Pacyna J. (1991) Europäische Test-Emissionsdatenbasis von Quecksilberkomponenten für Modellrechnungen. Umweltforschungsplan des Bundesministers für Umwelt, Naturschutz und Reaktorsicherheit—Luftreinhaltung—104 02 726. (See Petersen G. (1992b).)
- Bergström J. (1986) Mercury behavior in flue gases. *Waste Manag. Res.* **4**, 57–64.
- Bloom N. S. and Fitzgerald W. F. (1988) Determination of volatile mercury species at the picogram level by low-temperature gas chromatography with cold-vapor atomic fluorescence detection. *Analyt. Chim. Acta* **208**, 151–161.
- Brosset C. (1982) Total airborne mercury and its possible origin. *Water Air Soil Pollut.* **17**, 37–50.
- Brosset C. (1987) The behavior of mercury in the physical environment. *Water Air Soil Pollut.* **34**, 145–166.
- Brosset C. and Iverfeldt A. (1989) Interaction of solid gold with mercury in ambient air. *Water Air Soil Pollut.* **34**, 147–169.
- Brosset C. and Lord E. (1991) Hg in precipitation and ambient air. A new scenario. *Water Air Soil Pollut.* **56**, 493–506.
- Cachier H., Bremond M. P. and Buat-Menard P. (1990) Organic and black carbon aerosols over marine regions of the Northern Hemisphere. *Proc. Int. Conf. on Global Atmospheric Chemistry*, Beijing, 1989 (edited by Newman and Kian), pp. 249–261.
- Eliassen A. and Saltbones J. (1983) Modelling of long-range transport of sulphur over Europe: a two-year model run and some model experiments. *Atmospheric Environment* **17**, 1457–1473.
- Ferrara R., Maserti B. E., Morelli M., Edner H., Ragnarson P., Svanberg S. and Wallinder E. (1991) Vertical distribution of atmospheric mercury concentration over a cinnabar deposit. In *Proc. Int. Conf. on Heavy Metals in the Environment*, Edinburgh, 1991 (edited by Farmer J. G.), Vol. 1, pp. 247–250.
- Ferrara R., Maserti B. and Petrosino A. (1986) Mercury levels in the Atlantic and Mediterranean waters and in the Strait of the Tyrrhenian Sea. In *Rapp. Proces-Verb. Reunions, XXX Congr.*, Mallorca, Abstract C-17, 35, Monaco, CIEM.
- Ferrara R., Petrosino A., Maserti E. and Barghigiani C. (1982) The biogeochemical cycling of mercury in the Mediterranean. Part 2: mercury in the atmosphere, aerosol and in rainwater of a Northern Tyrrhenian area. *Envir. Technol. Lett.* **3**, 449–456.
- Graß H., Eppel D. P., Petersen G., Schneider B., Weber H., Gandraß J., Reinhardt K. H., Wodarg D. and Fließ J. (1989) Stoffeintrag in Nord- und Ostsee über die Atmosphäre. Umweltforschungsplan des Bundesministers für Umwelt, Naturschutz und Reaktorsicherheit—Luftreinhaltung—104 02 572. GKSS 89/E/8 External Report, GKSS Research Centre, D-21502 Geesthacht, Germany.
- Grennfelt P., Saltbones J. and Schjoldager J. (1987) Oxidant Data Collection in OECD-Europe 1985–87 (OXIDATE). NILU OR: 22/87; Norwegian Institute for Air Research, Postboks 64, N-2001 Lillestrom, Norway.
- Gronas G. and Hellevik O. (1982) A limited area prediction model at the Norwegian Meteorological Institute. Technical Report No. 61, Det Norske Meteorologiske Institutt, Oslo, Norway.
- Hellwig A. and Neske P. (1990) Zur komplexen Erfassung von Quecksilber in der Luft. In *Aktuelle Aufgaben der Meßtechnik in der Luftreinhaltung*, VDI-Berichte 838, pp. 457–466. VDI-Verlag Düsseldorf, Germany.
- Iverfeldt Å. (1991a) Occurrence and turnover of atmospheric mercury over the nordic countries. *Water Air Soil Pollut.* **56**, 151–165.

- Iverfeldt Å. (1991b) Mercury in forest canopy throughfall water and its relation to atmospheric dry deposition. *Water Air Soil Pollut.* **56**, 553–564.
- Iverfeldt Å. and Lindqvist O. (1986) Atmospheric oxidation of elemental mercury by ozone in the aqueous phase. *Atmospheric Environment* **20**, 1567–1573.
- Iversen T., Halvorsen N. E., Mylona S. and Sandnes H. (1991) Calculated budgets for airborne acidifying components in Europe 1985, 1987, 1988, 1989 and 1990. EMEP/MSC-W Report 1/91.
- Krüger O. (1993) Europaweite Deposition von Schwefel- und Stickstoffverbindungen: Neue Ansätze bei Trocken- und Naßdeposition. Ph.D. thesis, University of Hamburg, Germany. GKSS 93/E/23 External Report, GKSS Research Centre, D-21502 Geesthacht, Germany.
- Lindberg S. E., Turner R. R., Meyers T. P. and Schroeder W. H. (1991) Atmospheric concentrations and deposition of Hg to a deciduous forest at Walker Branch Watershed, Tennessee, USA. *Water Air Soil Pollut.* **56**, 577–594.
- Lindqvist O. and Rodhe H. (1985) Atmospheric mercury — a review. *Tellus* **37B**, 136–159.
- Lindqvist O. and Schager P. (1990) *Continuous Measurement of Mercury in Flue Gases from Waste Incinerators and Combustion Plants*. VDI-Berichte 838, pp. 401–422.
- Lindqvist O., Johansson K., Aastrup M., Andersson A., Bringmark L., Hovsenius G., Håkanson L., Iverfeldt Å., Meili M. and Timm B. (1991) Mercury in the Swedish environment. Recent research on causes, consequences and corrective methods. *Water Air Soil Pollut.* **55**.
- Munthe J. (1992) The aqueous oxidation of elemental mercury by ozone. *Atmospheric Environment* **26A**, 1461–1468.
- Munthe J. and McElroy W. (1992) Some aqueous reactions of potential importance in the atmospheric chemistry of mercury. *Atmospheric Environment* **26A**, 553–557.
- Munthe J., Xiao Z. F. and Lindqvist O. (1991) The aqueous reduction of divalent mercury by sulfite. *Water Air Soil Pollut.* **56**, 621–630.
- Nordeng T. E. (1986) Parametrization of physical processes in a three-dimensional weather prediction model. Technical Report No. 65, Det Norske Meteorologiske Institutt, Oslo, Norway.
- Penner J. E., Eddleman H. and Novakov T. (1993) Towards the development of a global inventory for black carbon emissions. *Atmospheric Environment* **27A**, 1277–1295.
- Petersen G. (1992a) Numerische Modellierung des Transports und der chemischen Umwandlung von Quecksilber über Europa. Ph.D. thesis, University of Hamburg, Germany. GKSS 92/E/51 External Report, GKSS Research Centre, D-21502 Geesthacht, Germany.
- Petersen G. (1992b) Belastung von Nord- und Ostsee durch ökologisch gefährliche Stoffe am Beispiel atmosphärischer Quecksilberverbindungen. Umweltforschungsplan des Bundesministers für Umwelt, Naturschutz und Reaktorsicherheit—Luftreinhaltung—104 02 726. GKSS 92/E/111 External Report, GKSS Research Centre, D-21502 Geesthacht, Germany.
- Petersen G., Weber H. and Graßl H. (1989) Modelling the atmospheric transport of trace metals from Europe to the North Sea and Baltic Sea. *Control and Fate of Atmospheric Trace Metals* (edited by Pacyna J. M. and Ottar B.), NATO-ASI Series, Series C: Mathematical and Physical Sciences Vol. 68, pp. 57–83. Kluwer Academic Publishers, Dordrecht.
- Sanemasa I. (1975) The solubility of elemental mercury vapor in water. *Bull. chem. Soc. Japan* **48**, 480–484.
- Schroeder W. H. (1982) Sampling and analysis of mercury and its compounds in the atmosphere. *Envir. Sci. Technol.* **16**, 394A–400A.
- Schroeder W. H. and Jackson R. A. (1987) Environmental measurements with an atmospheric mercury monitor having speciation capabilities. *Chemosphere* **16**, 183–199.
- Schroeder W. H., Yarwood G. and Niki H. (1991) Transformation processes involving mercury species in the atmosphere—results from a literature survey. *Water Air Soil Pollut.* **66**, 203 (1993).
- Simpson D. (1991) Long period modelling of photochemical oxidants in Europe. Calculations for April–September 1985, April–October 1989. EMEP MSC-West Report 2/91.
- Simpson D. (1992) Long period modelling of photochemical oxidants in Europe. Model calculations for July 1985. *Atmospheric Environment* **26A**, 1609–1634.
- Xiao Z. F., Munthe J., Schroeder W. H. and Lindqvist O. (1991) Vertical fluxes of volatile mercury over forest soil and lake surfaces in Sweden. *Tellus* **43B**, 267–269.



# Paper II



# NUMERICAL MODELING OF REGIONAL TRANSPORT, CHEMICAL TRANSFORMATIONS AND DEPOSITION FLUXES OF AIRBORNE MERCURY SPECIES

G. PETERSEN

*GKSS Research Center, Institute of Hydrophysics,  
Max-Planck-Strasse, D-21502 Geesthacht, Germany*

J. MUNTHE

*Swedish Environmental Research Institute (IVL),  
P.O.Box 47086, S-402 58 Goeteborg, Sweden*

R. BLOXAM

*Ontario Ministry of Environment and Energy,  
Science and Technology Branch,  
2 St.Clair Ave W, Toronto, ON M4V 1L5, Canada*

*Abstract.* This article reviews current knowledge of atmospheric mercury processes and describes activities in Europe and North America to simulate these processes by means of tropospheric chemistry/transport models for regional-scale applications. Advantages and limitations of relatively simple Lagrangian models are discussed within the context of issues currently facing the environmental scientific and policy-making communities. The current state and future direction of comprehensive Eulerian models in simulating the tropospheric chemistry and transport of mercury species is outlined. A number of central improvements in these models are discussed, with consideration of the key progress necessary to include feedbacks and interactions between formation and distribution of clouds and mercury atmospheric chemistry.

## 1. Introduction

The dispersion of atmospheric mercury emitted from point and areal sources is a process comprising local, regional and global geographical scales [7]. The present state of knowledge is mainly focused on environmental problems related to regional Hg dispersion and deposition. The mechanisms, major transport pathways and effects of mercury as a regional pollutant have been presented in a number of reports and conference proceedings including those from the international 'Mercury as a Global Pollutant' conferences and national summaries of research [24] [25] [34] [45]. The

resulting geographical scale of mercury dispersion from an emission source is governed by a series of atmospheric processes and chemical parameters where the changing mercury speciation is of central importance. The complexity of these physico-chemical processes makes results from comprehensive mercury measurement programs difficult to interpret without a clear conceptual model of the workings of the atmosphere. Further, measurements alone cannot be used directly by policy-makers to form balanced and cost-effective strategies for dealing with this problem: an understanding of individual processes within the atmosphere does not automatically imply an understanding of the entire system. A complete picture of individual mercury processes and their interactions with the atmospheric system as a whole can only be obtained by means of numerical modeling.

In a broad sense, two basic types of models have been developed to date, wherein the turbulent transport of mercury species is analyzed through either a Lagrangian or an Eulerian approach. Lagrangian models developed for mercury and currently in use are variants of the so-called trajectory models. These models are usually formulated under assumptions of simplified turbulent diffusion, no convergent or divergent flows, and no wind shear. In these approaches only first-order chemical reactions can be treated rigorously. However, the Lagrangian approach avoids many of the computational complexities associated with the simultaneous solution of many differential equations; this generally results in requiring significantly less computational resources and can facilitate an understanding of problems that do not require descriptions of interactive nonlinear processes. Further progress in understanding the atmospheric mercury cycle has emphasized the need for direct modeling of the complex nonlinear mercury chemistry of the atmosphere by comprehensive Eulerian models. These approaches employ extensive gas- and aqueous-phase chemical mechanisms and explicitly track numerous mercury species concentrations. Also, a more detailed numerical formulation for physical and chemical processes occurring within and below precipitating clouds is included. Typically, these models contain modules designed to calculate explicitly the chemical interactions that move gas-phase mercury into and among the various aqueous phases within clouds as well as calculate the aqueous-phase chemical transformations that occur within cloud and precipitation droplets.

In section 2, the state of knowledge on mercury species and their atmospheric processes from their inception in the 1970s through their most recent formulations is described. Section 3 discusses regional-scale atmospheric transport/chemistry models currently in use or under development. In this section, emphasis is given to individual physical and chemical mercury processes that are incorporated into a comprehensive Eulerian model. Finally, in section 4, conclusions are summarized and desirable features of future model developments are enumerated.

## 2. Atmospheric Processes of Mercury Species

### 2.1. MERCURY IN AIR

Several attempts have been made to speciate the mercury content of ambient air. The reason for this interest is that different forms of mercury will behave differently in air due to their different physical and chemical properties. While elemental mercury,  $\text{Hg}^0$ , is a relatively stable long-lived species, oxidized ( $\text{Hg(II)}$ ), methylated ( $\text{MeHg}$ ) and particulate ( $\text{HgP}$ ) forms will be rapidly removed from air by dry deposition or wash-out processes due to their higher water solubility.

The presence of different forms of Hg in ambient air has been investigated since the seventies. While measurements of total airborne Hg can be made with good reproducibility the development of reliable techniques for sampling and analysis of different Hg species is less straightforward due to the low concentrations present in air and to the risks for chemical conversion during the process.

#### 2.1.1. Total atmospheric mercury

Atmospheric Hg mainly consists of elemental Hg vapor at background concentrations around 1 to 4  $\text{ng m}^{-3}$  [3] [4] [9] [25] [41]. Measurements are today being made on a routine basis at a number of sites in Europe and North America, most often using gold trap techniques and atomic fluorescence or atomic absorption for detection. Recent data suggest that atmospheric Hg concentrations may be slowly increasing on a hemispheric or global scale [10] [42] but also that a significant decrease has occurred in Scandinavia during the last few years [19].

#### 2.1.2. Oxidized, methylated and particulate mercury in air

A small but significant fraction of the atmospheric Hg consists of vapor phase oxidized  $\text{Hg(II)}$ , gaseous  $\text{MeHg}$  and particulate bound species  $\text{HgP}$ . Several attempts have been made during the last few years to sample and detect these species in air. Of the three species,  $\text{Hg(II)}$  and  $\text{HgP}$  are of great importance for the total deposition of Hg from the atmosphere [31]. Although these species are typically present at less than 10 % of the total atmospheric Hg, they may still influence the deposition flux of Hg significantly.  $\text{MeHg}$  in air will not influence the deposition of Hg to any greater extent. It may, however, constitute an important contribution to the overall loadings of  $\text{MeHg}$  in terrestrial and aquatic ecosystems [16].

A summary of recently measured concentrations of  $\text{Hg(II)}$ ,  $\text{HgP}$  and  $\text{MeHg}$  in continental background air is given in Table 1. The presented concentrations represent examples of data from areas not directly influenced by local sources. In urban and industrial sites, considerably higher concentrations can be found, at least for  $\text{HgP}$ .

Some uncertainties still remain concerning the accuracy of the applied techniques.  $\text{HgP}$  and  $\text{Hg(II)}$  may be generated during sampling via chemical conversion of  $\text{Hg}^0$ . For  $\text{MeHg}$  the major difficulty is the low concentrations found in air which requires long sampling times and extremely good analytical capabilities.

Presently, no generally accepted method for sampling and analysis of these species

is available but many attempts of development and refinement are being made using different approaches such as mist chambers for Hg(II) [43], denuder separation [47] as well as filters [21] for HgP and aqueous stripping for MeHg [5]. Further development and method intercomparisons are needed before comparable data on these species can be generated on a more regular basis.

TABLE 1. Typical concentrations of Hg species in air ( $\mu\text{g m}^{-3}$ )

Species	Concentration range	Reference
HgP	1 to 86	Keeler [21]
Hg(II)	50 to 150	Stratton and Lindberg [43]
MeHg	< 1 to 8	Brosset and Lord [5]

## 2.2. MERCURY IN PRECIPITATION

Wet and dry deposition are equally important sources of Hg to forested ecosystems [17] [30]. In continental open field sites and marine location, wet processes are likely to be dominant.

Hg in rain is present in both the dissolved and the particulate phases. An exact chemical speciation is, in most cases, not possible to make due to the low concentrations of the individual species. Operational classification is sometimes used based on different analytical procedures [4]. This classification is often used to express the Hg concentrations as total Hg and reactive Hg. Total Hg is determined after chemical destruction of stable forms of Hg in the sample (oxidation or digestion) and reactive Hg is analyzed without extensive pretreatment of the sample and corresponds to dissolved inorganic forms of Hg.

A major fraction of the total Hg is associated with particles, at least in industrialized and urban regions [1] [8] [18]. The origin of the particulate bound Hg in precipitation is probably both wash-out or rain-out of HgP in air and adsorption of Hg compounds on soot particles in the cloud- and raindrops. Total Hg concentrations are generally in the range 2 to 100  $\text{ng l}^{-1}$  in remote or moderately affected areas [15] [18] [30]. The particulate fraction of this varies between less than 10 percent at remote sites up to > 90 % at polluted sites [18].

Methylmercury (MeHg) is present in precipitation at concentrations generally corresponding to around 5 % of the total Hg [2] [16] [30]. The source of this MeHg is not known. Several different sources are in principle possible such as formation of MeHg from  $\text{Hg}^0$  or Hg(II) in atmospheric reactions, volatilization of MeHg (or more volatile precursor species such as dimethylmercury) from anthropogenic sources. Combustion of fossil fuels or waste incineration was earlier thought to be of major importance but has recently been shown to be negligible or of minor importance [35]. The question of the origin of atmospheric MeHg remains one of the major sources of uncertainty when trying to evaluate the environmental impact of Hg emissions from specific sources.

### 2.3. ATMOSPHERIC REACTIONS OF IMPORTANCE

The major goal of studies of the atmospheric cycling of Hg is to be able to describe the pathways of transport and transformation of Hg on its way from emissions to deposition and possibly re-emissions. This knowledge can then be applied to make future predictions of Hg deposition, optimizing pollution control measures as well as for estimating how a specific region is affected by Hg emissions in other areas.

The main mechanisms for the wet removal of inorganic Hg from the atmosphere are direct wash- or rain-out of water soluble or particulate forms of Hg and oxidation of  $\text{Hg}^0$ . The oxidation of  $\text{Hg}^0$ , and consequently the transfer of Hg into cloud and rain drops, can be described via a set of key chemical reactions. These include oxidation of  $\text{Hg}^0$  to  $\text{Hg(II)}$  by ozone in the aqueous phase, formation of compounds of  $\text{Hg(II)}$  and various ligands (e.g.  $\text{Cl}^-$ ) and reduction of  $\text{Hg(II)}$  back to  $\text{Hg}^0$ . The concentration of  $\text{Hg(II)}$  is a function of the concentrations of  $\text{O}_3$ ,  $\text{SO}_2$ , pH etc., in a reaction system. Under given conditions, the  $\text{Hg(II)}$  concentrations in cloud- or raindrops is in a state of "dynamic equilibrium", i.e. when the rate of oxidation of  $\text{Hg}^0$  equals the rate of reduction of  $\text{Hg(II)}$  [28] [29].

## 3. Status of Current Atmospheric Chemistry/Transport Models

A variety of modeling techniques are being developed for exploration of atmospheric mercury processes. These include global cycle models that examine mercury exchange between various environmental compartments as well as local- and regional-scale models attempting to simulate the atmospheric transport and transformation of mercury over domains of several tens and hundreds to thousands of kilometers, respectively. In this section, existing local- and regional-scale models are briefly touched and an outline of how a comprehensive regional-scale Eulerian model is being advanced to address future demands on simulating atmospheric mercury processes is given.

### 3.1. MODELS IN USE

The first operational models for atmospheric transport and transformation of mercury were designed for different spatial and temporal scales and for different treatment of the mercury chemistry: A long-range transport model based on the Lagrangian approach of the EMEP Meteorological Synthesizing Center West with a simplified mercury chemistry scheme [31] and two local-scale models with a more detailed description of the chemistry in gas and aqueous phases [32] [33] [39].

The long-range transport model was applied over Europe to estimate mercury air concentration and deposition gradients keeping track of the most significant emitted inorganic species from a deposition perspective, i.e. vapor-phase elemental mercury ( $\text{Hg}^0$ ), divalent inorganic mercury compounds  $\text{Hg(II)}$ , and mercury associated with particles  $\text{HgP}$ . The model has been run for two full years, 1987 and 1988. The results

show that the atmospheric mercury load over Central Europe was characterized by considerable temporal variability during those two years. As an example for a winter maximum and a summer minimum, monthly averages of calculated concentrations of vapor-phase elemental mercury across the entire model domain for January and June 1988 are shown in Figure 1. Due to lower mixing heights, concentrations in the mixed layer are generally higher in winter months. In January 1988, mean concentrations of  $\text{Hg}^0$  in the main source areas of Central Europe were in the range of 12-16  $\text{ng m}^{-3}$  and the concentration pattern of  $\text{Hg}^0$  is substantially elongated towards Northern Europe, i.e. in the main wind direction during that month.

A focus of the model simulations was to confirm one of the most important results from the Nordic network for atmospheric mercury, i.e. a relatively weak south-to-north gradient of mercury concentrations in ambient air and a more pronounced one in precipitation over Scandinavia indicating a substantial impact from Central European anthropogenic mercury sources through long-range transport. Table 2 compares modeled and observed annual means of mercury in air and precipitation at eight measurement sites in Germany and Scandinavia forming a longitudinal corridor extending from the high emission region Halle/Leipzig/Bitterfeld in Germany to Overbygd in Northern Norway. In general, modeled concentrations of vapor-phase elemental mercury in air compare satisfactorily with observations from all stations. However, the scarcity of particulate mercury measurements and uncertainties in the quality of these data are such that no firm conclusions can be drawn from the comparison of those data. Modeled concentrations of mercury in precipitation both dissolved or 'reactive' mercury and total mercury agreed within a factor of 2 with observed values in nearly all cases, thus indicating that the model is capable of reproducing the observed south-to-north gradients. These results together with a good correlation between elevated levels in calculated mercury concentrations in precipitation and observed soot carbon concentrations do suggest that for long-term averages the chemical scheme in the model is based on an adequate parametrization of

TABLE 2. Atmospheric mercury concentrations in Central and Northern Europe - annual mean values 1988 (observations: IVL, Göteborg, Sweden and GKSS, Geesthacht, Germany)

	elemental mercury in air [ $\text{ng m}^{-3}$ ]		particulate mercury in air [ $\text{ng m}^{-3}$ ]		reactive mercury in precipitation [ $\text{ng l}^{-1}$ ]		total mercury in precipitation [ $\text{ng l}^{-1}$ ]	
	modeled	observed	modeled	observed	modeled	observed	modeled	observed
Halle/ Leipzig/ Bitterfeld*	10.1	8.2	0.279		9.2	29.4	330.5	462.5
Neuglobsow	4.9		0.208		6.6		233.9	
Langenbrügge*	4.1	4.2	0.111		4.3		65.8	52.0
Zingst*	3.6	2.5	0.107		4.0	16.5	61.6	49.0
Rörvik	2.5	2.8	0.025	0.06	2.3	1.9	17.4	35.0
Aspvreten	2.5		0.019		3.3	2.4	16.5	18.4
Vindeln	2.1	2.5	0.005	0.05	1.9	1.4	7.0	11.2
Overbygd	2.1	2.6	0.002		2.3	1.0	3.9	9.2

\* observations 1992 - 1994

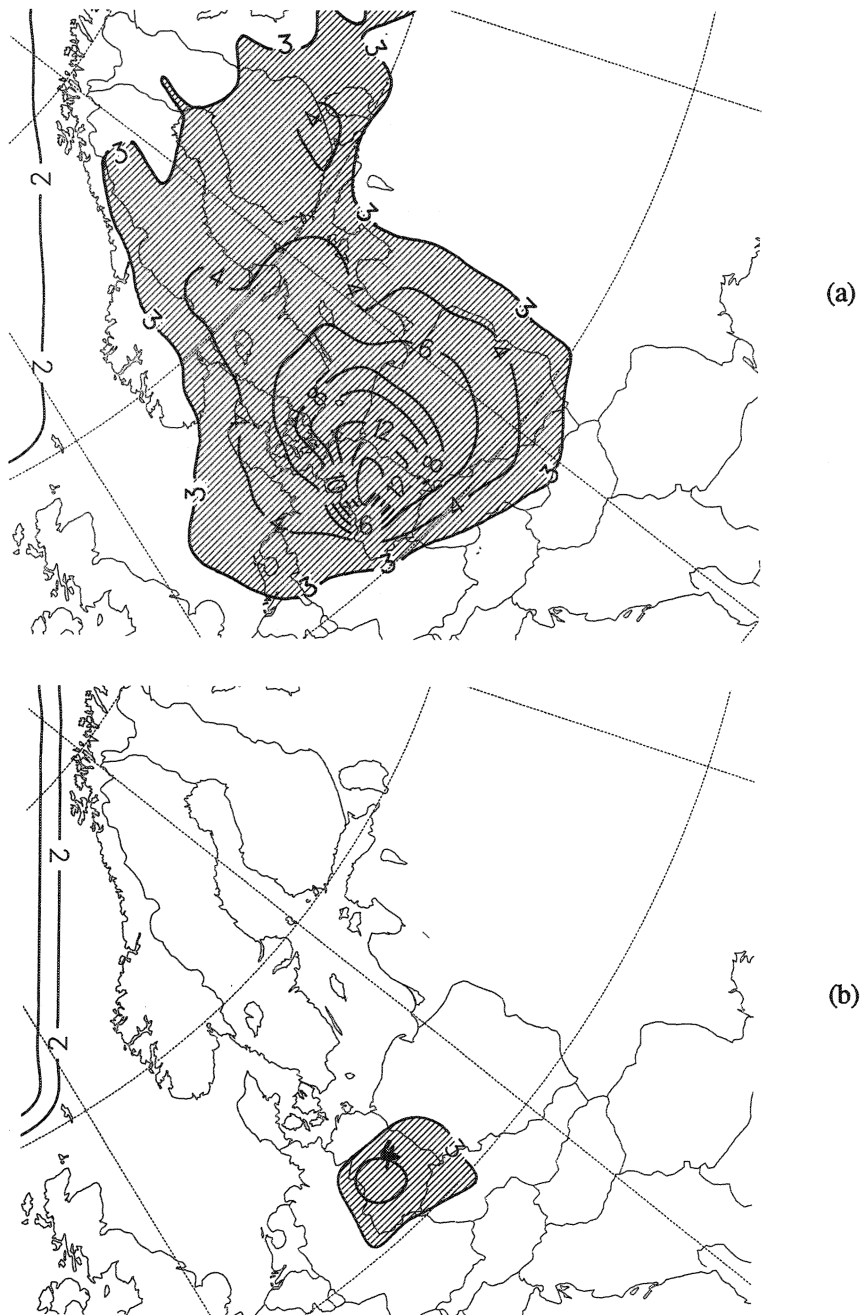


Figure 1. Calculated monthly average of vapor-phase elemental mercury in air (units  $\text{ng m}^{-3}$ ). (a) January 1988, (b) June 1988.

aqueous phase chemistry, i.e. redox reactions of  $\text{Hg}^0$  and adsorption of oxidized Hg on soot particles.

An extensive treatment of the mercury chemistry scheme employed in the model calculations can be found in Petersen et al. [31]. Similar schemes are used in several other models previously developed at the EMEP Meteorological Synthesizing Center East [13], the US Environmental Protection Agency [6], the US Argonne National Laboratory [40], and the National Power, UK [46].

### 3.2. APPROACH TO THE DEVELOPMENT OF A COMPREHENSIVE MODEL

The mercury chemistry so far used in atmospheric transport models is a simplified description of a complex series of chemical reactions and mass transfer processes. In Pleijel and Munthe [32] [33], considerably more complex chemical schemes were tested and evaluated. Concentrations of mercury in cloud droplets were calculated under varying conditions of gas and aqueous phase concentrations of mercury species,  $\text{O}_3$ ,  $\text{SO}_2$ ,  $\text{Cl}^-$  and others. The results of these tests have been used to devise a condensed chemical procedure consisting of 14 different mercury species and 21 reactions (Figure 2). The chemistry has been considerably simplified compared to the scheme described in Pleijel and Munthe (1995a, b) but contains one major addition: the gas phase reaction of  $\text{Hg}^0$  and  $\text{O}_3$  for which new kinetic data have recently been presented [14]. The description of the aqueous chemistry is based on the species  $\text{Hg}^{2+}$ , which is formed in the oxidation of  $\text{Hg}^0$  by  $\text{O}_3$ , via the intermediate species  $\text{HgO}$ . From  $\text{Hg}^{2+}$ , three different complexes can be formed including the S(IV) forms which are involved in the back reduction of  $\text{Hg}^{2+}$  to  $\text{Hg}^0$ .

#### 3.2.1. The ADOM Model System

Currently, the scheme depicted in Figure 2 is implemented into a comprehensive Eulerian model referred to as ADOM (Acid Deposition and Oxidant Model), which has been developed under the sponsorship of Environment Canada, Atmospheric Environment Service (AES), the Ontario Ministry of Environment and Energy (OMEE), the German Umweltbundesamt and the Electric Power Research Institute (EPRI) for simulating long-range transport and deposition of acidic pollutants in Europe and North America. Within the constraints of available resources and input data, this model incorporates detailed physical and chemical processes in the atmosphere [11] [12] [26] [44].

Figure 3 shows schematically the various components of the ADOM-model system modified for transport, transformations and deposition of mercury and to be applied over Eastern North America and Central and Northern Europe. The basic model time step is one hour. Horizontal and vertical wind fields along with the eddy diffusivity, temperature, humidity, surface precipitation and information about the distribution of clouds make up the input meteorological data set. This data set is derived diagnostically using the weather prediction model HIRLAM for Europe and the Canadian Meteorological Center's model for North America. Combining these data with information from a high resolution boundary layer model yields the final

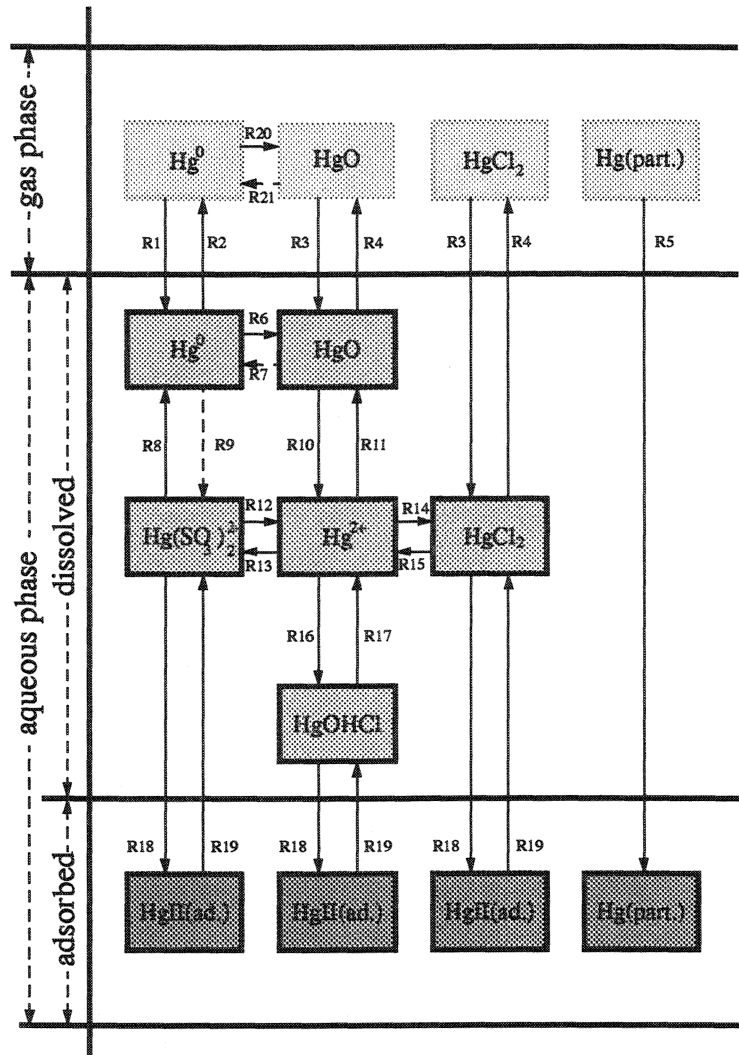


Figure 2. Atmospheric mercury chemistry scheme  
(R1 - R19 denote rate constants and equilibrium constants)

meteorological input files.

Other than meteorological data, the input and data requirements for ADOM are

- emissions,
  - initial and boundary conditions
- and
- geophysical data.

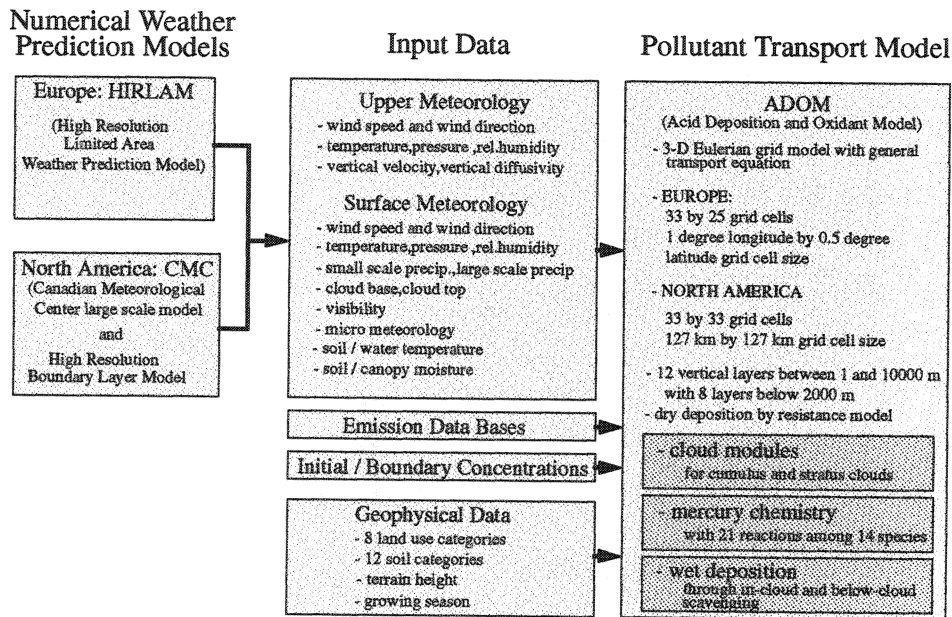


Figure 3. Overview of a comprehensive Eulerian model system for mercury.

Emission data bases include area and point source files. Emitted species are vapor-phase elemental mercury, mercury chloride and mercury associated with particles. The area sources are the grid cell total emissions while the point sources are emissions at a specific location in the grid.

Initial and boundary conditions are needed for all advected species in the model. This includes the emitted compounds and secondary compounds affecting the atmospheric chemistry of mercury.

The geophysical data include files for 8 land use categories (i.e. deciduous forests, coniferous forest, grassland, cropland, urban, desert, water and swamp.) and 12 soil categories. The database also includes information on terrain height and the growing season. This geophysical data affects meteorology, natural emissions of mercury and dry deposition processes.

The major modules making up the ADOM code are

- transport and diffusion,
- dry deposition,
- gas phase chemistry and
- cloud mixing/scavenging/aqueous phase chemistry.

These are integrated together within an Eulerian framework using the split-operator

approach as:

$$C^{n+1} = A_x A_y A_z A_c A_c A_z A_y A_x C^n$$

where  $C_n$  is the concentration of a species at time  $n$ ,  $A_x$  and  $A_y$  are the horizontal transport and diffusion operators,  $A_z$  is the vertical transport, diffusion, source injection and physical depletion operator and  $A_c$  is the operator containing cloud mixing, dry deposition and all chemical conversion terms.

The decomposition of each operator into two parts and its application in opposite order during each time step cause the errors of order  $t$  which build up during the first half of the cycle to be canceled out as the reverse operator application completes the time-marching cycle [27].

For transport and diffusion, the equations are solved by various numerical schemes. For advection in the horizontal, a sophisticated cell-center flux scheme based on the Blackman spline approach is used. Horizontal diffusion is solved by Crank-Nicolson time difference and three-point finite difference expressions. Vertical diffusion, advection, dry depletion and emissions injection are accomplished through a low-order mass conserving algorithm that operates in either Crank-Nicolson or fully implicit modes depending on stability criteria and the maximum number of iterations allowed.

Dry deposition proceeds according to a deposition velocity which is inversely proportional to the sum of the area weighted aerodynamic, surface and canopy resistances. The aerodynamic resistance is determined from meteorological input such as stability and applies to all species. The surface resistance is calculated from the land-use type and the physical and chemical properties of the species. The canopy resistance responds to the incoming solar radiation and meteorology.

Dry deposition rates of elemental mercury are difficult to assess. The very low solubility of elemental mercury suggests that dry deposition will be a slow process. However, since the large majority of the observed air concentrations is elemental mercury, even a small dry deposition rate could result in significant deposition. Two studies of mercury deposition to forests are those by Iverfeldt [17] and Lindberg et al. [23]. Iverfeldt had estimated total dry deposition of mercury using precipitation measurements under a spruce forest canopy compared to wet deposition in nearby clearings. The data indicated a strong seasonality to the dry deposition with very little deposition in the winter. Although the observed data would include particulate mercury deposition, measurements of air concentrations in the area indicate that gaseous mercury is responsible for most of the deposition. The summer-time dry deposition rate was estimated to be  $\sim 0.03 \text{ cm s}^{-1}$ .

Lindberg et al. [23] estimated Hg dry deposition using a multiple-resistance model of deposition to leaves. They also found a very pronounced seasonal cycle, with a summertime maximum dry deposition rate of about  $0.1 \text{ cm s}^{-1}$  and about  $0.01 \text{ cm s}^{-1}$  in the winter. Air temperatures had a significant effect on the modeled summertime dry deposition rate of elemental mercury.

For the model sensitivity tests performed for eastern North America, a dry deposition rate of  $0.03 \text{ cm s}^{-1}$  was used for summertime deposition to forest surfaces. A sensitivity test was then performed where this dry deposition rate was doubled to give a value closer to Lindberg's published estimates. The dry deposition rate of elemental mercury to all surfaces except forests was set to zero in these model simulations.

Since divalent mercury (e.g. in the form of  $\text{HgCl}_2$ ) has an aqueous solubility similar to that of nitric acid, the dry deposition parameters already used in ADOM for nitric acid are used for  $\text{Hg(II)}$ . Similarly the dry deposition rates used in ADOM for sulfate particles are used for particulate-phase mercury.

As can be seen from Figure 2 gas phase chemistry in the model is currently restricted to oxidation of  $\text{Hg}^0$  by ozone. Hence, the adaptations of ADOM required to model atmospheric mercury are primarily in the cloud mixing/scavenging/aqueous phase module. In view of its relevance to the model testing results presented in section 3.2.2, it is described in some detail subsequently.

Clouds are classified as stratus (layer clouds) or cumulus (convective clouds) according to diagnostic output from the weather prediction models. Observations of the fractional coverage and the vertical extent of clouds are combined with output from the diagnostic models to yield the input fields for the cloud physics modules.

The stratus module calculates the vapor condensation rate based on the vertical temperature profile of the grid column and the vertical velocity, and then divides the column into a maximum of four homogeneous zones depending on the relative position of the cloud base, cloud top, freezing and  $-20^\circ \text{C}$  levels. Kessler's bulk water technique [22] is used for the microphysical formulation.

The cumulus module has evolved from a highly parameterized version to a more detailed cloud-mixing model developed by Raymond and Blyth [36]. This model allows sub-parcels in each parcel of ascending cloud air to mix in different proportion with the environmental air and eventually to settle at its level of neutral buoyancy. The life cycle of a cumulus cloud is modeled in three stages, as shown in Figure 4. First, the active region is formed by ingestion of air from the cloud surroundings. Second, chemical reactions take place in the cloud water formed in the active region. This stage, referred to as the dwell-phase, is assumed to make up most of the life-cycle of the cloud. At the end of the dwell-phase, scavenging occurs. Finally, in the third stage, the cloud dissipates and the remaining pollutants are ejected into the cloudy region. Redistribution of pollutants occurs during both the cloud formation and the cloud dissipation stages.

Aqueous phase chemistry is performed whenever a cloud module is activated. For stratiform clouds the module is activated when a finite precipitation amount is given for that grid location. In the case of cumulus clouds, calculations are performed for both precipitating and non-precipitating clouds. As already mentioned above the mercury chemistry scheme has 21 reactions which includes transfer between the gas and aqueous phases. Mass transfer from gas to aqueous-phase makes use of forward and backward mass fluxes dependent on a sticking coefficient and the Henry's Law constant for the gas.

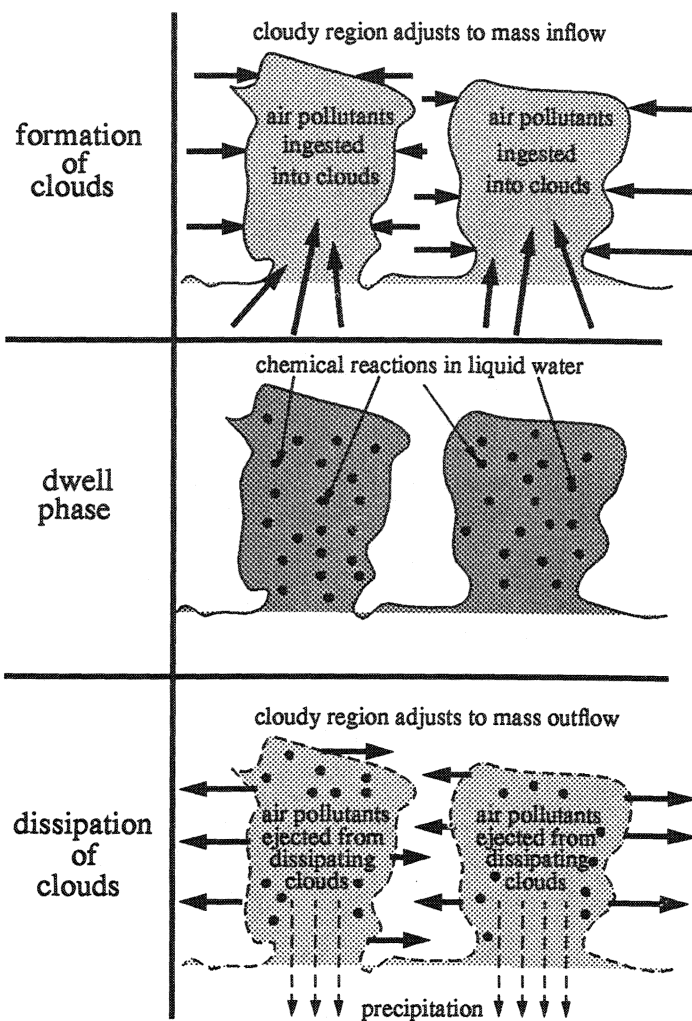


Figure 4. Lifecycle of a cumulus cloud system.  
(adapted from Karamchandani and Venkatram [20])

The present version of ADOM allows for the co-existence of stratus and cumulus clouds. Both modules consider in-cloud and below-cloud scavenging of mercury species. Removal of particulate-phase mercury is assumed to occur primarily by nucleation scavenging in clouds, analogous to the sulfate-scavenging mechanism employed in ADOM model for acidic compounds. However, there is also below-cloud collection/scavenging of particles (and, to a much lesser extent elemental mercury vapour) by falling rain drops [37] [38], but that is a much less efficient scavenging mechanism. The very soluble Hg(II) species is rapidly absorbed into water droplets. The model uses a Henry's Law gas-to-liquid partition coefficient for Hg in its

continuous wet-scavenging algorithm. At the end of each hour, the concentrations of all Hg species within the cloud water droplets are included in that grid cell's chemical inventory and are then used to set the initial concentrations for the next hour. As outlined in section 2.2., the majority of the mercury in rain water is in particulate form. Thus, the aqueous chemistry process in non-precipitating clouds results in a pathway producing particulate-phase mercury. In precipitating clouds there would be both wet scavenging and subsequent wet deposition of particulate-phase mercury as well as production of particulate-phase mercury through aqueous chemistry followed by evaporation of water droplets.

### 3.2.2. 'Stand Alone Model' for Cloud Mixing, Scavenging, Chemistry, and Wet Deposition

To test the aqueous chemistry equation set and the scavenging mechanisms for mercury species in stratus and cumulus clouds, a stand alone version of the cloud mixing, scavenging, aqueous chemistry and wet deposition module has been developed. This model is used to test the sensitivity of mercury wet deposition to various assumptions about the chemical reactions including the rate constants and the scavenging of mercury by water droplets. The sensitivity of the model to various cloud parameters such as the cloud depth, vertical temperature and moisture profiles, the lifetime of cumulus clouds, cloud fractional coverage and the precipitation rate can also be examined.

*Model design.* The model consists of one ADOM grid column with the same 12 vertical levels used in the full model. Initial concentration profiles of mercury species in ambient air as well as cloud-base height, cloud-top height, precipitation rates, and vertical profiles of temperature, pressure and relative humidity are needed as input. Moreover, a cloud fractional coverage is used to divide the grid cell into cloudy and clear regions. The model can be run for a single hour or for a sequence of hours with the clouds evaporated and the mercury species in the cloudy air averaged with the clear air concentrations to provide the starting concentration profiles for the next hour.

A cumulus cloud is created only when lifting of an air parcel from cloud base can support convection. Otherwise the stratiform cloud module is used. Because the cumulus cloud module only uses cloud-base height and ambient temperature, pressure and humidity profiles to create a cloud, it can treat both precipitating and non-precipitating clouds. The stratiform module is driven by the surface precipitation rate. To simulate non-precipitating stratiform clouds, a minimum precipitation rate of  $0.029 \text{ mm h}^{-1}$  is used to generate cloud water/ice profiles but no deposition is calculated.

Currently, development and testing of the stand alone model is focused on cumulus clouds. The sequential steps in the calculations for this cloud type are shown in Figure 5. For the basic model time step of 1 hour, the cloud physics sub-module calculates the mixing parameters (i.e. vertical profiles of air inflow and outflow) and the vertical distribution of liquid water and ice in the active region. All subsequent

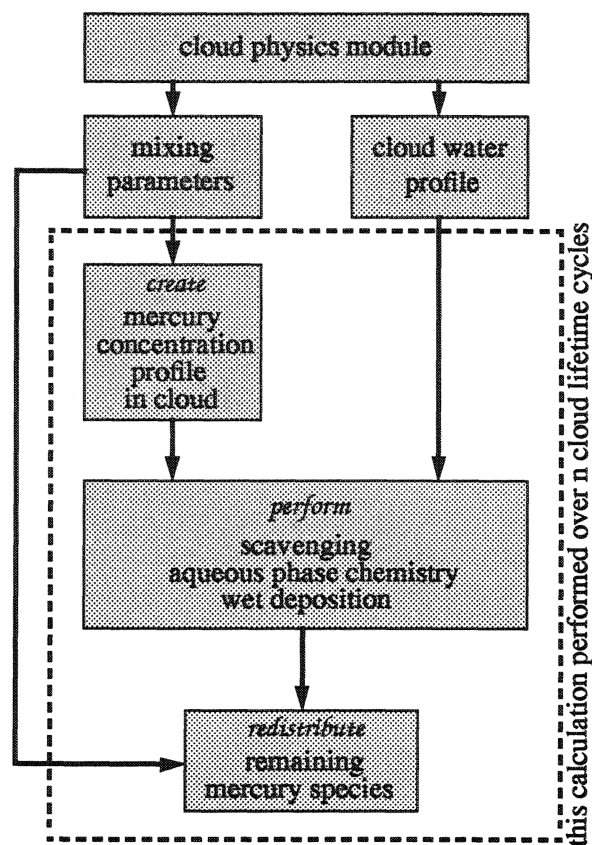


Figure 5. Steps in cloud mixing/scavenging/chemistry/wet deposition calculations.

steps in the calculations are repeated for each cloud life-cycle. Between 1 and 6 cycles can occur during a 1-h simulation, depending on the depth of the cloud and on the ratio of the cloud water content and the precipitation rate. Shallow cumulus clouds repeat the cycle more rapidly than deep cumulus clouds.

Concentration profiles of mercury species during cloud formation are created using the inflow profiles. Average concentrations in the active region which are being used as input for the aqueous phase processes sub-module are determined from the properties of the environmental air and the cloud-base air using the inflow of air into the cloud from each level as the weighting factor.

The aqueous phase processes sub-module comprises scavenging, chemistry and wet deposition. Scavenging in the active region is accomplished by dividing this region into a liquid-water and an ice reactor. Both aqueous phase chemistry and mass transfer processes are allowed to occur in the liquid water reactor. In the ice phase, only nucleation scavenging and equilibrium dissolution are considered. The

scavenging components employed in the 'stand alone model' test runs treat the reversible mass transfer of vapor-phase  $\text{Hg}^0$  and  $\text{Hg}(\text{II})$  to cloud water, irreversible scavenging of those two species by ice and irreversible  $\text{HgP}$  scavenging by cloud water and ice. Chemistry corresponds to the scheme used in Petersen et al., 1995, i.e. the scheme is restricted to the most important processes of aqueous oxidation of  $\text{Hg}^0$  by ozone, back-reduction of  $\text{Hg}(\text{II})$  to  $\text{Hg}^0$  and adsorption of  $\text{Hg}(\text{II})$  on soot particles. After scavenging and aqueous phase chemistry are simulated for the life-cycle of the cloud mercury species are removed from the cloud via wet deposition and the remaining pollutants are redistributed to form the input profile for the next cycle.

*Model testing.* The stand alone model has been tested under different environmental conditions. Figures 6a and 6b show the two temperature profiles and cloud depths used with the sensitivity tests and referred to as the 'warm' and the 'cold' cloud. Both cases share the same pressure and humidity profile. The fraction of the cloudy region in the grid square and the fraction of the active region in the cloudy region were fixed in both cases at 0.9 and 0.1, respectively. The precipitation rates used with the test runs were  $2 \text{ mm h}^{-1}$  for the warm cloud and  $0.3 \text{ mm h}^{-1}$  for the cold cloud.

Sensitivity studies were performed using the two basic temperature profiles and the other meteorological input data mentioned above. Figures 7 and 8 illustrate the output from the cumulus cloud physics sub-module in terms of cloud mixing and cloud water profiles. Both clouds have a base height of approximately 500 m. For the warm cloud a top height of 10,000 m and a maximum liquid water and ice content of nearly 4 and 1.5 grams per  $\text{m}^3$  of air, respectively, have been calculated whereas the cold cloud has considerably lower liquid water and ice contents and only extends to 4000 m height (Figure 7a and 7b). The vertical distribution of air flow into and out of the active region of the warm and cold cloud is shown in Figure 8a and 8b. The horizontal dotted lines represent the grid cell center heights in the vertical grid system, the bars indicate the inflow and outflow of the air. According to the mixing model of Raymond and Blyth [36] the active area in both clouds consists of 50 % cloud base air and 50 % entrained from the sides. In case of the warm cloud (Figure 8a), about 75 % of the air comprising the cloud flows out of the topmost layer, indicating that almost all combinations of air from the base and the sides are buoyant enough to reach the cloud top. The total airflow in the cold cloud is considerably lower and the outflow is more evenly distributed between several layers.

The effects of cloud mixing, scavenging and wet deposition on the vertical concentration profile of particulate mercury, which does not undergo chemical reactions, are depicted in Figure 9a and 9b. The lines represent 24 hour sequences of  $\text{HgP}$  concentration profiles after cloud dissipation at the end of each 1 hour time step. For both the warm and the cold cloud the model was started with the same vertical constant concentration profile. It is evident that in both cases final concentration profiles reflect the distribution of outflow of air shown in Figure 8a and 8b. In the case of the warm cloud, the concentrations decrease most rapidly at the 8-1/2 km level. This is expected since the cloud air, depleted in  $\text{HgP}$  due to wet deposition, has most of its outflow to the environment at this level. Mixing of the environmental air at

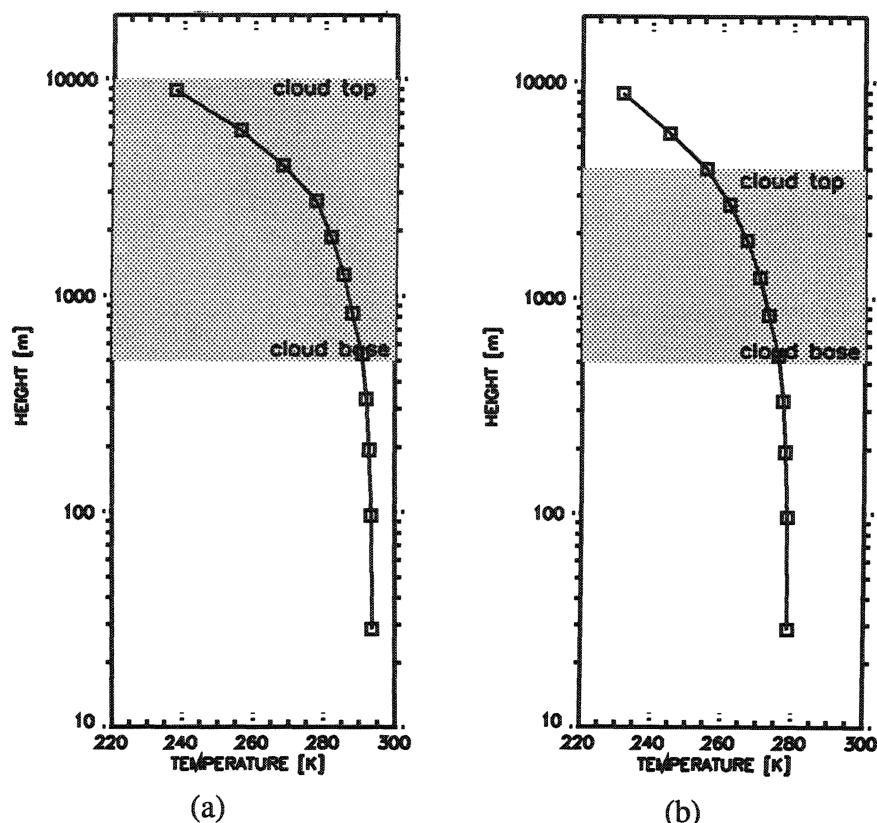


Figure 6. Temperature profiles and cloud base/top elevation for  
(a) warm cumulus (b) cold cumulus.

the 8-1/2 km level with lower layers results in the slow spread of the impact over the cloud depth.

For the cold cloud, the variation in concentrations and deposition with time are very different from the warm case. Figure 10a shows that concentration of particulate in the rain or cloud water are initially about ten times those of the warm cloud. This occurs because the particulate is assumed to be completely scavenged by nucleation and for the cold cloud, the liquid water content is about a tenth of that of the warm cloud. This leads to much more rapid depletion of the particulate concentration over the shallow cold cloud compared to the deep warm cloud. This depletion is further enhanced because the shallow cloud results in six cloud lifecycles per hour while the deep cumulus cloud has only one lifecycle per hour. The shallow cumulus can then process a much larger fraction of the cloudy region air in an hour, resulting in more rapid removal of the layer average particulate concentration in rainwater (Figure 10a) and hence in more rapid decrease of wet deposition fluxes (Figure 10b).

The warm cloud has been selected for additional sensitivity tests covering the

above mentioned aqueous redox reactions of  $\text{Hg}^0$ . Figures 11a and 11b show the losses of dissolved  $\text{Hg}(\text{II})$  in the grid column with time for different oxidation and reduction rate constants. The base case for oxidation (Figure 11a) is determined from the rate constant of Munthe [29] and an ozone ambient air concentration of 50 ppb. Cumulative column losses are almost linearly increasing within the 24 h time period and are directly proportional to ozone concentrations due to a linear relationship between ozone levels and dissolved  $\text{Hg}(\text{II})$  production rates. Figure 11b illustrates the column loss decrease for the oxidation base case caused by back reduction of dissolved  $\text{Hg}(\text{II})$  to  $\text{Hg}^0$  for various reduction rate constants ranging from 'no backreduction' to the two-fold base case value, which is determined from Munthe et al. [29].

Tests of the chemical scheme have been further extended by implementing adsorption of dissolved  $\text{Hg}(\text{II})$  on soot particles, assuming base case rate constants for redox reactions and an equilibrium constant for adsorption taken from Petersen et al. [31]. The model was initialized with vertical constant ambient air concentration profiles of  $3 \text{ ng m}^{-3}$  for  $\text{Hg}^0$  and  $1 \text{ } \mu\text{g m}^{-3}$  for soot. Results in terms of the influence of carbon soot on the partitioning of dissolved and adsorbed  $\text{Hg}(\text{II})$  in the warm cloud during a 48 h period is depicted in Figure 12a. As can be seen, most of the  $\text{Hg}(\text{II})$  is in the adsorbed phase over the entire time period but both dissolved and adsorbed  $\text{Hg}(\text{II})$  concentrations are significantly decreasing with time due to relatively high removal by precipitation.

The influence of different soot concentrations on the adsorbed  $\text{Hg}(\text{II})$  fraction has been investigated over a 48 h time period and a soot concentration range of  $0.1 - 100 \text{ } \mu\text{g m}^{-3}$ . Figure 12b shows that the adsorbed fraction covers a broad range and is increasing with time and with increasing soot concentrations. For the highest soot concentration, around 90 % of  $\text{Hg}(\text{II})$  has been adsorbed at the end of the time period, whereas only 20 % are present in adsorbed form for the lowest soot level at the beginning of the simulation period.

#### 4. Summary and Conclusions

Regional-scale tropospheric chemistry/transport model systems which can simulate numerous physico-chemical processes that are important in the transport and transformation of atmospheric mercury species and the resulting dry and wet deposition of these species have been presented.

In Lagrangian models previously used in Europe many of the processes have been neglected or highly simplified. Nevertheless, results in terms of monthly and annual means of mercury concentration and deposition fluxes that have been generated by this model type compare satisfactorily with observations from stations in Scandinavia and Germany, thus indicating that the model is an adequate tool to estimate regional monthly and annual average mercury concentration and deposition patterns and to generate matrices of international exchanges of mercury for the European countries.

Currently, a comprehensive mercury model system using the Eulerian reference

frame of the Acid Deposition and Oxidants Model (ADOM) is developed jointly by German, Swedish and Canadian institutions. This tropospheric transport, transformation, and deposition model is an evolving system of submodules which can be used to study the sensitivities of several physical and chemical processes assumed to be important for regional mercury deposition phenomena. Preliminary results from sensitivity studies with the cloud mixing, scavenging, chemistry, and wet deposition submodule demonstrate its capabilities in gaining scientific insights of tropospheric mercury transport, transformation and deposition problems which cannot be obtained through field measurements or experiments in the laboratory. The results also show that an enhanced emphasis on the further development of this submodule will have significant impact on the ultimate performance of the entire model system, which is expected to be operational within the next two years.

*Acknowledgment.* The authors wish to acknowledge the financial support for this work which was provided by the International Bureau of the GKSS Research Centre Geesthacht, Germany, in the framework of the German/Canada Science & Technology Agreement, Atmospheric Sector, Project ENV-58 'Air Toxics'.

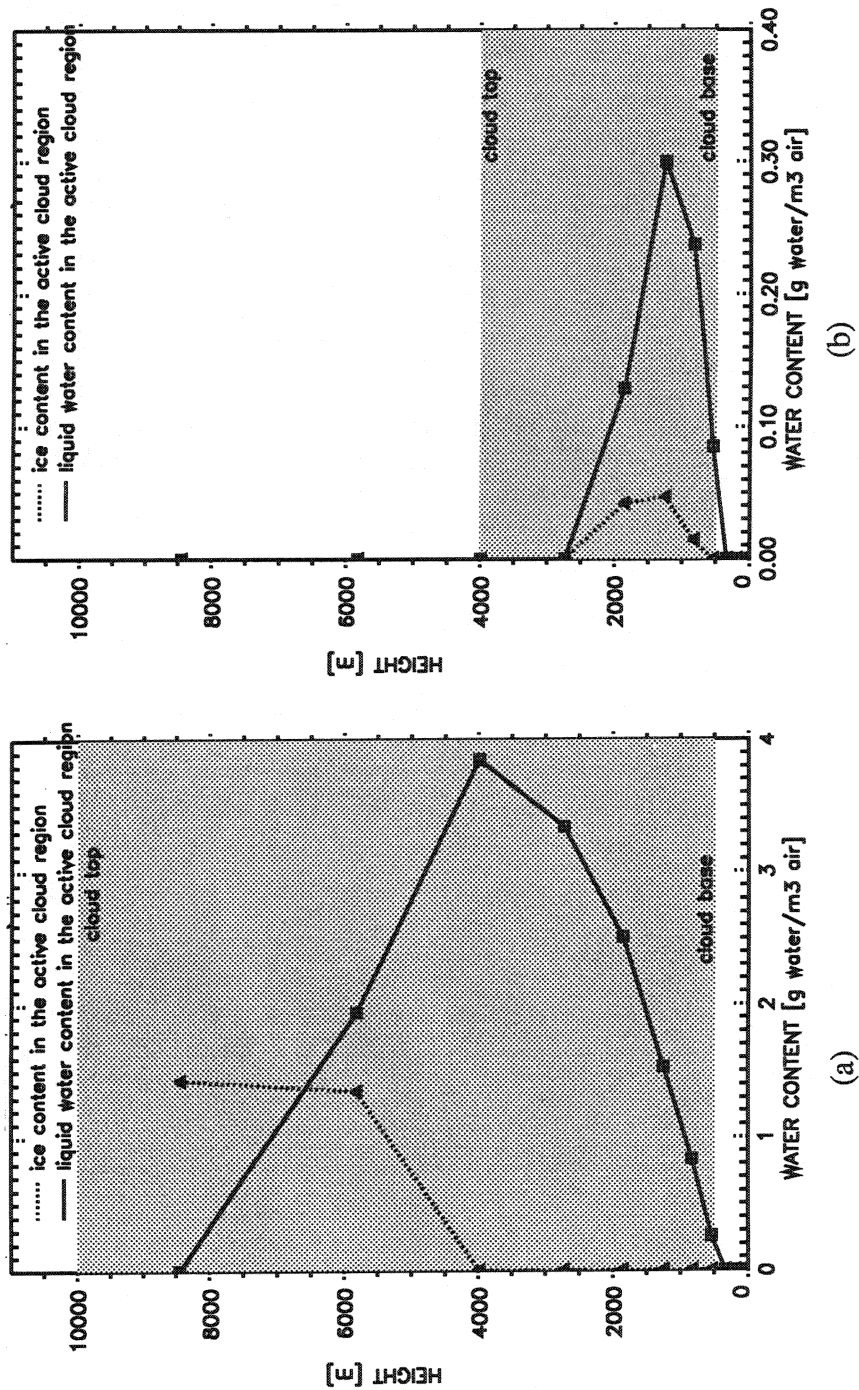


Figure 7: Cloud water/ice profiles for (a) warm cumulus (b) cold cumulus

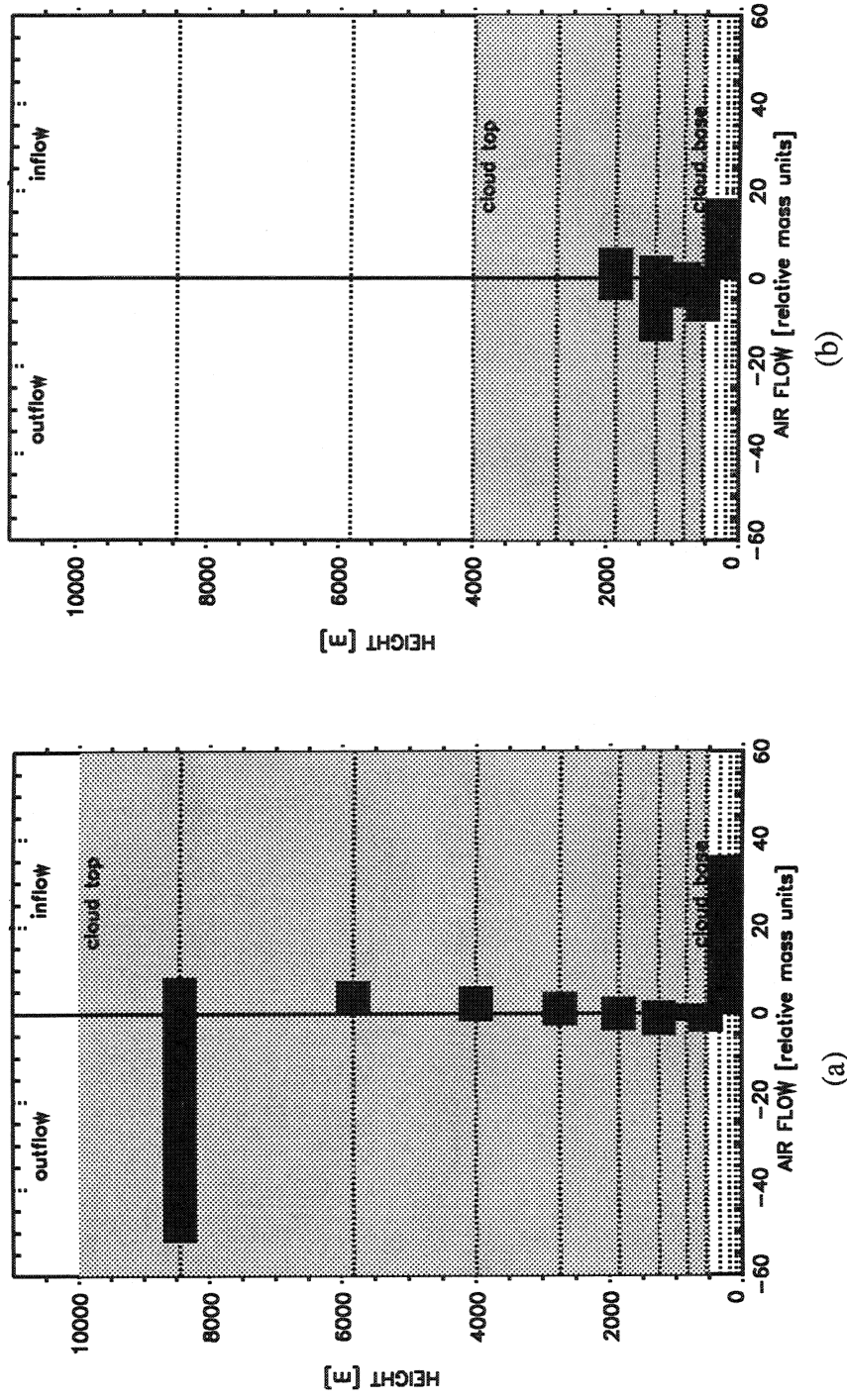


Figure 8: Air inflow and outflow  
 (a) warm cumulus (b) cold cumulus

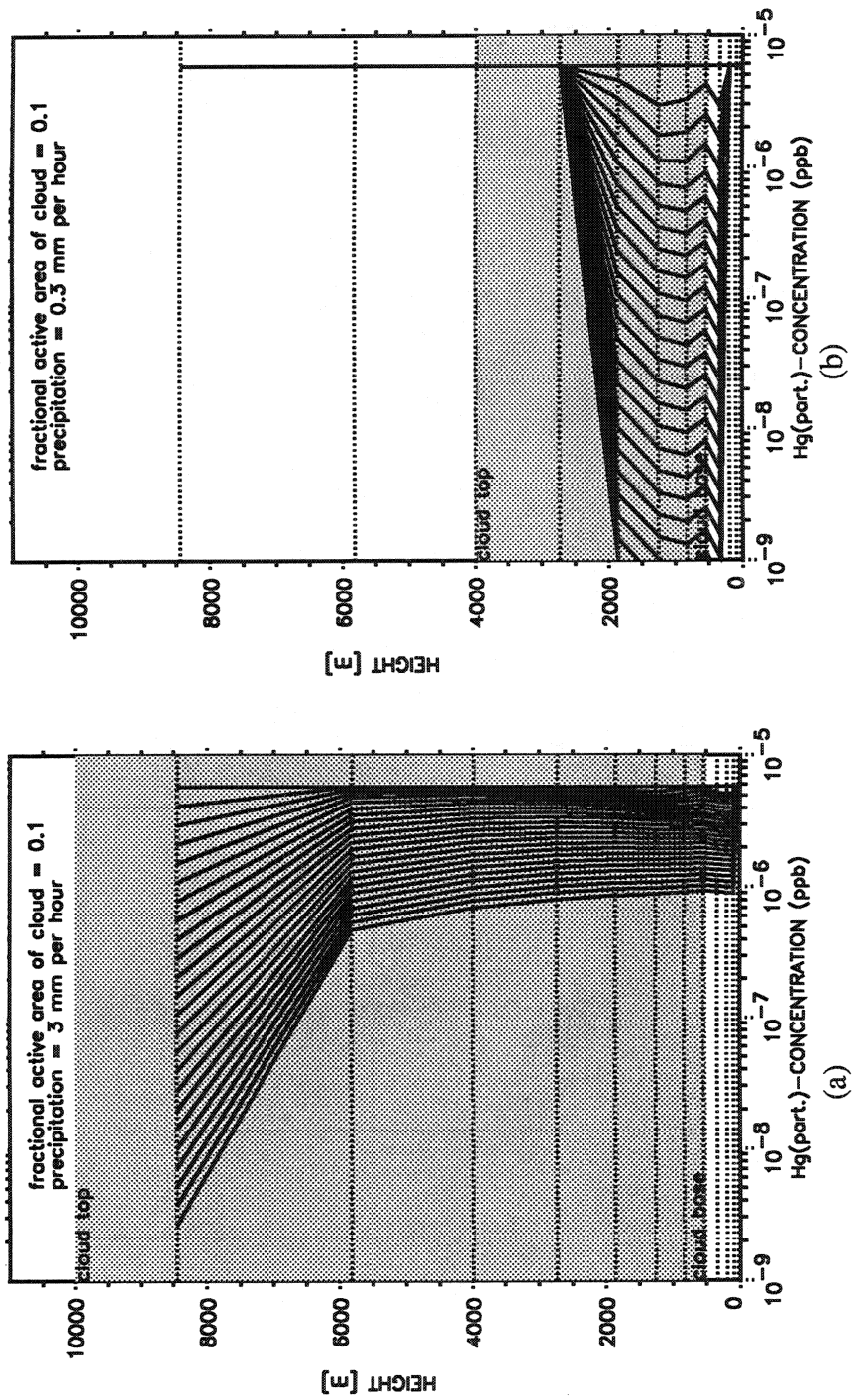


Figure 9. 24h-time evolution of vertical mercury concentration profiles in  
(a) warm cumulus (b) cold erulus.

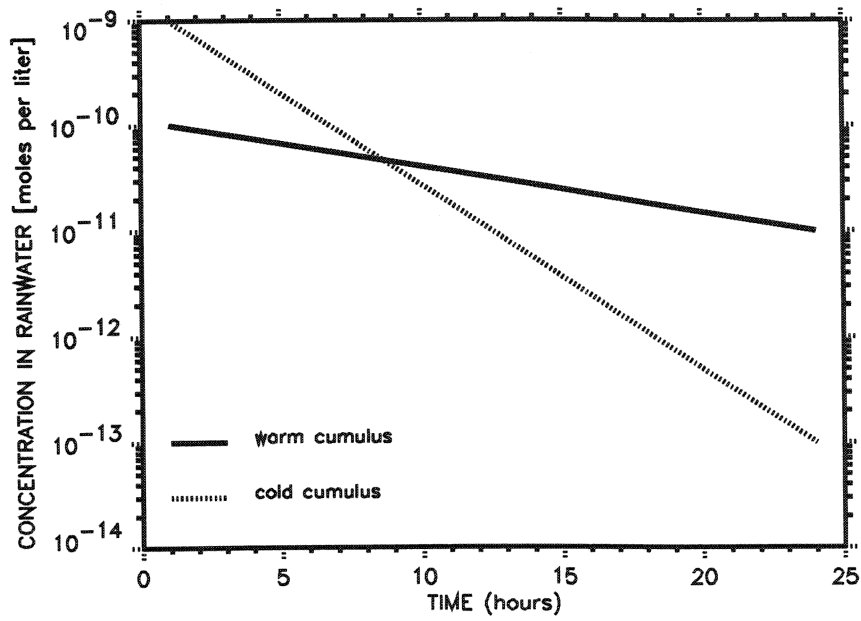


Figure 10a. Rainwater concentrations for “warm” and “cold” cloud cases over a 24-h period.

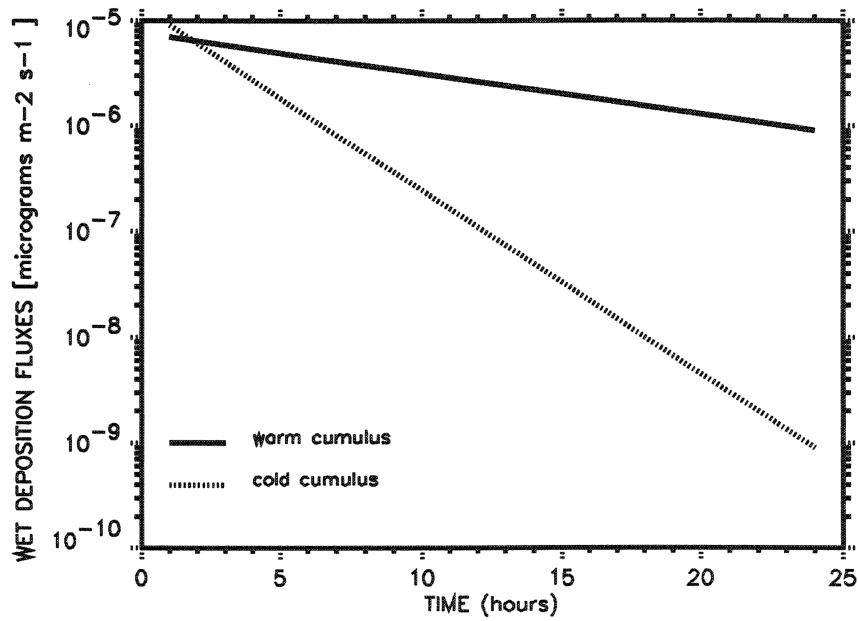


Figure 10b. Wet deposition fluxes for “warm” and “cold” cloud cases over a 24-h period.

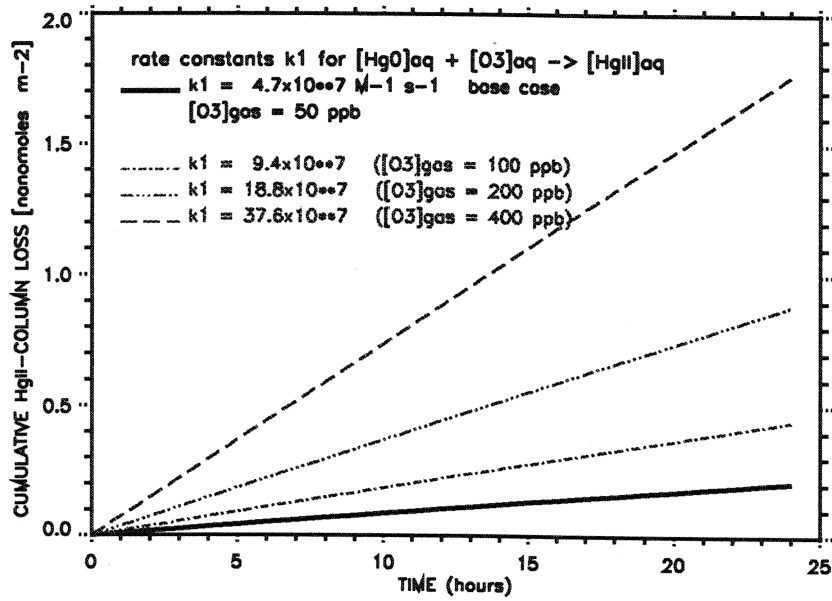


Figure 11a. Effect of  $\text{Hg}^0$ -oxidation on  $\text{Hg}^{\text{II}}$  - column loss over a 24 h period.

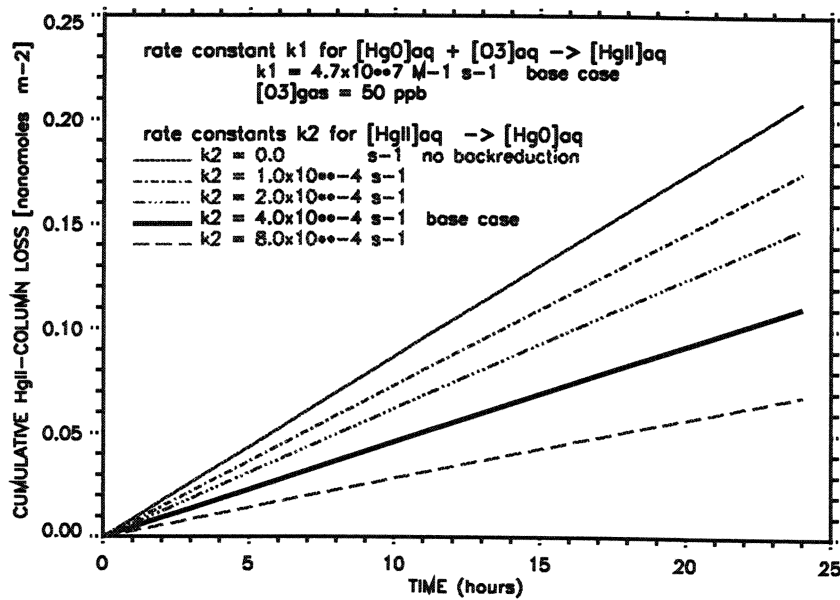


Figure 11b. Effect of  $\text{Hg}^{\text{II}}$  reduction on  $\text{Hg}^{\text{II}}$  column loss over a 24 h period.

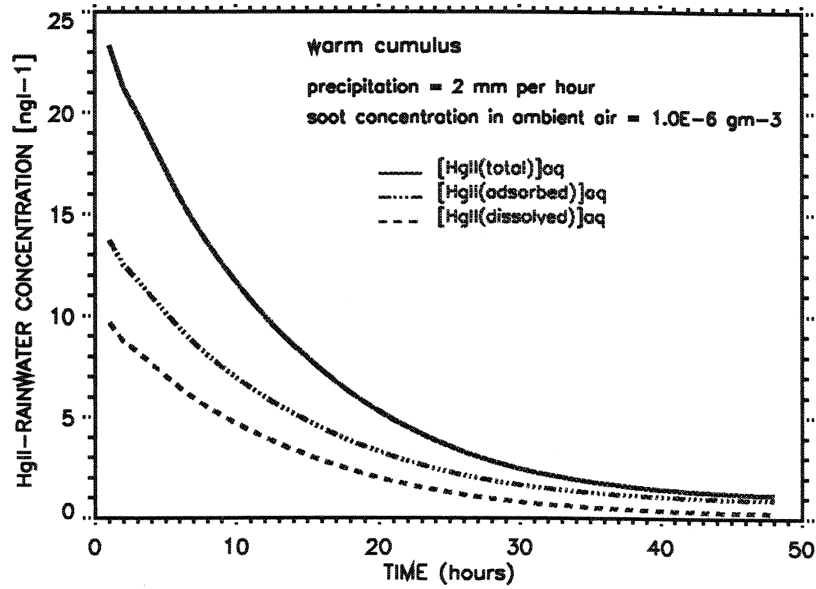


Figure 12a. Effect of soot particles on Hg(II) rainwater concentration over a 48 h period.

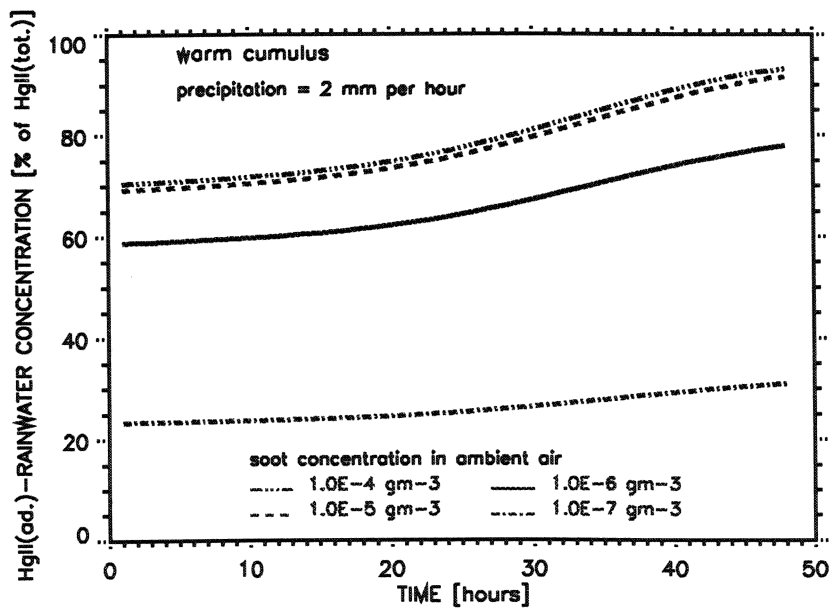


Figure 12b. Percentage of adsorbed Hg(II) for different soot concentration over a 48 h period.

## References

1. Ahmed, R., May, K., and Stoeppler, M. (1987) Wet Deposition of Mercury and Methylmercury from the Atmosphere, *Sci. Tot. Environ.* **60**, 249-261.
2. Bloom, N. S. and Watras, C. J. (1988) Observations of Methylmercury in Precipitation, *Sci. Tot. Environ.* **87/88**, 199-207.
3. Brosset, C. (1982) Total Airborne Mercury and its Possible Origin, *Water, Air and Soil Pollution* **17**, 37-50.
4. Brosset, C. (1987) The Behavior of Mercury in the Physical Environment, *Water, Air and Soil Pollution* **34**, 145-166.
5. Brosset, C. and Lord, E. (in press) Methylmercury in Ambient Air, Method of Determination and some Measurement Results, *Water, Air, and Soil Pollution*.
6. Bullock, O. R., Benjey, W., and Keating, M. H. (in press) The Modeling of Regional-Scale Atmospheric Mercury Concentration and Deposition Patterns using RELMAP, in J. E. Baker (ed.), *Atmospheric Deposition of Contaminants to the Great Lakes and Coastal Waters*.
7. EPRI (1994) Mercury Atmospheric Processes: A Synthesis Report, EPRI/TR-104214, Workshop Proceedings, Electric Power Research Institute, P.O.Box 10412, Palo Alto, CA 94303, U.S.A.
8. Ferrara, R., Maserti, B., Petrosino, A. and Bargagli, R. (1986) Mercury Levels in Rain and Air and the Subsequent Wash-out Mechanism in a Central Italian Region, *Atmospheric Environment* **20**, 125-128.
9. Fitzgerald, W. F. and Gill, G. A. (1979) Subnanogram Determination of Mercury by Two-Stage Gold Amalgamation and Gas Phase Detection Applied to Atmospheric Analysis, *Analyt. Chem.* **51**, 1714-1720.
10. Fitzgerald, W.F. (1995) Is Mercury Increasing in the Atmosphere? The Need for an Atmospheric Mercury Network (AMNET), *Water, Air and Soil Pollution* **80**, 245-254.
11. Fung, C., Misra, P.K., Bloxam, R., and Wong, S. (1991) A Numerical Experiment on the Relative Importance of H<sub>2</sub>O<sub>2</sub> and O<sub>3</sub> in Aqueous Conversion of SO<sub>2</sub> to SO<sub>4</sub>, *Atmospheric Environment* **25A**, 411-422.
12. Fung C., Bloxam R., Misra P.K., Wong S. and Yap, D. (1992) Evaluating the Comprehensive Model ADOM with Data from Three Seasons, Ontario Ministry of Environment Report PIBS 2064.
13. Galperin, M., Sofiev, M., Gusev, A., and Afinogenova, O. (1995) The Approaches to Modeling of Heavy Metals Transboundary and Long-Range Airborne Transport and Deposition in Europe, EMEP/MS-CHE Technical Report 7/95, EMEP Meteorological Synthesizing Center-East, Kedrova str.8-1, Moscow, Russia.
14. Hall, B. (1995) The Gas Phase Oxidation of Elemental Mercury by Ozone, *Water, Air and Soil Pollution* **80**, 301-315.
15. Hoyer, M., Burke, J., and Keeler, G. (1995) Atmospheric Sources, Transport and Deposition of Mercury in Michigan: Two Years of Event Precipitation, *Water, Air and Soil Pollution* **80**, 199-208.
16. Hultberg, H., Munthe, J. and Iverfeldt, A. (1995) Cycling of Methyl Mercury and Mercury - Responses in the Forest Roof Catchment to three Years of Decreased Atmospheric Deposition, *Water, Air and Soil Pollution* **80**, 415-424.
17. Iverfeldt, A. (1991a) Mercury in Forst Canopy Throughfall Water and its Relation to Atmospheric Deposition, *Water, Air and Soil Pollution* **56**, 553-564.
18. Iverfeldt, A. (1991b) Occurrence and Turnover of Atmospheric Mercury over the Nordic Countries, *Water, Air, and Soil Pollution* **56**, 251-265.
19. Iverfeldt, A., Munthe, J., Brosset, C. and Pacyna, J. M. (1995) Long-Term Changes in Concentration and Deposition of Atmospheric Mercury over Scandinavia, *Water, Air and Soil Pollution* **80**, 227-233.
20. Karamchandani, P. and Venkatram, A. (1992) The Role of Non-Precipitating Clouds in Producing Ambient Sulfate During Summer: Results from Simulations with the Acid Deposition and Oxidants Model (ADOM), *Atmospheric Environment* **26A**, 1041-1052.
21. Keeler, G., Glinsom, G. and Pirrone, N. (1995) Particulate Mercury in the Atmosphere: Its Significance, Transport, Transformation and Sources, *Water, Air and Soil Pollution* **80**, 159-168.
22. Kessler, E. (1969) On the Distribution and Continuity of Water Substances in Atmospheric Circulation, Meteorological Monographs 10, Number 32, American Meteorological Society, 45 Beacon St., Boston, Mass. 02108.
23. Lindberg, S. E., Turner, R. R., Meyers, T.P., Taylor, G.E., Jr. and Schroeder, W.H. (1991) Atmospheric Concentrations and Deposition of Hg to a Deciduous Forest at Walker Branch Watershed, Tennessee, U.S.A., *Water, Air and Soil Pollution* **56**, 577-594.
24. Lindqvist, O. (ed.) (1991) Mercury as an Environmental Pollutant, *Water, Air and Soil Pollution* **56**.
25. Lindqvist, O., Johansson, K., Aastrup, M., Andersson, A., Bringmark, L., Hovsenius, G., Hakanson, L., Iverfeldt, A., Meili, M. and Timm, B. (1991) Mercury in the Swedish Environment-Recent Research on Causes, Consequences and Corrective Methods, *Water, Air and Soil Pollution* **55**.
26. Misra, P. K., Bloxam, R., Fung, C., and Wong, S. (1989) Non-linear Response of Wet Deposition to Emissions Reduction: A Model Study, *Atmospheric Environment* **23**, 671-687.
27. Marchuk, G.I. (1975) *Methods of Numerical Mathematics*, Springer-Verlag, New York.

28. Munthe, J., Xiao, Z.F. and Lindqvist, O. (1991) The Aqueous Reduction of Divalent Mercury by Sulfite, *Water, Air, and Soil Pollution* **56**, 621-630.
29. Munthe, J. (1992) The Aqueous Oxidation of Elemental Mercury by Ozone, *Atmospheric Environment* **26A**, 1461 - 1468.
30. Munthe, J., Hultberg, H., and Iverfeldt, A. (1995) Mechanisms of Deposition of Mercury and Methylmercury to Coniferous Forests, *Water, Air and Soil Pollution* **80**, 363-371.
31. Petersen, G., Iverfeldt, A. and Munthe, J. (1995) Atmospheric Mercury Species over Central and Northern Europe. Model Calculations and Comparison with Observations from the Nordic Air and Precipitation Network for 1987 and 1988, *Atmospheric Environment* **29**, No. 1, 47-67.
32. Pleijel, K. and Munthe, J. (1995a) Modelling the Atmospheric Mercury Cycle - Chemistry in Fog Droplets, *Atmospheric Environment* **29**, No. 12, 1441-1457.
33. Pleijel, K. and Munthe, J. (1995b) Modeling the Atmospheric Chemistry of Mercury - The Importance of a Detailed Description of the Chemistry of Cloud Water. *Water, Air, and Soil Pollution* **80**, 317-324.
34. Porcella, D.B., Huckabee, J.W., and Wheatley, B. (eds.) (1995) Mercury as a Global Pollutant, Proceedings of the Third International Conference held in Whistler, British Columbia, July 10-14, 1994, Reprinted from *Water, Air and Soil Pollution* **80** (1-4), 1995, Kluwer Academic Publishers Dordrecht/Boston/London.
35. Prestbo, E.M. and Bloom, N.S. (1995) Mercury Speciation Adsorption (MESA) for Combustion Flue Gas: Methodology, Artifacts, Intercomparison, and Atmospheric Implications, *Water, Air and Soil Pollution* **80**, 145-158.
36. Raymond, D.J. and Blyth, A.M. (1986) A Stochastic Mixing Model for Nonprecipitating Cumulus Clouds, *J. Atmos. Sci.* **43**, 2708-2718.
37. Schroeder, W.H., Dobson, M., Kane, D.M., and Johnson, N.D. (1987) Toxic Trace Elements Associated with Airborne Particulate Matter: A Review, *J. Air Pollut. Control Assoc.* **37**, 1267-1285.
38. Schroeder, W.H. and Lane, D.A. (1988) The Fate of Toxic Airborne Pollutants, *Environ. Sci. Technol.* **22**, 240-246.
39. Seigneur, C., Wrobel, J. and Constantinou, E. (1994) A Chemical Kinetic Mechanism for Atmospheric Inorganic Mercury, *Environ. Sci. Technol.* **28**, 1589-1597.
40. Shannon, J.D. and Voldner, E.C. (1995) Modeling Atmospheric Concentrations of Mercury and Deposition to the Great Lakes, *Atmospheric Environment* **29**, 1649-1662.
41. Slemr, F., Schuster, G., and Seiler, F. (1985) Distribution, Speciation and Budget of Atmospheric Mercury, *Journal of Atmospheric Chemistry* **3**, 407-434.
42. Slemr, F. and Langer, E. (1992) Increase in Global Atmospheric Concentrations of Mercury Inferred from Measurements over the Atlantic Ocean, *Nature* **333**, 434-437.
43. Stratton, W.J. and Lindberg, S.E. (1995) Use of a Refluxing Mist Chamber for Measurement of Gas-Phase Mercury (II) Species in the Atmosphere, *Water, Air and Soil Pollution* **80**, 1269-1278.
44. Venkatram A., Karamchandani, P.K., and Misra, P.K. (1988) Testing a Comprehensive Acid Deposition Model, *Atmospheric Environment* **22**, 737-747.
45. Watras, C.J. and Huckabee, J.W. (eds.) (in press) *Mercury as a Global Pollutant-Towards Integration and Synthesis*, Lewis Publishers, Boca Raton, U.S.A.
46. Wright, R. (1995) Personal Communication.
47. Xiao, Z.F., Munthe, J. and Lindqvist, O. (1991) Sampling and Determination of Gaseous and Particulate Mercury in the Atmosphere Using Gold Coated Denuders, *Water, Air and Soil Pollution* **56**, 141-151.



# Paper III





## A COMPREHENSIVE EULERIAN MODELING FRAMEWORK FOR AIRBORNE MERCURY SPECIES: DEVELOPMENT AND TESTING OF THE TROPOSPHERIC CHEMISTRY MODULE (TCM)

G. PETERSEN,\* J. MUNTHE,† K. PLEIJEL,† R. BLOXAM‡  
and A. VINOD KUMAR§

\*GKSS Research Centre, Institute of Hydrophysics, Max-Planck-Strasse, D-21502 Geesthacht, Germany; †Swedish Environmental Research Institute (IVL), P.O. Box 47086, S-402 58 Goteborg, Sweden; ‡Ontario Ministry of Environment and Energy, Science and Technology Branch, 2 St.Clair Ave W, Toronto, ON M4V 1L5, Canada; and §Environmental Assessment Division, Bhabha Atomic Research Centre, Mumbai 400085, India

(First received 2 October 1996 and in final form 9 December 1996. Published March 1998)

**Abstract**—A comprehensive mercury model system using the Eulerian reference frame of the Acid Deposition and Oxidant Model (ADOM) is being developed to study the regional transport of atmospheric mercury species. A stand-alone version of the ADOM cloud mixing, scavenging, chemistry and wet deposition model components referred to as the Tropospheric Chemistry Module (TCM) is used to investigate the sensitivity of various chemical and meteorological parameters, assumed to be important for mercury deposition phenomena. The TCM chemistry scheme was developed by systematic simplification of the detailed Chemistry of Atmospheric Mercury (CAM) process model, which is based on the current knowledge of physico-chemical forms and transformation reactions of atmospheric mercury species. The first part of the paper describes the general approach to the TCM formulation. The second part presents sensitivity studies of the TCM behavior under different environmental conditions and a comparison of TCM results with observed concentrations of total mercury concentrations in precipitation (Hg(tot)). The results indicate that the TCM has capabilities to examine the relative importance and sensitivity of numerous mercury processes in the troposphere and to reproduce observed Hg(tot) concentrations reasonably well justifying its ultimate use in the full ADOM model. © 1998 Elsevier Science Ltd. All rights reserved.

**Key word index:** Mercury species, numerical modeling, Eulerian models; atmospheric mercury chemistry, cloud processes, wet deposition.

### 1. INTRODUCTION

In recent years there has been a remarkable revival of interest in mercury as an atmospheric pollutant on local, regional and global geographical scales. An important indicator of increasing interest regarding mercury species in Europe's atmosphere is the recent decision of the UN-ECE to prepare a protocol for heavy metals and persistent organic pollutants under its cooperative programme for monitoring and evaluation of the long range transmission of air pollutants (EMEP) with mercury as a priority substance. In North America, the 1990 U.S. Clean Air Act Amendments have identified mercury as one of the trace substances listed in the legislation as "hazardous air pollutants" because of its potentially significant effects on ecosystems and human health.

Since 1990, constant or decreasing mercury releases from anthropogenic emission sources have been observed in North America (Porcella *et al.*, 1996) and

Europe (Iverfeldt *et al.*, 1996), respectively. On the other hand, there are indications that the global background concentration in the atmosphere has increased during the past decade (Slemr and Langer, 1992), suggesting substantial contributions from anthropogenic combustion and industrial sources in China (Lindqvist *et al.*, 1996) and other parts of Asia, which overcompensate the above mentioned emission reductions.

An assessment of the potential ecological and health risks associated with atmospheric mercury species requires an understanding of the relationships between sources of emission to the atmosphere and the levels of concentrations measured in ambient air and precipitation in a given receptor area. However, the complexity of the physico-chemical processes of atmospheric mercury species makes results from measurement programs difficult to interpret without a clear conceptual model of the workings of the atmosphere. Further, measurements alone cannot be used

directly by policy-makers to form balanced and cost-effective strategies for dealing with this problem; an understanding of individual processes within the atmosphere does not automatically imply an understanding of the entire system. A complete picture of individual mercury processes and their interactions with the atmospheric system as a whole can only be obtained by means of numerical modeling.

In a broad sense, two basic types of models have been developed to date, wherein the turbulent transport of mercury species is analyzed through either a Lagrangian or an Eulerian approach (Petersen *et al.*, 1996). Lagrangian models developed for mercury and currently in use are variants of the so-called trajectory models (Bullock *et al.*, 1997; Shannon and Voldner, 1995; Petersen *et al.*, 1995). These models are formulated under assumptions of simplified turbulent diffusion, no convergent or divergent flows and no wind shear. In these approaches only first-order chemical reactions can be treated rigorously. However, the Lagrangian approach avoids many of the computational complexities associated with the simultaneous solution of many differential equations. This modeling approach requires significantly less computational resources than a comprehensive Eulerian model but can facilitate an understanding of problems that do not require descriptions of interactive nonlinear processes.

Recent progress in understanding the atmospheric mercury cycle has emphasized the need for direct modeling of the complex nonlinear mercury chemistry of the atmosphere by comprehensive Eulerian models. These approaches employ extensive gas and aqueous phase chemical mechanisms and explicitly track numerous mercury species concentrations. Also, a more detailed numerical formulation for physical and chemical processes occurring within and below precipitating clouds can be included. Typically, these models contain modules designed to calculate explicitly the chemical interactions that move gas phase mercury into and among the various aqueous phases within clouds as well as calculate the aqueous phase chemical transformations that occur within cloud and precipitation droplets. As a first step in this direction the cloud mixing, scavenging, chemistry and wet deposition components of the comprehensive three-dimensional Eulerian Acid Deposition and Oxidants Model (ADOM), originally designed for regional-scale acid precipitation and photochemical oxidants studies in North America and Europe (Venkatram *et al.*, 1988; Stern *et al.*, 1990; Fung *et al.*, 1991) are restructured to accommodate the most recent developments in atmospheric mercury chemistry. A stand-alone version of these components referred to as the Tropospheric Chemistry Module (TCM) has been developed and tested under different environmental conditions allowing changes to the chemistry and meteorology alone to be evaluated at different vertical TCM levels.

In Section 2, the TCM is described in more detail. Emphasis is given to individual physical and chemical mercury processes that are incorporated into the module. Section 3 discusses results from sensitivity runs to examine the influence of chemistry and meteorology on concentration levels of different mercury species in the grid column. Finally, in Section 4, conclusions are summarized and an outlook with respect to future application of the TCM as a major component of the full ADOM mercury version for North America and Europe is given.

## 2. DESCRIPTION OF THE TROPOSPHERIC CHEMISTRY MODULE

The module is designed to simulate the meteorology and chemistry of the entire depth of the troposphere to study cloud mixing, scavenging and chemical reactions associated with precipitation systems that generate wet deposition fluxes of atmospheric mercury species. The scavenging and chemistry components of the module are based on the mercury chemistry scheme depicted in Fig. 1. It incorporates 14 mercury species and 21 reactions including mass transfer reactions (R1–R5), aqueous-phase (R6–R17) and gas-phase (R20–R21) chemical reactions and equilibrium reactions for adsorption on soot particles (R18–R19).

In view of their relevance to the results from sensitivity studies presented in this paper the TCM components for cloud mixing, scavenging and chemistry are described in some more detail in the next three subsections. Special emphasis is given to chemical reaction mechanisms, which have been derived from a far more complex series of chemical reactions in the aqueous phase (Pleijel and Munthe, 1995a, b).

### 2.1. Cloud mixing

The cloud mixing submodule simulates the vertical distribution of mercury species in clouds. Two different modules are incorporated: one describes stratus (layer) clouds and the other simulates cumulus (convective) type clouds. One or the other or a combination (cumulus deck embedded in a stratus cloud) is used in the calculations depending upon the characteristics of the precipitation observed.

The stratiform cloud module solves the conservation equations for cloud water, rain water and snow. The 'Bulk Water' technique (Kessler, 1969) is used for the microphysical formulation. A Marshall–Palmer type size distribution is used for the precipitating fields and the cloud droplets are assumed to have a uniform size distribution. A continuous supply of water vapour is assumed to be available at all times for conversion to cloud water (via condensation) or snow (via vapour deposition), depending upon the temperature. The precipitating field concentrations, cloud water concentrations and the updraft velocities are determined by working backwards from surface

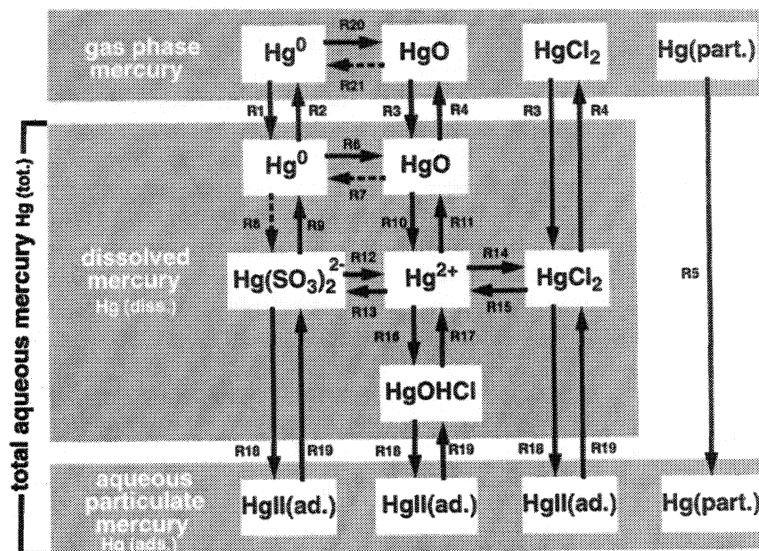


Fig. 1. The mercury chemistry scheme used with the Tropospheric Chemistry Module (TCM).

precipitation data. The following microphysical process rates are included in the model: vapor condensation to cloud water, cloud water autoconversion to rain, cloud water collection by rain, vapor deposition to snow, cloud water collection by snow (riming), evaporation of rain water below cloud base and sublimation of snow below cloud base. Vapour condensation rates are calculated based on the vertical temperature profile and the vertical velocity.

For cumulus clouds a detailed cloud mixing model is used (Raymond and Blyth, 1986). This model allows subparcels in each parcel of ascending cloud air to mix in different proportion with the environmental air and eventually to settle at its level of neutral buoyancy. The life cycle of a cumulus cloud is modelled in three stages, as shown in Fig. 2. First, an active region is formed by ingestion of air (also pollutants) from the cloud surroundings with 50% of the cloud air assumed to enter through the cloud base. Cloud water concentration profiles are generated, derived from observations made in cumulus clouds (Warner, 1970). Second, chemical reactions take place in the cloud water formed in the active region. This stage referred to as the dwell phase is assumed to make up most of the life cycle of the cloud. At the end of the dwell phase, scavenging occurs. Finally, in the third stage, the cloud dissipates and the remaining pollutants are ejected into the cloudy region. Redistribution of pollutants occurs during both the cloud formation and the cloud dissipation stages. The final concentration profile is the weighted average of the initial concentration in the inactive cloud air, the final concentration in the active cloud air and the well mixed concentrations corresponding to displaced cloud air.

Cumulus clouds with updrafts ranging from  $1\text{ m s}^{-1}$  to several meters per second, are characterised by cloud and precipitation mass contents from

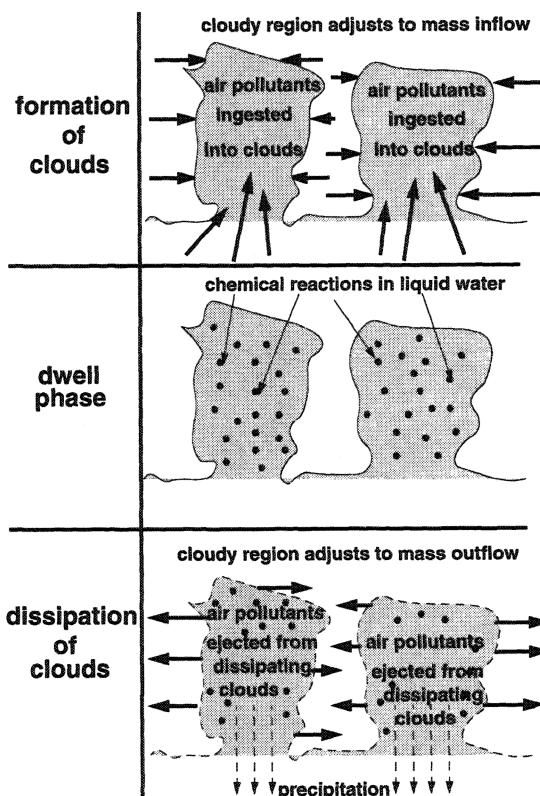


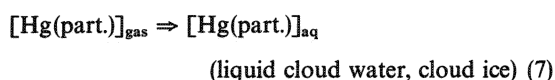
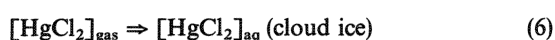
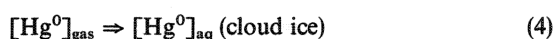
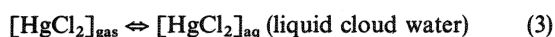
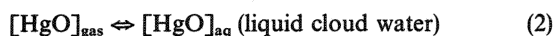
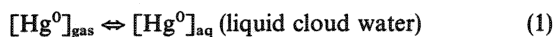
Fig. 2. Lifecycle of a cumulus cloud system (adapted from Karamchandani and Venkatram, 1992).

$0.1\text{ g m}^{-3}$  to  $10\text{ g m}^{-3}$  or more. Such rather large liquid water contents allow the cumulus clouds to be important in chemical transformations of various mercury species and the removal of gases and particulates by in-cloud and below-cloud scavenging.

Furthermore, cumulus clouds provide a means for quickly transporting boundary layer air (which may contain particularly large concentrations of pollutants) into the free troposphere.

## 2.2. Scavenging

This component of the module includes the reversible mass transfer of gaseous elemental mercury ( $\text{Hg}^0$ ) and oxidised gaseous mercury species ( $\text{HgO}$  and  $\text{HgCl}_2$ ) to liquid cloud water, irreversible scavenging of these species by cloud ice and irreversible scavenging of particulate mercury ( $\text{Hg}(\text{part.})$ ) by liquid cloud water and ice:



As an example for liquid cloud water scavenging Table 1 lists kinetic rate expressions for the mass transfer of gaseous and particulate mercury species. Reversible mass transfer processes of gaseous species (R1–R2, R3–R4) are treated as separate forward and backward reactions. The forward mass transfer rates ( $k_{f1}$ ,  $k_{f3}$ ) are estimated from collision theory and sticking coefficients. The calculations are based on the scavenging rate expression of Fuchs and Sutugin

(1971), using the parameters listed in the reference case column of Table 1. The backward mass transfer rates ( $k_{b1}$ ,  $k_{b3}$ ) are determined from the forward rates using Henry's law constant for  $\text{Hg}^0$  and  $\text{HgO}/\text{HgCl}_2$ , respectively.

Soluble gases are irreversibly scavenged by cloud ice in the model by determining the equilibrium composition of  $\text{Hg}^0$  and  $\text{HgO}/\text{HgCl}_2$  in liquid water and then freezing the liquid water so that these species are trapped in ice for the duration of the cloud life time. Particulate mercury is irreversibly scavenged by cloud water and cloud ice (R5). It is assumed that all of the mercury associated with particles is available as condensation nuclei for the formation of cloud water and ice.

## 2.3. Chemistry

One of the critical steps in the atmospheric modeling of mercury is the description of the chemical processes involved in the transformations. Atmospheric mercury consists of three major forms; elemental mercury ( $\text{Hg}^0$ ), oxidised species (e.g.  $\text{HgCl}_2$ ,  $\text{HgO}$ ) and particulate mercury ( $\text{Hg}(\text{part.})$ ). Methods capable of identifying individual species such as  $\text{HgCl}_2$  or  $\text{HgO}$  in ambient air are not available but operationally defined methods have been used to sample and measure these forms at different locations (e.g. Bloom *et al.*, 1996; Xiao *et al.*, 1996).

For a correct parameterization, conversions between these species need to be described in terms of mathematical expressions. In Pleijel and Munthe (1995a, b) an extensive chemistry was tested and evaluated in a sensitivity analysis aimed at determining the most important parameters and identifying

Table 1. Mass transfer rate expressions for gaseous and particulate mercury species

Mass transfer rate expression for cloud droplets (in cloud scavenging)	Reference case	Rate constant for Reference case [ $s^{-1}$ ]
R1 = $k_{f1}$ , $k_{r1} = f(\text{RAD}, \text{QCLD}, \text{MWT1}, \text{MFPL}, \text{STIK}, \text{TLIQ})$	RAD = 0.6600E-05 [m] (mass mean cloud droplet radius)	0.3156E-01
R2 = $k_{b1}$ , $k_{b1} = k_{f1} \cdot (\text{H1} \cdot \text{QCLD} \cdot \text{RGAS} \cdot \text{TLIQ} / \text{WDEN})$	QCLD = 0.1701E + 01 [ $\text{g m}^{-3}$ ] (cloud average liquid water content)	0.5997E + 04
R3 = $k_{f3}$ , $k_{r3} = f(\text{RAD}, \text{QCLD}, \text{MWT3}, \text{MFPL}, \text{STIK}, \text{TLIQ})$	MWT1 = 0.2000E + 03 [g] (molecular weight $\text{Hg}^0$ )	0.2911E-01
R4 = $k_{b3}$ , $k_{b3} = k_{f3} \cdot (\text{H3} \cdot \text{QCLD} \cdot \text{RGAS} \cdot \text{TLIQ} / \text{WDEN})$	MWT3 = 0.2160E + 03 [g] (molecular weight $\text{HgO}$ )	0.5348E-03
	MFPL = 0.1000E-06 [m] (mean free path length in air)	
	STIK = 0.1000E-02 [-] (sticking coefficient)	
	TLIQ = 0.2771E + 03 [K] (liquid water temperature)	
	H1 = 0.1361E-06 [ $\text{mole}^{-1} \text{ppm}^{-1}$ ] (Henry's law coefficient $\text{Hg}^0$ )	
	H3 = 0.1408E + 01 [ $\text{mole}^{-1} \text{ppm}^{-1}$ ] (Henry's law coefficient $\text{HgO}$ )	
	RGAS = 0.8205E + 05 [ $\text{cm}^3 \text{ppm mole}^{-1} \text{K}^{-1}$ ] (gas constant)	
	WDEN = 1.000E + 06 [ $\text{g m}^{-3}$ ] (water density)	
R5 = $k_{f5}$ , $k_{r5} = 0.0000E + 00$ (100% of $\text{Hg}(\text{part.})$ is nucleated at start of simulation)		0.0000E + 00

the critical processes in the atmospheric cycling of mercury. The model employed in those studies was considerably simplified in terms of physical processes and meteorology and only calculated cloud or fog droplet concentrations of mercury species. It is currently being modified to allow calculations of local to small regional scale transport and deposition processes with the full chemical description intact (Pleijel and Munthe, 1996).

Due to the constraints in computer resources and input data in comprehensive Eulerian modeling framework, it was necessary to significantly condense the chemistry described in Pleijel and Munthe (1995a). The results presented in the earlier full-chemistry studies was used as a basis for the design of the

condensed scheme depicted in Fig. 1. This condensed scheme consists of four gas phase species, six dissolved aqueous species and four aqueous particulate phase species. The reaction rates are derived from published data and from assumptions of the rates of complex formation.

The rate expressions used with the condensed scheme are presented in Tables 2–4. For each process in the gas and aqueous phase, the stoichiometric reaction rate expressions have been transformed into first order expressions where the first order rate constants are functions of the reactant species. In Tables 2–4 the expressions used with the calculations are given along with an example of the pseudo-first order reaction for the reference case. Only one gas phase reaction of

Table 2. Reaction rate expressions for aqueous phase chemistry

Reaction rate expression for aqueous phase chemistry	Reference case	Reaction rate constant for reference case [ $s^{-1}$ ]
R6 = $k_6 \cdot H_{O_3} \cdot [O_3(g)]$	$k_6 = 4.7E + 7 [M^{-1} s^{-1}]$ (Munthe, 1992)	
R7 = $k_7$	$H_{O_3} = 0.024 [M ppb^{-1}]$ $k_7 = 0.4E - 03 [s^{-1}]$ (Munthe <i>et al.</i> , 1991)	
R8 = $k_8$	$k_8 = 0.1E - 14 [s^{-1}]$	0.4000E - 03
R9 = $k_9$	$k_9 = 0.44E - 03 [s^{-1}]$	0.1000E - 14
R10 = $1.0E + 10 \times 1.0E - pH$	pH = 4.5	0.4400E - 03
R11 = $k_{11}$	$k_{11} = 0.4E + 00 [s^{-1}]$	0.3300E + 06
R12 = R13/1.17E + 24		0.4000E + 00
R13 = $1.1E - 21 \cdot ([SO_2(g)]/1.0E - 2 \cdot pH)^2$	$[SO_2(g)] = 1 [ppb]$ pH = 4.5	0.8547E - 27
R14 = $1.0E + 15 \cdot [Cl^-]^2$	$[Cl^-] = 2.0E - 6$ [mol $\ell^{-1}$ ]	0.1000E - 02
R15 = R14/1.66E + 17		0.1000E + 04
R16 = $1.0E + 15 \cdot [Cl^-] \cdot 1.0E - (14 - pH)$	$[Cl^-] = 2.0E - 6$ [mol $\ell^{-1}$ ]	0.6024E - 14
R17 = R16/3.16E + 17	pH = 4.5	0.6320E + 00
		0.2000E - 17

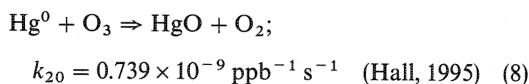
Table 3. Equilibrium rate expressions for adsorption processes

Equilibrium rate expression for adsorption processes	Reference case	Equilibrium rate constant for reference case [ $s^{-1}$ ]
R18 = $K_{18}$ , $K_{18} = 0.2000E - 01$		0.2000E - 01
R19 = R18/([csoot(g)] · W · equik/rsoot)	$[csoot(g)] = 1.0000E - 06 [g cm^{-3}]$ (soot particle concentration in air) $W = 0.5000E + 06 [-]$ (wash out ratio for soot particles) $equik = 0.5000E - 05 [m^4 g^{-1}]$ (equilibrium factor for dissolved and adsorbed mercury species) (Petersen <i>et al.</i> , 1995) $rsoot = 0.5000E - 06 [m]$ (soot particle mean radius)	0.4000E - 02

Table 4. Reaction rate expressions for gas phase chemistry

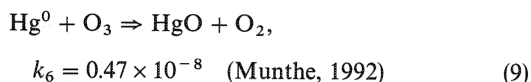
Reaction rate expression for gas phase chemistry	Reference case	Reaction rate constant for reference case [ $s^{-1}$ ]
R20 = $k_{20} \cdot [O_3(g)]$ , $k_{20} = 0.7389E - 09 [ppb^{-1} s^{-1}]$ [Hall, 1995]	$[O_3(g)] = 35 [ppb]$	0.2586E - 07
R21 = R20/1.0E + 3		0.2586E - 10

mercury is treated in the model; the oxidation of elemental mercury by ozone:



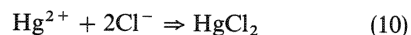
In the condensed chemistry description, this reaction is treated as a first order process with a constant ozone concentration so that  $R20 = k_{20} \cdot [\text{O}_3]$  (Table 4). For reasons of calculation procedure, all reactions in the TCM must have a reverse process. In the gas phase, no reduction of Hg(II) is known so the rate constant for this process was given a very low value ( $R21 = R20/1000$ ) making it insignificant in the overall process.

The same principle is used for the aqueous oxidation of  $\text{Hg}^0$  by ozone. The reaction is written as:



but is treated as a first order reaction in the model. The aqueous concentration of ozone is given by the gas phase concentration and the Henry's law constant. The product of both the gas and aqueous phase oxidations is assumed to be HgO. A low value for the reverse reaction is set for the same reasons as for the gas phase process. The HgO species is not very likely to be long lived in the aqueous phase and a rapid transformation to  $\text{Hg}^{2+}$  is assumed ( $\text{HgO} + \text{H}^+ \Rightarrow \text{Hg}^{2+} + \text{OH}^-$ ). In the subsequent calculation of oxidised mercury speciation in the aqueous phase,  $\text{Hg}^{2+}$  takes part in a number of reactions leading to the formation of three separate complexes;  $\text{HgCl}_2$ ,  $\text{Hg}(\text{SO}_3)_2^{2-}$  and  $\text{HgOHCl}$ .

The formation of  $\text{HgCl}_2$  is described as a hypothetical third order reaction:



for which the rate expression is

$$d[\text{HgCl}_2]/dt = k \cdot [\text{Hg}^{2+}] \cdot [\text{Cl}^-]^2 \quad (11)$$

where  $k$  is a third order reaction rate constant.

Ligand formation reactions of mercury are well known to be rapid so that the hypothetical third order rate constant can be given a value corresponding to the diffusion controlled limit, i.e. about  $10^{15} \text{ M}^{-2} \text{ s}^{-1}$ . Thus R14 is given the value  $10^{15} \cdot [\text{Cl}^-]^{-2} \text{ s}^{-1}$  where the chloride ion concentration is set in the model run. For  $\text{HgOHCl}$  a similar process is assumed except that the  $\text{OH}^-$  is given by the pH set before the model run. The rate expression for formation of  $\text{Hg}(\text{SO}_3)_2^{2-}$  is similar but slightly more complicated since the concentration of  $\text{SO}_3^{2-}$  is calculated from the air concentration of  $\text{SO}_2$  and the cloudwater pH:

$$\begin{aligned} [\text{SO}_3^{2-}] &= K_2 \cdot [\text{HSO}_3^-] / [\text{H}^+] \\ &= K_2 \cdot K_1 \cdot [\text{SO}_2(\text{aq})] / [\text{H}^+]^2 \\ &= K_2 \cdot K_1 \cdot H_{\text{SO}_2} \cdot [\text{SO}_2(\text{g})] / 10^{-2\text{pH}} \end{aligned} \quad (12)$$

where  $K_2$  and  $K_1$  are equilibrium constants for the dissociation of aqueous  $\text{SO}_2$  ( $\text{H}_2\text{SO}_3$ ) and  $\text{HSO}_3^-$  and  $H_{\text{SO}_2}$  is the Henry's law constant:

$$\begin{aligned} K_2 &= 6.42 \times 10^{-8} \\ K_1 &= 1.32 \times 10^{-2} \\ H_{\text{SO}_2} &= 1.24 \text{ mol } \ell^{-1} \text{ atm}^{-1} \\ &= 1.24 \times 10^{-9} \text{ mol } \ell^{-1} \text{ ppb}^{-1} \end{aligned}$$

With these values inserted, the expression becomes

$$[\text{SO}_3^{2-}] = 1.05 \times 10^{-18} \cdot [\text{SO}_2(\text{g})] / 10^{-2\text{pH}}. \quad (13)$$

For a hypothetical third order formation reaction,  $\text{Hg}^{2+} + 2[\text{SO}_3^{2-}] \Rightarrow \text{Hg}(\text{SO}_3)_2^{2-}$  the rate expression is given by

$$d[\text{Hg}(\text{SO}_3)_2^{2-}]/dt = k \cdot [\text{Hg}^{2+}] \cdot [\text{SO}_3^{2-}]^2. \quad (14)$$

In our case we assume a first order reaction which means that

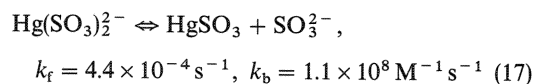
$$R13 = k \cdot [\text{SO}_3^{2-}]^2. \quad (15)$$

Our assumed reaction is a third order reaction for which the diffusion controlled limit is about  $10^{15} \text{ M}^{-2} \text{ s}^{-1}$  and R13 can be simplified to:

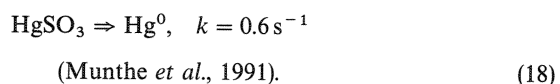
$$R13 = 1.1 \times 10^{-21} \cdot ([\text{SO}_2(\text{g})] / 10^{-2\text{pH}})^2. \quad (16)$$

For all the three major dissolved complexes  $\text{HgCl}_2$ ,  $\text{Hg}(\text{SO}_3)_2^{2-}$  and  $\text{HgOHCl}$ , equilibrium constants are well known and can be applied for the calculation of the reverse reaction rate constants R15, R12 and R17. The whole procedure described above for these complexes is meant to allow kinetic treatment of these processes without disturbing the known equilibrium properties.

Of the three major complexes nearly all the oxidised mercury exists in the chloride form. This is due to the relatively high chloride concentration found in the droplets (Plejdel and Munthe, 1995a).  $\text{HgOHCl}$  is the second most important complex and  $\text{Hg}(\text{SO}_3)_2^{2-}$  is added due to the possibility of back reduction of oxidised Hg to  $\text{Hg}^0$  via reaction R9. The stoichiometry of this reaction is written as:



and



The rate limiting step in this reaction scheme is the dissociation of  $\text{Hg}(\text{SO}_3)_2^{2-}$  and this rate constant has been used for reaction R9 in the condensed scheme. The reverse process is not considered to be a realistic process and R8 is given a sufficiently low value in order not to affect the process.

The parameterization of adsorption of dissolved mercury species on particles is based on an observed

empirical equilibrium relation between mercury concentrations (Petersen *et al.*, 1995) and the occurrence of soot particles in precipitation samples (Iverfeldt, 1991). To date, no alternative more theoretically strict description is available for this process. In general, the adsorption of airborne mercury onto carbon based surfaces (i.e. activated carbon) is well known and used in many applications for trapping vapour phase mercury. The reversibility of the aqueous adsorption of different mercury species, as described in the TCM, is to some extent an assumption necessary for computing reasons. Experimental studies on this process are a prerequisite for further development of models for atmospheric mercury.

In the TCM it is assumed that the adsorption rate is diffusion-controlled and the desorption rate is calculated from the adsorption rate and the empirical equilibrium relation mentioned above. The adsorption rate is calculated as the typical time for diffusion in an aqueous phase to be about  $0.02 \text{ s}^{-1}$  which is used for the forward rate constant R18 in the condensed scheme. Thus the reverse desorption rate constant R19 will depend on the soot particle concentration and the soot particle radius. For the reference case a value of  $4 \times 10^{-3} \text{ s}^{-1}$  is used (see Table 3).

### 3. TEST RESULTS

A schematic view of the TCM for cumulus and stratus clouds embedded into the ADOM three-dimensional grid system is presented in Fig. 3a and b, respectively. For both cloud types initial concentration profiles of mercury species in ambient air, cloud base height, precipitation rates and vertical profiles of temperature, pressure and relative humidity are needed as input. Cloud top heights are required input for stratus clouds while this is calculated in the cumulus cloud module. The module can be run for a sequence of hours with the clouds evaporated at the end of the one hour time step to provide the starting concentration profiles for the next hour.

The volume of a cumulus cloud is defined by the cloud cover i.e. the fraction of the cloudy region in a grid square and by the cloud base height and top height (Fig. 3a). This volume is subdivided into inactive and active regions. The dissipation of clouds is represented by the inactive regions. Subgrid scale vertical mixing, i.e. up and down motion of air parcels occurs in the active region. This motion is accompanied by the formation of cloud water and the redistribution of air and pollutants. The active region also represents the reactor for aqueous phase chemistry. During the aqueous phase chemistry submodule execution, the pollutant concentrations are assumed to be homogeneously mixed throughout this reactor.

Stratiform clouds always cover the entire grid square. The column is divided vertically into a maximum of four zones, depending on the microphysical processes occurring in them (Fig. 3b). The steady state

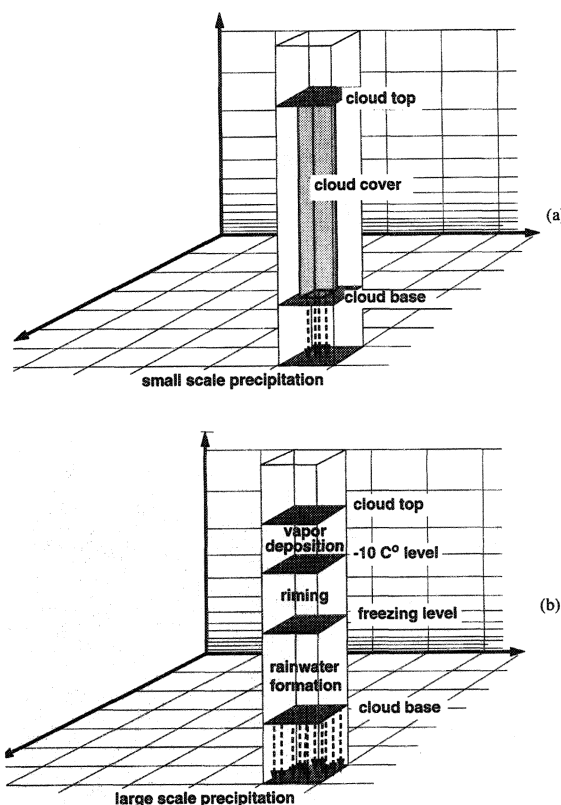


Fig. 3. Schematic view of the TCM: (a) cumulus cloud; (b) stratus cloud.

vertical distribution of cloud microphysical parameters is calculated in the zones and is provided as input to the aqueous phase chemistry submodule. In each of the zones, aqueous phase chemistry is simulated assuming homogeneously mixed pollutant concentrations.

In both cumulus and stratus clouds, mass transfer and chemistry equations are solved using the Young and Boris predictor corrector scheme (Young and Boris, 1977). After the aqueous phase processes are simulated mercury species in cloud water are removed via wet deposition, which is determined as the product of their liquid water and ice weighted average concentration and the precipitation amount. At the end of the model time step, remaining mercury species in the cloud are returned to the gas phase by cloud evaporation and redistribution of the species from the chemical reactor to the grid system of the entire column consisting of 12 unevenly spaced vertical layers between 1 m and 10000 m.

As has been mentioned in the previous section, gas phase chemistry is currently restricted to the oxidation of  $\text{Hg}^0$  by ozone. Nevertheless this process may have a significant impact on mercury concentration levels since gas phase chemistry acts during each time step and in each grid cell of the entire column.

TCM testing was conducted by incorporating the above described mechanisms for cloud mixing,

scavenging and chemistry into the grid columns depicted in Figs 3a and b. The main objective of the test runs described in the subsequent sections was to study the model behavior under different environmental conditions and to compare the results with observed mercury concentrations in precipitation at different sites in Europe.

### 3.1. Cloud sensitivity studies

This section illustrates the TCM behavior under different cloud conditions. Sensitivity runs were performed to test the scavenging mechanisms and the chemical equation set for mercury species in cumulus clouds and stratus clouds.

For cumulus clouds, two environmental temperature profiles were chosen. The profiles, referred to as the warm and cold profiles together with the input cloud base height and the cloud top height calculated from the cloud physics submodule are shown in Figs 4a and b. Both cases share the same pressure and humidity profile. The cloud cover in the grid square and the active cloudy region were fixed in both cases at 0.9 and 0.1, respectively. The precipitation rates used with the sensitivity tests were  $2 \text{ mm h}^{-1}$  for the warm case and  $0.3 \text{ mm h}^{-1}$  for the cold case. Both clouds have a base height of approximately 500 m.

For the warm cloud a top height of 10000 m and a maximum liquid water and ice content of nearly 4 and  $1.5 \text{ g per m}^3$  of air, respectively, have been calculated whereas the cold cloud has considerably lower liquid water and ice contents and only extends up to approximately 2000 m height. The vertical distribution of air flow into and out of the active region of the warm and the cold cloud is shown in Figs 5a and b. The horizontal dotted lines represent the grid cell center heights in the vertical grid system, the bars indicate the inflow and outflow of air. According to the mixing model of Raymond and Blyth the active area in both clouds consists of 50% cloud base air and 50% entrained from the sides. In case of the warm cloud (Fig. 5a), about 75% of the air comprising the cloud flows out of the topmost layer, indicating that almost all combinations of air from the base and the sides are buoyant enough to reach the cloud top. The total airflow in the cold cloud is considerably lower and the outflow is more evenly distributed between several layers.

The effects of cloud mixing, scavenging and wet deposition on the vertical concentration profile of particulate mercury ( $\text{Hg}(\text{part.})$ ), which does not undergo chemical reactions, are depicted in Figs 6a and b. The lines represent 24 h sequences of  $\text{Hg}(\text{part.})$

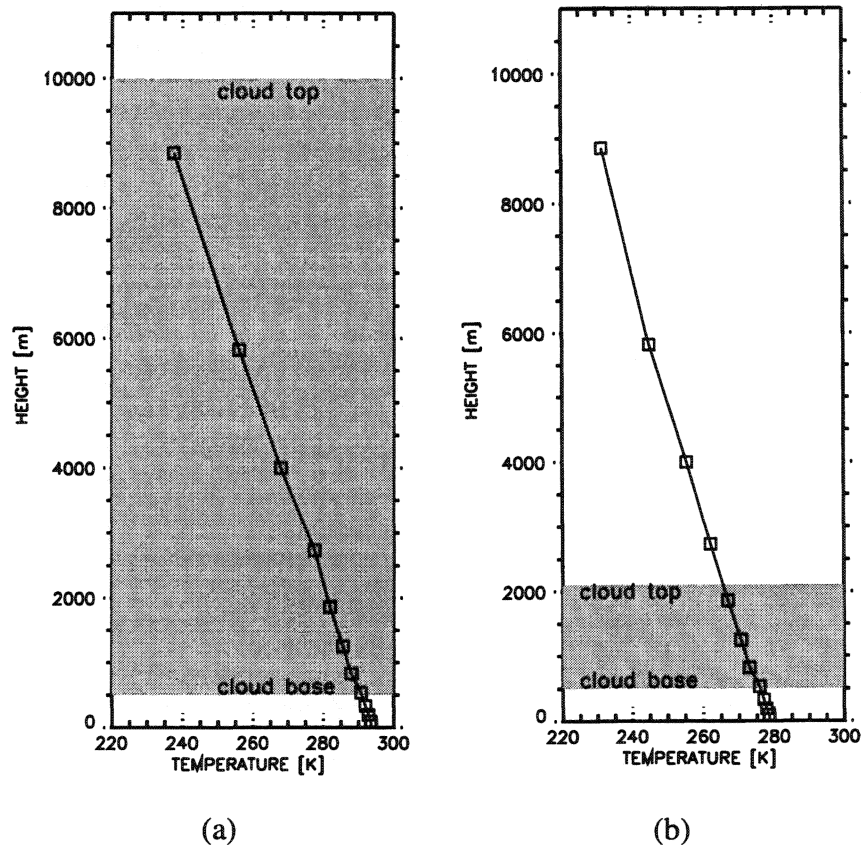


Fig. 4. Temperature profile and cloud base/top elevation: (a) cumulus cloud in a warm environment; (b) cumulus cloud in a cold environment.

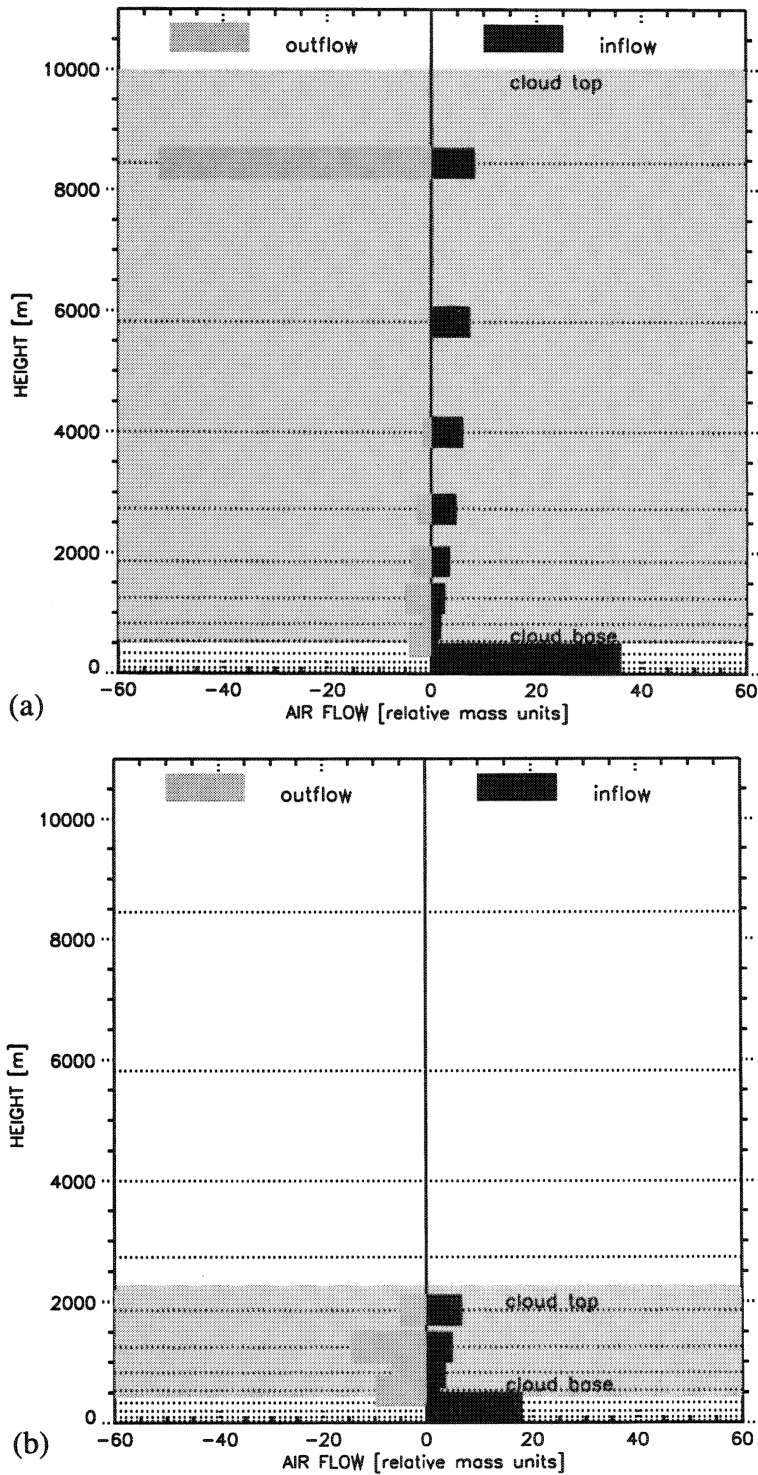


Fig. 5. Air inflow and outflow: (a) cumulus cloud in a warm environment; (b) cumulus cloud in a cold environment.

concentration profiles after cloud dissipation at the end of each one hour time step. For both the warm and the cold cloud the model was started with the same vertical constant concentration profile. It is evi-

dent that in both cases final concentration profiles reflect the distribution of outflow of air shown in Figs 5a and b. In case of the warm cloud, the concentrations decrease most rapidly at the 8500 m level. This is

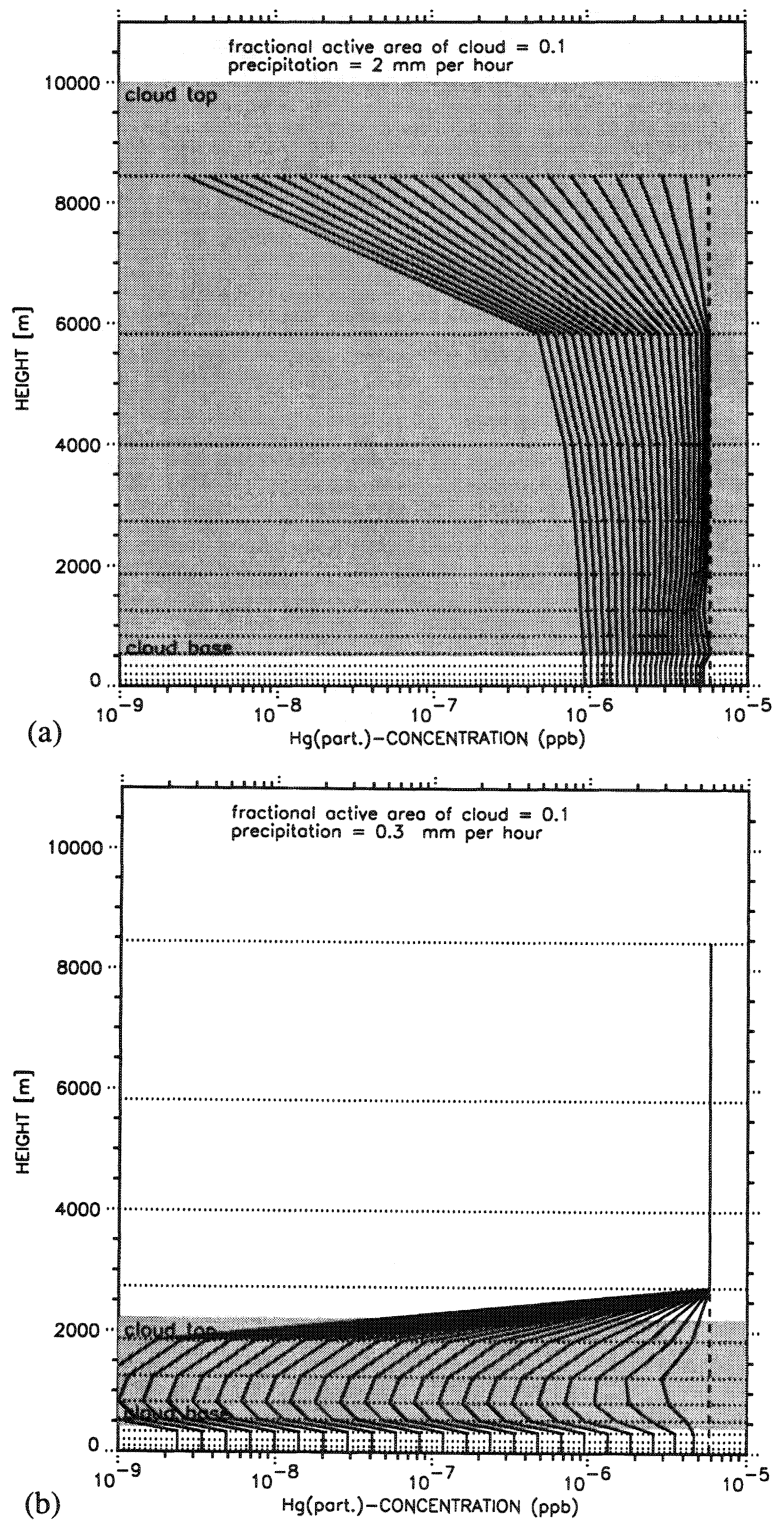


Fig. 6. 24-h time evolution of particulate mercury concentration profiles: (a) cumulus cloud in a warm environment; (b) cumulus cloud in a cold environment.

expected since the cloud air, depleted in Hg(part.) due to wet deposition, has most of its outflow to the environment at this level. Mixing of the environmental air at the 8500 m level with lower layers results in the

slow spread of the impact over the cloud depth. For the cold cloud case, cloud air is detrained over the 1500 m cloud depth, resulting in more uniform depletion of Hg(part.) concentration over a 24 h simulation.

The chemical scheme has undergone extensive testing comprising the warm and cold cumulus clouds described above and a stratus cloud with a base and top height of 500 and 4000 m, respectively and a precipitation rate of  $1.19 \text{ mm h}^{-1}$ . As an example, Figs 7a–c show the time evolution of vertical  $\text{Hg}^0$  concentration profiles in a one hour sequence starting with a vertical constant profile of  $3.75 \times 10^{-4} \text{ ppb}$ , which corresponds to  $3 \text{ ng m}^{-3}$  at ground level. As can be seen from the chemistry scheme depicted in Fig. 1 the  $\text{Hg}^0$  profiles are effected by both gas phase chemistry and mass

transfer to cloud droplets and subsequent aqueous phase chemistry. The effects of gas phase chemistry alone are reflected by a continuous decrease of the vertical constant concentration profiles in the regions above the top of the cold cumulus (Fig. 7b) and the stratiform cloud (Fig. 7c). For both the warm and the cold cumulus, additional effects of  $\text{Hg}^0$  scavenging followed by aqueous phase chemistry, which only takes place in the active part of the cloudy region, are comparatively small thus indicating that the gas phase oxidation of  $\text{Hg}^0$  is a more important pathway than the direct transfer of  $\text{Hg}^0$  to cloud droplets

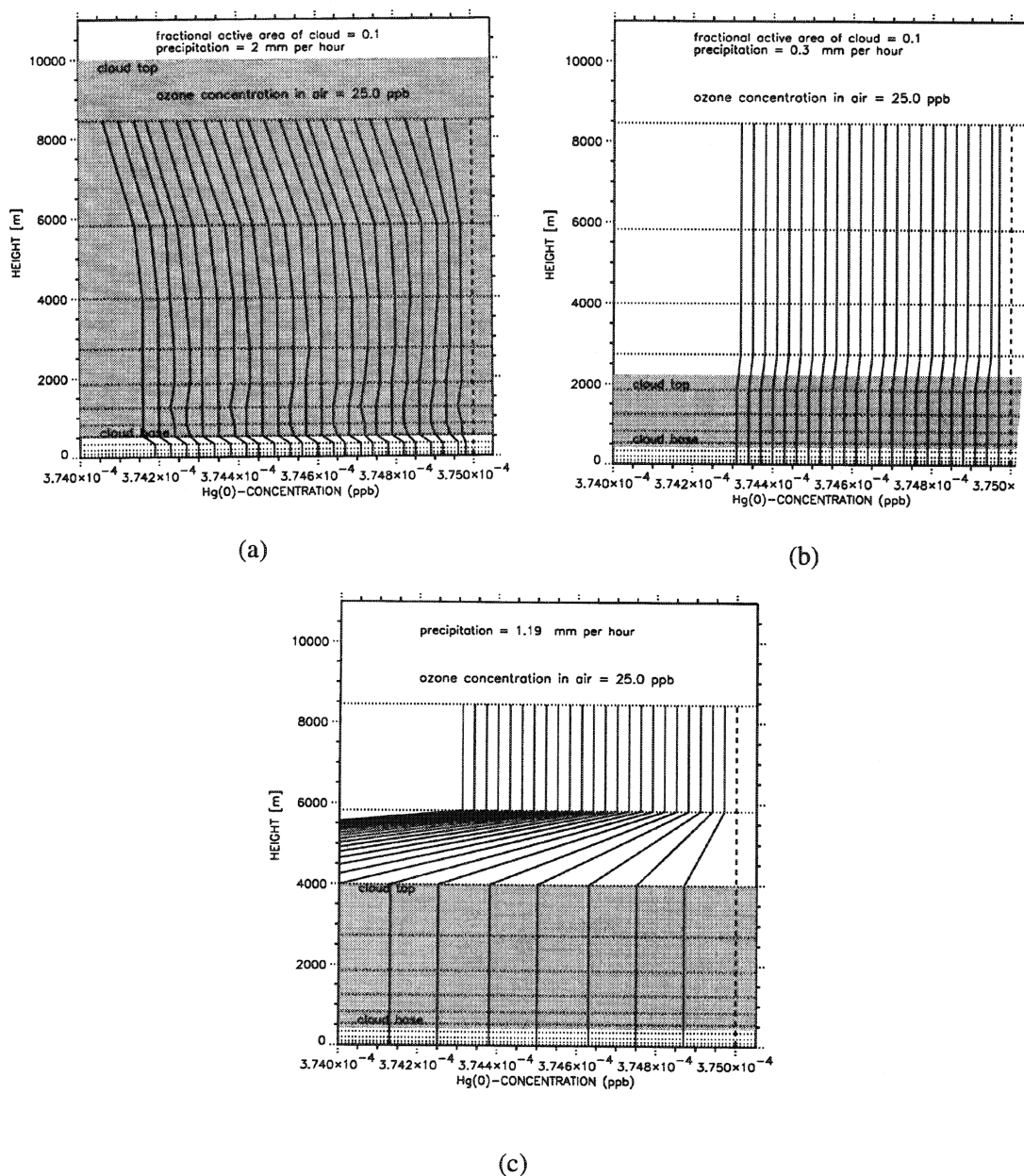


Fig. 7. 24-h time evolution of elemental mercury concentration profiles; (a) cumulus cloud in a warm environment; (b) cumulus cloud in a cold environment; (c) stratus cloud.

(Figs 7a and b). The decrease in the stratus cloud layers is more pronounced since aqueous phase chemistry is performed in the entire grid cell (Fig. 7c).

Tests of the chemical scheme have been further extended by investigating the formation of total mercury concentration in the aqueous phase ( $\text{Hg}(\text{tot.})$ ). This species represents the sum of all dissolved ( $\text{Hg}(\text{diss.})$ ) and adsorbed ( $\text{Hg}(\text{ads.})$ ) species originating from  $\text{Hg}^0$  in ambient air, i.e. for these tests  $\text{HgCl}_2$  and ( $\text{Hg}(\text{part.})$ ) in ambient air have been decoupled from the system depicted in Fig. 1, thus allowing to determine the formation of  $\text{Hg}(\text{tot.})$  in cloud and rainwater droplets as a function of the  $\text{Hg}^0$  depletion illustrated in Fig. 7. The development of  $\text{Hg}(\text{tot.})$  concentrations during a 48-h simulation is shown in Fig. 8. The solid line represents the formation of  $\text{Hg}(\text{tot.})$  in a non-precipitating warm cumulus. The dashed and the chaindashed line show the build up in the deep warm and in the shallow cold cloud with the same precipitation rate of  $0.3 \text{ mm h}^{-1}$ . Since aqueous phase chemistry occurs up to 10000 m height, the deep cloud processes a much larger mass of the cloudy region air in an hour resulting in a more effective build up of  $\text{Hg}(\text{tot.})$  concentration. The warm cloud with  $2 \text{ mm h}^{-1}$  precipitation (dotted line) shows a less effective  $\text{Hg}(\text{tot.})$  build up than the same cloud with a precipitation rate of  $0.3 \text{ mm h}^{-1}$  (dashed line), as expected due to more effective scavenging. The significant influence of the bigger cloud volume on  $\text{Hg}(\text{tot.})$  formation becomes evident when the curves for the deep warm cloud (precipitation rate  $2 \text{ mm h}^{-1}$ ) and the shallow cold cloud (precipitation rate  $0.3 \text{ mm h}^{-1}$ ) are compared; in the case of the warm cloud, enhanced production of  $\text{Hg}(\text{tot.})$  by aqueous phase

chemistry overcompensates the enhanced depletion by a higher precipitation rate resulting in a slightly higher build up of  $\text{Hg}(\text{tot.})$  than in the shallow cloud with a smaller precipitation rate.

### 3.2. Comparison with observations

Figure 9 shows TCM predictions of  $\text{Hg}(\text{tot.})$ ,  $\text{Hg}(\text{diss.})$  and  $\text{Hg}(\text{ads.})$  concentrations originating from  $\text{Hg}$  in air with an initial constant vertical profile of  $3.75 \times 10^{-4} \text{ ppb}$  as a function of soot concentration in ambient air for a warm cumulus cloud with no precipitation and with a precipitation rate of  $2 \text{ mm h}^{-1}$  after a 48 h simulation period. In both cases  $\text{Hg}(\text{ads.})$  increases and  $\text{Hg}(\text{diss.})$  decreases with increasing soot concentrations, but the concentration levels differ by one order of magnitude due to depletion of mercury species in the precipitating cloud. For soot concentrations greater than  $1 \times 10^{-6} \text{ g m}^{-3}$  almost all of the mercury is in the adsorbed phase, whereas for lower soot concentrations the major fraction is in the dissolved phase. These model results can be compared against observed  $\text{Hg}(\text{tot.})$  concentrations, which are routinely monitored within European research programs. Typical monthly averages of mercury in precipitation are in the range of  $2 \times 10^{-11}$ – $2 \times 10^{-10} \text{ mol l}^{-1}$  at monitoring sites at the Swedish west coast (Iverfeldt, 1991), the Irish west coast and the German coast of the North Sea (Ebinghaus *et al.*, 1995). The weighted annual average is around  $5 \times 10^{-11} \text{ mol l}^{-1}$ , which is in good agreement with the calculated range of  $\text{Hg}(\text{tot.})$  concentrations depicted in Fig. 9.

Comparisons of calculated  $\text{Hg}(\text{tot.})$  concentrations as a function of  $\text{Hg}^0$  in ambient air and simultaneous

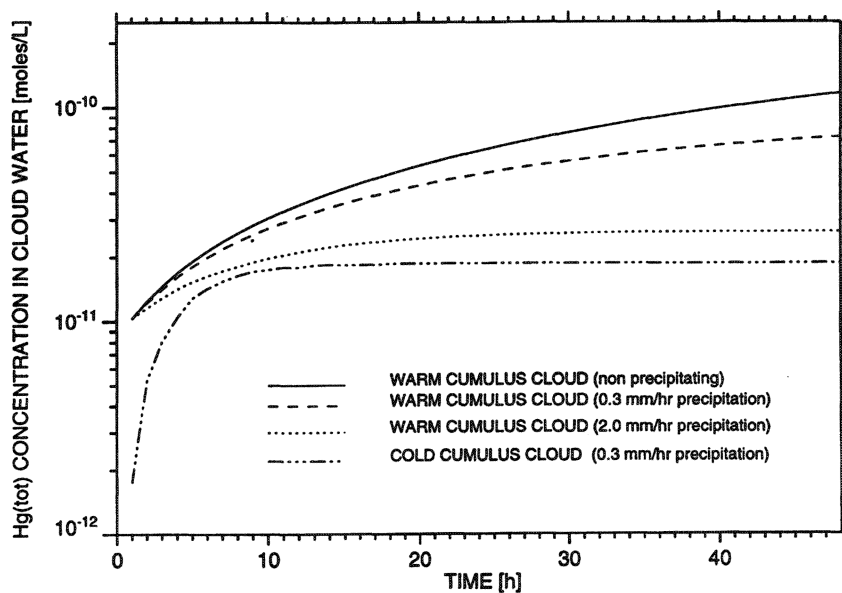


Fig. 8. Development of total mercury concentration in cloudwater and rain for different cloud conditions during a 48 h simulation period.

measurements of Total Gaseous Mercury (TGM) and Hg(tot.) obtained at four different sites in Sweden (Iverfeldt, 1991) and in Ireland and Germany (Ebinghaus *et al.*, 1995) are presented in Fig. 10. This comparison is between TCM calculations of Hg(tot.) in cloud and rainwater ranging from a non-precipitating cloud to a deep cumulus associated with a precipitation rate of  $2 \text{ mm h}^{-1}$  and measurements of Hg(tot.) at ground level associated with precipitation rates up to  $2 \text{ mm h}^{-1}$ .

In general, TCM predicted Hg(tot.) concentrations compare satisfactorily with observations from all the stations, indicating that the module is based on an adequate parameterization of cloud mixing, scavenging and chemistry. Compared to the linear fit of observed Hg(tot.) concentrations the TCM seems to underpredict Hg(tot.) at the upper end of the range shown in Fig. 10. This is most probably due to two factors which could adversely affect the skill of the model to reproduce the observed Hg(tot.)

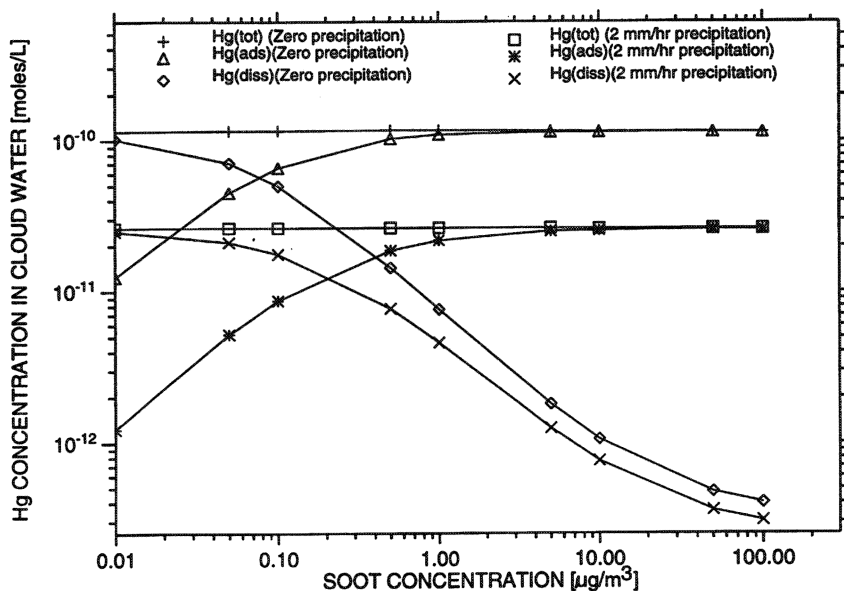


Fig. 9. Mercury concentrations in cloudwater and rain as a function of soot concentration in ambient air after a 48 h simulation period.

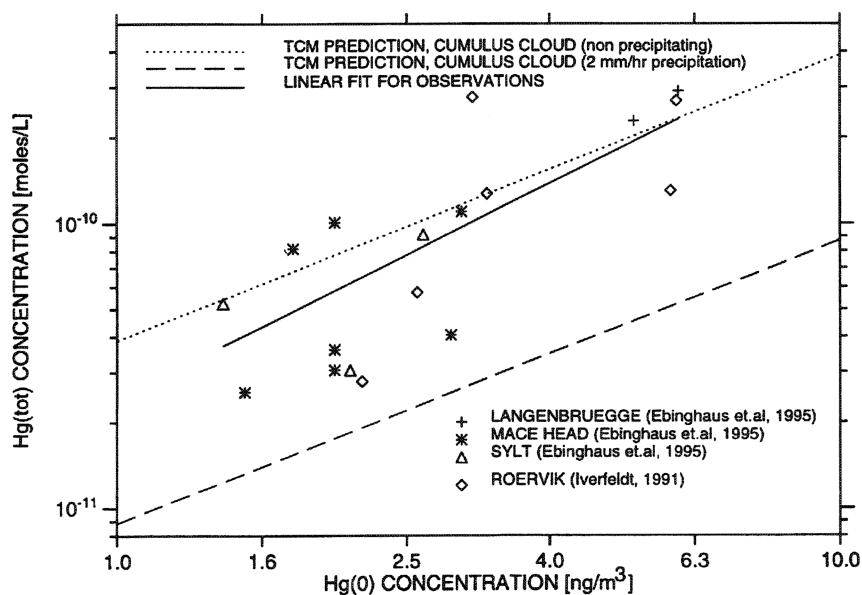


Fig. 10. Comparison of TCM predicted and observed total mercury concentrations in cloudwater and rain.

concentrations. First, slight differences between  $\text{Hg}^0$  model input and measured TGM could affect the comparison, at least at sites like Langenbrügge which is located in the vicinity of industrial sources with a potential of additional emissions of oxidised gaseous mercury species such as  $\text{HgCl}_2$  resulting in higher  $\text{Hg}(\text{tot.})$  concentrations at the measurement site. Second, the upper end of the range of observed TGM concentrations shown in Fig. 10 is frequently associated with soot concentrations greater than  $1.0 \times 10^{-6} \text{ g m}^{-3}$ . This value was used with the entire range of TCM simulations, thus suggesting that  $\text{Hg}(\text{tot.})$  concentrations at the upper end of the calculated range are underestimated. However, the limited data material does not allow to draw any firm conclusions and a larger data set is needed to evaluate the TCM performance with respect to adsorption of dissolved mercury species on soot particles and the impact of gaseous mercury species other than  $\text{Hg}^0$  on aqueous phase concentrations of both dissolved and adsorbed mercury species.

#### 4. SUMMARY AND CONCLUSIONS

The stand-alone version of a Tropospheric Chemistry Module (TCM) containing submodules for cloud mixing, scavenging and chemistry of atmospheric mercury species is presented. The chemical equation set used with the TCM is a condensed version of the comprehensive Chemistry of Atmospheric Mercury (CAM) process model. The TCM is consistent with current understanding of cloud processes and treats both cumulus and stratus clouds within the same framework. The module is computationally simple enough to be readily incorporated into comprehensive Eulerian models for atmospheric mercury species without significant increase of total computational time.

A number of sensitivity studies have been conducted with the TCM to investigate its cloud mixing, scavenging and chemical transformation characteristics. In general, results from these studies indicate that the TCM has capabilities to gain scientific insights of tropospheric mercury transport, transformation and deposition problems which cannot be obtained through field measurements or experiments in the laboratory. The evaluation of the module performance led to three main issues:

(1) TCM predictions of mercury concentrations in rainwater compare satisfactorily with observations at four European sites thus indicating that the module is based on an adequate parameterization of atmospheric mercury processes. However, the available data material is scarce and more simultaneous measurements of mercury concentrations in ambient air and precipitation are necessary to evaluate the ultimate TCM performance.

(2) Due to lack of analytical methods capable of identifying individual oxidised mercury species, the

TCM performance with respect to the impacts of  $\text{HgCl}_2$  and  $\text{HgO}$  on the atmospheric cycling of mercury cannot be evaluated at present.

(3) TCM test runs have shown that adsorption of mercury species to particulate matter is very important to the atmospheric fate of mercury. Currently, the TCM chemical equation set is restricted to adsorption of dissolved mercury species on soot particles based on an empirical adsorption coefficient. For further TCM development, a more accurate parameterization of adsorption processes is clearly needed.

Overall, the present development level of the TCM is such that its implementation in full ADOM mercury versions for Europe and North America is justified. These models with the TCM as their major component will be developed further according to advancements in the knowledge of atmospheric mercury processes to ensure that they maintain their capability to address effectively the scientific and policy questions that may arise over the next decade.

*Acknowledgements*—The authors wish to acknowledge the financial support for this work which was provided by the the International Bureaus of the GKSS Forschungszentrum Geesthacht and the Deutsche Forschungsanstalt für Luft- und Raumfahrt (DLR) in the framework of the Germany/Canada Science and Technology Agreement, Atmospheric Environment Sector, Project ENV58 "Air Toxics", and the Indo-German Bilateral Agreement on Cooperation in Science and Technology, Project, "Metal Ions Speciation in the Environment", respectively. The tropospheric chemistry module described in this paper has been developed in the framework of the European Union – MARine Science and Technology – BALTic Sea SYstem Study (EU-MAST-III-BASYS), Subproject 5 — Atmospheric Load.

#### REFERENCES

- Bloom, N. S., Prestbo, E. M. and Von der Geest, E. (1996) Determination of atmospheric gaseous  $\text{Hg}(\text{II})$  at the  $\text{pg/m}^3$  level by collection onto cation exchange membranes, followed by dual amalgamation/cold vapor atomic fluorescence spectrometry. In *4th Int. Conf. on Mercury as a Global Pollutant, Book of Abstracts* (edited by Ebinghaus R., Petersen, G. and von Tümpling, U.), GKSS Forschungszentrum, Max-Planck-Strasse, D-21502 Geesthacht, Germany).
- Bullock, O. R., Benjey, W. G. and Keating, M. H. (1997) The Modeling of Regional-scale Atmospheric Mercury Concentration and Deposition Patterns using RELMAP, *Environmental Toxicology and Chemistry*.
- Ebinghaus, R., Kock, H. H., Jennings, S. G., McCartin, P. and Orren, M. J. (1995) Measurements of atmospheric mercury concentrations in northwestern and central Europe — Comparison of experimental data and model results. *Atmospheric Environment* **29**, 3333–3344.
- Fuchs, N. A. and Sutugin, A. G. (1971) High-dispersed aerosols. *International Reviews of Aerosol Physics and Chemistry*, Vol. 2 (edited by Hidy, G. M. and Brock, J. R.), pp. 1–60, Pergamon Press, New York.
- Fung, C., Misra, P. K., Bloxam, R. and Wong, S. (1991) A numerical experiment on the relative importance of  $\text{H}_2\text{O}_2$  and  $\text{O}_3$  in aqueous conversion of  $\text{SO}_2$  to  $\text{SO}_4^{2-}$ . *Atmospheric Environment* **25A**, 411–422.

- Hall, B. (1995) The gas phase oxidation of elemental mercury by ozone, *Water, Air and Soil Pollution* **80**, 301–315.
- Iverfeldt, A. (1991) Occurrence and turnover of atmospheric mercury over the nordic countries. *Wat. Air Soil Pollut.* **56**, 251–265.
- Iverfeldt, A., Munthe, J. and Hultberg, H. (1996) Terrestrial mercury and methylmercury budgets for Scandinavia. *Regional and Global Mercury Cycles, Fluxes and Mass Balances* (edited by Baeyens W., Ebinghaus R. and Vassiliev O. F.), NATO-ASI Series, Series 2: Environment, Vol. 21, pp. 381–401. Kluwer Academic Publishers, Dordrecht, the Netherlands.
- Karamchandani, P. K. and Venkatram, A. (1992) The role of non-precipitating clouds in producing ambient sulfate during summer: Results from simulations with the Acid Deposition and Oxidant Model (ADOM). *Atmospheric Environment* **26A**, 1041–1051.
- Kessler, E. (1969) On the distribution and continuity of water substances in atmospheric circulation. *Met. Monographs* **10**, Number 32, American Meteorological Society, 45 Beacon St., Boston, Massachusetts 02108, U.S.A.
- Lindqvist, O., Wei, S. and Tan, S. (1996) Inventory of anthropogenic mercury emissions from Guizhu Province, China. In *4th Int. Conf. on Mercury as a Global Pollutant, Book of Abstracts* (edited by Ebinghaus, R., Petersen, G. and von Tümpling, U.), GKSS Forschungszentrum, Max-Planck-Strasse, D-21502 Geesthacht, Germany).
- Munthe, J. (1992) The aqueous oxidation of elemental mercury by ozone. *Atmospheric Environment* **26A**, 1461–1468.
- Munthe, J., Xiao, Z. F. and Lindqvist, O. (1991) The aqueous reduction of divalent mercury by sulfite, *Water, Air and Soil Pollution* **56**, 621–630.
- Petersen, G., Iverfeldt, A. and Munthe, J. (1995) Atmospheric mercury species over Central and Northern Europe. Model calculations and comparison with observations from the Nordic air and precipitation network for 1987 and 1988. *Atmospheric Environment* **29**, 47–67.
- Petersen, G., Munthe, J. and Bloxam, R. (1996) Numerical modeling of regional transport, chemical transformations and deposition fluxes of airborne mercury species. *Regional and Global Mercury Cycles, Fluxes and Mass Balances* (edited by Baeyens W., Ebinghaus R. and Vassiliev O. F.), NATO-ASI Series, Series 2: Environment, Vol. 21, pp. 191–217, Kluwer Academic Publishers, Dordrecht, the Netherlands.
- Pleijel, K. and Munthe, J. (1995a) Modelling the atmospheric mercury cycle—chemistry in fog droplets. *Atmospheric Environment* **29**, 1441–1457.
- Pleijel, K. and Munthe, J. (1995b) Modeling the atmospheric chemistry of mercury — the importance of a detailed description of the chemistry of cloud water. *Water, Air and Soil Pollution* **80**, 317–324.
- Pleijel, K. and Munthe, J. (1996) Modeling the atmospheric chemistry of mercury — validation and sensitivity analysis of different deposition processes. In *4th Int. Conf. on Mercury as a Global Pollutant, Book of Abstracts* (edited by Ebinghaus, R., Petersen, G. and von Tümpling, U.), GKSS Forschungszentrum, Max-Planck-Strasse, D-21502 Geesthacht, Germany).
- Porcella, D. B., Chu, P. and Allan, M. A. (1996) Inventory of North American Hg emissions to the atmosphere. *Regional and Global Mercury Cycles, Fluxes and Mass Balances* (edited by Baeyens W., Ebinghaus R. and Vassiliev O. F.), NATO-ASI Series, Series 2: Environment, Vol. 21, pp. 179–190. Kluwer Academic Publishers, Dordrecht, the Netherlands.
- Raymond, D. J. and Blyth, A. M. (1986) A stochastic mixing model for nonprecipitating cumulus clouds. *Journal of Atmospheric Science* **43**, 2708–2718.
- Shannon, J. D. and Voldner, E. C. (1995) Modeling atmospheric concentrations of mercury and deposition to the Great Lakes. *Atmospheric Environment* **29**, 1649–1662.
- Slemr, F. and Langer, E. (1992) Increase in global atmospheric concentrations of mercury inferred from measurements over the Atlantic Ocean. *Nature* **333**, 434–437.
- Stern, R., Scherer, B. and Schubert, S. (1990) Modeling of photochemical oxidant formation in North-Western Europe with special emphasis on the non-linearity issue in the SO<sub>x</sub>/NO<sub>x</sub>/VOC system. Presented at the *EMEP Workshop on the Progress of Transport Modelling of Nitrogen Compounds*, Potsdam, Germany, October 1990.
- Venkatram, A., Karamchandani, P. K. and Misra, P. K. (1988) Testing a comprehensive acid deposition model. *Atmospheric Environment* **22**, 737–747.
- Warner, J. (1970) On steady state one-dimensional models of cumulus convection. *Journal of Atmospheric Science* **27**, 1035–1040.
- Xiao, Z. F., Sommar, J., Wei, S. and Lindqvist, O. (1996) Sampling and determination of gas phase divalent mercury with KCl coated denuders. In *4th Int. Conf. on Mercury as a Global Pollutant, Book of Abstracts* (edited by Ebinghaus, R., Petersen, G. and von Tümpling, U.), GKSS Forschungszentrum, Max-Planck-Strasse, D-21502 Geesthacht, Germany).
- Young, T. R. and Boris, J. P. (1977) A numerical technique for solving stiff ordinary differential equations associated with the chemical kinetics of reactive flow problems, *J. Phys. Chem.* **81**, 2424–2427.



# Paper IV



## NUMERICAL SIMULATION MODELS FOR AIRBORNE HEAVY METALS IN EUROPE: A REVIEW

G. PETERSEN

GKSS-Research Centre, Institute of Hydrophysics  
Max-Planck-Strasse, D-21502 Geesthacht, GERMANY

### Abstract

In view of the decision of the United Nations-Economic Commission Europe (UN-ECE) to prepare a protocol for heavy metals and persistent organic pollutants under its Convention on Long-range Transboundary Air Pollution an attempt is made to summarize European activities on modeling the atmospheric long-range transport of heavy metals. Special emphasis is placed on mercury, lead and cadmium which have been defined by the UN-ECE to be the priority heavy metals of concern. In this paper, numerical models for atmospheric transport, transformations and deposition of heavy metals are discussed chronologically with respect to their development and first applications. Basic features of the models together with input data and main results are summarized in a table. Limitations of present models and the improvements that are needed to address effectively the issues presently facing the atmospheric scientific and policy-making communities are briefly outlined.

### 1. Introduction

Over the past two decades, significant efforts have been devoted in Europe to the monitoring of heavy metals as a result of the general awareness of the potential impacts of atmospheric long-range transport on sensitive ecosystems such as European marginal seas [17], [1], [15], [71], [24], [65], [67], [19], inland lakes and forest areas [66], [75], [39] and the Norwegian Arctic [45], [43], [44]. Relatively little attention has been given to numerical modeling of the long-range transport and deposition of heavy metals over Europe so far. However, in recent years it has been widely recognized, that the use of numerical models is important in formulating effective control strategies for the reduction of atmospheric deposition fluxes of heavy metals to the above mentioned ecosystems, because the only way of delineating their atmospheric transport pathways and hence the emitter-receiver relationship is through numerical modeling [51], [26], [27], [38].

In a broad sense, two basic types of models have been developed to date, wherein the turbulent transport of heavy metals is analyzed through either a Lagrangian or an Eulerian approach. Lagrangian models developed for heavy metals and currently

TABLE 1. A Comparative Summary of Models Applied to Heavy Metals in Europe

model							reference
name	type	institution	input		output		
			meteorological input	calculated substances	receptor area	typical time scale	
<b>EMEP</b> (European Monitoring and Evaluation Program)	Lagrangian 1-layer trajectory model	NILU Norsk Institutt for Luftforskning Kjeller, Norway	6-hourly from the Norwegian Numerical Weather Prediction Model	Pb,Cd,As V,Mn,Sb,Se	Birkenes, Southern Norway	months	Pacyna et al., 1984
<b>TREND</b>	statistical approach of a Gaussian plume model and a trajectory model	RIVM National Institute of Public Health and Environmental Protection Bilthoven, the Netherlands	long-term averages from the Dutch Meteorological Office and from the European Centre for Medium-Range Weather Forecast (ECMWF).	As,Sb,Cd,Cr; Cu,Ni,Zn	North Sea	years	van Jaarsveld et al., 1986
<b>OPS</b> (Operational Priority Substances)		TNO Netherlands Organization for Applied Research Delft, the Netherlands		Cd,Cr,Cu,Pb Hg,Ni,Zn	North Sea, Dutch Wadden Sea River Rhine drainage basin		Warmenhoven et al., 1989
<b>EUTREND</b>				Pb,Cd	Europe North Sea		Baart et al., 1995
<b>HHLRT</b> (Hamburg Long-Range Transport Model)	three-dimensional stochastic model	Meteorological Institute, University of Hamburg Germany	6-hourly analyses from the ECMWF	Pb,Cd	North Sea	months	Krell and Roeckner, 1988

TABLE 1 (continued)

name		type	model				application			reference
			institution	input	input	output	calculated substances	receptor area	typical time scale	
<b>HMET</b> (Heavy Metals Eulerian Transport)	1-layer (plus 1 residence layer) Eulerian model	EMEP Meteorological Synthesizing Centre West Oslo, Norway	6-hourly from the Norwegian Numerical Weather Prediction Model	Pb,Cd,Zn,As	Europe	months	Bartnicki et al., 1993 Bartnicki, 1994 Bartnicki, 1996			
	4-layer Eulerian model	EMEP Meteorological Synthesizing Centre East Moscow, Russia	6-hourly from the Russian Hydro-meteorological Centre	Pb,Cd	Europe	years				
<b>ASIMD</b> (asymmetric advection scheme)	4-layer Eulerian model	EMEP Meteorological Synthesizing Centre East Moscow, Russia	6-hourly from the Russian Hydro-meteorological Centre	Pb,Cd	Europe	years	Pekar, 1996			
<b>LPMOD</b> (Large Particle Model)	4-layer Eulerian model	EMEP Meteorological Synthesizing Centre East Moscow, Russia	6-hourly from the Russian Hydro-meteorological Centre	Pb,Cd	Europe	years	Pekar, 1996			
<b>MSC-E</b> (Meteorological Synthesizing Centre East)	1-layer Eulerian model with a vertical Gaussian pollutant profile	EMEP Meteorological Synthesizing Centre East Moscow, Russia	6-hourly from the Russian Hydro-meteorological Centre	Pb,Cd,Zn,As Hg	Europe Northern Hemisphere	years	Galperin et al., 1995 Galperin et al., 1996			
<b>CAM</b> (Chemistry of Atmospheric Mercury)	1-layer chemical process (box) model	Swedish Environmental Research Institute (IVL) Göteborg, Sweden	hourly from the High Resolution Limited Area Weather Prediction Model (HIRLAM)	Hg	Europe	hours	Pleijel and Munthe, 1995a Pleijel and Munthe, 1995b			
<b>ADOM</b> (Acid Deposition and Oxidant Model)	12-layer Eulerian model	GKSS Research Centre Geesihacht Germany	hourly from the High Resolution Limited Area Weather Prediction Model (HIRLAM)	Hg	Europe	days	Petersen et al., 1996a			

TABLE I (continued)

model							reference
name	type	institution	application			output	
			meteorological input	input	output		
			calculated substances	receptor area	typical time scale		
<b>GKSS-EMEP</b>	Lagrangian 1-layer trajectory model	GKSS Research Centre Geesthacht Germany	6-hourly from the Norwegian Numerical Weather Prediction Model	Pb	North Sea Baltic Sea	months	Grassl et al., 1989 Petersen et al., 1989 Krüger, 1996
				Pb, Cd, Zn, As			
<b>GESIMA</b> (Geesthacht Simulation Model of the Atmosphere)	high-resolution non-hydrostatic mesoscale model	GKSS Research Centre Geesthacht Germany	Prediction Model	Hg			Petersen et al., 1995 Petersen, 1992a
			numerical weather prediction models e.g. 'Deutschland' model of the German Weather Service	Pb	North Sea coastal areas in Germany	days	Eppel et al., 1992 Kapitza and Eppel, 1995
<b>TRACE</b> (Trace Metal Atmospheric Concentrations in Europe)	climatological model	IIASA International Institute for Applied System Analysis Laxenburg Austria	climatological input	Pb, Cd, Zn, As	Europe	years	Alcamo et al., 1991 Alcamo et al., 1992

in use are variants of the so-called trajectory models. These models are usually formulated under assumptions of simplified turbulent diffusion, no convergent or divergent flows, and no wind shear. In these approaches only first-order chemical reactions can be treated rigorously. However, the Lagrangian approach avoids many of the computational complexities associated with the simultaneous solution of many differential equations; this generally results in requiring significantly less computational resources and can facilitate an understanding of problems that do not require descriptions of interactive nonlinear processes. Further progress in understanding the atmospheric cycling of heavy metals has emphasized the need for direct modeling of complex nonlinear processes (e. g. the physico-chemical transformations of atmospheric mercury species) by comprehensive Eulerian models. These approaches employ extensive gas- and aqueous-phase chemical mechanisms and explicitly track numerous species concentrations. Also, a more detailed numerical formulation for physical and chemical processes occurring within and below precipitating clouds is included. Typically, these models contain modules designed to calculate explicitly the chemical interactions that move gas-phase species into and among the various aqueous phases within clouds as well as calculate the aqueous-phase chemical transformations that occur within cloud and precipitation droplets. The scope and the general structure of such a comprehensive Eulerian modeling framework has been extensively discussed by Peters *et al.* [54].

Despite intense interest in using both types of models for heavy metals only a few number of operational models, which are validated through comparison with experimental data, are currently available in Europe. These models have been designed to simulate long-range and long-term transport of heavy metals assumed to be chemically inert and in association with particulate matter using a combined trajectory-climatologic approach [4], statistical approaches of a Gaussian plume model and a trajectory model [30] and an EMEP type Lagrangian trajectory model [55], [59], [36]. More recently, three-dimensional models using an Eulerian reference frame have been introduced simulating various inert species on regional geographic scales in Europe [11], [22], [53] and for high-resolution nonhydrostatic mesoscale applications [21]. Moreover, the development and application of dispersion models for heavy metals has progressed from formulations for inert species to models accounting for the physico-chemical transformations of atmospheric mercury species [56], [57], [58]. An extensive treatment of the chemistry scheme employed with the model calculations can be found in Petersen *et al.* [60]. Similar schemes are used in several other models previously developed at the EMEP Meteorological Synthesizing Center East [23], the U. S. Environmental Protection Agency [16] and at the U. S. Argon National Laboratory [68].

The major sources of information for the subsequent review on results from the above mentioned types of models are those listed in the reference section. A number of sources cited in these publications were also used in preparing this review. In addition, information was obtained from internal reports and personal communication with scientists from European and North American research institutes and environmental protection agencies.

## 2. Results From Models Applied in Europe

The first model for long-range transport of heavy metals [45] similar to that developed in the OECD program on long-range transport of sulphur compounds in Europe [42] was presented soon after the first European emission survey was completed [46]. The model was used to verify emission data by comparison of measured and calculated concentrations of heavy metals in ambient air. The results show that measured concentrations at a location in southern Norway can be related to calculated anthropogenic emissions for a number of elements, e. g. vanadium, lead, cadmium, manganese and chromium. It was concluded from this work that future emphasis should be placed on the deposition of heavy metals in addition to estimating air concentrations to create the opportunity to assess the contribution of emissions from various source regions to a certain receptor site in a more complete way.

A first overview of results from atmospheric transport and deposition models for heavy metals in Europe was given in the framework of a multidisciplinary study on the status of the North Sea [3]. There, attempts to calculate atmospheric inputs to the North Sea by means of transport models developed in the Netherlands are summarized [2], [30]. With these models, whose latest versions are called TREND [31] and OPS [32], annually or seasonally averaged concentrations and depositions of heavy metals over the North sea are calculated from emission data bases prepared for cadmium, zinc, lead, chromium, copper and nickel for the years 1979 and 1980 [46].

TREND and its more operational versions OPS and EUTREND use statistical approaches of a Gaussian plume model for source distances within 20km and of a trajectory model for greater distances. Meteorological input data are provided by the Dutch national air quality monitoring network with additional data from the Dutch meteorological office and the European Centre for Medium-Range Weather Forecast (ECMWF). Dry deposition of particle associated metals is taken into account by deriving dry deposition velocities from different particle size and atmospheric stability classes. Wet deposition includes washout processes parameterized by a scavenging coefficient and a raindrop size distribution function and rainout is modeled on the basis of empirical scavenging ratios.

In more recent research projects commissioned by the Dutch Ministry of Housing, Physical Planning and Environment different TREND versions were used to estimate atmospheric input to the North Sea and the Dutch Wadden Sea focussing on the contributions of the surrounding countries to the total input [74]. In this study, recent updates to the above mentioned emission inventories, including mercury, are used [49], [50]. The model results concerning the contributions of the surrounding countries are considered to be realistic, because the model has been successfully validated through comparison with data from the Dutch National Air Quality Monitoring Network and because the emission data from the surrounding countries are relatively reliable. The EUTREND version covers the entire European continent including its marginal seas and calculates deposition as a function of surface characteristics. This version has been applied within the European Soil and Sea Quality and Atmospheric Deposition of Selected Substances (ESQUAD) project to assess the deposition fluxes of heavy metals to the European continent and the North Sea [28], [9].

In the framework of research contracts with the German Umweltbundesamt (UBA), the three-dimensional stochastic model HHLRT (Hamburg Long Range Transport Model) has been developed and applied at the University of Hamburg for episode studies of atmospheric sulphur transport in Europe [37] and subsequently modified for heavy metal transport and deposition [34]. The meteorological input data for the model, such as windfields and precipitation rates, are prescribed according to 6-hourly analyses of the ECMWF. Mixed-layer height analyses are from the Norwegian Weather Service. Emission data are adopted from the first European emission survey on heavy metals [46]. Results for two species, i. e. lead and cadmium, have been presented for the months of July 1984 and January 1985. From these explicit simulations, annual input of lead and cadmium into the North Sea has been extrapolated assuming no significant month-to-month variability of deposition. The annual values are considerably smaller than estimates based on extrapolated measurements at coastal sites but they are comparable to the results from the above mentioned Dutch models.

In 1985 the long-period model for sulphur [20] used under the European Monitoring and Evaluation Programme (EMEP) has been modified at the GKSS-Research Centre Geesthacht for transport and deposition of heavy metals. The model is a one-layer trajectory model. Columns of air in the atmospheric boundary layer are followed along specified 96-hours trajectories picking up emissions of heavy metals from the underlying grid. The mass balance equations are integrated along each trajectory, taking into account emission inputs, possible chemical reactions, dry and wet removal, and the influence of relevant meteorological parameters. The 6-hourly meteorological data are taken from the output of the Norwegian Numerical Weather Prediction (NWP) model.

In the first phase of a comprehensive research project funded by the German Umweltbundesamt, the model was used to calculate atmospheric lead input into the North Sea and the Baltic Sea [25], [55]. Anthropogenic lead emissions in Europe used with the model were based on emission surveys available by 1986 and published by 1988 [49], [50]. Model results in terms of weekly averages of lead concentrations compare well with observations at various sites at the North Sea coast. The calculated total annual atmospheric lead input into the North Sea is in agreement with previous model results [2], [30]. The conclusion drawn in earlier studies [2], [34], that extrapolations from measurements at coastal sites tend to overpredict the total input, is supported by the model results obtained at GKSS. These findings initiated the development of more advanced extrapolation methods [67] whose results in terms of total lead input the Baltic Sea compare well with model calculations [27].

More recent updates to emission databases for lead, cadmium, zinc and arsenic [7] are used with the GKSS model in the second phase of the project [59]. Model validation has been extended to the Baltic Sea area since data from the HELCOM monitoring network have been available. The results show that the model again performs well in predicting annual lead input into the North Sea and the Baltic Sea. Emission reduction scenario runs concerning introduction of best available flue gas cleaning technology for the entire European non-ferrous metal industry and use of lead free gasoline in all European countries have been performed resulting in 90% lead input reduction for both sea areas approximately, if both scenarios are applied [36].

In comparison with observations, calculated concentrations of cadmium and zinc in ambient air and precipitation and hence deposition fluxes are significantly underpredicted by the GKSS-model. This is in accordance with results from other modelers, who have used the same emission data [2], [30], [34], [74] indicating that the European emission inventories for these two substances are still incomplete. The model performance for arsenic is about the same as for lead but measurement data for arsenic are too scarce to draw any firm conclusions. As a follow-up activity, the GKSS-model for the long-range transport of particle-associated and inert heavy metals has been extended to mercury and mercury species [56], [60]. The chemical equation set used in this model is a simplified description of a complex series of chemical reactions and mass transfer processes of atmospheric mercury species. An update to earlier emission inventories including three most relevant species for atmospheric long-range transport, i. e. elemental gaseous mercury, particulate mercury and divalent inorganic mercury compounds [6] is used with the model. Model runs are focused on estimates of atmospheric mercury input into the North Sea [57] and the Baltic Sea [58] and on scenario runs concerning inorganic mercury compounds and the role of soot particles for the mercury load in Europe's atmosphere. Since the model has been successfully validated through comparison with observations from the Nordic Network [29], the calculated range of 5-12 tones for the North Sea and 6-13 tones for the Baltic are considered to be the most reliable data currently available.

Five years ago a study was conducted at the University of Hamburg investigating the ability of the three models TREND, HHLRT and GKSS-EMEP to simulate atmospheric long-range transport of lead to the North Sea [35]. The models have been applied for a defined time period using identical emission databases. Modeling results are compared against each other and with measured data from a network of seven monitors around the North Sea. In conclusion it was found that the models perform well in predicting total annual input but that mainly due to errors associated with precipitation fields over sea areas substantial differences can occur as far as spatial and temporal variability of predicted monthly wet deposition fluxes over the North Sea is concerned.

The International Institute for Applied System Analysis (IIASA) at Laxenburg, Austria, has developed a set of two numerical models to quantify the long-range transport of particle-associated and inert heavy metals in Europe [4], [5]. The metals selected are those which have been recommended by PARCOM and HELCOM for monitoring, i. e. lead, cadmium, zinc and arsenic. A modified version of the EMEP-model is used for generating time- and space-average inputs for a climatologic model called TRACE (TRACE Metal Atmospheric Concentrations in Europe). The advantage of this combined approach is that the climatologic model can be conveniently run for all Europe and several years, and can thus make use of the very scattered measurements available for metals in Europe. Most TRACE model calculations for lead and arsenic agree within a factor of two of observed annual air concentrations and deposition. Zinc and cadmium computations clearly underestimate observations.

In recent years an Eulerian high-resolution non-hydrostatic mesoscale model called GESIMA (GEesthacht SIMulation Model of the Atmosphere) has been developed at the GKSS Research Centre Geesthacht within an Umweltbundesamt research contract. The model is applicable for a variety of problems comprising large-

eddy simulations, short-term weather prediction, or environmental problem studies such as pollutant transport. As a first application for atmospheric heavy metal transport the model has been used to simulate two episodes of atmospheric lead transport and deposition over the German North Sea coast [21].

One of the regional-scale Eulerian models currently in use for simulating heavy metal transport over Europe is the HMET (HeuMetEulerian TransPort) model, which has been developed to study the long-range and long-term transport, deposition and overall budget of As, Cd, Pb and Zn in Europe [10], [11], [12]. The main purpose of developing the model was the computation of atmospheric transboundary fluxes of heavy metals. The emission data used with the study are the above-mentioned recent updates to databases for arsenic, cadmium, lead and zinc in the EMEP-grid [7]. The model can be used both for long-term (one year or longer) as well as shorter (one week) episodes. Up to now, model applications are restricted to long-term averages, i. e. calculation of annual concentrations and deposition fluxes for 1985. Due to the small number of observations available for that year it was difficult to validate the model. The results indicate that model calculations for Cd and Pb are in good agreement with observations, but only satisfactory for As. Concentrations and deposition fluxes of Zn calculated by HMET are significantly lower than the observed values, but are in agreement with results from other models [5], [59].

The EMEP Meteorological Synthesizing Centre East (MSC-E) has developed an Eulerian model called MSC-E capable to calculate concentrations and deposition fluxes of heavy metals on both regional and hemispheric geographical scales [22]. Emission databases for lead, cadmium, zinc and arsenic [7] and mercury [6] are used with the models. In the mercury version, natural emissions and air-sea exchange processes of both organic and inorganic mercury species are treated but the chemical equation set used in this model is in the early stages of evaluation at the moment [23]. Recently, the three-dimensional Eulerian Large Particle MODEl (LPMOD) and ASIMD have been developed and applied at the EMEP MSC-E to calculate Pb and Cd transport and deposition over Europe [53] using emission data bases for 1990 from the ESQUAD project [13]. These two model approaches employ different advanced numerical advection schemes but incorporate the same detailed description of the atmospheric boundary layer with respect to dry and wet deposition of particle-associated heavy metals. Observed Pb concentrations from the PARCOM air and precipitation monitoring network are quite well reproduced by both models. For Cd, the models overestimate concentrations in air and underpredict concentrations in precipitation. This is most probably due to both incomplete European emission inventories for Cd and insufficient precipitation fields at coastal sites obtained from numerical weather prediction models.

Recent progress in understanding the atmospheric mercury cycle has emphasized the need for direct modeling of the complex nonlinear mercury chemistry of the atmosphere by comprehensive Eulerian models. As a first step in this direction the cloud mixing, scavenging, chemistry and wet deposition components of the comprehensive three-dimensional Eulerian Acid Deposition and Oxidants Model (ADOM), originally designed for regional-scale acid precipitation and photochemical oxidants studies in North America and Europe [73], [70] are restructured to accommodate the most recent developments in atmospheric mercury chemistry [14],

[61]. The chemistry scheme of this ADOM mercury version was developed by systematic simplification of the detailed Chemistry of Atmospheric Mercury (CAM) process model, which was tested and evaluated in a sensitivity analysis aimed at determining the most important parameters and identifying the critical processes in the atmospheric cycling of mercury [63], [64].

A stand-alone version of the ADOM mercury model referred to as the Tropospheric Chemistry Module (TCM) has been developed and tested under different environmental conditions allowing changes to the chemistry and meteorology alone to be evaluated at different vertical TCM levels [61], [62]. Overall, the present development level of the TCM is such that its implementation in full ADOM mercury versions for Europe and North America is justified. These models with the TCM as their major component will be developed further according to advancements in the knowledge of atmospheric mercury processes to ensure that they maintain their capability to address effectively the scientific and policy questions that may arise over the next decade.

### 3. Conclusions

This review has produced strong evidence that long-range transport models with relatively simple formulations, extensively used in simulating European transboundary transport of acidifying pollutants and modified for heavy metals associated with particulate matter, are now in an operational stage. Results from a model intercomparison study for lead demonstrate their capability to predict annual and monthly means of concentrations in ambient air and in precipitation as well as dry and wet deposition fluxes within a factor of two of observations over spatial scales from about 100 km to continental [69]. Recent progress in understanding physico-chemical processes of atmospheric mercury and the availability of European emission data bases for different mercury species has permitted to investigate mercury transport and deposition in Europe's atmosphere by means of EMEP-type models and by comprehensive Eulerian modeling frameworks. Currently, efforts are made to implement atmospheric transport of heavy metals in complex mesoscale models, but pollutant transport in these models is in the early stages of evaluation at the moment. Although there have been significant advancements in the knowledge of heavy metal properties and in the understanding of the processes which determine control and fate of heavy metals in Europe's atmosphere, our knowledge is far from complete. Listed below are the main areas of uncertainties and required activities toward further development of transport models for heavy metals:

- 1) In general, the accuracy of calculated deposition fluxes could be improved simply by improving the model inputs such as emissions and meteorological data. There is evidence from model testing that the European emission inventories are still incomplete for some substances and that precipitation fields obtained from numerical weather prediction models are insufficient to calculate wet deposition patterns over sea areas in some cases.
- 2) Because there is no coordinated atmospheric monitoring program for heavy metals in Europe it was difficult for all model applications to assemble

measurements suitable for comparing to computed values. Hence, a reliable identification of the main sources of model uncertainties and a quantitative analysis of uncertainties in model results cannot be performed at present. Air and precipitation measurements of heavy metals are few and highly uncertain in some cases. To verify model predictions, high quality monitoring networks especially over sea areas and at coastal zones are required.

3) To improve model-derived estimates of heavy metal deposition to receptor areas such as the North Sea and the Baltic Sea it is essential that suitable emission inventories for countries surrounding these two sea areas are compiled. At the moment the quality of the emission data for some substances such as zinc and cadmium limits the confidence with which the results of different control options can be predicted.

4) Sensitivity analysis performed for two long-range and long-term models showed that deposition parameters and assumptions are no major sources of model uncertainties, as these models are relatively robust with respect to large variabilities in dry and wet deposition parameters [25], [5].

5) Model calculations underestimate Cd observations, but are correlated and within a factor of two of observations. Zn calculations greatly underestimate observations [11], [72], although calculations are correlated to measurements [5], [59], thus indicating that current Cd and Zn emissions in Europe are underestimated.

6) In case of mercury sufficient information on speciation and mechanisms and kinetics of chemical reactions exists to model the main atmospheric pathways of mercury. It is well established now that redox reactions of elemental mercury [40], [41] and adsorption of oxidized mercury on soot particles in the aqueous phase [60] and subsequent wet deposition together with dry and wet deposition of particulate phase mercury emitted from industrial sources are the most important processes in polluted air masses over Europe. Values predicted by a model which contains simplified representations of these processes agree with observations from the Scandinavian network within a factor of two [60]. Additional laboratory and field measurements close to the main European industrial sources would be necessary to get a more complete picture of existing atmospheric mercury species, e. g. organic and inorganic gaseous mercury compounds. These species are hard to identify with currently available analytical techniques but they could have a significant influence on the deposition pattern close to sources.

7) Mesoscale modeling capabilities are necessary to quantify the subgrid scale variability of heavy metal concentrations simulated by regional scale models. Mesoscale models should be interfaced with large scale Eulerian models to obtain a 'nested' modeling system capable to simulate long-range transport induced, local effects with a spatial resolution of 20 km or less.

#### 4. References

1. van Aalst, R. M., van Ardenne, R. A. M., de Kruk, F. J., and Lems, T. (1983a) Pollution of the North Sea from the Atmosphere. TNO Report CL 182/152, Delft, the Netherlands.

2. van Aalst, R. M., Duyzer, J. H., and Veldt C. (1983b) Atmospheric deposition of lead and cadmium in the southern part of the North Sea. I. Emissions and preliminary model calculations. TNO Report R 83/222, Delft, the Netherlands.
3. van Aalst, R. M. (1988) Input from the Atmosphere, in W. Salomons, B. L. Bayne, E. K. Duursma and U. Förstner (eds. ), *Pollution of the North Sea - An Assessment*, Springer Verlag Berlin, pp. 275-283.
4. Alcamo, J., Bartnicki, J., and Olendrzynski, K. (1991) Modeling Heavy Metals in Europe's Atmosphere: A Combined Trajectory - Climatologic Approach, in H. van Dop and D. G. Steyn (eds. ), *Air Pollution Modeling and its Application VIII*, Plenum Press, New York, pp. 389-398. .
5. Alcamo, J., Bartnicki, J., Olendrzynski, K. and Pacyna, J. (1992) Computing heavy metals in Europe's atmosphere - I. Model development and testing, *Atmospheric Environment* 26A, 3355-3370.
6. Axenfeld, F., Münch, J., and Pacyna, J. M. (1991) Europäische Test-Emissionsdatenbasis von Quecksilberverbindungen für Modellrechnungen. In: G. Petersen (1992). Belastung von Nord- und Ostsee durch ökologisch gefährliche Stoffe am Beispiel atmosphärischer Quecksilberverbindungen. Abschlußbericht des Forschungsvorhabens 104 02 726 des Umweltforschungsplanes des Bundesministers für Umwelt, Naturschutz und Reaktorsicherheit. Im Auftrag des Umweltbundesamtes, Berlin.
7. Axenfeld, F., Münch, J., Pacyna, J. M., Duiser, J. A. and Veldt, C. (1992) Test-Emissionsdatenbasis der Spurenelemente As, Cd, Hg, Pb, Zn und der speziellen organischen Verbindungen Lindan, HCB, PCB und PAK für Modellrechnungen in Europa. Abschlußbericht des Forschungsvorhabens 104 02 588 des Umweltforschungsplanes des Bundesministers für Umwelt, Naturschutz und Reaktorsicherheit. Im Auftrag des Umweltbundesamtes, Berlin.
8. Baart, A. C. and Diederens, H. S. M. A. (1991) Calculation of the Atmospheric Deposition of 29 Contaminants to the Rhine Catchment Area. TNO-rapport R 95/138. Instituut voor Milieuwetenschappen. TNO (IMW), 2600 JA Delft, The Netherlands.
9. Baart, A. C., Berdowski, J. J. M., and van Jaarsveld, J. M. (1995) Calculation of Atmospheric Deposition of Contaminants to the North Sea. TNO-rapport R 91/219. Instituut voor Milieuwetenschappen. TNO (IMW), 2600 JA Delft, The Netherlands.
10. Bartnicki, J., Modzelewski, H., Szewczuk-Bartnicka, H., Saltbones, J., Berge, E., and Bott, A. (1993) An Eulerian model for atmospheric transport of heavy metals over Europe: Model description and testing. DNMI Technical report no. 117. Norwegian Meteorological Institute, Oslo, Norway.
11. Bartnicki, J. (1994) An Eulerian model for atmospheric transport of heavy metals over Europe: Model description and preliminary Results, *Water, Air and Soil Pollution* 75, 227-263.
12. Bartnicki, J. (1996) Computing atmospheric transport and deposition of heavy metals over Europe: Country budgets for Europe. *Water, Air and Soil Pollution* 92, 343-374.
13. Berdowski, J. J. M., Pacyna, J. M., and Veldt, C. (1994) Emissions, in K. D. van den Hout (ed. ) *The Impact of Atmospheric Deposition of Non-Acidifying*

*Compounds on the Quality of European Forest Soils and the North Sea*, TNO-rapport R 93/329, Instituut voor Milieuwetenschappen. TNO (IMW), 2600 JA Delft, the Netherlands.

14. Bloxam, R., Schroeder, W. H., and Petersen, G. (1996) An Eulerian model of mercury atmospheric transport, chemistry and deposition, in R. Ebinghaus, G. Petersen and U. von Tümpling (eds. ), *Fourth International Conference on Mercury as a Global Pollutant, Book of Abstracts*, GKSS Forschungszentrum, Max-Planck-Strasse, D-21502 Geesthacht, Germany, p. 40
15. Brüggemann, L. (1986) Contamination of the Baltic Sea Atmosphere by Metals - Concentration Levels and Inputs. - Proceedings of the Seminar on Diffusivity, Transport and Deposition of Atmospheric Pollutants to the Baltic Sea, pp. 81-98. Neubrandenburg, GDR, May 7-8, 1986.
16. Bullock, O. R., Benjey W. G., and Keating M. H. (1996) The Modeling of Regional-scale Atmospheric Mercury Concentration and Deposition Patterns using RELMAP, *Environmental Toxicology and Chemistry*. (in press)
17. Cambray, R. S., Jefferies, D. F., and Topping G. (1975) An Estimate of the Input of Atmospheric Trace Elements into the North Sea and the Clyde Sea. AERE-Report R 7733, AERE, Harwell.
18. Cambray, R. S., Jefferies, D. F., and Topping G. (1979) The atmospheric input of trace elements to the North Sea, *Marine Science Communications* 5, 175-194.
19. Ebinghaus, R., Kock, H. H., Jennings, S. G., McCartin, P., and Orren, M. J. (1995) Measurements of atmospheric mercury concentrations in northwestern and central Europe - Comparison of experimental data and model results, *Atmospheric Environment* 29, 3333-3344.
20. Eliassen, A. and Saltbones, J. (1983) Modelling the long-range transport of sulphur over Europe: a two year model run and some model experiments, *Atmospheric Environment* 17, 1457-1473.
21. Eppel, D. P., Kapitza, H., Claußen, M., Jacob, D., Koch, W., Levkov, L., Mengelkamp, H. -T., Resch, E., and Wermann N. (1992) Untersuchung und Bewertung des Schadstoffeintrags über die Atmosphäre im Rahmen von PARCOM (Nordsee) und HELCOM (Ostsee). Teilbericht: Simulation des Transports und der Deposition atmosphärischen Bleis in der norddeutschen Küstenregion. Abschlußbericht des Forschungsvorhabens 104 02 583 des Bundesministers für Umwelt, Naturschutz und Reaktorsicherheit. Im Auftrag des Umweltbundesamtes, Berlin.
22. Galperin, M., Sofiev, M., Gusev, A., and Afinogenova, O. (1995) The Approaches to Modeling of Heavy Metals Transboundary and Long-Range Airborne Transport and Deposition in Europe, EMEP/MSC-E Technical Report 7/95, EMEP Meteorological Synthesizing Center-East, Kedrova str. 8-1, Moscow, Russia.
23. Galperin, M., Sofiev, M., and Mantseva, E. (1996) A model of the chemical transformation of mercury and its long-range atmospheric transport, in W. Baeyens, R. Ebinghaus, and O. F. Vassiliev (eds. ), *Regional and Global Mercury Cycles, Fluxes and Mass Balances*, NATO-ASI Series, Series C: Mathematical and Physical Sciences, Kluwer Academic Publishers, Dordrecht, the Netherlands, pp. 219-227.

24. GESAMP (1989) The Atmospheric Input of Trace Species to the World Ocean. IMO/FAD/UNESCO/WMO/IAEA/UN/UNEP. WMO Reports and Studies 38.
25. Graßl, H., Eppel, D. P., Petersen, G., Schneider, B., Weber, H., Gandraß, J., Reinhardt, K. H., Wodarg, D., and Fließ J. (1989) Stoffeintrag in Nord- und Ostsee über die Atmosphäre. Abschlußbericht des Forschungsvorhabens 104 02 572 des Umweltforschungsplanes des Bundesministers für Umwelt, Naturschutz und Reaktorsicherheit. Im Auftrag des Umweltbundesamtes, Berlin.
26. HELCOM (1989) Deposition of Airborne Pollutants to the Baltic Sea Area 1983 - 1985 and 1986. Baltic Sea Environment Proceedings No. 32. Baltic Marine Environment Protection Commission - Helsinki Commission -
27. HELCOM (1991) Airborne Pollution Load to the Baltic Sea 1986-1990. Baltic Sea Environment Proceedings No. 39. Baltic Marine Environment Protection Commission - Helsinki Commission -
28. van den Hout K. D. (ed.) (1994) The Impact of Atmospheric Deposition of Non-Acidifying Compounds on the Quality of European Forest Soils and the North Sea. TNO-rapport R 93/329. Instituut voor Milieuwetenschappen. TNO (IMW), 2600 JA Delft, The Netherlands.
29. Iverfeldt, Å. (1991) Occurrence and Turnover of Atmospheric Mercury over the Nordic Countries, *Water, Air and Soil Pollution* 56, 251-165.
30. van Jaarsveld, J. A., van Aalst, R. M., and Onderdelinden, D. (1986) Deposition of metals from the Atmosphere into the North Sea: model calculations. Report No. 84 20 15 002, National Institute of Public Health and Environmental Protection (RIVM), Bilthoven, The Netherlands.
31. van Jaarsveld, J. A. and Onderdelinden, D. (1989) Dispersion and deposition of dioxins, dibenzofurans and heavy metals emitted by a municipal waste incinerator (in Dutch). Report No. 73 84 73 007, National Institute of Public Health and Environmental Protection (RIVM), Bilthoven, the Netherlands.
32. van Jaarsveld, J. A. (1990) An operational atmospheric transport model for priority substances; specification and instruction for use. Report No. 222 501 002, National Institute of Public Health and Environmental Protection (RIVM), Bilthoven, the Netherlands.
33. Kapitza, H. and Eppel, D. P. (1992) The Non-Hydrostatic Mesoscale Model GESIMA. Part I: Dynamical Equations and Tests, *Beiträge zur Physik der Atmosphäre* 65, 129-146.
34. Krell, U. and Roeckner, E. (1988) Model simulation of the atmospheric input of lead and cadmium into the North Sea, *Atmospheric Environment* 22, 375 - 381.
35. Krell, U. (1991) Vergleich von Modellen für den Eintrag von Spurenstoffen aus der Atmosphäre in die Nordsee - Beispiel Blei. GKSS Forschungszentrum Geesthacht, externer Bericht GKSS 91/E/79.
36. Krüger O. (1996) Atmospheric deposition of heavy metals to North European marginal seas: Scenarios and trend for lead, *GeoJournal* 39. 2, 117-131.
37. Lehmhaus, J., Roeckner, E., Bernhardt, I., and Pankrath, J. (1984) A Monte Carlo model for the simulation of long-range transport of air pollutants, in C. de Wispelaere (ed.), *Air Pollution Modeling and its Application III*, Plenum Press, New York, pp. 149-163.

38. Lindqvist, O., Johansson, K., Aastrup, M., Andersson, A., Bringmark, L., Hovsenius, G., Hakanson, L., Iverfeldt, A., Meili, M., and Timm, B. (1991) Mercury in the Swedish Environment-Recent Research on Causes, Consequences and Corrective Methods, *Water, Air and Soil Pollution* 55.
39. Michaelis, W., Schönburg, M., and Stöbel, R. -P. (1989) Deposition of Atmospheric Pollutants into a North German Forest Ecosystem, in H. -W. Georgii (ed. ), *Mechanisms and Effects of Pollutant-Transfer into Forests*, Kluwer Academic Publishers, pp 3-12.
40. Munthe, J., Xiao, Z. F., and Lindqvist, O. (1991) The Aqueous Reduction of Divalent Mercury by Sulfite, *Water, Air and Soil Pollution* 56, 621-630.
41. Munthe, J. (1992) The Aqueous Oxidation of Elemental Mercury by Ozone, *Atmospheric Environment* 26A, 1461 - 1468.
42. OECD (1979) The OECD Programme on Long-Range Transport of Air Pollutants. Measurements and Findings, 2nd edn. Organization for Economic Co-operation and Development, Paris.
43. Ottar, B. and Pacyna, J. M. (1984) Sources of Ni, Pb and Zn during the Arctic Episode in March 1983, *Geophysical Research Letters* 11, 441-444.
44. Ottar, B., Pacyna, J. M. and Berg, T. C. (1985) Aircraft measurements of air pollution in the Norwegian Arctic, *Atmospheric Environment* 20, 87-100.
45. Pacyna, J. M., Semb, A., and Hansen, J. E. (1984) Emission and long-range transport of trace elements in Europe, *Tellus* 36B, 163-174.
46. Pacyna, J. M. (1984) Estimation of the atmospheric emissions of trace elements from anthropogenic sources in Europe, *Atmospheric Environment* 18, 41-50.
47. Pacyna, J. M., Ottar, B., Tomza, U., and Maenhaut, W. (1985) Long-Range Transport of Trace Elements to Ny Ålesund, Spitsbergen, *Atmospheric Environment* 19, 857-865.
48. Pacyna, J. M., Bartonova, A., Cornville, P., and Maenhaut, W. (1988) Modelling of Long-Range Transport of Trace Elements. A Case Study, *Atmospheric Environment* 23, 107-114.
49. Pacyna, J. M. (1988) Atmospheric Lead Emissions in Europe 1982. NILU-Report 18/88. Norwegian Institute for Air Research, Lillestrom, Norway.
50. Pacyna, J. M. and Münch, J. (1988) Atmospheric Emissions of Arsenic, Cadmium, Mercury and Zinc in Europe 1982. NILU-Report 17/88. Norwegian Institute for Air Research, Lillestrom, Norway.
51. Pacyna, J. M., and Ottar, B. (eds. ) (1989) *Control and Fate of Atmospheric Trace Metals*, NATO ASI Series. Series C: Mathematical and Physical Sciences - Vol. 268, Kluwer Academic Publishers.
52. PARCOM (1988) Interim Report on Atmospheric Input to the North Sea. Convention for Prevention of Marine Pollution from land-based Sources. Sixth Meeting of the Working Group on the Atmospheric Input of Pollutants to Convention Waters, Paris, November 15-17, 1988, (ATMOS 5/6/4-E).
53. Pekar, M. (1996) Regional Models LPMOD and ASIMD. Algorithms, Parameterization and Results of Application to Pb and Cd in Europe Scale for 1990, EMEP / MSC-E Report 9/96, EMEP Meteorological Synthesizing Center-East, Kedrova str. 8-1, Moscow, Russia.

54. Peters, L. K., Berkowitz, C. M., Carmichael, G. R., Easter, R. C., Fairweather, G., Ghan, S. J., Hales, J. M., Leung, R. L., Pennell, W. R., Potra, F. A., Saylor, R. D., and Tsang, T. T. (1995) The current state and future direction of Eulerian models in simulating the tropospheric chemistry and transport of trace species: A review, *Atmospheric Environment* 29, 189 - 222.
55. Petersen, G., Weber, H., and Graßl, H. (1989) Modelling the Atmospheric Transport of Trace Metals from Europe to the North Sea and the Baltic Sea, in J. M. Pacyna and B. W. Ottar (eds. ), *Control and Fate of Atmospheric Trace Metals*, NATO-ASI Series, Series C: Mathematical and Physical Sciences - Vol. 268, Kluwer Academic Publishers, Dordrecht, the Netherlands, pp. 57-83.
56. Petersen, G. (1992a) Belastung von Nord- und Ostsee durch ökologisch gefährliche Stoffe am Beispiel atmosphärischer Quecksilberverbindungen. Abschlußbericht des Forschungsvorhabens 104 02 726 des Bundesministers für Umwelt, Naturschutz und Reaktorsicherheit. Im Auftrag des Umweltbundesamtes, Berlin. Externer Bericht GKSS 92/E/111.
57. Petersen, G. (1992b) Atmospheric Input of Mercury to the North Sea. Paris Convention for the Prevention of Marine Pollution. Ninth Meeting of the Working Group on the Atmospheric Input of Pollutants to Convention Waters. London: 5-8 November 1991 (PARCOM-ATMOS 9/13/1).
58. Petersen, G. (1992c) Atmospheric Input of Mercury to the Baltic Sea. Baltic Marine Environment Protection Commission - Helsinki Commission -. Ninth Meeting of the Group of Experts on Airborne Pollution of the Baltic Sea Area (EGAP). Solna, Sweden: 19-22 Mai 1992 (HELCOM-EGAP 9/2/5).
59. Petersen, G. and Krüger, O. (1993) Untersuchung und Bewertung des Schadstoffeintrags über die Atmosphäre im Rahmen von PARCOM (Nordsee) und HELCOM (Ostsee) Teilvorhaben: Modellierung des großräumigen Transports von Spurenmetallen. Abschlußbericht des Forschungsvorhabens 104 02 583 des Bundesministers für Umwelt, Naturschutz und Reaktorsicherheit. Im Auftrag des Umweltbundesamtes, Berlin. Externer Bericht GKSS 93/E/28.
60. Petersen, G., Iverfeldt, A. and Munthe, J. (1995) Atmospheric Mercury Species over Central and Northern Europe. Model Calculations and Comparison with Observations from the Nordic Air and Precipitation Network for 1987 and 1988, *Atmospheric Environment* 29, 47-67.
61. Petersen, G., Munthe, J., and Bloxam, R. (1996) Numerical modeling of regional transport, chemical transformations and deposition fluxes of airborne mercury species, in W. Baeyens, R. Ebinghaus, and O. F. Vassiliev (eds. ), *Regional and Global Mercury Cycles, Fluxes and Mass Balances*, NATO-ASI Series, Series C: Mathematical and Physical Sciences, Kluwer Academic Publishers, Dordrecht, the Netherlands, pp. 191-217.
62. Petersen, G., Munthe, J., Pleijel, K., Bloxam, R., and Vinod Kumar, A. (in press) A Comprehensive Eulerian Modeling Framework for Airborne Mercury Species : Development and Application of a Tropospheric Chemistry Module, *Atmospheric Environment* 31.
63. Pleijel, K. and Munthe, J. (1995a) Modelling the Atmospheric Mercury Cycle - Chemistry in Fog Droplets, *Atmospheric Environment* 29, 1441-1457.

64. Pleijel, K. and Munthe, J. (1995b) Modeling the Atmospheric Chemistry of Mercury - The Importance of a Detailed Description of the Chemistry of Cloud Water, *Water, Air and Soil Pollution* 80, 317-324.
65. Remoudaki, E., Bergametti, O., and Buat-Ménard, P. (1991) Temporal Variability of Atmospheric Lead Concentrations and Fluxes over the Northwestern Mediterranean Sea, *Journal of Geophysical Research* 96, No. D1, 1043-1055.
66. Rühling, A., Rasmussen, L., Pilegaard, K., Mäkinen, A. and Steinness, E. (1987) Survey of Atmospheric Heavy Metal Deposition in the Nordic Countries in 1985. Report NORD 1987: 21, prepared for 'The Steering Body for Environmental Monitoring', The Nordic Council of Ministers.
67. Schneider, B. (1992) Untersuchung und Bewertung des Schadstoffeintrags über die Atmosphäre im Rahmen von PARCOM (Nordsee) und HELCOM (Ostsee) - Teilvorhaben: Messungen von Spurenmetallen - Abschlußbericht des Forschungsvorhabens 104 02 583 des Umweltforschungsplanes des Bundesministers für Umwelt, Naturschutz und Reaktorsicherheit. Im Auftrag des Umweltbundesamtes, Berlin.
68. Shannon, J. D. and Voldner, E. C. (1995) Modeling Atmospheric Concentrations of Mercury and Deposition to the Great Lakes, *Atmospheric Environment* 29, 1649-1662.
69. Sofiev, M., Maslyayev, A., and Gusev, A. (1996) Heavy metal model intercomparison. Methodology and results for Pb in 1990. EMEP/MSC-E Technical Report 2/96, EMEP Meteorological Synthesizing Center-East, Kedrova str. 8-1, Moscow, Russia.
70. Stern, R., Scherer, B., and Schubert, S. (1990) Modeling of Photochemical Oxidant Formation in North-Western Europe with special Emphasis on the non-linearity issue in the SOX / NOX / VOC System. Presented at the EMEP Workshop on the Progress of Transport Modelling of Nitrogen Compounds, Potsdam, Germany, October 1990.
71. Stössel, R. P. (1987) Untersuchungen zur Naß- und Trockendeposition von Schwermetallen auf der Insel Pellworm. GKSS Forschungszentrum Geesthacht, externer Bericht GKSS 87/E/34.
72. Swietlicki, E., Bartnicki, J., Jalkanen, L., Kemp, K., Wahlin, P., and Krejci, R. (1996) Heavy Metals in the Atmosphere. Comparison of source-receptor relationship estimated by means of receptor and meteorological dispersion modeling, Lund University Report No. LUTFD2 / (TFKF-3079) / 1-29 / (1996). Lund University, Division of Nuclear Physics, Sölvegatan 14, Lund, Sweden.
73. Venkatram, A., Karamchandani, P. K., and Misra P. K. (1988) Testing a Comprehensive Acid Deposition Model, *Atmospheric Environment* 22, 737-747.
74. Warmenhoven, J. P., Duiser, J. A., de Leeuw, L. T., and Veldt, C. (1989) The Contribution of the Input from the Atmosphere to the Contamination of the North Sea and the Dutch Wadden Sea. TNO Report R 89/349A, Delft, The Netherlands.
75. Xiao, Z. F., Munthe, J., Schroeder, W. H., and Lindqvist, O. (1991) Vertical fluxes of volatile mercury over forest soil and lake surfaces in Sweden, *Tellus* 43B, 267-279.



# Paper V



# **AIRBORNE HEAVY METALS OVER EUROPE: EMISSIONS, LONG-RANGE TRANSPORT AND DEPOSITION FLUXES TO NATURAL ECOSYSTEMS**

G.PETERSEN

*GKSS Research Centre, Institute of Hydrophysics  
Max-Planck-Strasse, D-21502 Geesthacht, GERMANY*

## **Abstract**

This paper presents a brief review of the processes by which airborne heavy metals are transported from the main emission areas in Europe and become subject to deposition and absorption into terrestrial and aquatic ecosystems with subsequent transport and transformation within the biotic and abiotic media that comprise these ecosystems. Results from numerical simulation models capable of simulating long-range transport of heavy metals over Europe together with measurement data of heavy metal concentrations in air and precipitation and the corresponding dry and wet deposition fluxes are reported. European wide inventories of anthropogenic heavy metal emissions based on location and capacity of their dominating source categories such as fossil fuel burning in power plants, industrial and residential combustion, waste incineration and road traffic are briefly described. Emission reduction scenarios with respect to introduction of lead free gasoline are outlined.

The critical gaps of knowledge on heavy metals in the atmosphere are identified focusing on uncertainties associated with emission fluxes in Eastern Europe and the scarcity of measurement data in that area. Future research is needed to estimate the effects of emission reductions on deposition fluxes of heavy metals to sensitive ecosystems such as forested areas in Europe is recommended. Special emphasis is placed on mercury, lead and cadmium which have been defined within the European convention on long-range transboundary air pollution of the United Nations-Economic Commission Europe (UN-ECE) to be the priority heavy metals of concern.

## **1. Introduction**

Heavy metals emitted into the atmosphere by anthropogenic activities are deposited partly in the vicinity of emission sources but mostly 'en route' during their long-range transport over spatial scales from about 100 km to continental. Therefore, environmental policy strategies aiming at the reduction of emissions and deposition fluxes of heavy metals require international agreements. In Europe, such agreements

are now underway within the United Nations Economic Commission for Europe, Convention on Long-Range Transboundary Air Pollution (UN-ECE-LRTAP).

In view of the protocol for heavy metals within the UN-ECE-LRTAP and the already existing Arctic Monitoring and Assessment Program (AMAP), the Oslo and Paris Commission (OSPAR) and Helsinki Commission (HELCOM) programmes on inputs of atmospheric heavy metals to the Arctic, the North Sea and the Baltic Sea, respectively, significant efforts have been devoted in Europe to the monitoring of heavy metals to European marginal seas eg. [1-3], inland lakes and forest areas [4-6], and the Norwegian Arctic [7]. Recently, a data base has been established by the EMEP Co-operative Programme for Monitoring and Evaluation of the Long-range Transmission of Air Pollutants in Europe [8]. This data base contains concentrations of heavy metals in ambient air and precipitation for the time period 1987 to 1996 from 69 measurement sites in 20 European countries.

Increasing attention is now given to numerical modeling of the long-range transport and deposition of heavy metals over Europe. In recent years it has been widely recognized that the use of numerical models is important in formulating effective control strategies for the reduction of atmospheric deposition fluxes of heavy metals to the above mentioned ecosystems. The only way of delineating their atmospheric transport pathways and hence the emitter-receiver relationship is through numerical modeling. The major sources of information for this review are those listed in the reference section. In addition, information was obtained from internal reports and personal communication with scientists from European and North American research institutes and environmental protection agencies.

## **2. Atmospheric cycling of heavy metals**

Once they are released into the atmosphere, heavy metals are subjected to various physical and chemical processes that determine their ultimate environmental fate. Fig.1 shows the fundamental features of the atmospheric cycle for heavy metals, beginning with emissions to the atmosphere and ending with deposition on the Earth's surface. The physical and chemical properties of a particular heavy metal and the prevailing environmental conditions determine the atmospheric pathways that it will follow during its residence time in the atmosphere. The term 'atmospheric pathways' refers to the multitude of possible processes and interactions in which heavy metals may participate from the time it enters the atmosphere until it leaves this environmental compartment.

### **2.1. ANTHROPOGENIC EMISSIONS**

High temperature processes, such as coal and oil combustion in electric power generating stations and in district heating and industrial plants, roasting and smelting of

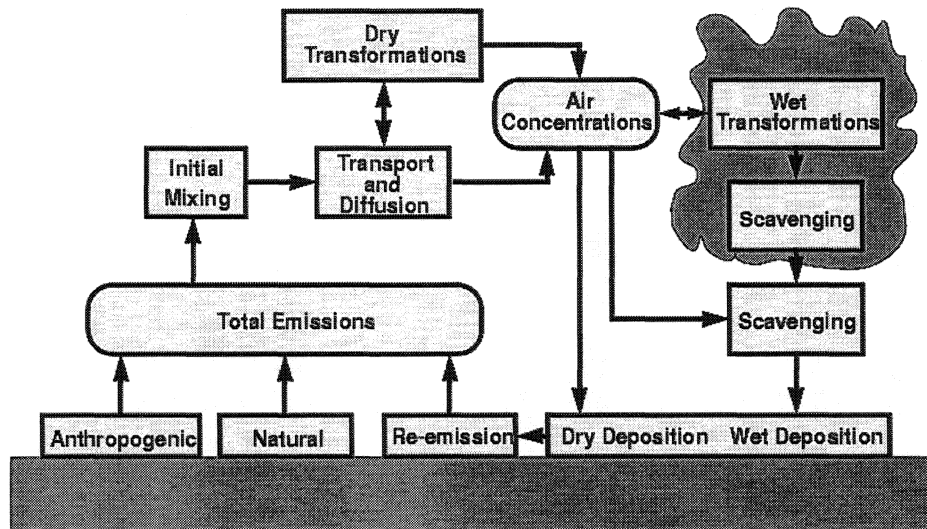


FIGURE 1. Airborne heavy metals: emission-to-deposition cycle

ores in non-ferrous metal smelters, melting operations in ferrous foundries, and waste incinerators, emit various heavy metals.

The quantity of atmospheric emissions from these sources depends upon:

- the contamination of fossil fuels and other raw materials
- physico-chemical properties of heavy metals, affecting their behavior during the industrial processes
- the technology of industrial processes
- the type and efficiency of control equipment

A detailed discussion as to what extent the above parameters affect the emission of heavy metals is presented in [9]. The first quantitative worldwide estimate of the annual industrial input of 16 heavy metals into the air, soil, and water has been published in [10]. This study illustrated that human activities are significantly altering the cycling of many heavy metals in the environment on a global scale. One of the first attempts to estimate atmospheric emissions of heavy metals from anthropogenic sources was completed at the beginning of the 1980s [11]. This work included information on emissions of 16 compounds. Previous works have dealt with either a single metal or a given source category. Most of the effort was spent on making inventories for emissions of lead, cadmium and mercury [12, 13].

In Central and Eastern Europe, the political changes of the 1990s initially brought a sharp decline of industrial activities, followed by significant restructuring of the economy and industry. The resulting emission reductions for lead, cadmium and mercury together with the relative changes of the main source categories are shown in Fig. 2.

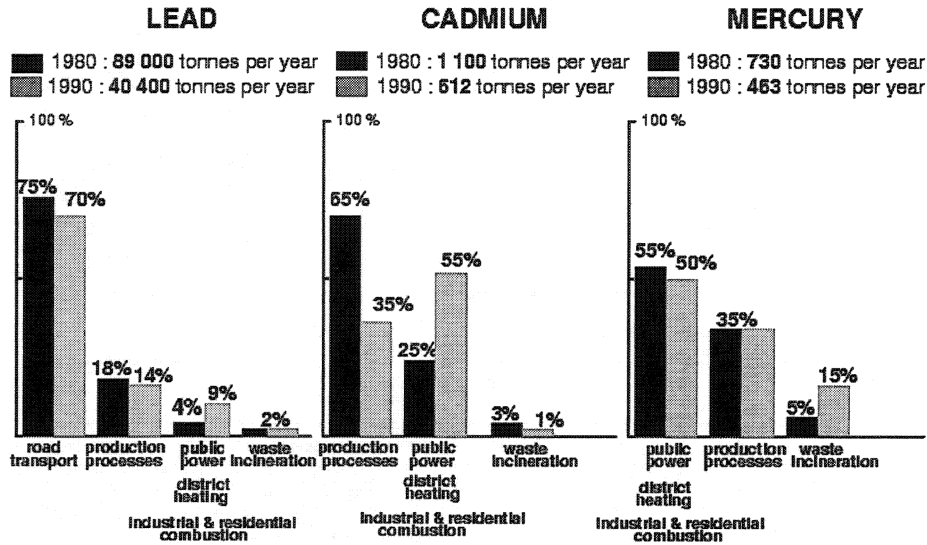


FIGURE 2. Main emission categories for heavy metals in Europe 1980 [12, 13] and 1990 [14].

## 2.2. INITIAL MIXING, TRANSPORT AND TRANSFORMATIONS

Initial mixing refers to the physical processes that act on heavy metals immediately after their release from an emission source into the mixed layer, which is the lower region of the troposphere with typical extensions of 1-2 km during daytime and a few hundred meters at night. In this layer, heavy metals are relatively free to circulate and disperse vertically as well as horizontally due to small-scale turbulence, which promotes intimate contact between vapor phase and aerosol associated heavy metals. Such direct contact is important for physico-chemical transformations of heavy metals near the source before extensive dilution has occurred and while air concentrations are still relatively high.

Diffusion and transport processes occur simultaneously in the atmosphere. Diffusion is caused by turbulent motion or eddies which develop in air that is unstable or influenced by strong wind shear. Pollutant transport results from air mass circulations driven by local or global forces. The actual distance travelled by pollutants depends strongly on the amount of time a specific heavy metal resides in the atmosphere. As a result of dispersive and removal processes such as precipitation scavenging, some heavy metals associated with relatively large particles are deposited from the mixing layer quickly. Metals on small particles or in gaseous and water insoluble form, which are removed more gradually, can be transported over several hundred or even thousands of kilometers. During transport and diffusion through the atmosphere some of the metals such as selenium and mercury can participate in complex chemical reactions. These processes can transform a metal from its primary

physical and chemical state to another state that may have similar or very different characteristics. For example, mercury is mainly present in the atmosphere in its gaseous elemental form but undergoes a series of physico-chemical reactions. These reactions include oxidation by ozone in the gas and aqueous phase, complex formation of oxidized mercury with subsequent back-reduction and adsorption on particulate matter in the aqueous phase (Fig.3).

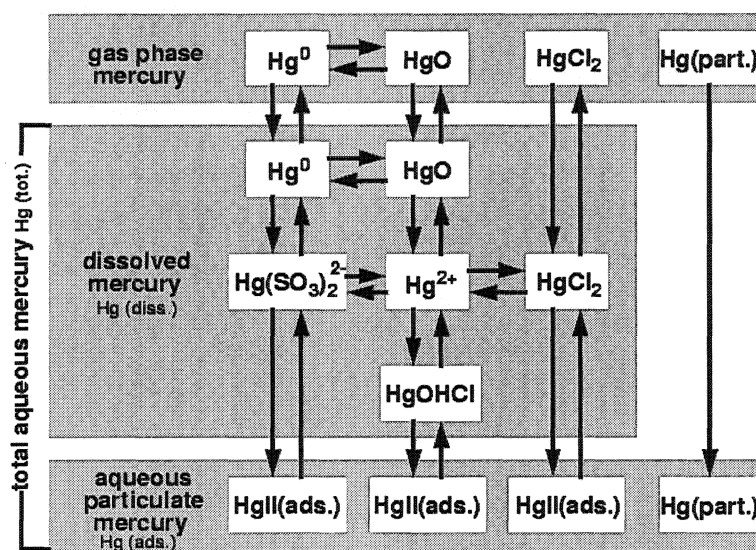


FIGURE 3. Chemical transformations of atmospheric mercury species, ( adopted from [15] )

### 2.3. DEPOSITION PROCESSES

Removal processes of heavy metals can be conveniently grouped into two categories: dry deposition and wet deposition. Dry deposition denotes the direct transfer of gaseous and particulate heavy metals to the Earth's surface. Wet deposition encompasses all processes by which heavy metals are transferred to the Earth's surface in aqueous form (i.e. rain, snow, fog). The current understanding of wet deposition far exceeds the knowledge of dry deposition. Wet deposition is relatively simple to measure, even though considerable uncertainty exists if one attempts rigorous conceptual or mathematical description. By comparison, dry deposition is difficult to measure; therefore, the existing data base on this process is relatively small and contains many uncertainties. For both, dry and wet deposition the atmospheric pathways are much better described and understood for heavy metals associated with particles than for metals in gaseous form. Current knowledge of dry and wet deposition processes of heavy metals are extensively reviewed in [16] and [17].

## 2.4. OBSERVED ATMOSPHERIC CONCENTRATIONS

Observations of heavy metals in the atmosphere have been reported over the last 15 to 20 years for a number of locations throughout the European continent. However, the scarcity of measurements and uncertainties in the quality of data in parts of Eastern and Southern Europe is such that no generalized conclusions for Europe can be drawn. Nevertheless, the following trends are apparent: individual heavy metal concentrations vary widely with location, ranging from less than one nanogram per cubic meter in remote areas to tens of micrograms per cubic meter in polluted urban areas. The remote areas recorded measurable concentrations of some of the elements, indicative of anthropogenic sources, and supports the thesis of long-range atmospheric transport into these areas. Data obtained for urban areas in central and Northern Europe, although having considerable variation, generally show a decreasing temporal trend in most elements.

TABLE 1. Observed annual mean concentration of lead and cadmium in ambient air at 5 locations in Europe. Units:  $\text{ng m}^{-3}$  ( adopted from [8] )

	Ispra (Italy)		Deuselbach (Germany)		Liesek (Slovakia)		Preila (Lithuania)		Lista (Norway)	
	Cd	Pb	Cd	Pb	Cd	Pb	Cd	Pb	Cd	Pb
1988			0.74	41	0.83	38				
1989	243		0.68	36	1.09	29				
1990	162		0.50	30	0.89	31				
1991	123		0.52	27	0.80	19			0.06	2
1992	120		0.46	21	1.18	39	0.17	13	0.05	2
1993	105		0.36	19	1.07	11	0.17	9	0.07	3
1994	104		0.34	15			0.41	12	0.08	3

Heavy metals have not yet been officially included in the UN-ECE convention on long-range transboundary air pollution in Europe, but in the framework of the preparatory phase of the heavy metal protocol the EMEP Chemical Coordinating Centre has established a data base containing observations from 1987 and onwards from different national and international European programmes such as HELCOM, AMAP, and OSPARCOM [8]. Twenty European countries have contributed data from 69 measurement sites. In Table 1, observations at 5 selected locations ranging from a densely populated area with considerable road traffic in Italy to a remote station in Norway are shown to reflect typical concentrations and temporal trends for cadmium and lead in Europe.

## 2.5 NUMERICAL SIMULATION MODELS

Because processes involved in atmospheric transport of heavy metals are so complex, numerical simulation models are invaluable in understanding the cause-and-effect relationship between the emissions of heavy metals from particular sources in Europe and the spatial pattern of atmospheric deposition fluxes to various ecosystems. These models aid in predicting which proposed control strategy can succeed in reducing these fluxes to acceptable levels. An example of numerical model capabilities is illustrated for a model predicting exposure of the Baltic Sea to lead emissions in Europe in 1980 is shown in Fig. 4. The black bars indicate the predicted contribution of 6 European countries to the atmospheric deposition fluxes of lead to the Baltic Sea. Comparison between the black and grey bars reveals the substantial flux reduction if only lead free gasoline would be used in road traffic of these countries.

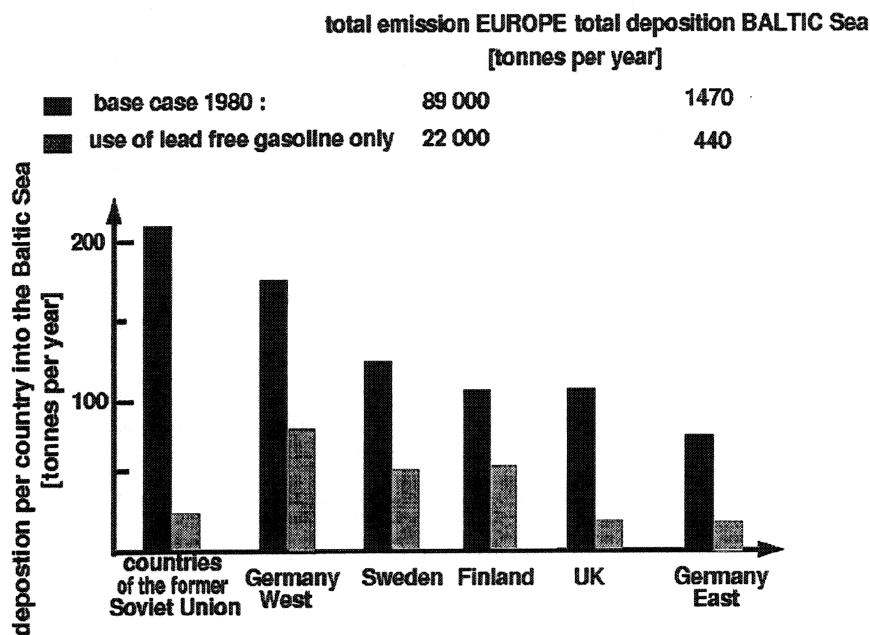


FIGURE 4. Emission reduction scenario 'lead free gasoline in Europe' 1980  
(adopted from [18])

Despite intense interest in using models for heavy metals only a few operational models, which are validated through comparison with experimental data, are currently available in Europe. These models have been designed to simulate long-range and long-term transport of heavy metals assumed to be chemically inert and in association with particulate matter using a combined trajectory-climatologic approach [19], namely statistical approach using a Gaussian plume model and a trajectory model [3] and an EMEP type Lagrangian trajectory model [2], [18], [20]. More recently, three-

dimensional models using an Eulerian reference frame have been introduced simulating various inert species on regional geographic scales in Europe [21 - 23] . Moreover, the development and application of dispersion models for heavy metals has progressed from formulations for inert species to models accounting for the physico-chemical transformations of atmospheric mercury species [15] , [24 - 26].

### 3. Conclusions

The current knowledge of airborne heavy metals over Europe has been briefly reviewed. There is strong evidence that recent progress in understanding atmospheric physico-chemical processes has permitted investigation of atmospheric heavy metal transport, transformation and deposition by means of field measurements and numerical simulation models. However, growing international concerns about heavy metals in Europe's atmosphere, as demonstrated in the recent agreement of the Heavy Metals Protocol of the UN-ECE, have led to a realization that the underlying scientific knowledge is incomplete and requires additional interdisciplinary analysis of heavy metals in the atmosphere. Listed below are the three main areas of uncertainty and the required activities needed to improve assessments of heavy metal deposition fluxes to terrestrial and aquatic ecosystems in Eastern Europe:

- A coordinated atmospheric monitoring programme for heavy metals does not yet exist in Europe. Hence, it is not possible at present to get a complete picture of deposition fluxes and their spatial and temporal variability especially in Eastern Europe, where air and precipitation measurements are few and highly uncertain in some areas.
- Field measurements close to the main industrial sources in Eastern Europe would be necessary to identify existing heavy metals and their chemical speciation, e.g mercury and organic and inorganic mercury species. These species are hard to identify with currently available analytical techniques but they could have a significant influence on the deposition pattern close to sources.
- Results from a model intercomparison study for lead have demonstrated their capability to predict monthly and annual deposition fluxes within a factor of two of observations over spatial scales from about 1000 km to continental [27]. However, model calculations for other metals such as cadmium and zinc greatly underestimate observations, even though calculations are correlated to measurements[18] , [19]. This shows that emissions for some heavy metals are underestimated.

### 4. References

1. HELCOM (1991) Airborne Pollution Load to the Baltic Sea 1986-1990. Baltic Sea Environment Proceedings No. 39. Baltic Marine Environment Protection Commission - Helsinki Commission -.
2. Petersen, G., Weber, H., and Grassl, H. (1989) Modelling the Atmospheric Transport of Trace Metals from Europe to the North Sea and the Baltic Sea, in J.M. Pacyna and B.W. Ottar (eds.), *Control and Fate of Atmospheric Trace Metals*, NATO-ASI Series, Series C: Mathematical and Physical Sciences -

- Vol.268,pp 57-83,Kluwer Academic Publishers, Dordrecht.
3. van Jaarsveld, J.A., van Aalst ,R.M., and Onderdelinden, D. (1986) Deposition of metals from the Atmosphere into the North Sea: model calculations. Report No. 84 20 15 002, National Institute of Public Health and Environmental Protection (RIVM), Bilthoven, The Netherlands.
  4. Michaelis, W., Schönburg, M., and Stöbel, R.-P. (1989) Deposition of Atmospheric Pollutants into a North German Forest Ecosystem, in H.-W. Georgii (ed.), *Mechanisms and Effects of Pollutant-Transfer into Forests*, Kluwer Academic Publishers, pp 3-12.
  5. Rühling, A., Rasmussen, L.,Pilegaard, K.,Mäkinen, A. and Steinnes, E. (1987) Survey of Atmospheric Heavy Metal Deposition in the Nordic Countries in 1985.Report NORD 1987: 21, prepared for 'The Steering Body for Environmental Monitoring', The Nordic Council of Ministers.
  6. Iverfeldt,A ., Munthe, J., and Hultberg,H. (1996) Terrestrial Mercury and Methylmercury Budgets for Scandinavia, in W. Baeyens, R. Ebinghaus, and O.F.Vassiliev (eds.), *Regional and Global Mercury Cycles,Fluxes and Mass Balances*,NATO-ASI Series, Series C: Mathematical and Physical Sciences,Kluwer Academic Publishers,Dordrecht, pp.381-401.
  7. Ottar, B. and Pacyna, J.M. (1984) Sources of Ni, Pb and Zn during the Arctic Episode in March 1983,*Geophysical Research Letters* 11,441-444.
  8. Berg, T.,Hjellbrekke,A.G. and Skjelmoen, J.E. (1996) Heavy Metals and POPs within the ECE Region,EMEP/CCC-Report 8/96,Norwegian Institute for Air Research,P.O.Box 100, N-2007 Kjeller,Norway.
  9. Pacyna, J.M. (1989) Technological Parameters Affecting Atmospheric Emissions of Trace Elements from Major Anthropogenic Sources, in J.M. Pacyna and B.W. Ottar (eds.),*Control and Fate of Atmospheric Trace Metals*, NATO-ASI Series, Series C: Mathematical and Physical Sciences - Vol.268,pp 15-39,Kluwer Academic Publishers,Dordrecht.
  10. Nriagu, J.O. and Pacyna, J.M. (1988) Quantitative Assessment of Worldwide Contamination of Air,Water and Soils with Trace Metals, *Nature* 333,134-139.
  11. Pacyna, J.M. (1984) Estimation of the atmospheric emissions of trace elements from anthropogenic sources in Europe,*Atmospheric Environment* 18,41-50.
  12. Axenfeld, F., Münch, J., and Pacyna, J.M. (1991) Europäische Test-Emissionsdatenbasis von Quecksilberverbindungen für Modellrechnungen. In: G. Petersen (1992). Belastung von Nord- und Ostsee durch ökologisch gefährliche Stoffe am Beispiel atmosphärischer Quecksilberverbindungen. Abschlußbericht des Forschungsvorhabens 104 02 726 des Umweltforschungsplanes des Bundesministers für Umwelt, Naturschutz und Reaktorsicherheit. Im Auftrag des Umweltbundesamtes, Berlin.
  13. Axenfeld, F., Münch, J., Pacyna, J.M., Duiser,J.A. and Veldt,C. (1992) Test-Emissionsdaten-basis der Spurenelemente As, Cd, Hg, Pb, Zn und der speziellen organischen Verbindungen Lindan, HCB, PCB und PAK für Modellrechnungen in Europa. Abschlußbericht des Forschungsvorhabens 104 02 588 des Umweltforschungsplanes des Bundesministers für Umwelt, Naturschutz und Reaktorsicherheit. Im Auftrag des Umweltbundesamtes, Berlin.
  14. Umweltbundesamt (1997) The European Atmospheric Emission Inventory of Heavy Metals and Persistent Organic Pollutants.Umweltbundesamt (Federal Environmental Agency) P.O. Box 330022, D-14191 Berlin,Germany.
  15. Petersen, G.,Munthe,J.,Bloxam,R.,and Vinod Kumar,A. (1998) A Comprehensive Eulerian Modelling Framework for Airborne Mercury Species: Development and Testing of the Tropospheric Chemistry Module (TCM)*Atmospheric Environment - Special Issue on Atmospheric Transport,Chemistry,and Deposition of Mercury* (edited by S.E.Lindberg,G.Petersen and G.Keeler),Vol.32,No.5,pp.829-843.
  16. Davidson, C. and Yee-Lin, W. (1989) Dry Deposition of Trace Elements, in J.M. Pacyna, B.W. Ottar (eds.),*Control and Fate of Atmospheric Trace Metals*, NATO-ASI Series, Series C: Mathematical and Physical Sciences - Vol.268,pp 147-202,Kluwer Academic Publishers,Dordrecht.

17. Barrie, L.A. and Schemenauer, R.S. (1989) Wet Deposition of Heavy Metals, in J.M. Pacyna and B.W. Ottar (eds.), *Control and Fate of Atmospheric Trace Metals*, NATO-ASI Series, Series C: Mathematical and Physical Sciences - Vol.268, pp 203-231, Kluwer Academic Publishers, Dordrecht.
18. Petersen, G. and Krüger, O. (1993) Untersuchung und Bewertung des Schadstoffeintrags über die Atmosphäre im Rahmen von PARCOM (Nordsee) und HELCOM (Ostsee) Teilvorhaben: Modellierung des großräumigen Transports von Spurenmetallen. Abschlußbericht des Forschungsvorhabens 104 02 583 des Bundesministers für Umwelt, Naturschutz und Reaktor sicherheit. Im Auftrag des Umweltbundesamtes, Berlin. Externer Bericht GKSS 93/E/28.
19. Alcamo, J., Bartnicki, J., and Olendrzynski, K. (1991) Modeling Heavy Metals in Europe's Atmosphere: A Combined Trajectory - Climatologic Approach, in H. van Dop and D.G. Steyn (eds.), *Air Pollution Modeling and its Application VIII*, Plenum Press, New York, pp.389-398..
20. Krüger O. (1996) Atmospheric deposition of heavy metals to North European marginal seas: Scenarios and trend for lead, *GeoJournal* 39.2, 117-131.
21. Bartnicki, J. (1994) An Eulerian model for atmospheric transport of heavy metals over Europe: Model description and preliminary results, *Water, Air and Soil Pollution* 75, 227-263.
22. Galperin, M., Sofiev, M., Gusev, A., and Afinogenova, O. (1995) The Approaches to Modeling of Heavy Metals Transboundary and Long-Range Airborne Transport and Deposition in Europe, EMEP/MSC-E Technical Report 7/95, EMEP Meteorological Synthesizing Center-East, Kedrova str.8-1, Moscow, Russia.
23. Pekar, M. (1996) Regional Models LPMOD and ASIMD. Algorithms, Parameterization and Results of Application to Pb and Cd in Europe Scale for 1990, EMEP / MSC-E Report 9/96, EMEP Meteorological Synthesizing Center-East, Kedrova str.8-1, Moscow, Russia.
24. Petersen, G. (1992) Atmospheric Input of Mercury to the North Sea. Paris Convention for the Prevention of Marine Pollution. 9th Meeting of the Working Group on the Atmospheric Input of Pollutants to Convention Waters. London: 5-8 Nov. 1991 (PARCOM-ATMOS 9/13/1).
25. Petersen, G. (1992) Atmospheric Input of Mercury to the Baltic Sea. Baltic Marine Environment Protection Commission - Helsinki Commission -. Ninth Meeting of the Group of Experts on Airborne Pollution of the Baltic Sea Area (EGAP). Solna, Sweden: 19-22 Mai 1992 (HELCOM-EGAP 9/2/5).
26. Petersen, G., Iverfeldt, A. and Munthe, J. (1995) Atmospheric Mercury Species over Central and Northern Europe. Model Calculations and Comparison with Observations from the Nordic Air and Precipitation Network for 1987 and 1988, *Atmospheric Environment* 29, 47-67.
27. Sofiev, M., Maslyayev, A., and Gusev, A. (1996) Heavy metal model intercomparison Methodology and results for Pb in 1990. EMEP/MSC-E Technical Report 2/96, EMEP Meteorological Synthesizing Center-East, Kedrova str.8-1, Moscow, Russia.

# Paper VI



# Atmospheric Pb and Cd input into the Baltic Sea: a new estimate based on measurements

B. Schneider<sup>a,\*</sup>, D. Ceburnis<sup>b</sup>, R. Marks<sup>c</sup>, J. Munthe<sup>d</sup>, G. Petersen<sup>e</sup>, M. Sofiev<sup>f</sup>

<sup>a</sup> *Baltic Sea Research Institute, Inst. für Ostseeforschung, Warnemuende, Seestrasse 15, 18119 Rostock, Germany*

<sup>b</sup> *Institute of Physics, Vilnius, Lithuania*

<sup>c</sup> *Institute of Oceanology, Sopot, Poland*

<sup>d</sup> *Environmental Research Institute, Gothenburg, Sweden*

<sup>e</sup> *GKSS Research Center, Geesthacht, Germany*

<sup>f</sup> *Finnish Meteorological Institute, Helsinki, Finland*

Received 18 October 1999; received in revised form 24 May 2000; accepted 1 June 2000

## Abstract

Bulk deposition samples were collected during a summer (1997) and a winter (1998) measurement campaign at four coastal stations along the southern Baltic Sea coast and on the Island of Gotland. The data were used to construct Pb and Cd deposition fields over the Baltic Sea. A weak gradient with decreasing deposition rates from the southwest towards the east and north was obtained for Pb. In the case of Cd, the spatial distribution pattern was characterized by an extreme deposition maximum at the Polish station on the Hel Peninsula. The total atmospheric input of Pb and Cd into the Baltic Sea was 550 and 33 t/year, respectively, and exceeds the riverine input by approximately about 50%. Previous measurement-based estimates were higher by a factor 2–3 and indicate a decrease of the atmospheric deposition during the past 10–15 years. The comparison with modelled deposition data yielded partly large differences and was impaired by the fact that 1990 emission inventories were used whereas our measurements were performed in 1997/1998.

Relating our deposition estimate and the Pb/Cd input by rivers to the mean concentrations in Baltic Sea water, residence times of 0.29 and 3.6 years were obtained for Pb and Cd, respectively. © 2000 Elsevier Science B.V. All rights reserved.

*Keywords:* Atmospheric deposition; Cadmium; Lead; Baltic Sea

## 1. Introduction

The Baltic Sea is exposed to the input of many anthropogenically derived chemicals which are released into the environment mainly in the highly industrialized and densely populated areas in central

Europe. These substances enter the Baltic Sea via atmospheric deposition and riverine input where they may accumulate and potentially exert toxic effects on the ecosystem. Accumulation of contaminants in the Baltic Sea is favoured by the low water depth (mean: 52 m) and the limited water exchange with the North Sea which results in a mean seawater residence time of 20–30 years (HELCOM, 1986), which is much longer than in other coastal seas, e.g. in the North Sea (1–2 years; Otto et al., 1990).

\* Corresponding author. Fax: +49-381-5197302.

E-mail address: bernd.schneider@io-warnemuende.de (B. Schneider).

About 20–30 years ago, it became evident that atmospheric deposition plays an important role for the marine cycles of trace metals (e.g. Buat-Menard, 1986) and, in particular, for the contamination of coastal seas (e.g. Rodhe et al., 1980). This applies especially to the Baltic Sea where strong trace metal emission sources exist in countries bordering on the southern and eastern coast. However, the impact of these sources on the deposition into the Baltic Sea depends on the atmospheric transport pattern. The frequency distribution of the wind direction in the central Baltic Sea shows that southwesterly winds prevail. The relative frequency for the 60° southwest sector is 26%, whereas the corresponding southeast sector accounts for only 9%. As a consequence, sources located southwest of the Baltic Sea are of enhanced importance. Model studies have shown that emissions in Western European countries that are not neighbouring the Baltic Sea account for about 25% of the trace metal deposition to the Baltic Sea (Krüger, 1996).

Several attempts have been made to estimate the atmospheric input of trace metals into the Baltic Sea on the basis of measurements. A very first estimate was presented by Rodhe et al. (1980). Although based on fragmentary data, the results indicated the importance of atmospheric deposition for the trace metal budget of the Baltic Sea. In the following years, the Helsinki Commission for the Protection of the Baltic Sea Environment (HELCOM) initiated an airborne pollution monitoring programme (EGAP) which included the deposition of trace metals. Based on these data and on results from research projects (Grassl et al., 1989), new experimental input estimates were established, mainly for Pb, Cd and Zn (HELCOM, 1989, 1991; Duce et al., 1989; Schnei-

der, 1993). The data for Pb and Cd (Table 1) reveal discrepancies as large as a factor 2, which is probably due to inadequate sampling/analytical techniques, shortcomings in the sampling strategy, and different methods for extrapolation of coastal data to the entire Baltic Sea. Moreover, the estimates refer only to the time span between 1980 and 1990. Subsequent EGAP monitoring data were not used for input calculations due to questionable data quality (HELCOM, 1997).

In parallel to the experimental efforts, progress was achieved in modelling the long-range transport and deposition of atmospheric trace metals. Petersen and Krüger (1993) published modelled input fluxes (Pb, Cd, Zn, As), and the latest HELCOM deposition estimate (Pb, Cd) was based on model computations (HELCOM, 1997) as well. The differences between the model results (Table 1) are also considerable. However, it has to be taken into account that the computations refer to different years (1984/1985 vs. 1990) and therefore are based upon different emission inventories. Also, the fact that Petersen and Krüger (1993) applied a Lagrangian transport model, whereas an Eulerian-type model was used for the HELCOM (1997) estimate, and that different process parameterizations were included in the two models, may have contributed to different results. The agreement between the experimental and modelled estimates is also not satisfactory. For 1989/90, the input estimates for both Pb and Cd differ by a factor of 2–3.

In view of this situation, trace metal deposition was included in the “Atmospheric Load” subproject within the EU research project Baltic Sea System Studies (BASYS). By the use of both measurements and models, it was intended to establish an improved

Table 1  
Input estimates for Pb and Cd by measurements and models

Year	Pb [t/year]	Cd [t/year]	Reference	Type
1980	2400	80	Rodhe et al., 1980	measurements
1983–1986	1560	35	HELCOM, 1989	
1985–1987	1000	60	Duce et al., 1989	
1986–1990	1285	–	HELCOM, 1991	
1986–1989	1600	77	Schneider, 1993	
1984–1985	1400	18	Petersen and Krüger, 1993	models
1990	640	27	HELCOM, 1997	

current atmospheric input estimate as part of an overall trace metal budget for the Baltic Sea. Here we describe our experimental approach and present the results in comparison to model calculations (Sofiev et al., 2000). We concentrate on Pb and Cd since these elements show opposite biogeochemical characteristics in seawater. Cd is linked to the cycling of nutrients (“nutrient-like element”) and has relatively long residence times in seawater, whereas Pb is easily removed from the water column by adsorption to mineral particles and subsequent sedimentation (“scavenged element”) resulting in much shorter residence times.

## 2. Experimental

### 2.1. Sampling

Deposition samples were collected during a summer (June 16–August 8, 1997) and a winter period (February 1–March 31, 1998) at four coastal stations (Fig. 1) located at Kap Arkona on the Island of Ruegen (KAP), the Hel Peninsula (HEL), at Preila (PRE), and at Hoburg on the Island of Gotland (HOB). The main criterion for the selection of these sites was the absence of local sources such as heavy traffic or other human activities. Simple precipitation samplers consisting of a PE funnel with a surface area of 110 cm<sup>2</sup> screwed to a PE collection bottle (150 cm<sup>3</sup>) were deployed at each station. All materi-

als that get in contact with the samples were carefully cleaned with HNO<sub>3</sub> (pH = 0) and subsequently rinsed with suprapure deionized water. Since the samplers were kept open during dry periods, the samples comprised wet and dry deposition as well (bulk deposition). During most of the sampling periods, the collection bottles were changed each second day, provided that precipitation had occurred. During two 2-week periods in July 1997 and March 1998, daily samples were collected. In some cases, e.g. during the winter experiment at PRE, the funnel was rinsed with 30–50 cm<sup>3</sup> suprapure water after sampling intervals with no precipitation in order to get pure dry deposition samples.

A total of 175 deposition samples were obtained and shipped to the Baltic Sea Research Institute which acted as the central laboratory for the trace metal analysis.

### 2.2. Chemical analysis

For the determination of Pb and Cd in the deposition samples, total-reflection X-ray fluorescence (TXRF) and graphite furnace atomic absorption spectrometry (GFAAS) were applied using the following stepwise procedure.

Prior to the analysis, the samples were acidified with concentrated suprapure HNO<sub>3</sub> to a pH of about 0 in order to avoid adsorption of dissolved trace metals on the walls of the collection bottle. To suspend particles homogeneously, the samples were shaken vigorously and 20 µl of the sample were pipetted onto the center of the TXRF sample holder. Ten microliters of yttrium standard solution containing 1 ng Y was added, the sample was evaporated to dryness, and the X-ray fluorescence spectrum obtained by excitation with the Mo(Kα) line was recorded for 1000 s (Atomika, Model EXTRA II). By multiplication of the Pb/Y fluorescence intensity ratio with a calibration factor, the Pb concentration in the sample was calculated. For each deposition sample, two TXRF subsamples were prepared and measured. Details of trace metal analysis by TXRF are given by Knoth and Schwenke (1980).

Since the sensitivity of the TXRF method is low for Cd, GFAAS was applied (Perkin-Elmer, Model 5000). However, the concentrations in most of the samples were also too low for direct Cd determina-

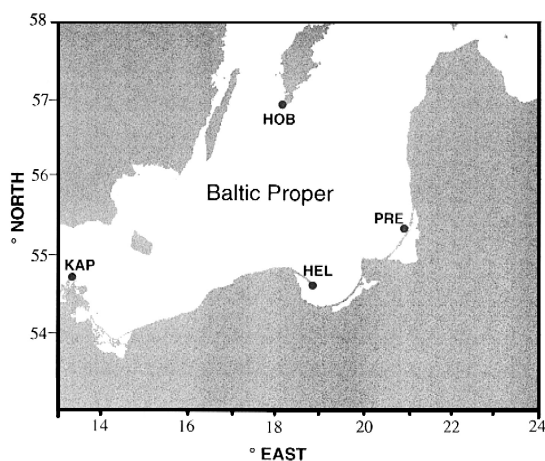


Fig. 1. Location of the sampling stations.

tion by GFAAS. Therefore, these samples were freeze-dried and then redissolved in a volume of 1 N HNO<sub>3</sub> that was 1/10 of the original sample volume. After this enrichment procedure, the detection limit for Cd in bulk deposition was reduced to 0.018 nmol/l. The uncertainty of the method is estimated to be about 15%.

The concentrated samples were also used to determine Pb by GFAAS and to repeat the TXRF determination. Hence, the Pb data were obtained using three different procedures: direct TXRF, GFAAS and TXRF after enrichment by freeze-drying. Since the differences between the results did not show any systematic trend, the mean was used to represent the Pb concentration. The mean differences between the three determinations indicated that the uncertainty of the Pb values is about 10–15%. Due to the freeze-drying enrichment, the sensitivity of the Pb determination was increased and a detection limit of 0.1 nmol/l was attained for both the TXRF and GFAAS method.

At the beginning of each measurement period, a field blank test was performed at each station using ultra-clean deionized water to simulate a rain event. Handling of the samples and chemical analysis were identical with the treatment of the real samples. For Pb, the concentrations in the blank samples (30–50 cm<sup>3</sup>) varied between 0.15 and 1.9 nmol/l with a mean value of 0.87 nmol/l. In the case of Cd, only three samples contained detectable Cd concentrations with a mean of 0.09 nmol/l, which thus represents an upper blank limit.

### 3. Results and discussion

#### 3.1. Pb and Cd concentrations in the deposition samples

The Pb and Cd concentrations in the bulk deposition samples at the four stations are plotted as a function of the precipitation height in Fig. 2. No blank corrections were performed because of the uncertainties of blank determination and because the effect on the measured concentrations was within the uncertainty of the method.

The Pb data cover a range of approximately two orders of magnitude and increase during periods of

low precipitation (Fig. 2a). To compare the concentrations at the different stations, means weighted to the amount of precipitation were calculated (Table 2). The mean values for Pb refer to both measurement periods and show a steady decline in the sequence KAP–HEL–PRE–HOB, indicating a west/east and a south/north gradient.

The variability of the Cd concentrations is similar to that of Pb if only the stations KAP, PRE and HOB are considered (Fig. 2b). However, at station HEL exceptionally high Cd concentrations were observed mainly, but not only, during sampling periods with little precipitation. Some samples contained as much as 240 nmol/l Cd and, when associated with relatively high precipitation amounts, yielded strong deposition pulses. Hence, a completely different regional distribution pattern was obtained for the mean Cd concentrations in the bulk deposition samples (Table 2). Whereas almost uniform values were found for KAP, PRE and HOB, an extremely high mean concentration was observed at HEL, which exceeded those at the other stations by a factor of about 20.

In view of these unexpected results, the question arises whether the samples could have been contaminated during handling. We think this is unlikely because only the Cd concentrations were high in the respective samples, whereas other elements such as Zn and Pb, which are known as indicators for contamination, did not show any anomaly. Moreover, data from the HELCOM monitoring station Leba, located about 75 km east of HEL, have also shown markedly elevated (factor 5) Cd concentrations in bulk deposition compared to the neighbouring stations in Germany and Lithuania (HELCOM, 1997). From these findings, we conclude that a strong Cd source must exist in northern Poland, which has a pronounced impact on the deposition at HEL. Backward trajectories calculated by the Finnish Meteorological Institute (M. Hongisto, K. Jylha, pers. communication) are presented (Fig. 3) for the sampling interval with the maximum concentration in bulk deposition (Fig. 2b). The trajectories show that the air masses passed the area south/southeast of HEL before arriving at the sampling site. Hence, one may speculate that the City of Gdansk, which is located about 25 km south of HEL, is the suspected Cd emission source. However, for the other sampling intervals with high Cd deposition, the trajectories

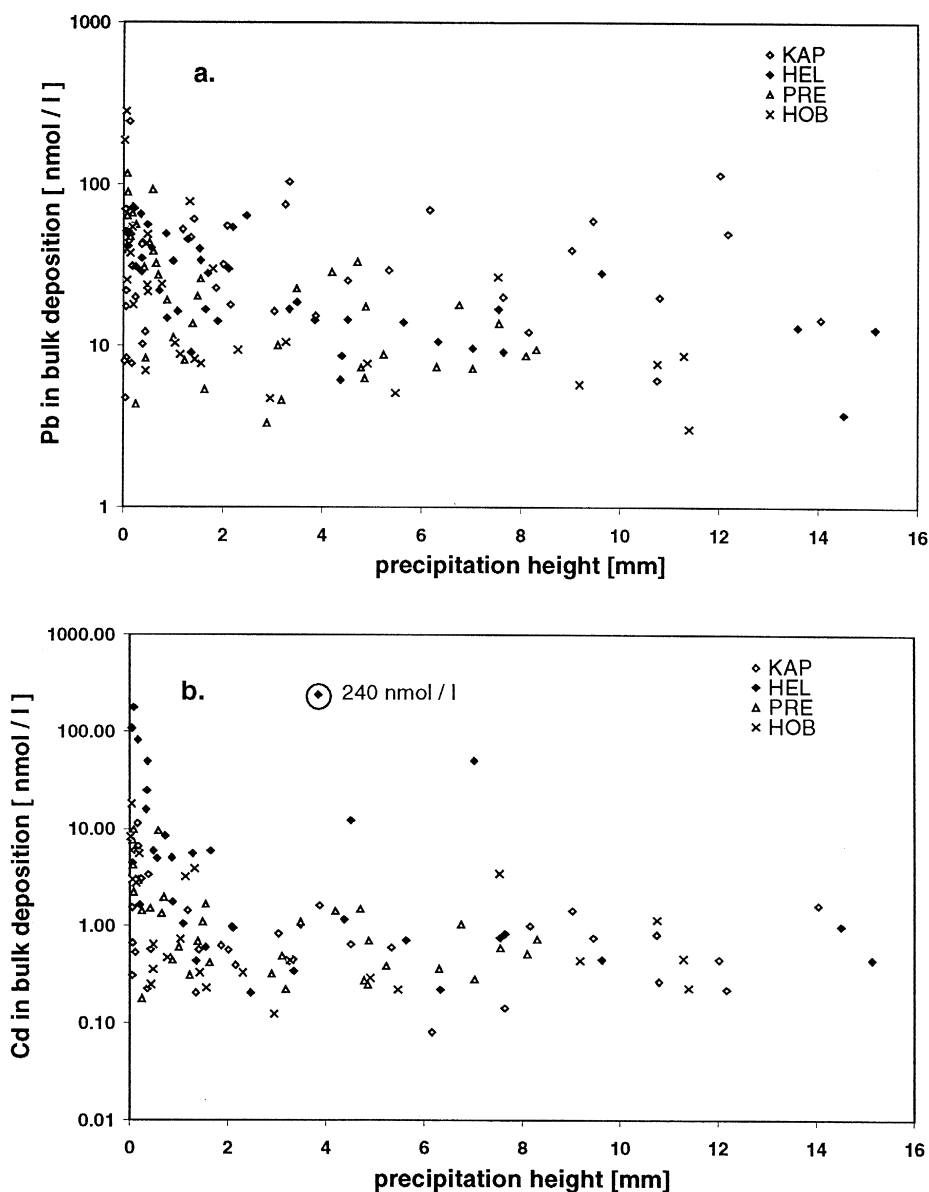


Fig. 2. Concentrations of Pb (a) and Cd (b) in the bulk deposition samples as a function of precipitation height.

were not unequivocally indicative of a Gdansk Cd source.

### 3.2. Dry deposition of Pb and Cd

To approximately estimate the contribution of dry deposition to the bulk deposition, the data from the

winter experiment at PRE were analyzed, where nine dry-only samples were collected during 2 weeks without any precipitation. The concentrations in water used to rinse the funnel ranged over one order of magnitude and showed mean values of 3.1 nmol/l and 0.13 nmol/l for Pb and Cd, respectively. Although the blanks may have contributed significantly

Table 2

Mean Pb and Cd concentrations in bulk deposition ( $c$ ), measured precipitation ( $h$ ) and deposition rates ( $D_b$ ), and deposition rates normalized to the mean annual precipitation rate ( $D_t$ )

Pb	$c$ [nmol/l]	$h$ [mm/year]	$D_b$ [ $\mu\text{mol}/\text{m}^2 \text{ year}$ ]	$D_t$ [ $\mu\text{mol}/\text{m}^2 \text{ year}$ ]
KAP	25	454	12.0	14.6
HEL	17	447	7.5	9.3
PRE	14	326	4.9	7.5
HOB	11	266	3.4	6.1

Cd	$c$ [nmol/l]	$h$ [mm/year]	$D_b$ [ $\mu\text{mol}/\text{m}^2 \text{ year}$ ]	$D_t$ [ $\mu\text{mol}/\text{m}^2 \text{ year}$ ]
KAP	0.69	454	0.32	0.39
HEL	16.2	447	7.24	8.91
PRE	0.72	326	0.25	0.38
HOB	0.89	266	0.28	0.49

to these low concentration levels, no correction was performed because of the uncertainties involved in the blank determinations, especially in the case of Cd. Therefore, the data may slightly overestimate the dry deposition and are considered as an upper limit estimate.

Dry deposition for the 2-week dry period was 0.085 and 0.0036  $\mu\text{mol}/\text{m}^2$  for Pb and Cd, respectively. Assuming that dry deposition took place with the same intensity during the period when precipitation occurred, the dry deposition for the entire sampling period (54 days) was calculated: 0.30  $\mu\text{mol}/\text{m}^2$  for Pb and 0.013  $\mu\text{mol}/\text{m}^2$  for Cd. Subtracting these values from the bulk deposition yielded the wet deposition, which after normalization to the mean climatological precipitation height was 1.0  $\mu\text{mol}/\text{m}^2$  (Pb) and 0.053  $\mu\text{mol}/\text{m}^2$  (Cd). Hence, the dry deposition contributed about 20% to the total (wet + dry) deposition for both Pb and Cd. Model calculations (Petersen and Krüger, 1993; HELCOM, 1997) give dry deposition estimates that account for about 10% or even less of the total deposition. However, such a comparison must take into account both the difficulty in parameterizing particle deposition in the models and the uncertainties involved in our estimate. In addition to a potential blank effect, the limited sampling period and the problems related to any attempt to sample dry deposition (e.g. Dolske and Gatz, 1985) may have introduced a bias to our estimate.

### 3.3. Input estimates for Pb and Cd

The mean precipitation ( $h$ ) and bulk deposition ( $D_b$ ) rates which include the contribution of the dry-only samples are given for each station in Table 2. To estimate the annual total deposition ( $D_t$ ) of Pb and Cd to the Baltic Sea requires extrapolation of the local bulk deposition rates in time and space. Whereas the concentrations in bulk deposition were assumed to be representative for an entire year, the deposition rates were adjusted to the climatological mean precipitation rate ( $H$ ). Since normalization to  $H$  must be confined to the wet fraction ( $D_{\text{wet}}$ ) of the bulk deposition, the total deposition ( $D_t$ ) is expressed by:

$$D_t = D_{\text{dry}} + D_{\text{wet}} * H/h \quad (1)$$

Using the previously determined ratio  $D_{\text{dry}}/D_t = 0.20$  and replacing  $D_{\text{wet}} = D_b - D_{\text{dry}}$  gives:

$$D_t = D_b * 1 / (0.20 + (1 - 0.20) * h/H) \quad (2)$$

On the basis of Eq. (2),  $D_t$  was calculated for each station using the bulk deposition and precipitation rates (Table 2) and the mean annual precipitation rate for the Baltic Sea  $H = 584 \text{ mm/year}$  (HELCOM, 1986). The uncertainties related to the

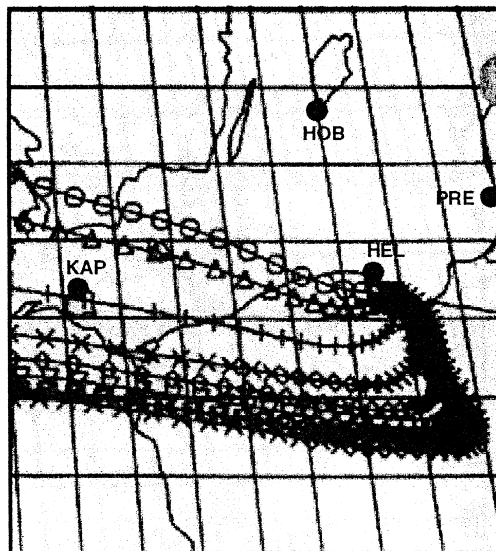


Fig. 3. Air mass trajectories for the sampling interval with the maximum Cd deposition at station HEL (see Fig. 2b).

determination of the  $D_{\text{dry}}/D_{\text{t}}$  are relevant for the determination of  $D_{\text{t}}$  only if the measured precipitation rates deviate strongly from the climatological mean. This effect was tested for the stations HOB and PRE where a low ratio  $h/H$  of about 0.5 was observed. However, a reduction of  $D_{\text{dry}}/D_{\text{t}}$  to the model-derived value of 0.1 (Petersen and Krüger, 1993; HELCOM, 1997) affected  $D_{\text{t}}$  only by about 5%.

In order to extrapolate the annual Pb and Cd deposition rates from the four stations to the entire Baltic Sea, the following simplifications and assumptions were made.

(a) The Baltic Sea (415 000 km<sup>2</sup>) is considered as a rectangle (Fig. 4) with the line KAP–HEL–PRE (500 km) representing the southern “continental” coast, whereas HOB represents the conditions 300 km north of the “continental” coast. In order to extrapolate the deposition measurements to the areas north of HOB, bulk deposition measurements made in 1995 at the Finnish monitoring station Hailuoto (HAI) on the northern coast of the Bothnian Bay (HELCOM, 1997) were assumed to be representative of the upper boundary of the Baltic Sea rectangle. The mean concentrations at HAI were 8.7 and 0.44 nmol/l for Pb and Cd, respectively. The calculation of the total deposition rates followed the procedure for our data and yielded 4.49  $\mu\text{mol}/\text{m}^2$  year for Pb and 0.23  $\mu\text{mol}/\text{m}^2$  year for Cd.

(b) Due to dispersion and deposition, concentrations of atmospheric trace substances decrease approximately exponentially with increasing distance from the source area. Therefore, it was assumed that deposition between the stations also follow an exponential function. Fields for the total deposition were calculated by interpolation, first between the stations along the “continental” coast, then between this baseline and the uniform deposition at a distance of 300 km (HOB) and finally between HOB and HAI. The calculations were performed for cells of 50 km  $\times$  50 km.

Fig. 4a shows the calculated spatial distribution of the Pb deposition, which is characterized by a weak gradient with decreasing deposition from the southwest (KAP) towards the east and north. The mean deposition rate was 6.37  $\mu\text{mol}/\text{m}^2$  year and corresponds to a Pb input into the Baltic Sea of 550 t/year. The distinct decrease of the Pb deposition

with regard to previous experimental estimates (Table 1) is consistent with the reduction of Pb emissions due to the restricted use of Pb additives in gasoline and with the decreasing trend of Pb concentrations in Baltic Sea surface water (Kremling and Streu, 2000). However, we cannot exclude that methodological improvements also contributed to the differences in the estimates.

Sofiev et al. (2000) calculated the Pb input into the Baltic Sea for the period of our measurements by model simulations that are based on modifications of the ADOM model (Venkatram et al., 1988) and the HILATAR model (Hongisto, 1998). Extrapolating their monthly data to an entire year yields Pb inputs of 680 and 596 t/year for the ADOM and the HILATAR model, respectively, which agrees well with HELCOM (1997) model estimate (Table 1). The agreement with our estimate (550 t/year) seems also reasonable, taking into account the uncertainties involved in both the model calculations and the experimental approach. However, the comparison is impaired by the fact that the model calculations are based on a 1990 Pb emission inventory which, due to emission reductions in Europe, does not apply to 1997/1998.

The distribution of the Cd deposition (Fig. 4b) is centered around the deposition hot spot at HEL with about 9  $\mu\text{mol}/\text{m}^2$  year. The relative contributions of the individual deposition events to the total deposition during the sampling campaigns are presented in Fig. 5 and show that the three highest deposition peaks accounted for about 70% of the total deposition. With increasing distance from HEL, the gradient decreased, but it still existed between HOB (0.49  $\mu\text{mol}/\text{m}^2$  year) and HAI (0.23  $\mu\text{mol}/\text{m}^2$  year). A mean Cd deposition rate of 0.71  $\mu\text{mol}/\text{m}^2$  year was calculated, yielding a total input of 33 t/year. About 20% of this input occurred in a narrow 50-km band along the southern coast. Most of the previous experimental input data (Table 1) were higher than our estimate by a factor of about 2. Again, it is difficult to assess the effect of methodological artefacts on these differences. However, the decreasing Cd concentrations in Baltic Sea surface waters during the time span 1982 to 1993/1995 (HELCOM, 1996; Kremling and Streu, 2000) support the conclusion that a real decrease of the Cd input occurred during the past 10–15 years.

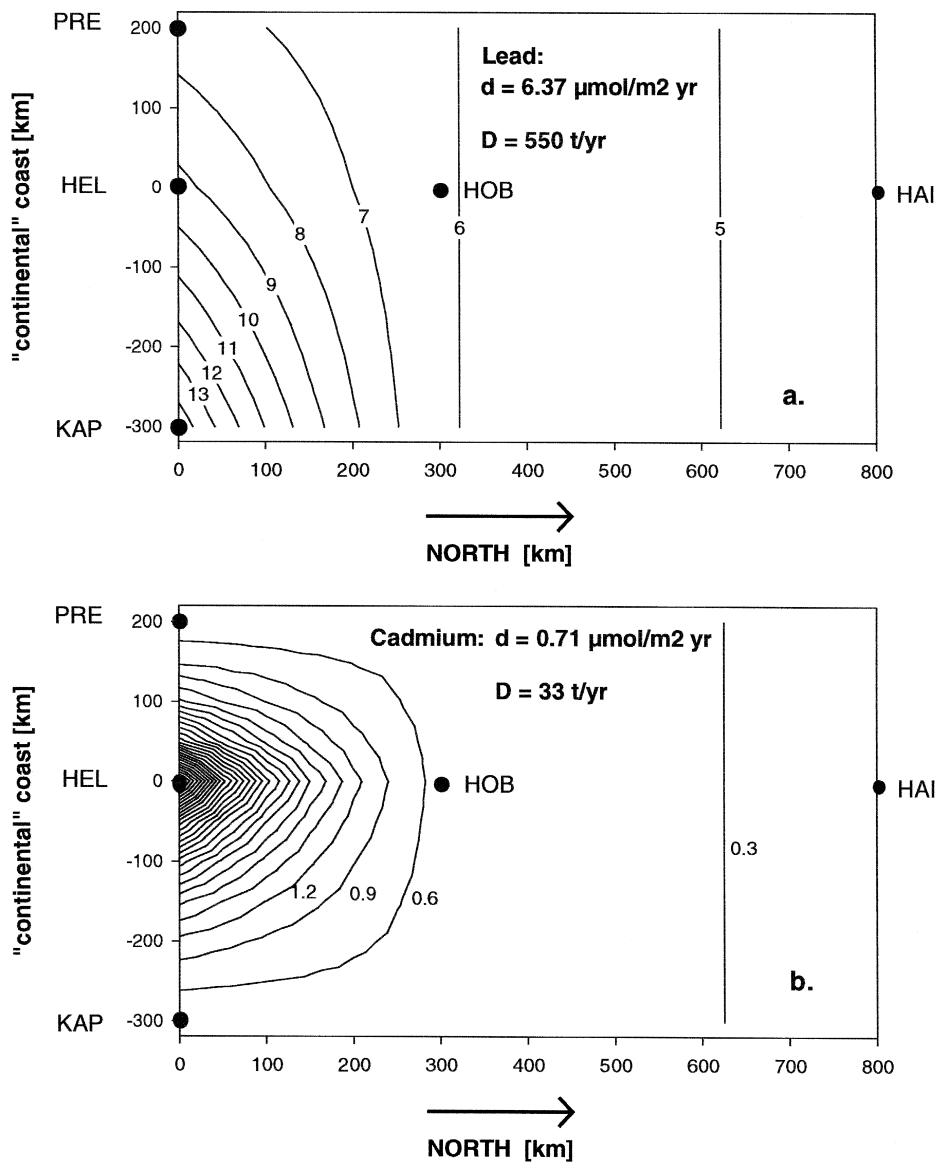


Fig. 4. Spatial distribution of the Pb (a) and Cd (b) deposition rates.

The comparison with model calculations by Sofiev et al. (2000) revealed major differences. Both the ADOM (9.4 t/year) and the HILATAR (9.0 t/year) model produced input estimates which were a factor of 3.7 below the values based on measurements. This discrepancy can only partly be attributed to the extreme deposition at HEL, which is not reproduced by the model (Sofiev et al., 2000). If the HEL data

are excluded from our deposition calculations, a total Cd input of 18 t/year is still obtained. On the other hand, the HELCOM (1997) Cd model calculations generated an input of 28 t/year, which differs by only 20% from our estimate.

The comparison between our input data and the model results must consider the uncertainties of the different approaches. With regard to model calcula-

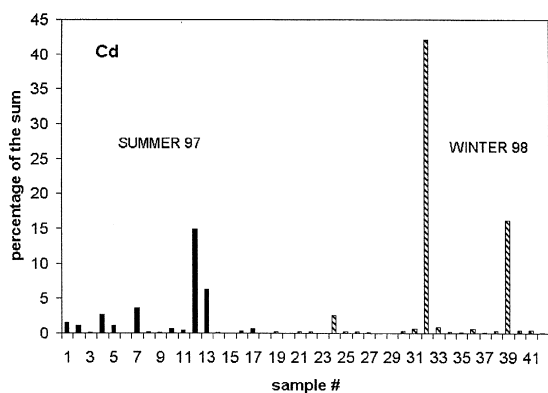


Fig. 5. Cd deposition at station HEL as percentage of total deposition during the summer and winter measurement period.

tions, inaccurate and obsolete emission inventories are very likely the main error sources, which according to Sofiev et al. (2000) may lead to uncertainties of roughly a factor 2. To give a well-grounded estimate of the uncertainty of our estimate is difficult as well. The error of 10–15% given for the chemical analysis of the samples is probably magnified by the procedure to extrapolate the deposition data in space and time.

Considerable effort has been made to estimate the atmospheric trace metal deposition to the North Sea since the neighbouring countries are highly industrialized and many potential emission sources are concentrated close to the coast. A compilation of measured deposition rates covering the period up to 1993 is given by Injuk and van Grieken (1995). Mean Pb and Cd deposition rates for the entire North Sea area are reported (e.g. Rojas et al., 1993) exceeding those in the Baltic Sea by a factor of 4–5. Subsequent investigations by Injuk et al. (1998), which did not include Cd, yielded somewhat lower Pb deposition rates. However, their Pb flux estimate of 17.9  $\mu\text{mol}/\text{m}^2$  year, which included a dry contribution of about 14%, is still a factor 3 higher than our data and indicates that the North Sea is more heavily subjected to atmospheric trace metal deposition than the Baltic Sea.

### 3.4. Importance of the atmospheric input for the Baltic Sea Pb and Cd budget

In addition to atmospheric deposition, riverine input plays an important role for the Baltic Sea Pb

and Cd budget. According to HELCOM (1998), the Pb and Cd river loads are approximately 340 and 24 t/year, respectively. Thus, the atmosphere contributes about 60% to the total input of both Pb and Cd into the Baltic Sea.

To establish a mass balance, the water exchange between the Baltic Sea and the North Sea must be considered as a potential sink/source for Pb and Cd. Mean concentrations for dissolved Pb and Cd in the central Baltic Sea surface waters are 0.041 and 0.080 nmol/l, respectively (Kremling and Streu, 2000). Taking into account a particulate Pb and Cd fraction of about 30% and 5% (Pohl and Hennings, 1999) results in total concentrations of 0.058 and 0.085 nmol/l, respectively. For the northeastern North Sea, Haarich and Schmidt (1993) reported total Pb and Cd concentrations of 0.21 and 0.19 nmol/l, respectively. Combining these data with the water exchange rates between the Baltic Sea and the North Sea (HELCOM, 1986: outflow = 947 km<sup>3</sup>/year; inflow = 471 km<sup>3</sup>/year) yields a net import into the Baltic Sea of 11 t/year for Pb and of 1 t/year for Cd. Compared to the atmospheric and riverine inputs, these are negligible quantities.

Whereas decreasing trends of the Pb and Cd concentrations in Baltic Sea surface waters were identified for the time span between 1982 and 1993/1995 (Kremling and Streu, 2000; HELCOM, 1996), the concentrations have stabilized during the

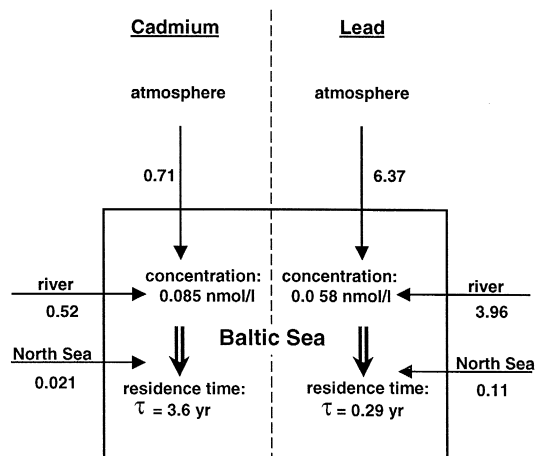


Fig. 6. Pb and Cd budget for the Baltic Sea, all inputs are related to the Baltic Sea surface area and are presented as [ $\mu\text{mol}/\text{m}^2$  year].

last 5 years (Pohl and Hennings, 1999; Pohl, unpublished monitoring data). This indicates that the present Pb and Cd inputs are compensated by sedimentation and that the budget is at steady state. Relating the sum of the input fluxes to the mean concentrations (Fig. 6) results in mean residence times of 0.29 and 3.6 years for Pb and Cd, respectively. This confirms and specifies the “scavenged” behaviour of Pb and “nutrient-like” properties of Cd.

#### 4. Conclusions

Pb and Cd input estimates for the Baltic Sea are presented which, with the exception of the HAI data, are based on a sampling network with uniform sampling equipment and on identical analytical methods. A methodological bias of the data was thus avoided and a homogeneous data set was obtained. The discrepancy between the experimental and modelled Pb/Cd input data that we were confronted with at the start of the project could not be resolved. The fact that the emission inventories used by the models do not apply to the time of the measurements is the major obstacle to identifying the reasons for the deviations.

Uncertainties in the experimental estimates are related to the representativeness of our measurements. Although seasonal differences in the air mass transport pattern and deposition were taken into account by performing a winter and a summer experiment, our measurements covered only one third of a year. The question of representativeness also arises with regard to the selection of sampling sites. The site selection is especially critical along the southern Baltic Sea coast, which is closest to the source areas. This was demonstrated by the input estimate that ignored the deposition maximum at HEL and yielded an input of 18 t/year instead of 33 t/year. To achieve representativeness, the stations must be located both in “low” and “high” deposition areas, but must avoid local sources which have no long-range effect. This is an extremely difficult task because it requires knowledge of the deposition distribution pattern along the coastline and because the establishment of a sampling network is restricted by logistical limitations. Future measurement programmes should

use model calculations to optimize the site selection, presuming that the models are based on correct emission inventories.

Despite these potential sources of errors, we are confident that our effort has improved the knowledge about the present Pb and Cd deposition to the Baltic Sea. The data indicate that atmospheric deposition of Pb and Cd exceeds the input by rivers and thus has a major impact on the Pb and Cd budget of the Baltic Sea. Compared to estimates for the time before 1990, the input of Pb and Cd decreased by a factor of 2–3. This is consistent with the decreasing trends for Pb and Cd in Baltic Sea surface waters reported by HELCOM (1996) and Kremling and Streu (2000).

#### Acknowledgements

This study was the result of a collaborative effort that included contributions from many scientists, technicians, students and a lighthouseman during the operation of the sampling stations. Many thanks to all of them, but especially to Ines Petersohn and Hildegard Kubsch, who analyzed the large number of samples with great care and skill. The study was part of the EU funded Baltic Sea System Study BASYS (MAS3-CT96-0058), subproject “Atmospheric Load”.

#### References

- Buat-Menard, P., 1986. Air to sea transfer of anthropogenic trace metals. In: Buat-Menard, P. (Ed.), *The Role of Air–Sea Exchange in Geochemical Cycling*. NATO ASI Series C vol. 185, Reidel, Dordrecht, Holland.
- Dolske, D.A., Gatz, D.F., 1985. A field intercomparison of methods for the measurement of particle and gas dry deposition. *J. Geophys. Res.* 90, 2076–2084.
- Duce, R.A., Liss, P.S., Merrill, J.T., Buat-Menard, P., Hicks, B.B., Miller, J.M., Prospero, J.M., Arimoto, R., Church, T.M., Ellis, W., Galloway, J.M., Hansen, L., Jickells, T.D., Knapp, A.H., Reinhardt, K.-H., Schneider, B., Soudine, A., Tokos, J.J., Tsunogai, S., Wollast, R., Zhou, M., 1989. The input of atmospheric trace species to the world ocean. *Rep. Stud. GESAMP*, 38.
- Grassl, H., Eppel, D., Petersen, G., Schneider, B., Weber, H., Gandrass, J., Reinhardt, K.-H., Wodarg, D., Fliess, J., 1989. Stoffeintrag in Nord-und Ostsee über die Atmosphäre. GKSS Research Center, Geesthacht, Germany, GKSS 89/E/8.
- Haarich, M., Schmidt, D., 1993. Heavy metals in the North Sea, 2.

- Results of the large-scale ZISCH survey from 28.1.–6.3.87. Dtsch. Hydrogr. Z. 45, 371–431.
- HELCOM, 1986. Water balance of the Baltic Sea. Baltic Sea Environ. Proc. No. 16.
- HELCOM, 1989. Deposition of Airborne Pollutants to the Baltic Sea Area 1983–1985 and 1986. Baltic Sea Environ. Proc. No. 32.
- HELCOM, 1991. Airborne Pollution Load to the Baltic Sea 1986–1990. Baltic Sea Environ. Proc. No. 39.
- HELCOM, 1996. Third Periodic Assessment of the Marine Environment of the Baltic Sea. Baltic Sea Environ. Proc. No. 64B.
- HELCOM, 1997. Airborne Pollution Load to the Baltic Sea 1991–1995. Baltic Sea Environ. Proc. No. 69.
- HELCOM, 1998. The Third Baltic Sea Pollution Load Compilation (PLC-3). Baltic Sea Environ. Proc. No. 70.
- Hongisto, M., 1998. HILATAR, a Regional Scale Grid Model for the Transport of Sulphur and Nitrogen Compounds. Finnish Meteorological Institute, Contributions 21, 152 pp.
- Injuk, J., van Grieken, R., 1995. Atmospheric concentrations and deposition of heavy metals over the North Sea: A literature review. J. Atmos. Chem. 20, 179–212.
- Injuk, J., van Grieken, R., de Leeuw, G., 1998. Deposition of atmospheric trace elements into the North Sea: Coastal, ship, platform measurements and model predictions. Atmos. Environ. 32, 3011–3025.
- Knoth, J., Schwenke, H., 1980. A new totally reflecting X-ray fluorescence spectrometer with detection limits below  $10^{-11}$  g. Z. Anal. Chem. 301, 7–9.
- Kremling, K., Streu, P., 2000. Further evidence for a drastic decline of potentially hazardous trace metals in Baltic Sea surface waters. Mar. Pollut. Bull., in press.
- Krüger, O., 1996. Atmospheric deposition of heavy metals to North European marginal seas: Scenarios and trends for lead. GeoJournal 39.2, 117–131.
- Otto, L., Zimmermann, J.T.F., Furnes, G.K., Mork, M., Saetre, R., Becker, G., 1990. Review of the physical oceanography of the North Sea. Neth. J. Sea Res. 26, 161–238.
- Petersen, G., Krüger, O., 1993. Untersuchung und Bewertung des Schadstoffeintrags ueber die Atmosphaere im Rahmen von PARCOM (Nordsee) und HELCOM (Ostsee)–Teilvorhaben: Modellierung des grossraeumigen Transports von Spurenmetallen. GKSS Research Center, Geesthacht, Germany, GKSS 93/E/28.
- Pohl, C., Hennings, U., 1999. The effect of redox processes on the partitioning of Cd, Pb, Cu, and Mn between dissolved and particulate phases in the Baltic Sea. Mar. Chem. 65, 41–53.
- Rodhe, H., Soederlund, R., Ekstedt, J., 1980. Deposition of airborne pollutants on the Baltic Sea. Ambio 9, 168–173.
- Rojas, C.M., Injuk, J., Laane, R.W., van Grieken, R., 1993. Dry and wet deposition fluxes of Cd, Cu, Pb and Zn into the Southern Bight of the North Sea. Atmos. Environ. 27A, 251–259.
- Schneider, B., 1993. Untersuchung und Bewertung des Schadstoffeintrags ueber die Atmosphaere im Rahmen von PARCOM (Nordsee) und HELCOM (Ostsee)–Teilvorhaben: Messungen von Spurenmetallen. GKSS Research Center, Geesthacht, Germany, GKSS 93/E/53.
- Sofiev, M., Petersen, G., Krüger, Schneider, B., Hongisto, M. and Jylha, K., 2000. Model simulations of atmospheric trace metal concentrations and depositions over the Baltic Sea. Submitted to Atmos. Environ.
- Venkatram, A., Karamchandani, P.K., Misra, P.K., 1988. Testing a comprehensive acid deposition model. Atmos. Environ. 22, 737–747.



# Paper VII





PERGAMON



Atmospheric Environment 35 (2001) 1395–1409

ATMOSPHERIC  
ENVIRONMENT

www.elsevier.com/locate/atmosenv

# Model simulations of the atmospheric trace metals concentrations and depositions over the Baltic Sea

M. Sofiev<sup>a,\*</sup>, G. Petersen<sup>b</sup>, O. Krüger<sup>c</sup>, B. Schneider<sup>d</sup>, M. Hongisto<sup>a</sup>, K. Jylha<sup>a</sup>

<sup>a</sup>Finnish Meteorological Institute, Vuorikatu 19, Helsinki 00100, Finland

<sup>b</sup>GKSS Research Centre, Geesthacht, Germany

<sup>c</sup>Meteorological Institute, University of Hamburg, Bundesstr. 55, D-20146 Hamburg, Germany

<sup>d</sup>Baltic Sea Research Institute, Warnemünde, Germany

Received 13 March 2000; accepted 14 July 2000

## Abstract

The results of application of two nested Eulerian atmospheric transport models for investigation of airborne heavy metal pollution are presented. The distribution and deposition over Europe and Baltic Sea region were simulated for Pb, Cd and Zn for 2 two-months periods: June–July 1997 and February–March 1998. The European-wide calculations were made with the ADOM model from the GKSS Research Centre, and the Baltic regional calculations were made with the HILATAR model from the Finnish Meteorological Institute. The one-way 3-D nesting was used: hourly concentrations from the ADOM model were used by the HILATAR as vertically resolved boundary conditions. Input data for both models were taken from the weather forecast model HIRLAM and UBA/TNO emission inventory. This allows interpreting of some diversity in the calculation results in terms of different internal parameterization and spatial resolution of the models. Simulation results were compared with high-resolution atmospheric measurements carried out at four stations in the southern part of the Baltic Sea for the same period. Manifesting quite good agreement with observations, the models missed several high deposition events of Cd observed at coastal station Hel. Study of this phenomenon enabled to build a 2-D probability function for potential location of the unknown Cd source. © 2001 Elsevier Science Ltd. All rights reserved.

**Keywords:** Toxic pollution; Nested modeling; Cadmium; Lead; Zinc

## 1. Introduction

The problem of toxic pollution of the European continent is taken as one of the prioritized directions of environmental investigations and policy. Contrary to acid substances, the toxic species (heavy metals and persistent organic pollutants) have direct negative influence on human health. One of specific fields of investigations is the toxic pollution of marine ecosystems, in particular, of the Baltic Sea and the North Sea.

The main difficulty in this area is the lack of reliable measurement data as well as emission inventories and knowledge about atmospheric transformations and

removal characteristics of the substances. These obstacles enforce complex approach (when intensive monitoring is combined with numerical simulations) to be implemented in the study of toxic pollution.

This is the way adopted for current study, which was performed within the framework of the EU Baltic Sea System Study (BASYS) project. The paper presents the modelling results for the distribution of three particle-carried heavy metals – Pb, Cd and Zn, model verification against measurements and discussion about potential unknown source of Cd in the southern Baltic.

## 2. Description of the model calculations

Considerable distance of the Baltic Sea region from the main pollution sources in Central Europe as well as

\* Corresponding author. Tel.: +358-9-1929-3151; fax: +358-9-1929-3146.

E-mail address: mikhail.sofiev@fmi.fi (M. Sofiev).

existence of several powerful local sources justified the application of two models nested one into another. The European-wide model was built from a chemical transport model for acid compounds ADOM (Venkatram et al., 1988) and adapted to simulations of particle-carried metals at the GKSS Research Centre. The regional model for the Baltic Sea was made from another Eulerian acid model HILATAR developed at the Finnish Meteorological Institute FMI (Hongisto, 1998).

The off-line one-way 3-D nesting procedure was used. Hourly concentrations over Europe for 4 months of simulations (June, July 1997 and February, March 1998) calculated by the ADOM model were transmitted from GKSS to FMI, where the nesting routine was applied sequentially for each hourly data set. The vertically resolved ADOM concentrations at the boundary of the HILATAR domain were picked up and interpolated vertically between the model grids (the ADOM grid contains 12 layers up to 10 km height, the HILATAR one has 13 layers up to  $\sim 10$  km). The horizontal interpolation was void since both models follow the grid formulations of weather forecast model HIRLAM (1990), but with different resolution (the ADOM grid has  $0.5^\circ$  cell size, the HILATAR one  $\sim 0.25^\circ$ ).

### 3. Common input data for the nested models

One of the advantages of the current study is the harmonized input data, which enables interpreting the similarity/diversity of the results in terms of the model formulations rather than in differences between the input data.

Emission information was derived from the UBA/TNO inventory for toxic substances in Europe (Berdowski et al., 1997). This inventory provides grid data with spatial resolution of  $50 \text{ km} \times 50 \text{ km}$  in polar stereographic projection for several pollutants and, in particular, for Pb, Cd and Zn. The data were re-scaled into the ADOM and HILATAR grids.

The emission inventory was compiled for the reference year 1990, which results in uncertainties connected with emission trends between 1990 and 1997/1998. Measures undertaken in Europe during 1990s (in particular, ban of leaded gasoline) resulted in significant decreasing of Pb emission – about factor of 2 for Eastern Europe. The Pb data for the reference year 1995 are becoming available (Pacyna, personal communication), but so far the complex up-to-date estimates do not exist. For Cd and Zn the trends are even less known but not so significant as for Pb (Ryaboshapko et al., 1999).

Meteorological data for both models were based on HIRLAM numerical weather forecast routinely made at FMI (HIRLAM, 1999; Järvenoja, 1999). The HIRLAM output contains large number of parameters extensively describing the 4-d atmospheric conditions. For ADOM runs, the 1 h data were pre-processed in FMI and transmitted to GKSS with a resolution  $0.5^\circ$ . For HILATAR

the 6 h data were used for the boundary layer pre-processing routine, which produced the data with  $0.25^\circ$  spatial horizontal and 1 h time resolutions. One-hour HIRLAM information was not used because the HILATAR is aimed at simulations of acid pollutants distribution since 1993, when only 6 h data are available.

### 4. Similarities and differences in the model formulations

The core principles of both models used for the nesting calculations are quite similar. They are based on the Eulerian advection–dispersion algorithms, multi-layer representation of the vertical structure of concentrations with the top located around 10 km above the sea level. The diversities discussed below are quantitative and located in the parameterization of the emission time variation, transport and deposition of the pollutants.

Although the emission data were the same for both models (apart from the minor deviations in the spatial distribution caused by re-projecting to grids with different resolutions) the time variation coefficients were different. In the European-wide ADOM model the emission rate was taken constant for all metals, whereas in the regional model HILATAR a non-uniform time variation for Pb was assumed.

According to Berdowski et al. (1997), one of the biggest individual contributions into Pb emission comes from the use of leaded gasoline (almost 70% in 1990 in Europe). So, time variation of Pb emission can be correlated with nitrogen emission, which also has large traffic fraction.  $\text{NO}_x$  daily coefficients for 1990 were taken from Lenhart and Friedrich (1995). For other years the monthly and weekly cycles were derived from these data. For diurnal variation, the hourly relative traffic intensity for Finland was used (Hongisto, 1998).

For Cd and Zn the situation is not so evident and there is no clear way to justify any time non-uniformity, so for these metals no variation was taken into account in both models.

Another source of difference is particle size. In the ADOM model the mean diameter is taken to be  $0.56 \mu\text{m}$ , while in HILATAR about  $0.8 \mu\text{m}$  was accepted in order to reflect the condensation of water on fine aerosol in the marine atmosphere.

There are some other dissimilarities between the models, originated in their internal structure, different thickness of the vertical layers, split algorithms, consideration of water-phase processes, scavenging, etc. The influence of the above differences to the final results is considered in the discussion part of the paper.

### 5. Results of the simulations and discussion

The simulation results are stored in form of maps of the metal concentrations in aerosol, dry and wet

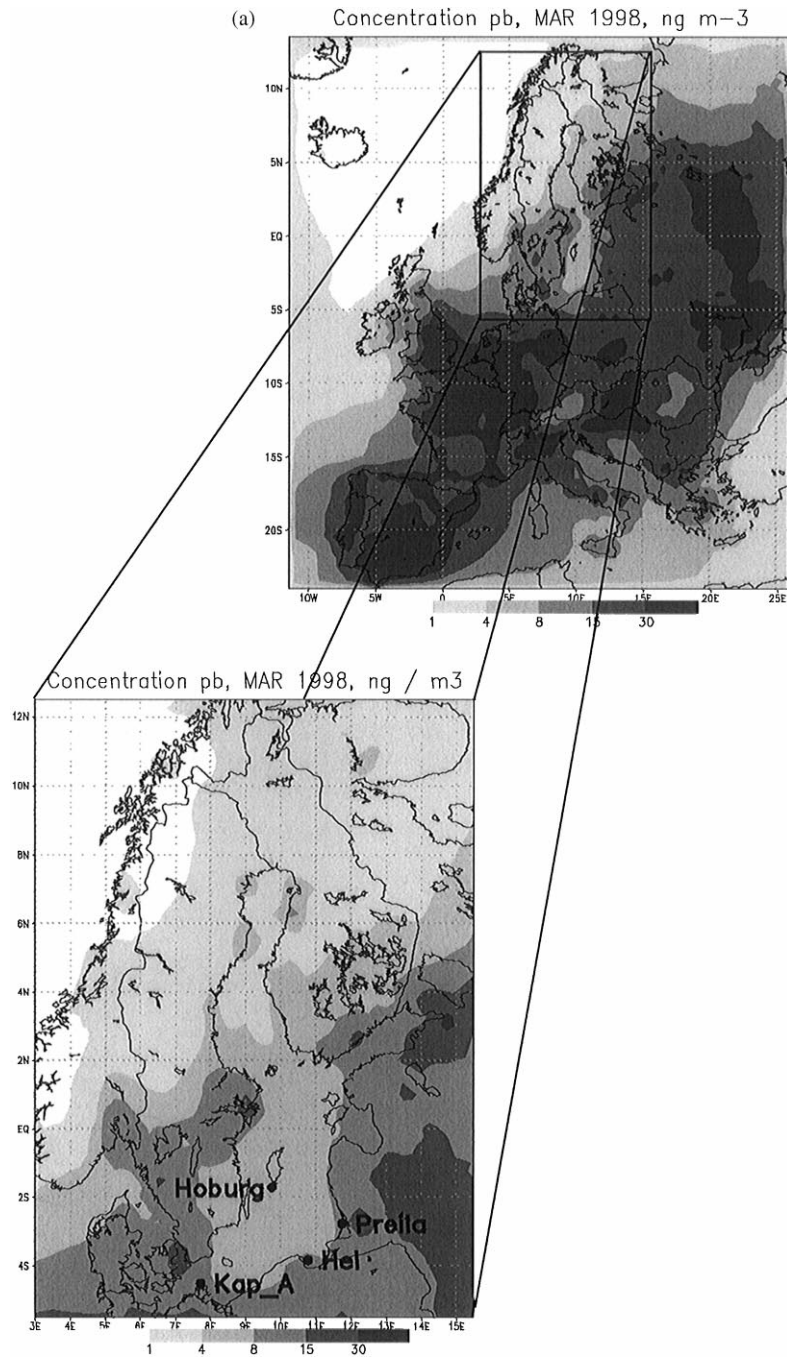


Fig. 1. Nested surface concentration for March 1998 for Pb, Cd, Zn ( $\text{ng m}^{-3}$ ).

deposition. All layers are stored separately. The ADOM maps are recorded with 1 h time resolution, the HILATAR output contains 6 h data, which enables to reduce the size of the output archives without loss of diurnal cycle representation.

### 5.1. Distribution patterns

An example for March 1998 of monthly mean values is shown in Fig. 1. The ADOM model produced the maps for Europe, while the Baltic ones are from HILATAR.

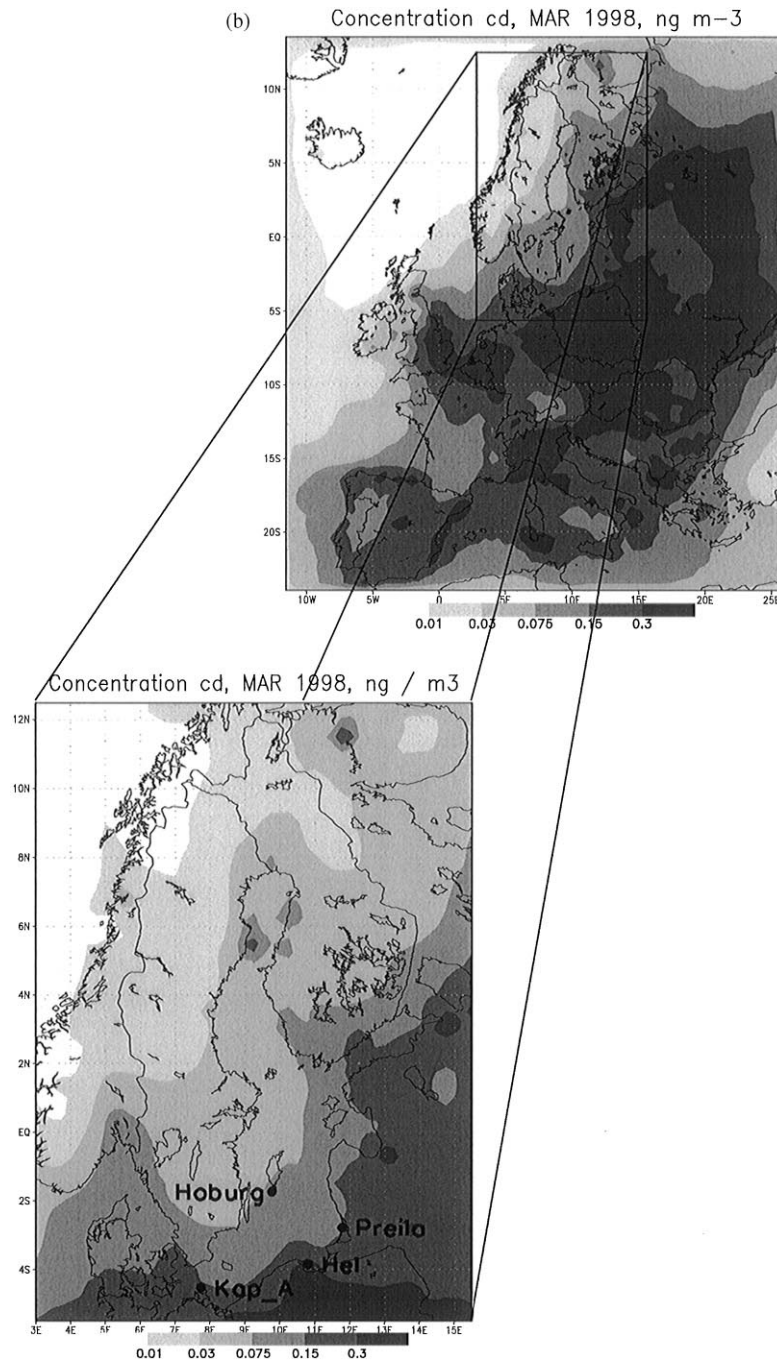


Fig. 1. (continued).

The first conclusion, which can be derived from the European map is that the Baltic area is comparably clean – the characteristic concentrations are about one order of magnitude less than those in Central Europe. There is also considerable gradient of concentrations

from the South to the North – the difference between the southern and the northern Baltic is again almost one order of magnitude.

Both models are coherent in reproducing these main patterns, but finer details are reported quite differently.

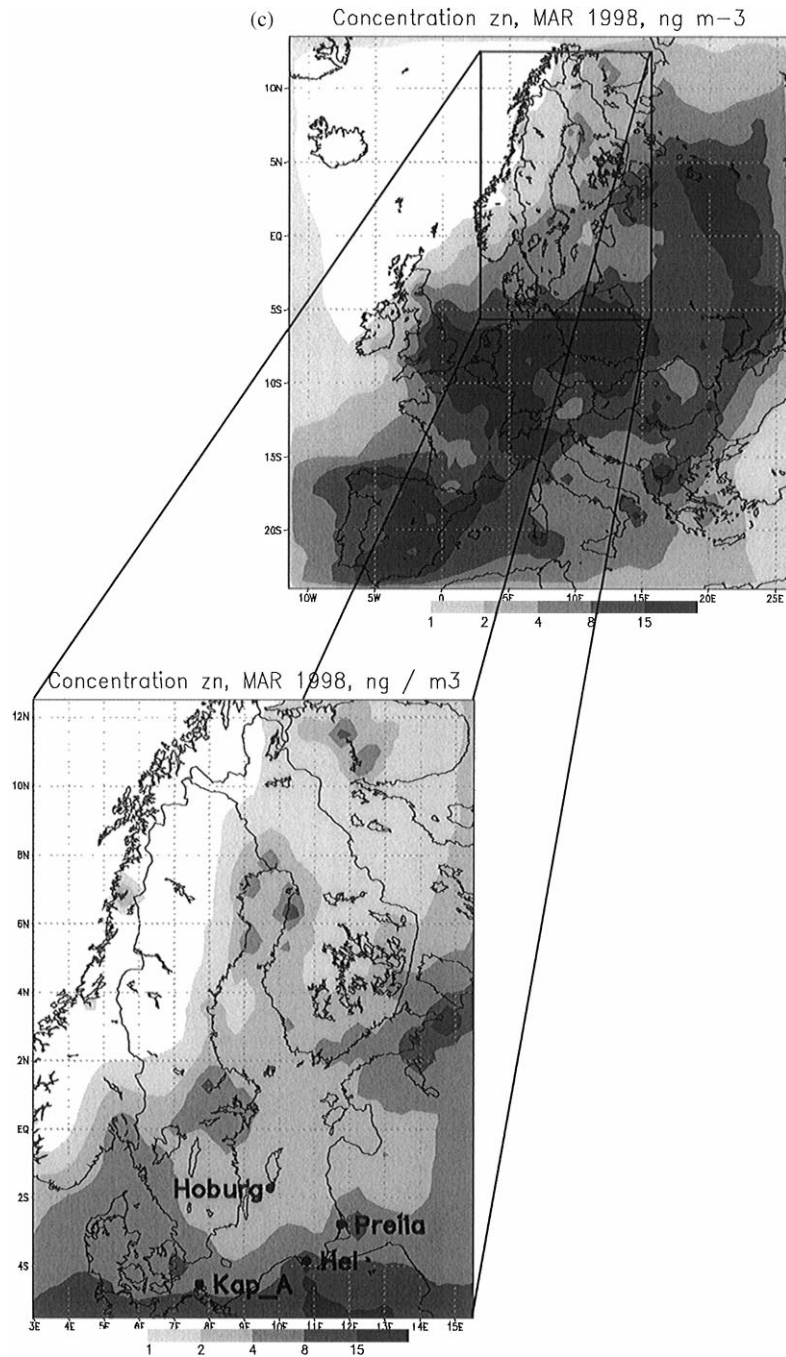


Fig. 1. (continued).

As it can be expected, the treatment of regional sources by HILATAR is more detailed. It is especially true for the clean northern part of the Baltic, as well as for the Kola Peninsula. Also, concentration isolines in the coastal zone are better resolved and closer to the coastal line in the regional HILATAR output than in European maps.

In March the coast-to-sea gradient is practically not seen in the Gulf of Finland, which reflects the high percentage of the ice cover during winter and early spring. Above the open sea in central Baltic this gradient is more pronounceable. It is the biggest for Pb and moderate for Cd and Zn, which is caused by higher

effective source heights assumed for these metals. Thus, in HILATAR 100% of Pb emission is concentrated in the first layer of  $\sim 45$  m thickness. For Cd it is spread over almost 500 m (the first, the second and the third layers of the model). Zn is distributed over 200 m (the first and the second layers). Consequently, the changes of the mixing conditions between the open sea and the land have smaller influence to the near-surface concentrations of Cd and Zn.

For the southern part of the Baltic region the models reported somewhat different concentration patterns. In particular, the HILATAR values are generally lower than the ADOM ones. The deviation is negligible in the south-west corner and reaches its maximum in the southeastern part of the Baltic domain. Such spatial irregularity is caused by the prevailing wind direction in March 1998. In the southwestern part of the domain the wind flow was incoming for more than 85% of the month. As a result, the concentration level was mainly dictated by the transport from outside. This information is directly accepted by the HILATAR from the ADOM boundary conditions, hence the patterns are very similar near the border line. On the contrary, in the southeastern part of the Baltic domain, the inflow wind was only during 35% of the time, and concentration patterns were primarily created by regional sources covered by the HILATAR, whose treatment of small-scale processes differs from that of ADOM.

Near the powerful sources, the HILATAR generally shows higher values than the ADOM, while in remote areas the difference is the opposite and can be accounted up to a factor of 2. There are several reasons for such deviation. First, initial horizontal dilution caused by coarse resolution of the ADOM model provokes more intensive dispersion of the pollutants and thus decreases the local concentrations in comparison with the HILATAR. Second, the assumed size of aerosol particles is bigger in HILATAR, which increases the removal processes and decreases transport to remote areas. For Pb the time variation coefficients applied in HILATAR result in bulk of emission occurred during daytime, when vertical mixing is generally more intensive in comparison with night. Consequently, the dilution along the height becomes higher than that in the ADOM, where the intensity is the same during day and night. It also decreases the regional Pb surface concentrations in comparison with European fields.

## 5.2. Total deposition on to the sea surface

Deposition maps for March 1998 are presented in Fig. 2. Total values obtained from the HILATAR are summarized in Table 1, together with the mean load from the ADOM, recent measurements (Schneider et al., 2000) and other model estimates (Ryaboshapko et al., 1999).

Absolute values of lead deposition (both modelled and derived from measurements) obtained in the BASYS

project are close to each other and twice as much as the results of the other model exercise. The difference between the model estimates is explained by the specific scenario for the Pb emission in 1996, used by Ryaboshapko et al. (1999). According to it, the total reduction of Pb emission in HELCOM countries between 1990 and 1996 is about a factor of 2.5, except for Russia, where it was almost constant. It resulted in difference in emission between current study and (Ryaboshapko et al., 1999) about a factor of 2, which approximately reflects the trend from 1990 to 1996. As atmospheric distribution of particle-carried pollutants is practically linear with regard to their emission, similar scaling should be attributed to the deposition onto the Baltic Sea. This makes the model estimates fully comparable with each other.

Accepting the above rough estimate of Pb emission trend between 1990 and 1997/98 and scaling the deposition figures, we end up with 300–350 t of Pb as a mean annual load reported by all models. This value is about a half of the number derived from the measurements. Reflecting the main tendency of the models to underestimate the load, this comparison is quite uncertain for several reasons: the actual emission trend is unknown; the original inventory is subject for  $\geq 25\%$  of uncertainty (Pacyna, 1994); and the extrapolation of coastal deposition measurements to the open sea also creates some errors, which are not easy to assess.

Comparison for Cd looks similar. The model values are close to each other, while the measurements-based load estimate is 2–3 times higher. For this metal, the situation is more complicated because of several very strong deposition events registered at the station Hel but missed by the models. These episodes are discussed below, but even without this station the difference is as large as a factor of 2 (the lower measurement-based value in the Table 1).

It is difficult to assess the accuracy of the modelled deposition of Zn (according to HILATAR, it is about  $400 \text{ t yr}^{-1}$ ). All calculated values are much lower than the observed ones (see also the next section, Table 3). Such under-estimation has quite a long history (Galperin et al., 1994) and still is not fully explained. Current study has also not resolved this problem and the results are of high degree of uncertainty.

So, the model assessments of annual deposition onto the Baltic sea are about 300–350 t for Pb (after 1995), about 9–10 t for Cd and about 400 t for Zn. The estimates made by different models and for different years are quite close to each other and are 1.5–2 times lower than those derived from the measurements.

The load appeared to be quite sensitive to the dispersion conditions. It consists of two main parts – fairly constant deposition caused by local/regional input and highly polluted episodes, when the air masses come from Central Europe. If they correlate with rain or

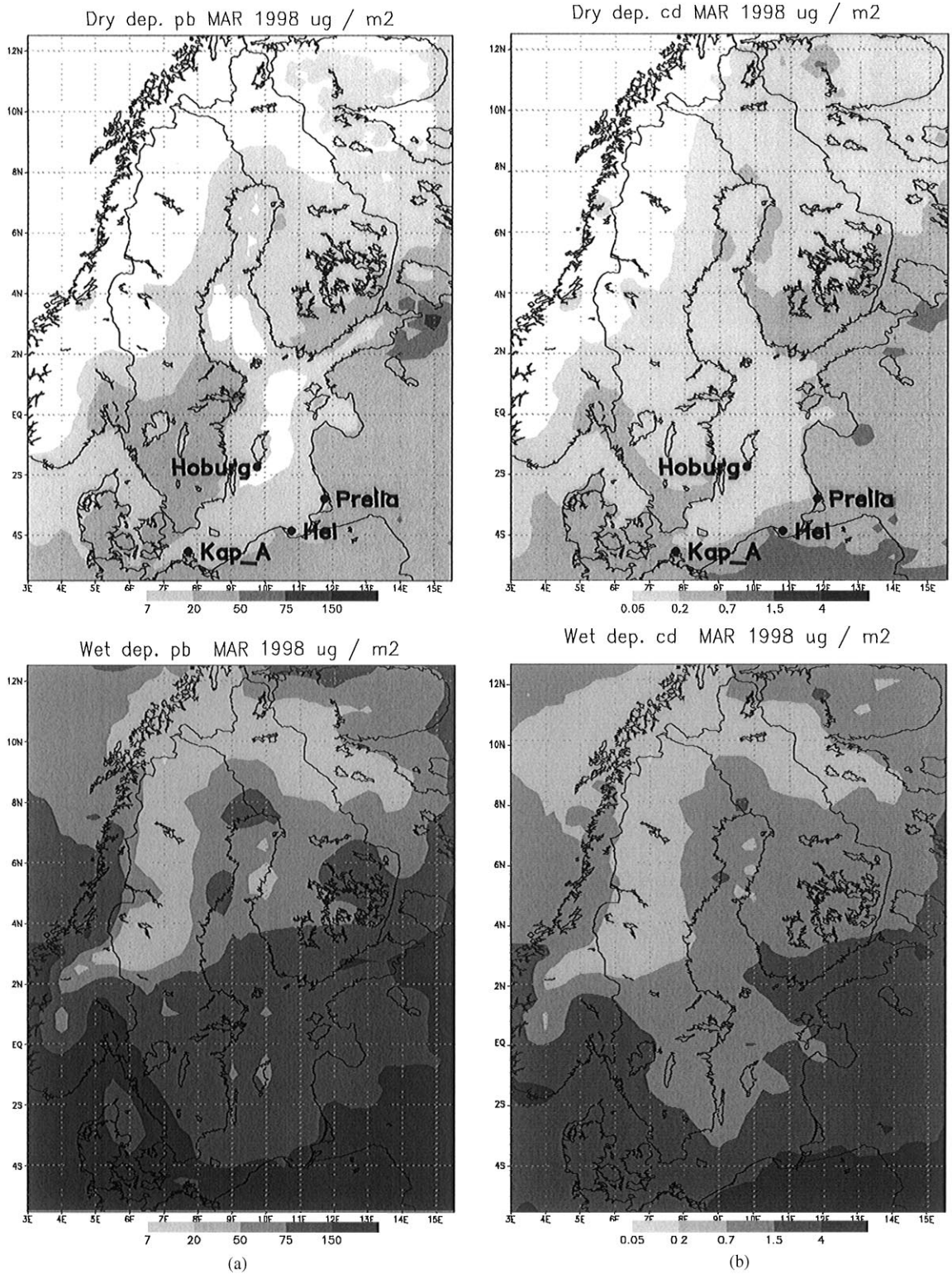


Fig. 2. Deposition maps for March 1998 for Baltic area.

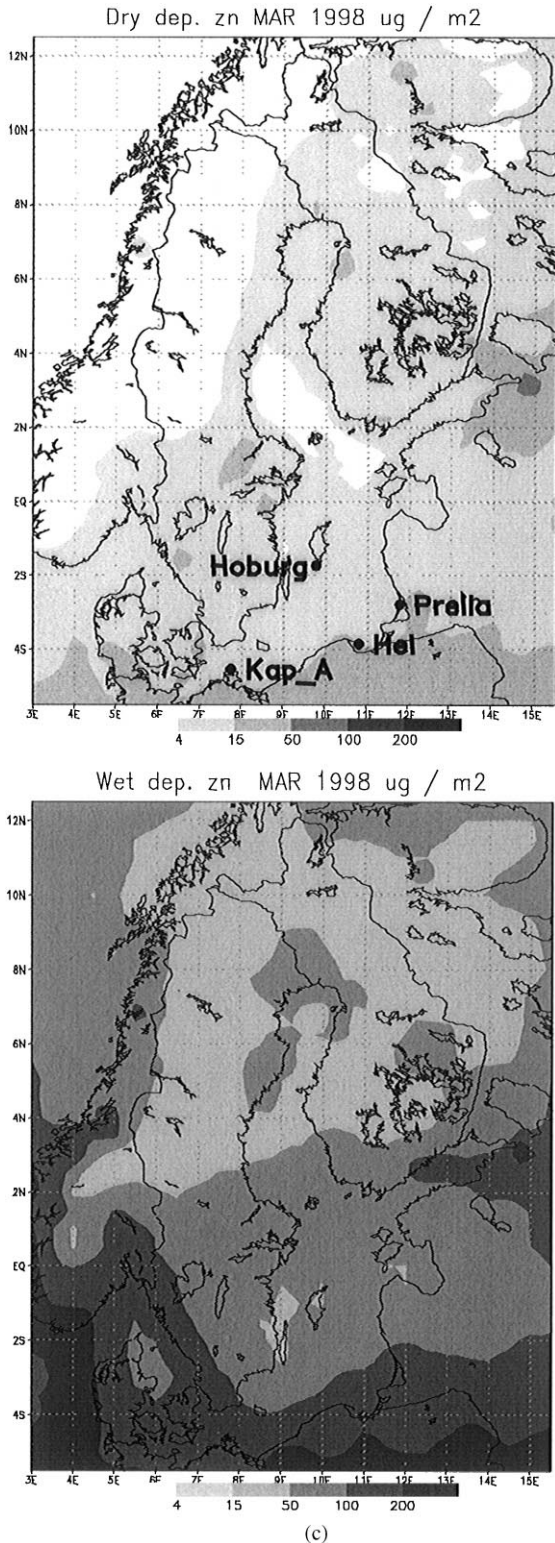


Fig. 2. (continued).

Table 1  
Deposition of Pb, Cd, Zn onto the Baltic Sea (tons of Pb Cd<sup>-1</sup> Zn<sup>-1</sup> yr<sup>-1</sup>)

	Dry	Wet	Total
<i>Pb</i> (t)			
June 1997	2.3	39	41
July 1997	1.9	29	31
February 1998	5.9	71	77
March 1998	4.6	45	49
Scaled annual	44	552	596
ADOM annual deposition			680
Schneider et al. (1999) from measurements			550
Ryaboshapko et al. (1999) for 1996			295
<i>Cd</i> (t)			
June 1997	0.04	0.8	0.8
July 1997	0.03	0.5	0.5
February 1998	0.07	0.8	0.9
March 1998	0.07	0.7	0.8
Scaled annual	0.59	8.4	9.0
ADOM annual deposition			9.4
Schneider et al. (1999) from measurements			18–33
Ryaboshapko et al. (1999) for 1996			9
<i>Zn</i> (t)			
June 1997	1.1	30	31
July 1997	0.7	18	19
February 1998	3.3	47	51
March 1998	2.7	32	34
Scaled annual	23	381	404

snow shower episodes, the monthly deposition can be generated within a couple of days (Hongisto et al., 2000). For the considered 4 months the standard deviations of both observed and modelled wet deposition values were between 100 and 200% of the mean values for all three metals depending on the station. Switching from 24–48 h to monthly averaging results in ~20–50% as a monthly standard deviation. Consequently, annual deposition onto the Baltic Sea will contain internal meteorological uncertainties of 5–15%.

5.3. Model-measurement comparison

The application of the modelling system was accompanied with the monitoring campaign at four stations established in the southern part of the Baltic region (see map in Fig. 2). High-resolution measurements were performed during two periods – summer (June, July, August in 1997) and winter (February, March 1998). For these months time averaging of the measured heavy metal aerosol concentration and deposition was kept within 24–48 h, which enabled detailed verification of the model results, both for aerosol concentrations and wet

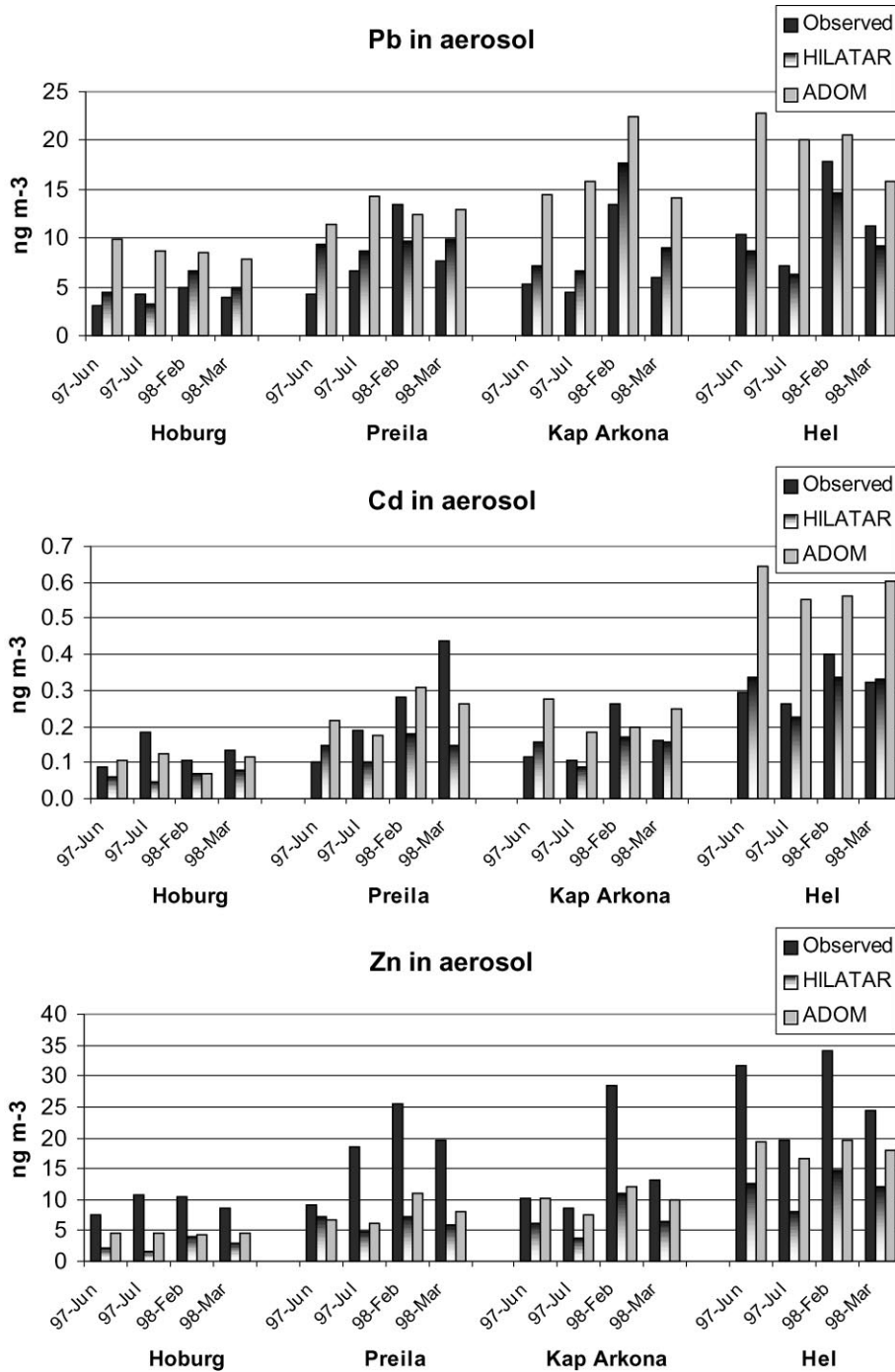


Fig. 3. Monthly mean concentrations in aerosol observed and simulated at 4 stations.

deposition. The monthly results are shown on Fig. 3; the correlation coefficients calculated for each set of samples are presented in Table 2. Examples of time series, observed at the stations and calculated by the HILATAR are presented in Fig. 4. Accumulated wet deposition over

the simulated period is presented in Table 3 together with the standard deviation of the deposition time series.

The main episodes with high concentrations (and conversely, clean periods) are reproduced quite well by the models, although the agreement varies for different

Table 2  
Correlation coefficients between observed and modelled concentrations

	Pb		Cd		Zn	
	ADOM	HILATAR	ADOM	HILATAR	ADOM	HILATAR
Hoburg	0.51	0.44	0.47	0.33	0.44	0.32
Preila	0.36	0.33	0.13	0.16	0.31	0.18
Kap Arkona	0.56	0.75	0.74	0.81	0.66	0.84
Hel	0.38	0.60	0.15	0.22	0.37	0.39

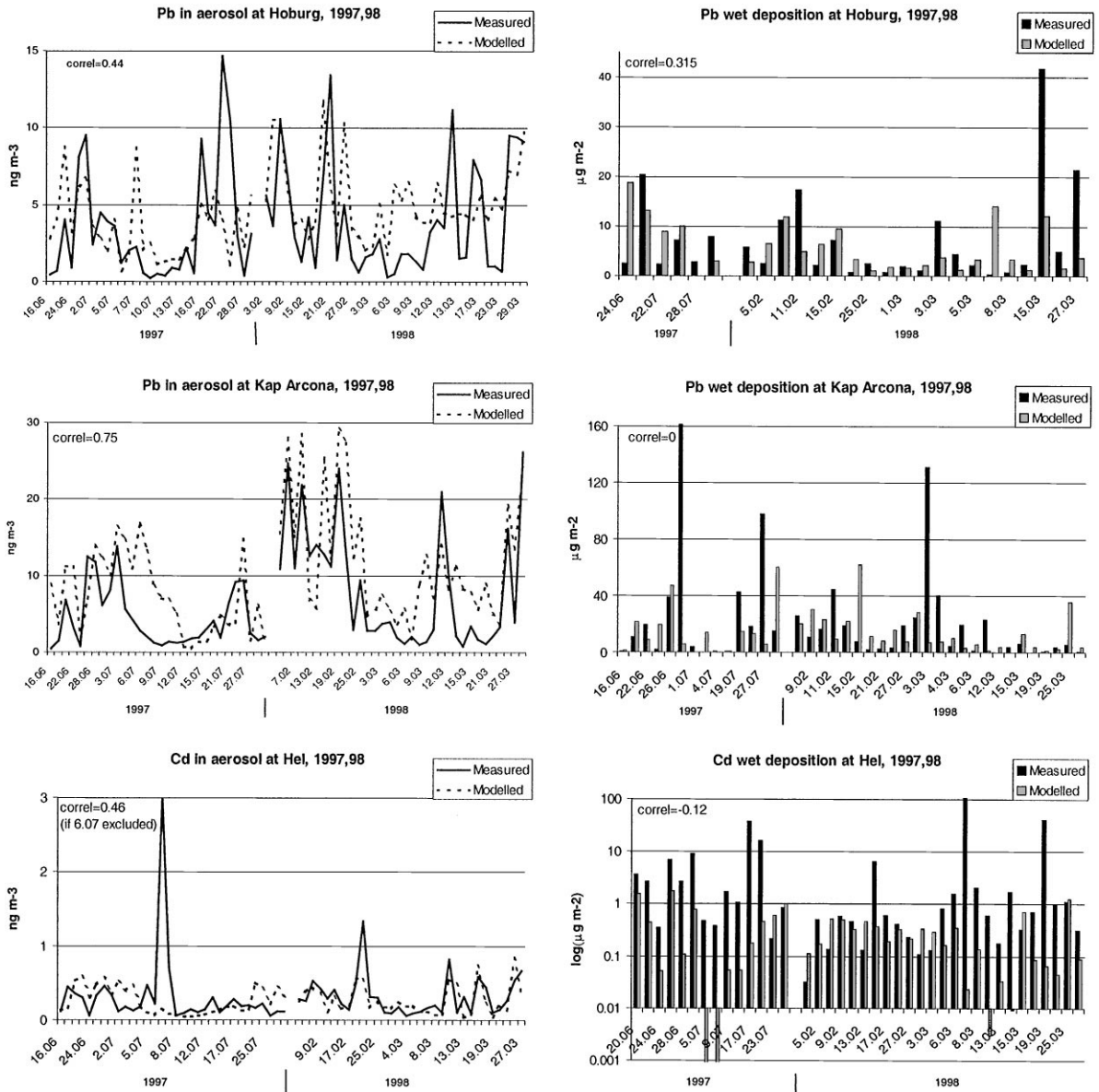


Fig. 4. Examples of observed and simulated time series for Pb and Cd. Model output is averaged/integrated to fit to the sampling periods.

Table 3  
Observed and modelled accumulated wet deposition and its variability

	Pb				Cd				Zn			
	Observed 4-mon sum ( $\mu\text{g m}^{-2}$ )	S.D. of episodes (%)	HILATAR ( $\mu\text{g m}^{-2}$ )	Observed 4-mon sum ( $\mu\text{g m}^{-2}$ )	S.D. of episodes (%)	HILATAR ( $\mu\text{g m}^{-2}$ )	Observed 4-mon sum ( $\mu\text{g m}^{-2}$ )	S.D. of episodes (%)	HILATAR ( $\mu\text{g m}^{-2}$ )	Observed 4-mon sum ( $\mu\text{g m}^{-2}$ )	S.D. of episodes (%)	HILATAR ( $\mu\text{g m}^{-2}$ )
Hoburg	155	135	132	7.0	192	1.5	596	102	1.5	596	102	78
Preila	218	108	354	5.8	102	4.9	967	93	4.9	967	93	136
Kap Arkona	569	158	459	8.6	135	6.5	4549	163	6.5	4549	163	355
HEL	370	109	427	233.5	276	11.1	2756	125	11.1	2756	125	429

metals and periods. Better coherence is seen for Hoburg and Kap Arkona, while correlation coefficients for Preila and Hel are quite low. This might point out to the incomplete emission inventory for the Eastern Europe, which damages the shape of the simulated pollution plumes coming to the sites.

Stochastic features of short-term precipitation events also disturb the model-measurement comparison, especially for the wet deposition. One to two days averaging is insufficient to smooth the fluctuations, which are well seen in Fig. 4 and quantified in Table 3.

The mean level of Pb concentrations is also problematic taking into account high uncertainties of the total European emission. As it was mentioned above, there was a strong and spatially inhomogeneous reduction of Pb emission in Western and Central Europe. So, it can be expected that the models overestimate surface concentrations, but its magnitude depends on several unknown factors and can vary in time. Both models reported such over-prediction, but values from HILATAR were closer to measured ones than the results of ADOM. This question can only be clarified by up-to-date emission inventories.

For Cd and Zn the emission trends since 1990 are not so strong, but the initial data for the basic year are less precise. Following Pacyna (1994), the uncertainty of Pb emission data is 25%, for Cd it is 50% and for Zn it is 100%. So, as well as for lead it is possible to expect the deviation from mean measured values within a factor of 2. In the light of agreement of both the models with measurements, looks surprisingly good for Cd, although still not convincing for Zn, where the under-estimation exceeds a factor of 2.

#### 5.4. Investigation of the high Cd deposition episodes at the site Hel

As it is seen from Fig. 4, the station Hel located on the southern coast of Baltic Sea has reported several high Cd wet deposition events, which were not reproduced by the models and were not always correlated with the other metals. There might be two reasons for such behavior – contamination of the samples or a powerful unknown local/regional source. Following (Schneider et al., 2000) we accepted that no evident contamination occurred and tried to locate the source with the aid of numerical experiments.

The study was performed under the following assumptions. First, the transport and deposition of the particle-carried pollutants like Cd is linear with regard to the emission intensity. Second, it is possible that the model might not reproduce some episodes at all. Indeed, small deviation of the predicted wind or time of precipitation may be enough for the polluted parcel not to correlate with the precipitation at the site and thus, no manipulations with emission result in reproducing the observed deposition peak.

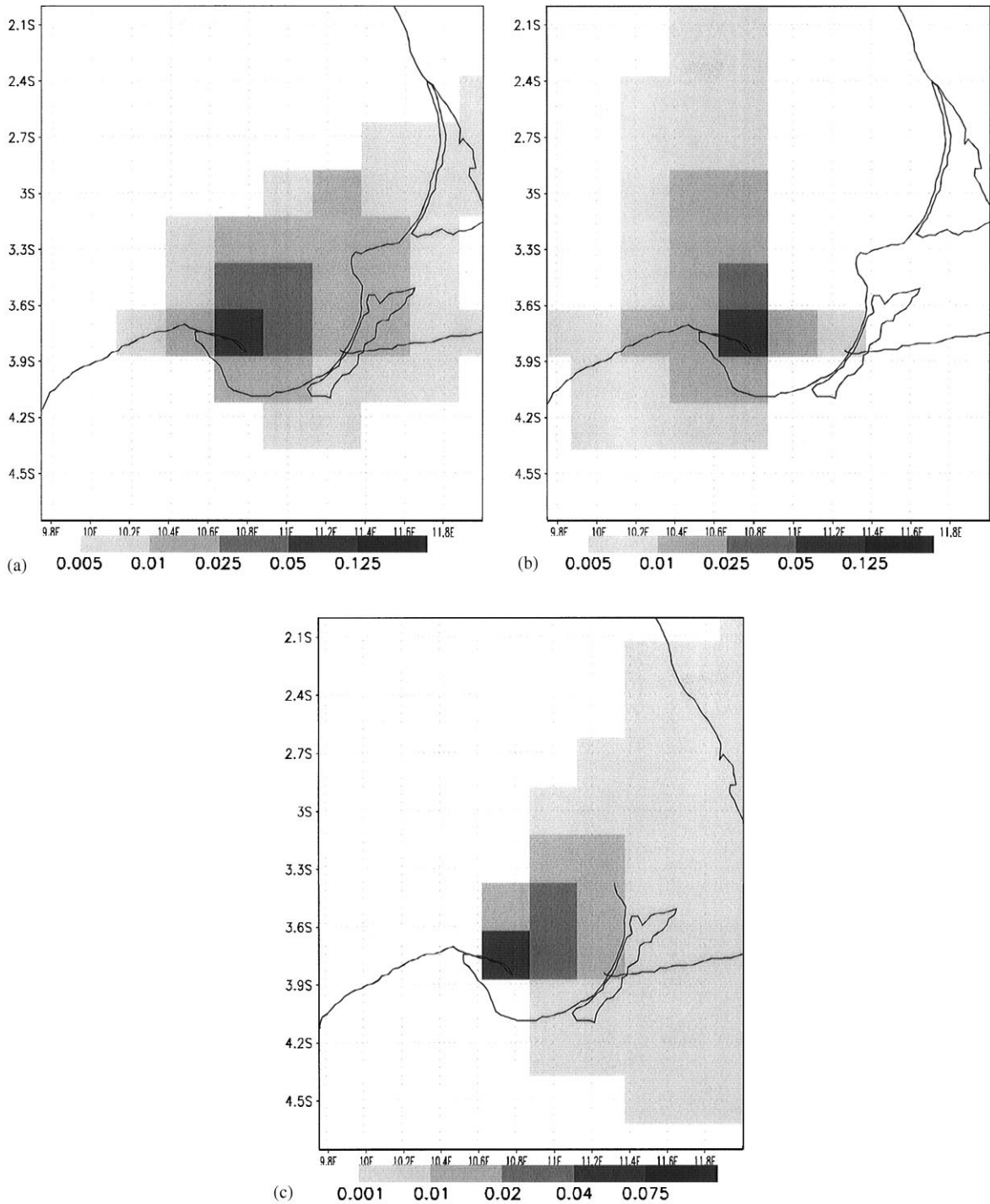


Fig. 5. Mean probability density matrices for July 1997 and March 1998.

The outcome from the first assumption is that new source is hardly located in the same grid cell already known as powerful source. The model deviation from the measurements for some episodes was

up to two orders of magnitude, which implies proportional under-estimation of the emission rate in the grid cells responsible for the particular episode. Consequently, if some sources are already

reported there, the final estimate would be unreasonably large.

Two periods – 1–23 July 1997 and 1–23 March 1998 – were chosen for the analysis. During that time 21 samples were collected reporting five episodes, particularly high, and 16 with moderate and low wet deposition (Fig. 4).

The next question was the selection of a mathematical approach for the source detection. Qualitative consideration of the wind flow patterns and backward trajectories were used by Schneider et al. (2000) and has not provided unequivocal answer. In general, it is believed that deterministic inverse task (which ends up with source coordinates plus some uncertainty/sensitivity analysis) is not useful in current case. Indeed, deposition measurements had comparably long time averaging, provided the samples are affected by many sources. The second problem would be caused by chaotic features of convective precipitation fields. Finally, wet deposition collects pollutants from different altitudes, often originated from different sources. These and other inevitable uncertainties reduce precision of the deterministic approach and can completely destroy the results.

In the current study the task was formulated in terms of probability  $p(i, j)$  of the unknown source to be located in the grid cell  $(i, j)$ . Corresponding matrix  $P = p(i, j)$  was built in three steps.

First, the “deposition influence matrix”  $M_E = m_E(i, j)$  for each episode  $E$  is computed. An element  $m_E(i, j)$  equals to the deposition at the monitoring site produced by an emission source located in the cell  $(i, j)$  with intensity of  $1 \text{ t Cd yr}^{-1}$ . One element  $m_E(i, j)$  is computed by the model run with zeroed emission field and artificial source in the cell  $(i, j)$ . Simulations go through all considered episodes  $E_1 \dots E_N$  with registration of the deposition at the monitoring site. To end up with reasonable computation time, the size of the influence matrices were taken as  $25 \times 25$  cells with the monitoring site situated in the center.

When built, the matrix  $M_E$  shows the influence pattern from the analyzed area to the monitoring site for the specific episode  $E$ . The set of 21 matrices covers the selected time periods. The next step is to normalize each matrix so that the spatial integral over the domain ( $25 \times 25$  cells) is equalled to 1, which gives the probability density matrix  $p_E$  for each episode  $E$ .

The final step involves grouping of the episodic probability matrices into two families in accordance with the measured deposition amount – “clean” and “polluted” ones. The arithmetic averaging inside each group produces the probability density functions (Fig. 5), which describe the locations of the emission sources responsible for “clean” and “polluted” episodes.

Analysis of Fig. 5 shows that there is evident difference in locations of the cells affecting the site during clean and polluted episodes. For the high-deposition events the contaminant was primarily coming from the east–north-

Table 4  
Correlation of the episodic probability densities with the mean ones

Start date, hour; duration	Mean polluted matrix	Mean clean matrix
Polluted episodes		
03071997, 13; 43 h	0.91	0.41
17071997, 12; 93 h	0.83	0.15
21071997, 12; 45 h	0.77	0.26
07031998, 12; 21 h	0.72	0.46
19031998, 12; 45 h	0.29	0.65
Clean episodes		
Range for 16 episodes	0.08–0.69	0.22–0.90
Range for 13 episodes	0.08–0.32	0.43–0.90

eastern sector, while the impact from the sources in other sectors was virtually negligible. On the contrary, during clean episodes the sources were located everywhere except for the northeastern sector. Table 4 confirms this conclusion by presenting the correlation coefficients between the probability matrices for the individual episodes and the mean ones. Both groups show that probability to get the deposition “from itself” is the highest, but for polluted episodes it is almost twice as for clean ones. So, it is possible that the source is located at a distance of few tens of kilometers to the east–northeast from the site and belongs to the same grid cell. The model horizontal resolution ( $\sim 28 \text{ km}$ ) is insufficient for more detailed investigation of this phenomena, so this cell was excluded from the calculations of Table 4.

As one can see, the matrix of the high-deposition episode around 20 March 1998 better correlates with the “clean” mean matrix than with the “polluted” one. There are also three outlining “clean” episodes, better correlated with the “polluted” mean rather than with the “clean” one. Anyway, 75–80% of the episodes in both groups show almost perfect correlation inside own family. So good correspondence decreases the chance for coincidence and supports the hypothesis of unknown source (rather than contamination of samples).

Some explanation for outlining of the episode around 20 March can be found from the comparison of its budget with that of another event, e.g. in the beginning of the month (Table 5). It is seen that the sources of deposition for these two periods are very different. The most drastic change appeared in the fraction of the long-range transport from Europe, which was 5 times more for the outlining period than for “normal” high deposition episode. The long-range transported pollution could itself create high load, which partially explains the diversity of this episode from the others. The reasons for missing of this particular episode by the models can be of pure meteorological origin.

Table 5  
Fractions of the modelled Cd wet deposition for episodes in March 1998

	7.03.1998	19.03.1998
Input from European sources (ADOM model)	5% ( $\sim 0.001 \mu\text{g m}^{-2}$ )	25% ( $\sim 0.015 \mu\text{g m}^{-2}$ )
Input from remote regional sources (HILATAR)	50% ( $\sim 0.01 \mu\text{g m}^{-2}$ )	50% ( $\sim 0.03 \mu\text{g m}^{-2}$ )
Neighborhood (< 75 km distance – HILATAR)	45% ( $\sim 0.01 \mu\text{g m}^{-2}$ )	25% ( $\sim 0.015 \mu\text{g m}^{-2}$ )

Concluding the case study, it is possible to state that practically all episodes of high Cd deposition at the coastal observation site of Hel are characterized by very similar potential locations of the influencing sources. The unknown emitter is to be located somewhere in the area outlined by mean probability density for high deposition episodes in Fig. 5. The probability to have the unknown Cd emitter at a specific place is dropping with distance from the monitoring site and has pronounced non-uniformity – the source can be located only to the east-northeast direction from the site.

The suspected area is largely covered with sea, which has two aspects. In agreement with the above assumptions, the reported emission in that area is very low or zero, so any powerful source can result in very high-deposition peaks. From the other side, we either have to assume existence of an island with some cadmium-emitting activity, or look for the source located very near the site, or quite far to the east. These options should be checked by further emission inventories.

## 6. Conclusions

1. The models demonstrated qualitatively similar patterns of the heavy metal pollution of the Baltic Sea region. Some quantitative deviations originate from the different resolution and parameterization of the models. The regional-scale model better resolved local patterns and coast-to-sea gradients, while the European-wide model provided the long-range transported fraction of contaminants. Both parts appeared to be significant, which justified the application of nested modelling system to the pollution simulation over the Baltic Sea.

2. Total deposition of heavy metals to the Baltic Sea was calculated from results of both models and compared with measurements and other modelling data. All models give comparable estimates both for Pb and Cd, while the measurements manifest higher values. The model assessment of Pb load is  $600\text{--}680 \text{ t yr}^{-1}$  if 1990 emission values are taken, which stands for  $300\text{--}350 \text{ t yr}^{-1}$  for 1995/96 emission. Cd total deposition was estimated to  $9\text{--}9.5 \text{ t yr}^{-1}$ . Zn load was  $\sim 400 \text{ t yr}^{-1}$ .

3. The comparison with high-resolution measurements carried out at 4 stations in the southern part of the Baltic Sea highlighted the episodic character of the regional pollution and proved the ability of the models to reproduce highly polluted events. The quantitative comparison was weakened due to uncertain emission data.

4. An investigation of high Cd deposition episodes at the site of Hel enabled to delimit the area where the unknown local/regional source of Cd could be located and to build the corresponding probability density function.

## Acknowledgements

Financial support of EU BASYS project through the MAST programme (contract: MAS3-CT96-0058), of the Nordic Council of ministers and of Academy of Finland are kindly acknowledged. We also would like to thank FMI HIRLAM group for the meteorological data.

## References

- Berdowski, J., Baas, J., Bloos, J.J., Visschedijk, A.J.H., Zandveld, P.Y.J., Bousardt, F.L.M., 1997. The European atmospheric emission inventory of heavy metals and persistent organic pollutants. UBA/TNO, June 1997, CD-ROM.
- Galperin, M., Sofiev, M., Erdman, L., Chechukina, T., 1994. Model evaluation of airborne trace metal transport and deposition. Short model description and preliminary results. EMEP/MSC-E Report 3/94, Moscow, 50pp.
- HIRLAM, 1990. In: Kallberg, P. (Ed.), HIRLAM Forecast Model Level 1. On-Line Documentation Manual. SMHI S-60176, Norrköping, Sweden.
- HIRLAM, 1999. The operational HIRLAM system. On-line documentation <http://www.fmi.fi/TUT/MET/hirlam/EWGLAM99/node2.html>
- Hongisto, M., 1998. HILATAR, a regional scale grid model for the transport of sulphur and nitrogen compounds. Finnish Meteorological Institute, Contributions 21, 152 pp.
- Hongisto, M., Sofiev, M., Jylhä, K., Joffre, S., 2000. High resolution numerical simulation of nutrient and trace element deposition to the Baltic, in press.

- Järvenoja, S., 1999. Towards new operational HIRLAM system at FMI – results from the pre-operational parallel tests. HIRLAM Newsletter 34, 33–42.
- Lenhart, L., Friedrich, R., 1995. European emission data with high temporal and spatial resolution. Air Pollution III, Vol. 2. Computational Mechanisms publication, Southampton, UK, pp. 285–292.
- Pacyna, J.M., 1994. Emissions of heavy metals in Europe. In: Modelling and Assessments of Heavy metals and Persistent Organic Pollutants. Background Document for the EMEP Workshop on European Monitoring. Beekbergen, the Netherlands, 3–6 May 1994, EB.AIR/GE.1/R.92.
- Ryaboshapko, A., Ilyin, I., Gusev, A., Afinogenova, O., Berg, T., Hjellbrekke, A.-G., 1999. Monitoring and modelling of lead, cadmium and mercury transboundary transport in the atmosphere of Europe. EMEP MSC-E and CCC Joint Report 1/99, 124pp.
- Schneider, B., Ceburnis, D., Marks, R., Munthe, J., Petersen, G., Sofiev, M., 2000. Atmospheric Pb and Cd input into the Baltic Sea: a new estimate based on measurements. Marine Chemistry 71 (3–4), 297–307.
- Venkatram, A., Karamchandani, P.K., Misra, P.K., 1988. Testing a comprehensive acid deposition model. Atmospheric Environment 22, 737–747.



# Paper VIII





PERGAMON

Atmospheric Environment 35 (2001) 3063–3074

ATMOSPHERIC  
ENVIRONMENT

www.elsevier.com/locate/atmosenv

# A comprehensive Eulerian modelling framework for airborne mercury species: model development and applications in Europe

G. Petersen<sup>a,\*</sup>, R. Bloxam<sup>b</sup>, S. Wong<sup>b</sup>, J. Munthe<sup>c</sup>, O. Krüger<sup>d</sup>,  
S.R. Schmolke<sup>a</sup>, A. Vinod Kumar<sup>e</sup>

<sup>a</sup>GKSS Research Centre, Institute of Hydrophysics, Max-Planck-Strasse, D-21502 Geesthacht, Germany

<sup>b</sup>Ontario Ministry of Environment, Environmental Monitoring and Reporting Branch, 125 Resources Road, Etobicoke ON M9P 3V6, Canada

<sup>c</sup>Swedish Environmental Research Institute (IVL), PO Box 47086, S-402 58 Göteborg, Sweden

<sup>d</sup>University of Hamburg, Institute of Meteorology, Bundesstrasse 55, D-20146 Hamburg, Germany

<sup>e</sup>Environmental Assessment Division, Bhabha Atomic Research Centre, Mumbai 400085, India

Received 20 February 2000; received in revised form 10 July 2000; accepted 16 July 2000

## Abstract

A comprehensive mercury model system using the Eulerian reference frame of the Acid Deposition and Oxidant Model (ADOM) has been developed under the Canada–Germany Science & Technology Co-operation Agreement and applied within the European Union Marine Science and Technology–Baltic Sea SYstem Study (MAST-III-BASYS) and the Environment & Climate project Mercury Species over Europe (MOE), to study the regional transport and deposition fluxes of atmospheric mercury species. The model is able to simulate long-range transport of mercury over the entire depth of the troposphere with a basic time step of 1 h and incorporates current knowledge of physico-chemical forms and transformation reactions of atmospheric mercury species. Model predicted concentration and deposition pattern of mercury species over Europe are presented and concentrations of total gaseous mercury in ambient air and total mercury in precipitation calculated by the model are compared with observed values from a BASYS monitoring network study in February/March 1998. Concentrations in air agree within a factor of about 2 with observed values, thus indicating that the model is capable of reproducing observations satisfactorily even on an hourly basis. Observed monthly average concentrations in precipitation at four monitoring stations at the Baltic Sea coast are reproduced by the model within a factor of 1.3 suggesting that the chemical scheme in the model is based on an adequate parameterisation of aqueous phase chemistry. © 2001 Elsevier Science Ltd. All rights reserved.

**Keywords:** Mercury species; Numerical modelling; Eulerian models; Atmospheric mercury chemistry; Mercury deposition

## 1. Introduction

Unlike other heavy metals that are associated with atmospheric aerosols, mercury exists in ambient air

predominantly in gaseous elemental form, which is estimated to have a global atmospheric residence time of about one year making it subject to long-range atmospheric transport over spatial scales from about 100 km to continental and global. Hence, mercury is a pollutant of concern in remote areas far away from anthropogenic sources, such as the polar regions, European regional seas, and inland lakes in the Northern US, Canada and Scandinavia.

\*Corresponding author.

E-mail address: [petersen@gkss.de](mailto:petersen@gkss.de) (G. Petersen).

The 1990 US Clean Air Act Amendments, the major European marine environment protection conventions (OSPAR, HELCOM and MEDPOL), the Arctic Monitoring and Assessment Program (AMAP), the US/Canada Great Lakes Water Quality Agreement (GLWQA) and the recently signed UN-ECE protocol on reducing the atmospheric transboundary transport of mercury in Europe have intensified the scientific interest to relate the spatial and temporal information on the release of mercury into the atmosphere with the pattern of atmospheric deposition fluxes to various ecosystems by means of numerical modelling on continental scales. In this context, efforts have been made to simulate the atmospheric transport and fate of mercury and to derive estimates of ambient concentrations and dry and wet deposition fluxes of mercury over North America (Shannon and Voldner, 1995; Bullock et al., 1997; Pai et al., 1997) and Europe (Petersen et al., 1995; Ryaboshapko et al., 1998) through either relative simple Lagrangian formulations or Eulerian approaches employing extensive gas- and aqueous phase chemical mechanisms and tracking explicitly numerous species concentrations.

This paper describes the development, testing and evaluation of a comprehensive Eulerian mercury simulation model as a joint activity within the Canada–Germany Science & Technology Co-operation agreement and the first model applications within the EU Baltic Sea System Study.

## 2. Development of the ADOM mercury model

Recent progress in understanding the atmospheric mercury cycle (Schroeder and Munthe, 1998) has allowed for direct modelling of the complex nonlinear mercury chemistry by fully three-dimensional Eulerian models. As a first step in this direction, the cloud mixing, scavenging, chemistry and wet deposition modules of the Acid Deposition and Oxidants Model (ADOM), originally designed for regional-scale acid precipitation and photochemical oxidants studies (Venkatram et al., 1988; Misra et al., 1989) have been restructured to accommodate recent developments in atmospheric mercury chemistry. A stand-alone version of these modules referred to as the Tropospheric Chemistry Module (TCM) was designed to simulate the meteorology and chemistry of the entire depth of the troposphere to study cloud mixing, scavenging and chemical reactions associated with precipitation systems that generate wet deposition fluxes (Petersen et al., 1998). The TCM chemistry scheme was developed by systematic simplification of the detailed Chemistry of Atmospheric Mercury (CAM) process model, which is based on the current knowledge of physico-chemical forms and

transformation reactions of atmospheric mercury species (Pleijel and Munthe, 1995).

After comprehensive testing under different environmental conditions the TCM has been implemented into both a North American and a European version of the full ADOM model. Within the constraints of the available computer resources and input data, these models incorporate an up-to-date understanding of the detailed physical and chemical processes in the atmosphere. In both models, the vertical grid consists of 12 unequally spaced levels between the surface and the top of the model domain at 10 km. The North American and the European versions are run for a grid cell size of  $127 \times 127$  km (fine mesh Canadian Meteorological Center (CMC) grid) over a  $33 \times 33$  grid domain and of  $55 \times 55$  km (High Resolution Limited Area Model (HIRLAM) grid) over a 76 by 76 domain, respectively.

The major modules making up the mercury version of ADOM together with the model input data sets are schematically depicted in Fig. 1. The transport and diffusion module uses a sophisticated cell-centred flux formulation solver for the 3-dimensional advection-diffusion equation. Dry deposition is modelled in terms of a deposition velocity for gaseous and particle associated mercury species, which is calculated as the inverse of the sum of the aerodynamic, deposition layer and surface canopy resistance. The mass transfer, chemistry and adsorption component of the model is illustrated in Fig. 2. It incorporates 14 mercury species and 21 reactions including mass transfer (R1–R5), aqueous phase (R6–R17) and gas phase (R20–R21) chemical reactions and adsorption processes on particles (R18–R19). The reaction rates are derived from published data and from assumption of the rates of complex formation. The cloud physics module simulates the vertical distribution of mercury species in clouds. Two different modules are incorporated: one describes stratus (layer) clouds and the other simulates cumulus (convective) type clouds. One or the other or a combination (cumulus deck embedded in a stratus cloud) is used in the calculation depending on the characteristics of the precipitation observed.

The details of each module comprising the original ADOM version for acid rain studies are given in ERT (1984). The development and testing of the mercury wet scavenging module consisting of cloud physics and mercury gas and aqueous phase chemistry sub-modules is described in detail in Petersen et al. (1998).

## 3. Preparation of model inputs

### 3.1. Emissions

The database for anthropogenic mercury emissions in Europe employed in the model calculations has been

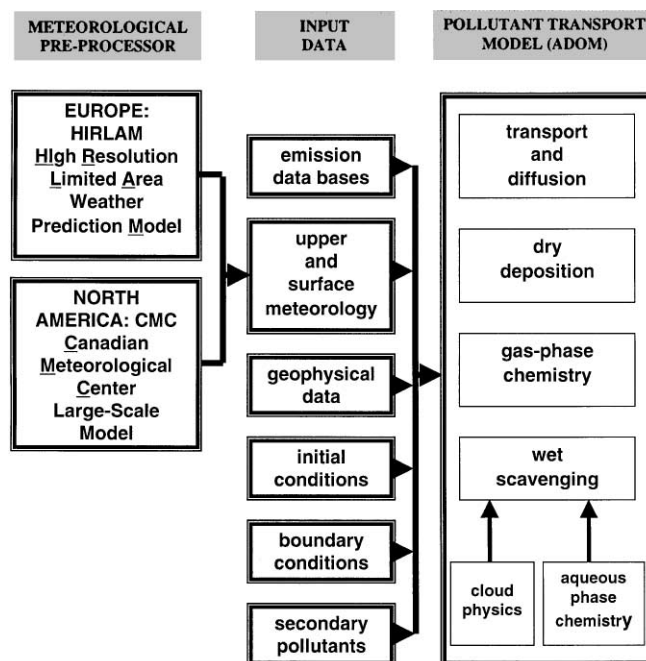


Fig. 1. Relationship between ADOM modules and input parameters.

compiled for 1990 (Umweltbundesamt, 1994). Potential changes in emissions between 1990 and 1998, the year for which the model simulation results are presented subsequently, are under investigation, but emission rates in the ADOM grid system for 1998 are not available at present. The emission rates and their spatial distribution in the model grid depicted in Fig. 3 are based on location and capacity of their dominating source categories such as combustion of fossil fuels in power plants, non-ferrous metal smelters, waste incinerators, chlor-alkaline factories and other industrial installations. The emission in each grid square are speciated with respect to gaseous elemental mercury ( $\text{Hg}^0$ ), gaseous divalent mercury ( $\text{HgCl}_2$ ), and particulate mercury ( $\text{Hg}(\text{part.})$ ), using estimated sector speciation percentages (Lindqvist et al., 1991). For modelling purposes, this speciation provides a possibility of separate treatment of mercury emitted in different physico-chemical forms and hence an assessment of the potential importance of these species for the mercury deposition pattern in Europe.

Prior to the political changes of the 1990s the total European anthropogenic mercury emissions into the air were estimated to be about  $700 \text{ t yr}^{-1}$  (Axenfeld et al., 1991). Due to the sharp decline of industrial activities in Eastern Europe mercury emissions have been reduced to about 450 in 1990. Compared to  $\text{SO}_2$  and  $\text{NO}_x$ , mercury emissions in Europe still show a

distinct geographical distribution characterised by a single very pronounced emission peak in Central Europe, which is clearly reflected in almost all of the model predicted mercury concentration and deposition patterns.

### 3.2. Meteorological fields

The meteorological input data needed by ADOM are three-dimensional fields of wind speed, wind direction, pressure, temperature, relative humidity, vertical velocity and vertical diffusivity, and two-dimensional fields of surface winds, surface pressure, surface air temperature, friction velocity, Monin-Obukhov length, mixing height, cloud base and top height, amount of cloud cover and the amount of precipitation at every 1 h model time step. These data sets are derived diagnostically using the weather prediction model HIRLAM for Europe and the Canadian Meteorological Center's model for North America.

### 3.3. Geophysical data

The geophysical data include files for 8 land use categories (i.e. deciduous forest, coniferous forest, grassland, cropland, urban, desert, water and swamp) and 12 soil categories. The database also includes information on terrain height and the growing season.

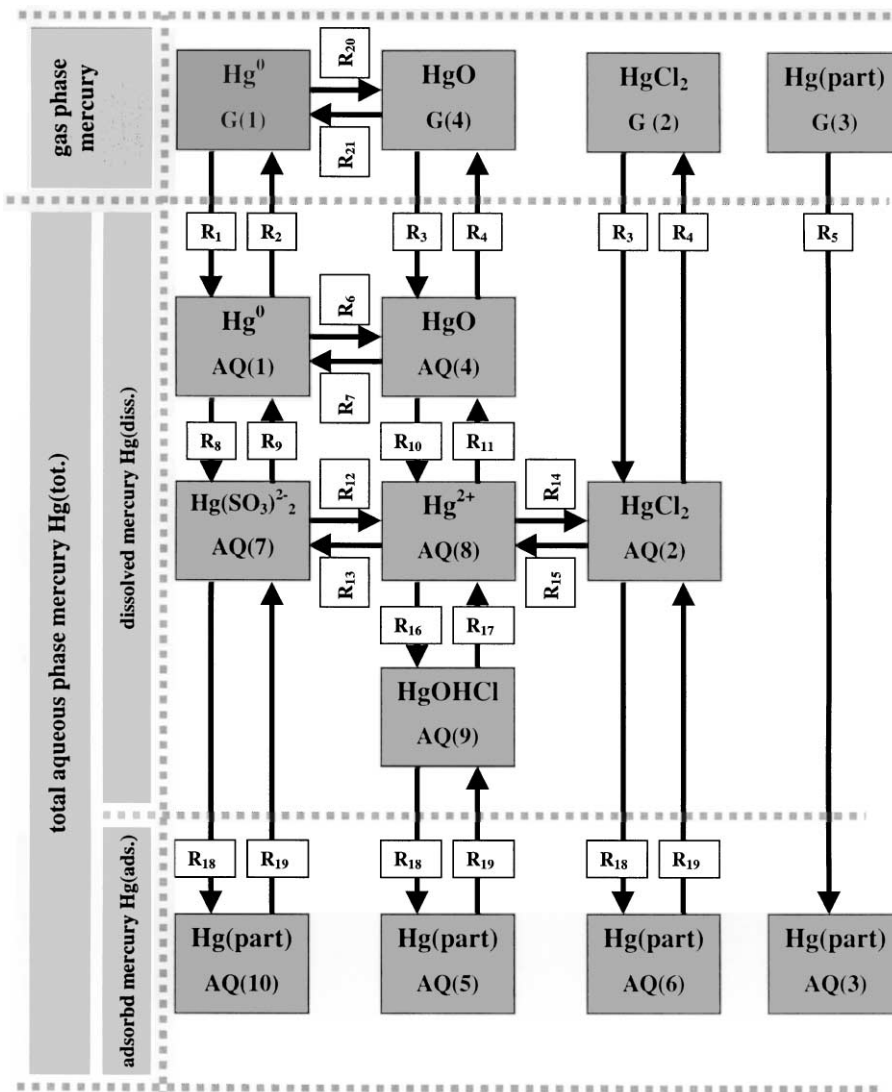


Fig. 2. The ADOM mass transfer, chemistry and adsorption scheme.

This geophysical data affect meteorology, dry deposition processes and air-surface exchange of gaseous mercury species.

### 3.4. Initial and boundary conditions

Initial and boundary conditions are needed for all advected species in the model. This includes the emitted compounds and mercuric oxide ( $\text{HgO}$ ) formed by gas phase oxidation of  $\text{Hg}^0$ . A typical European background mixing ratio of 0.18 ppt corresponding to a mass per unit volume concentration of about  $1.5 \text{ ng m}^{-3}$  is used for  $\text{Hg}^0$  in the atmospheric boundary layer (layers 1–4 in the vertical model grid) with a slight vertical mixing ratio decrease of approximately 80% of the boundary

layer value at the top of the modelling domain (Ebinghaus and Slemr, 2000).

Observations for mercury species other than  $\text{Hg}^0$  are still scarce in Europe and vertical profiles are not available at all. Therefore, initial and boundary concentrations of 2 and  $20 \text{ pg m}^{-3}$  estimated to be the average values from a limited number of observations in Europe are used for  $\text{HgCl}_2$  and  $\text{Hg}(\text{part.})$  in the boundary layer. Due to their relative short atmospheric residence time and due to anthropogenic emissions near the ground (layers 1–3) on the European continent concentrations of  $\text{HgCl}_2$  and  $\text{Hg}(\text{part.})$  are allowed to decrease with height to a value of about 10% of the boundary value at the model top.

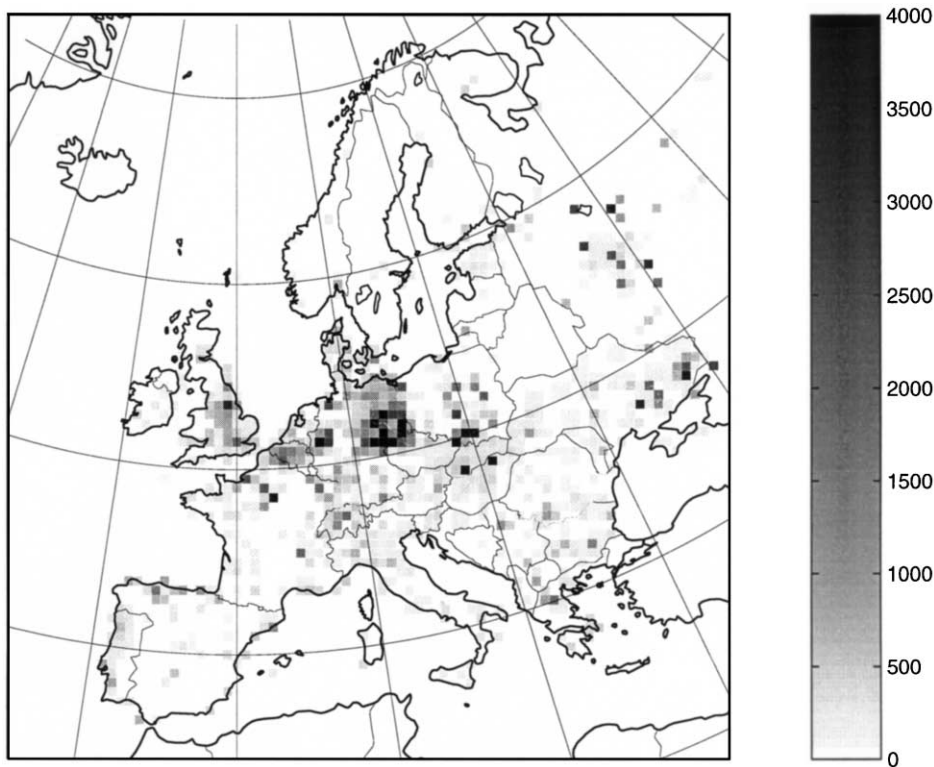


Fig. 3. The 1990 UN-ECE/OSPARCOM/HELCOM emission data base for mercury. Units:  $\text{kg yr}^{-1}$ .

In addition to  $\text{HgCl}_2$ , boundary concentrations for  $\text{HgO}$  are also given.  $\text{HgO}$  is believed to be the initial product from the gas phase reaction with  $\text{Hg}^0$  and  $\text{O}_3$  and is included in the chemistry scheme employed in the model. No information on ambient air concentrations of  $\text{HgO}$  or its physical/chemical properties such as Henry's law constant are available. For this reason,  $\text{HgO}$  is treated using the same parameterisation as for  $\text{HgCl}_2$ , believed to be the main gaseous divalent species in the atmosphere. In the absence of reliable measurement data, a very low initial value of  $0.7 \times 10^{-6} \text{ pg m}^{-3}$  constant with height is used for  $\text{HgO}$ . The more realistic initial value for  $\text{HgCl}_2$  ( $2 \text{ pg m}^{-3}$ ) is thus assumed to represent all divalent mercury compounds in the boundary air masses.

### 3.5. Chemical concentrations

The mercury chemistry in ADOM, described in Petersen et al., 1998, requires the specification of  $\text{O}_3$ ,  $\text{SO}_2$ , and soot carbon concentrations in ambient air as well as  $\text{Cl}^-$  concentrations in cloud water and cloud water pH. For the results with the European version of ADOM, the concentrations of  $\text{O}_3$ ,  $\text{SO}_2$ , and

soot carbon were fixed at 35 ppb, 1 ppb and  $1 \mu\text{g m}^{-3}$ . The cloudwater concentration of  $\text{Cl}^-$  and the cloudwater pH were specified as  $2 \times 10^{-6} \text{ mol l}^{-1}$  and 4.5, respectively.

## 4. Results of model applications

The model has been applied to various mercury deposition episodes in North America and Europe. As an example for model testing and application in Europe, a winter 1998 simulation period is described subsequently. This episode has been studied as a part of the European Union-Marine Science and Technology (EU MAST III) Baltic Sea System Study (BASYS). The BASYS data base, which includes mercury measurements in ambient air and in precipitation at four sites in the Baltic Sea area, provides a unique opportunity to test the European version of the ADOM mercury model.

### 4.1. Concentrations in ambient air

Figs. 4a–c show calculated  $\text{Hg}^0$ ,  $\text{HgCl}_2$  and  $\text{Hg}(\text{part.})$  air concentration patterns obtained from the BASYS

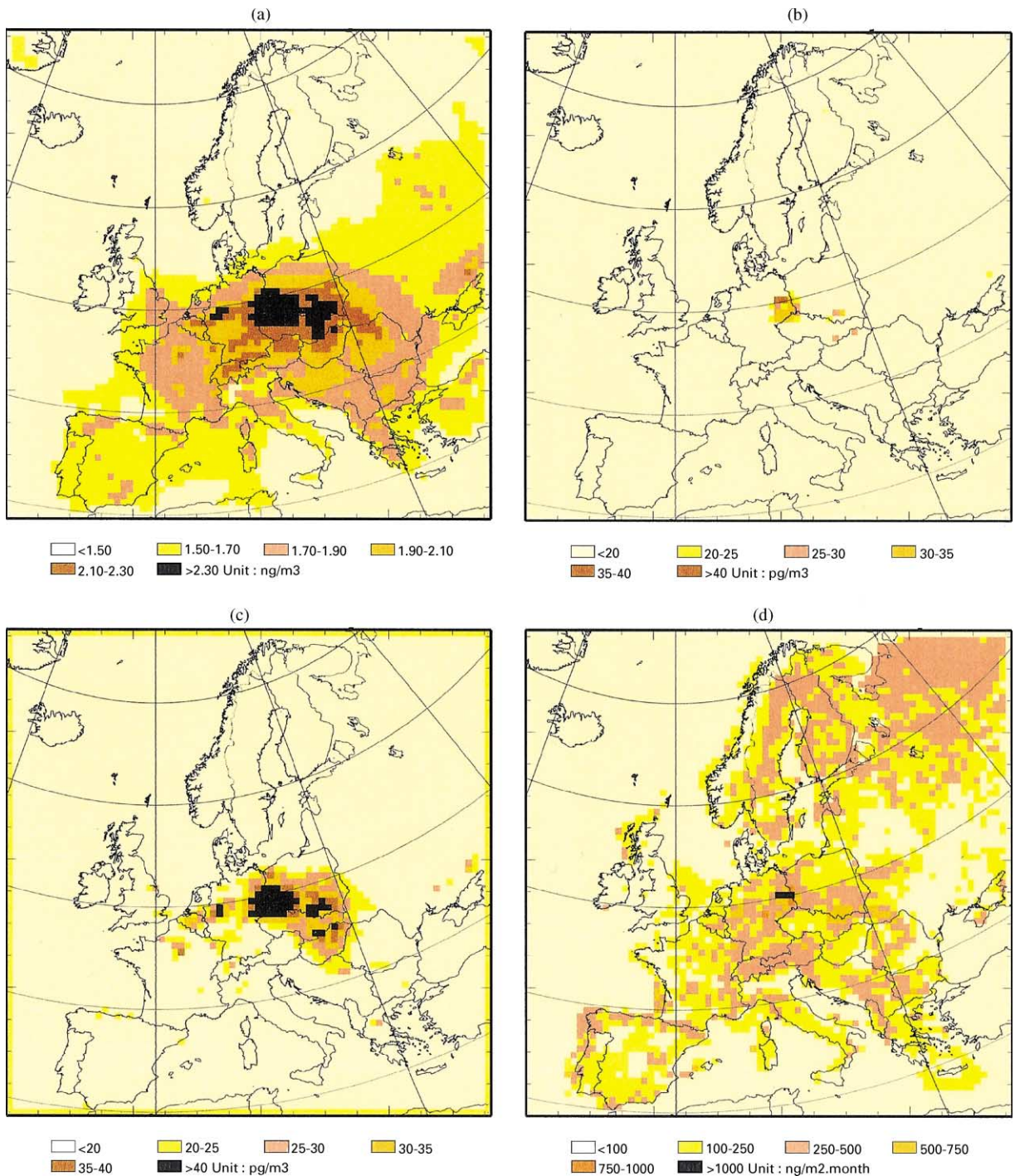


Fig. 4. Model predicted monthly average concentration in ambient air and dry deposition flux, February 1998; (a) elemental mercury ( $\text{Hg}^0$ ); (b) mercury chloride ( $\text{HgCl}_2$ ); (c) particulate mercury ( $\text{Hg}(\text{part.})$ ); (d) total dry deposition flux of  $\text{Hg}^0$ ,  $\text{HgCl}_2$  and  $\text{Hg}(\text{part.})$ .

study averaged over the entire month of February 1998. The concentrations refer to a vertical averaging over the first model layer (1–56 m). As expected the maximum concentrations of all three species are closely related to

the source areas. Concentration values of  $\text{Hg}^0$  generally range from about  $1.1 \text{ ng m}^{-3}$  in remote locations to  $3.0 \text{ ng m}^{-3}$  in the main emission area in Central Europe. The concentration pattern of  $\text{Hg}^0$  is substantially

elongated towards Eastern Europe, i.e. in the direction of the mean wind during that month. In the main emission areas, concentrations of  $\text{HgCl}_2$  and  $\text{Hg}(\text{part.})$  are about two orders of magnitude lower than  $\text{Hg}^0$  concentrations due to lower emission rates of these species. The elongation of the concentration patterns towards Eastern Europe is less pronounced for  $\text{HgCl}_2$  and  $\text{Hg}(\text{part.})$ , since these species have a significantly shorter atmospheric lifetime mainly due to their effective dry and wet depositions.

#### 4.2. Dry and wet depositions

The dry deposition fluxes shown in Fig. 4d denote the sum of  $\text{Hg}^0$ ,  $\text{HgCl}_2$  and  $\text{Hg}(\text{part.})$  deposition across the entire model domain. As can be seen, dry mercury deposition fluxes mainly occur over land surfaces with elevated levels in the major emission areas. The reason for that is twofold: First, due to its very low solubility the dry deposition rate of  $\text{Hg}^0$  to all surfaces was set to zero except forests where dry deposition velocities in the range of  $0.001\text{--}0.03\text{ cm s}^{-1}$  have been determined from experimental studies (Iverfeldt, 1991b; Lindberg et al., 1991). Second,  $\text{HgCl}_2$  and  $\text{Hg}(\text{part.})$  are readily dry deposited in the vicinity of sources resulting in very minor dry deposition over sea areas.

For precipitating clouds, the total monthly wet deposition flux depicted in Fig. 5a is derived by summing up the product of the hourly average cloud-water concentration of all aqueous species (AQ(1)–AQ(10) in Fig. 2) and the hourly precipitation amount over the entire month. As expected, wet deposition is determined by the precipitation distribution (Fig. 5b) and to a certain extent by the concentrations of mercury species in ambient air (see Figs. 4a–c) yielding a deposition pattern that comprises areas of high precipitation amounts as well as areas of elevated levels of  $\text{Hg}^0$ ,  $\text{HgCl}_2$  and  $\text{Hg}(\text{part.})$  concentrations in ambient air.

Concerning the physicochemical composition of mercury in cloudwater and precipitation, the scheme shown in Fig. 2 is based on the assumption, that the total wet deposition flux  $\text{Hg}(\text{tot.})$  can be divided into a dissolved fraction  $\text{Hg}(\text{diss.})$  and a fraction adsorbed on particles  $\text{Hg}(\text{ads.})$  depicted in Figs. 5c and d, respectively. The very distinct pattern in these two figures clearly reflect the design of two important and sensitive parts of the scheme:

1. In general,  $\text{Hg}(\text{diss.})$  and  $\text{Hg}(\text{ads.})$  are based on an equilibrium relation depending on gaseous and aqueous species concentration and rate expressions (R1–R21). However, in areas of relatively high  $\text{HgCl}_2$  (G(2)) concentrations in ambient air (i.e. close to major sources) the equilibrium is shifted towards a higher  $\text{Hg}(\text{diss.})$  fraction and hence a relative high  $\text{Hg}(\text{diss.})$  deposition flux as shown in Fig. 5c, since

$\text{HgCl}_2$  is highly water soluble and the mass transfer rate of this species into the aqueous phase is much higher than the adsorption rate of aqueous  $\text{HgCl}_2$  on particles.

2. In areas of low  $\text{HgCl}_2$  concentrations in ambient air (i.e. far from sources) the  $\text{Hg}(\text{diss.})$  and  $\text{Hg}(\text{ads.})$  equilibrium relation is more determined by  $\text{Hg}^0$  (AQ(1)) and its oxidation products and by aqueous phase reactions of  $\text{Hg}^{2+}$  (AQ(8)) leading to the formation of complexes, namely  $\text{HgCl}_2$  (AQ(2)),  $\text{HgOHCl}$  (AQ(9)) and  $\text{Hg}(\text{SO}_3)_2^{2-}$  (AQ(7)). Compared to  $\text{HgCl}_2$  the concentration level of  $\text{Hg}^0$  in ambient air is almost uniform in areas far from sources and hence the deposition pattern in these areas is mainly governed by precipitation, but elevated  $\text{Hg}^0$  concentrations in source areas are also reflected to a certain extent (see Figs. 5b and c).

A comparison of Figs. 4d and 5a shows, that the total mercury deposition over Central Europe is dominated by wet deposition during February 1998. The dry deposition of all mercury species, shown in Fig. 4d, indicates that over most of the main source areas in Central Europe the model estimated monthly dry deposition is in the range of  $100\text{--}500\text{ ng m}^{-2}$ , whereas the wet deposition flux (Fig. 5a) exceeds  $1000\text{ ng m}^{-2}$  despite relatively low precipitation amounts (less than  $50\text{ mm month}^{-1}$ ) in that area.

For further evaluation of the role of  $\text{HgCl}_2$  in the mass transfer and chemistry scheme and its influence on total mercury deposition, model predicted daily averages of  $\text{HgCl}_2$  concentrations in ambient air and daily dry and wet deposition fluxes in a grid cell at the German coast of the Baltic Sea during a two months monitoring network study are illustrated in Fig. 6. This grid cell was selected because of its surface characteristics (sea area, i.e. no dry deposition of  $\text{Hg}^0$ ), its geographical location relatively close to major sources implying high  $\text{HgCl}_2$  concentrations, and because observations from the Kap Arkona monitoring site located in this grid cell are available for comparison with model results (see Section 3.3). The coinciding peaks in ambient air concentrations and dry deposition fluxes (Figs. 6a, and b, respectively) indicate that high dry deposition events are dominated by  $\text{HgCl}_2$  due to its high dry deposition velocity. Wet deposition fluxes consist of a dissolved ( $\text{Hg}(\text{diss.})$ ) and an adsorbed ( $\text{Hg}(\text{part.})$ ) fraction (see Figs. 2). These fractions are determined by both the air concentrations of all gaseous species and their transfer into the aqueous phase with subsequent chemical transformations and adsorption processes. As can be seen from Fig. 6c  $\text{Hg}(\text{part.})$  is the major fraction for most of the days when wet deposition occurred, but  $\text{Hg}(\text{diss.})$  becomes more important at high wet deposition events (e.g. 16 February and 27 March). On these two particular days  $\text{HgCl}_2$  concentrations in air are relatively low suggesting

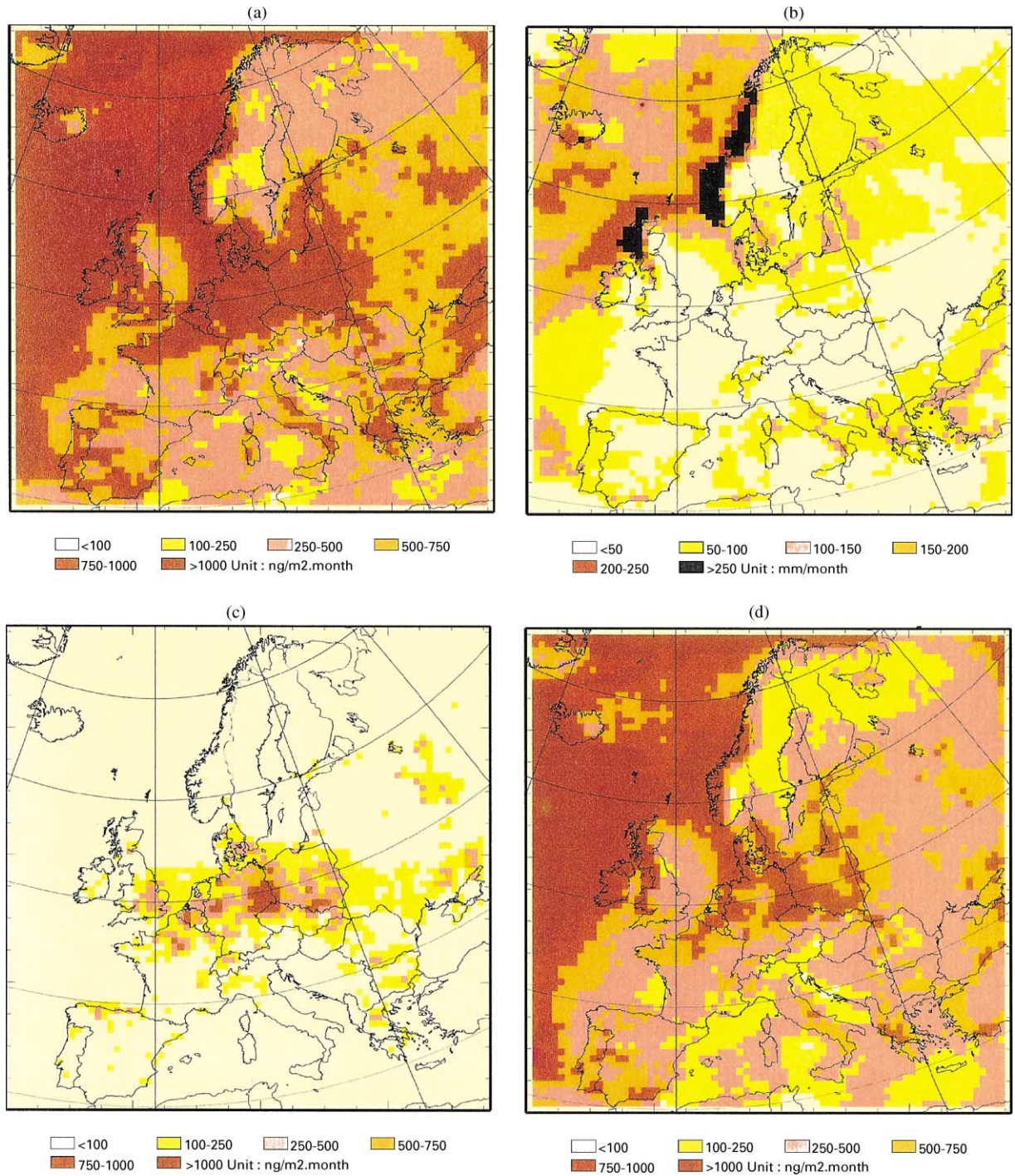


Fig. 5. Model predicted monthly wet deposition fluxes and precipitation, February 1998; (a) total wet deposition (Hg(tot.)); (b) precipitation; (c) wet deposition of dissolved species (Hg(diss.)); (d) wet deposition flux of adsorbed species (Hg(ads.)).

that  $HgCl_2$  has been readily scavenged mainly into the dissolved phase only because scavenging of this species is a much faster process than its adsorption on particles in the aqueous phase. Overall, there is evidence from

Fig. 6, that ambient  $HgCl_2$  concentrations typically occurring in the vicinity of high-emission areas can provide substantial contributions to both dry and wet mercury deposition. Hence, mercury emission rates

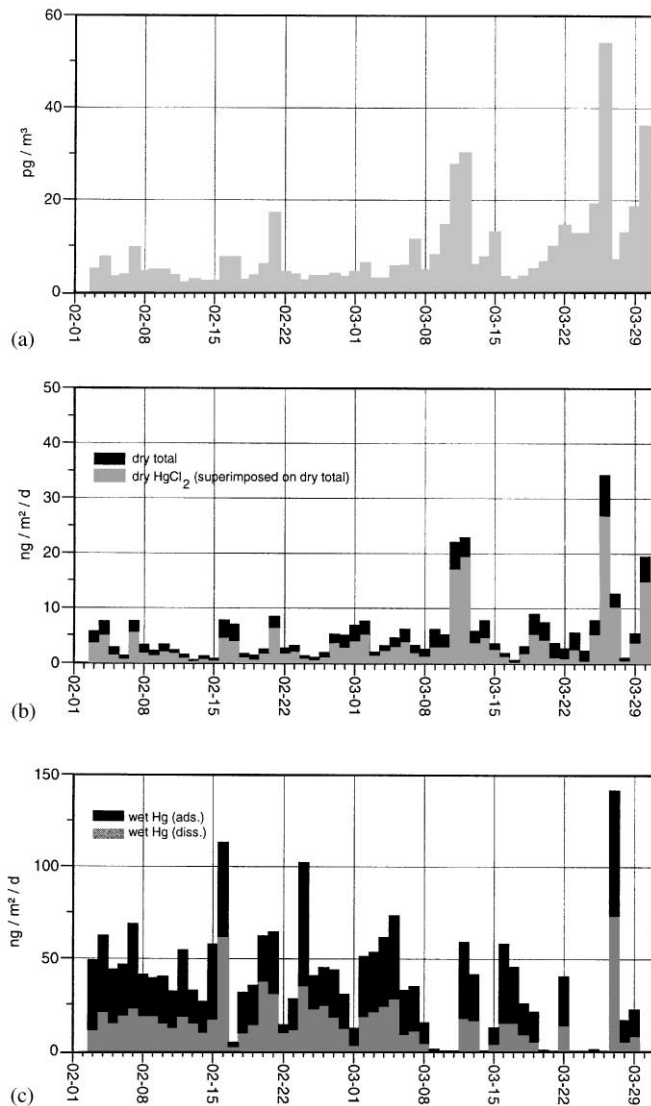


Fig. 6. Model predicted concentrations and fluxes, Kap Arkona, February/March 1998; (a) daily average  $\text{HgCl}_2$  concentration in ambient air; (b) daily dry deposition; (c) daily wet deposition flux.

speciated with respect to  $\text{HgCl}_2$  in particular are of crucial importance for model predicted deposition fluxes.

#### 4.3. Comparison with observations

Compared to other heavy metals mercury measurements are still scarce in space and time and individual mercury species in air and precipitation are hard to identify with currently available analytical techniques. However, in February and March 1998 total gaseous mercury (TGM) concentrations in ambient air and total mercury concentration in precipitation ( $\text{Hg}(\text{tot.})$ ) have

been measured in the framework of the BASYS study with a temporal resolution of the ADOM model time step of 1 h and 2 months averages, respectively. These data are of high quality and, although restricted to a two month period, provide an opportunity for some initial tests of the model performance.

Fig. 7 shows the time series of 1 h average total gaseous mercury concentration calculated for the Kap Arkona grid cell and the observed concentrations at the Kap Arkona monitoring station for the winter 1998 simulation period. Observations and model predictions are in reasonable agreement. One should note, however, that there are two major discrepancies: First, the model

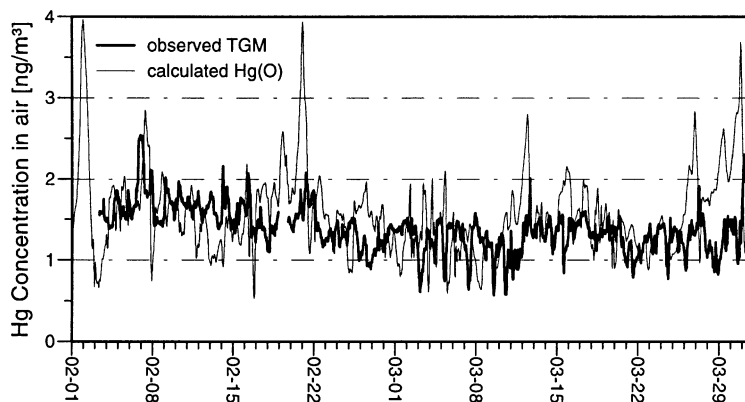


Fig. 7. Time series of observed and calculated hourly average concentrations of mercury in ambient air, Kap Arkona, February/March 1998.

predicted time series shows some peak events with calculated hourly concentrations exceeding  $2.5 \text{ ng m}^{-3}$ . Almost coinciding peaks have also been observed but on a lower level, indicating that the model is able to simulate elevated concentrations with a tendency of over-prediction most probably due to both overestimated emissions near the measurement site and underestimated vertical exchange of air masses in the grid cell in which the measurement site is located. Second, observed concentrations in March are generally lower than in February with quite a few concentrations less than  $1 \text{ ng m}^{-3}$ , mainly during the first decade, when air masses arriving at Kap Arkona were originating in Arctic regions. Since frequent episodic depletions in mercury vapor concentrations have been observed in the Arctic in springtime (Schroeder et al., 1998) the low level concentrations at Kap Arkona in the first decade of March can possibly be explained by this Arctic phenomenon. However, the limited data material does not allow to draw any firm conclusions at present and a larger data set comprising additional time series from other measurement sites north of Kap Arkona would be needed. The scatter plot of the Kap Arkona data (Fig. 8) indicates an agreement within a factor of two in more than 90% of the cases but the correlation coefficient would be low, since the model tends to overpredict peak concentrations as mentioned above.

In Fig. 9 average levels of observed and model predicted concentrations of mercury in precipitation at 4 monitoring stations in Baltic Sea coastal areas are compared. The observed data are based on 64 samples during the monitoring network study from 3 February to 30 March 1998, whereas the calculated numbers are obtained from hourly values during that time period. The overall agreement is good with a tendency in the model to overpredict concentrations relatively close to sources (Kap Arkona at the German coast) and under-

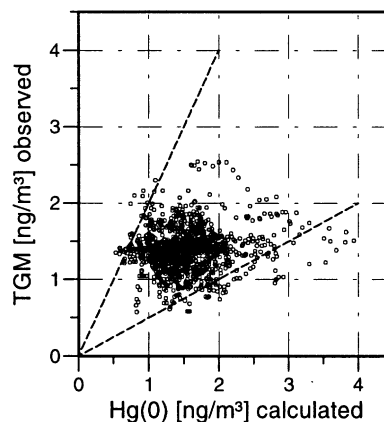


Fig. 8. Scatter plot of observed and calculated hourly average concentrations of mercury in ambient air, Kap Arkona, February/March 1998.

predict concentrations at more remote locations (Hoburg on the Swedish island of Gotland in the Central Baltic). Since mercury concentrations in precipitation are dominated by air concentrations of  $\text{HgCl}_2$  (see Fig. 6) and  $\text{Hg}(\text{part.})$  the discrepancies for Kap Arkona and Hoburg could be caused by uncertainties associated with emission rates of  $\text{HgCl}_2$  and  $\text{Hg}(\text{part.})$  and/or by a mispredicted south-to-north decrease of these two species. The discrepancies could also be due to misrepresentations in the chemistry scheme, e.g. if the reduction of oxidised mercury is underestimated close to sources the model will tend to overestimate the amount of Hg removed by precipitation. In the case of remote marine environment sites such as Hoburg, an underestimation of the oxidation of  $\text{Hg}^0$  would underestimate the amount of oxidised Hg removed by precipitation.

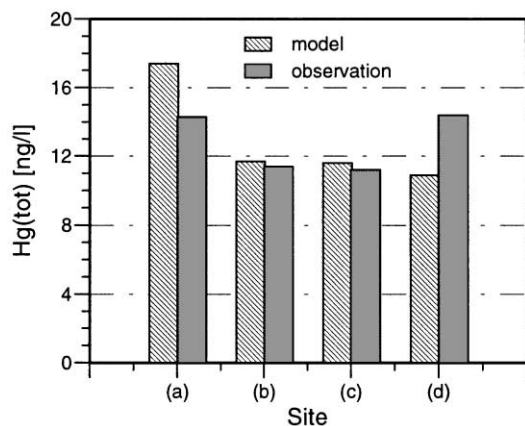


Fig. 9. Observed and calculated average total mercury concentration in precipitation (Hg(tot.)) at four Baltic Sea coastal sites, February/March 1998; (a) Kap Arkona (Germany); (b) Hel (Poland); (c) Preila (Lithuania); (d) yHoburg (Sweden).

## 5. Summary and conclusions

A comprehensive mercury model system using the Eulerian reference frame of the ADOM has been developed to calculate the atmospheric long-range transport, chemical transformations and deposition fluxes of mercury species in North America and Europe. The cloud mixing, scavenging, chemistry and wet deposition modules of ADOM restructured for recent developments in atmospheric mercury processes were used as a starting point in the model development. Model results in terms of monthly concentration and deposition patterns over Europe were presented. Hourly averages of total gaseous mercury concentrations in ambient air were compared against observations from a European monitoring network study in 1998. The evaluation of the model performance led to six main issues:

(1) Model predictions of hourly  $\text{Hg}^0$  concentrations in ambient air compared with observations at a location in the Baltic Sea coastal area within a factor of two in more than 90% of the cases, suggesting that  $\text{Hg}^0$  emissions and transport calculations are simulated satisfactorily by the European version of the model. However, the available data material is scarce, and more simultaneous measurements from representative locations with an hourly time resolution are necessary to evaluate the ultimate model performance with respect to  $\text{Hg}^0$  emission and transport.

(2) To improve model derived estimates of mercury deposition it is necessary to compile emission inventories based on measurements of mercury species in flue gases of the most important source categories. At present the quality of the emission data for  $\text{HgCl}_2$  and  $\text{Hg}(\text{part.})$

limits the confidence with which the effects of these species on the deposition pattern can be predicted.

(3) Model results suggest that up to 75% of mercury in cloud and rain droplets is associated with particles in polluted areas of Europe due to adsorption on soot particles determined by an empirically derived equilibrium rate expression for the adsorption process. The predicted percentages are in general agreement with observations from the nordic air and precipitation network for 1987 and 1988 (Iverfeldt, 1991a), but lower percentages (2–35%) of adsorbed Hg have been obtained in precipitation samples in North America (Seigneur et al., 1998). Clearly, the understanding of the interaction of Hg species with soot is limited at present and further experimental work is necessary to improve the model description.

(4) Observed mercury concentrations in precipitation are quite well reproduced by the model. However, there are indications of over- and underpredicted concentrations as a function of geographical separation from source areas, probably due to both insufficient emission speciation and inadequate parameterisation of redox reactions of  $\text{Hg}^0$  in the mercury chemistry scheme.

(5) Air/surface exchange fluxes of gaseous mercury species as a function of meteorological and geophysical parameters need to be measured in order to implement these processes into the model system.

(6) Time dependent vertical  $\text{Hg}^0$  concentration profiles at the model inflow boundaries calculated by hemispheric or global scale models should be introduced. There is evidence now from long-term measurements at a location close to the western boundary of the European modelling domain (Ebinghaus and Schmolke, 2000), that  $\text{Hg}^0$  concentrations show a pronounced seasonal variability which may have a significant effect on the temporal deposition pattern in the model domain at least in areas far from the major anthropogenic sources.

Overall, the development level of the model is such, that it can be considered as an essential step towards decisive assessments of the sources or source types most responsible for mercury contamination in Europe through the atmospheric pathway. Although the model incorporates significant progress in the understanding of mercury atmospheric processes our knowledge is far from complete. The model system will be developed further as additional information on emission speciation, atmospheric chemistry, air–soil exchange and vertical profiles of time dependent boundary conditions becomes available. Similarly, very little is known about other issues such as the role of methyl mercury compounds on observed deposition pattern. As research on these issues matures and more data exist, an explicit treatment of methyl mercury processes in ADOM is the next logical step.

## Acknowledgements

This work is a part of the MARine Science and Technology–BAltic Sea SYstem Study (MAST-III-BASYS), Subproject 5 ‘Atmospheric Load’ (Contract MAS3-CT96-0058) and of the Environment & Climate project Mercury Species over Europe (MOE) (Contract ENV4-CT97-0595). MOE is part of the EU European-Land-Ocean Interaction Studies (ELOISE) (Ref. No. 211). BASYS and MOE are funded by the European Commission DG XII. The authors wish to acknowledge the financial support for this work which was provided by the International Bureaus of the GKSS Forschungszentrum Geesthacht (GKSS) and the Deutsche Forschungsanstalt für Luft-und Raumfahrt (DLR) in the framework of the Germany/Canada Science and Technology Co-operation Agreement (Project No. CAN 99/002). The authors would like to express their appreciation of the peer reviewers’ suggestions for improving the manuscript.

## References

- Axenfeld, F., Münch, J., Pacyna, J.M., 1991. Europäische Test-Emissionsdatenbasis von Quecksilberkomponenten für Modellrechnungen. Umweltforschungsplan des Bundesministers für Umwelt, Naturschutz und Reaktorsicherheit—Luftreinhaltung—10402726. Umweltbundesamt (Federal Environmental Agency), P.O. Box 33 00 22, D-14191 Berlin, Germany.
- Bullock, R.O., Benjey, W.G., Keating, M.H., 1997. Modeling of regional scale atmospheric mercury transport and deposition using RELMAP. In: Baker, J.E. (Ed.), *Atmospheric Deposition of Contaminants to the Great Lakes and Coastal Waters*. SETAC Press, Pensacola, pp. 323–347.
- Ebinghaus, R., Schmolke, S.R., 2000. Spatial and temporal variability of atmospheric mercury concentrations in north-western and central Europe. Proceedings of the NIMD 99 Forum, Minamata, Japan, October 11–13, 1999, in press.
- Ebinghaus, R., Slemr, F., 2000. Aircraft measurements of atmospheric mercury over southern and eastern Germany. *Atmospheric Environment* 34, 895–903.
- ERT, 1984. ADOM/TADAP Model Development Program, Vols. 1–8. ERT No. P-B980-535, Environmental Research and Technology, Inc., Newbury Park, California 91320, USA, July 1984.
- Iverfeldt, A., 1991a. Occurrence and turnover of atmospheric mercury over the nordic countries. *Water, Air and Soil Pollution* 56, 151–165.
- Iverfeldt, A., 1991b. Mercury in forest canopy throughfall water and its relation to atmospheric deposition. *Water, Air and Soil Pollution* 56, 533–564.
- Lindberg, S.E., Turner, R.R., Meyers, T.P., Taylor, G.E., Schroeder, W.H., 1991. Atmospheric concentration and deposition of Hg to a deciduous forest at Walker Branch Watershed, Tennessee, USA. *Water, Air and Soil Pollution* 56, 577–597.
- Lindqvist, O., Johansson, K., Aastrup, M., Andersson, A., Bringmark, L., Hovsenius, G., Hakonson, L., Iverfeldt, A., Meili, M., Timm, B., 1991. Mercury in the Swedish environment—recent research on causes, consequences and corrective methods. *Water, Air, and Soil Pollution* 55, 23–32.
- Misra, P.K., Bloxam, R., Fung, C., Wong, S., 1989. Non-linear response of wet deposition to emission reductions: a case study. *Atmospheric Environment* 23, 671–687.
- Pai, P., Karamchandani, P., Seigneur, C., 1997. Simulation of the regional atmospheric transport and fate of mercury using a comprehensive Eulerian model. *Atmospheric Environment* 31, 2717–2732.
- Petersen, G., Iverfeldt, A., Munthe, J., 1995. Atmospheric mercury species over Central and Northern Europe. Model calculations and comparison with measurements from the Nordic air and precipitation network for 1987 and 1988. *Atmospheric Environment* 29, 47–67.
- Petersen, G., Munthe, J., Pleijel, K., Bloxam, R., Kumar, A.V., 1998. A comprehensive Eulerian modeling framework for airborne mercury species: development and testing of the tropospheric chemistry module (TCM). *Atmospheric Environment* 32, 829–843.
- Pleijel, K., Munthe, J., 1995. Modeling the atmospheric mercury cycle—chemistry in fog droplets. *Atmospheric Environment* 29 (12), 1441–1457.
- Ryaboshapko, A., Ilyin, I., Gusev, A., Afinogenova, O., 1998. Mercury in the atmosphere of Europe: concentrations, deposition patterns, transboundary fluxes. EMEP Meteorological Synthesizing Center-East, EMEP/MSC-E Report 7/98.
- Schroeder, W.H., Anlauf, K.G., Barrie, L.A., Lu, J.Y., Steffen, A., Schneeberger, D.R., Berg, T., 1998. Arctic springtime depletion of mercury. *Nature* 394, 331–332.
- Schroeder, W.H., Munthe, J., 1998. Atmospheric mercury—an overview. *Atmospheric Environment* 32, 809–822.
- Seigneur, C., Abeck, H., Chia, G., Reinhard, M., Bloom, N.S., Prestbo, E., Saxena, P., 1998. Mercury adsorption to elemental carbon (soot) particles and atmospheric particulate matter. *Atmospheric Environment* 32, 2649–2657.
- Shannon, J.D., Voldner, E.C., 1995. Modeling atmospheric concentrations of mercury and depositions to the Great Lakes. *Atmospheric Environment* 29, 1649–1661.
- Umweltbundesamt, 1994. The European atmospheric emission inventory of heavy metals and persistent organic pollutants for 1990. Umweltbundesamt (Federal Environmental Agency), P.O. Box 33 00 22, D-14191 Berlin, Germany.
- Venkatram, A., Karamchandani, P., Misra, P.K., 1988. Testing a comprehensive acid deposition model. *Atmospheric Environment* 22, 2717–2732.

# Paper IX



# EXAMINING SOURCE-RECEPTOR RELATIONSHIPS FOR MERCURY IN SCANDINAVIA

## *Modelled and Empirical Evidence*

JOHN MUNTHE<sup>1\*</sup>, KARIN KINDBOM<sup>1</sup>, OLAF KRUGER<sup>2</sup>, GERHARD  
PETERSEN<sup>2</sup>, JOZEF PACYNA<sup>3</sup> and ÅKE IVERFELDT<sup>1</sup>

<sup>1</sup> IVL Swedish Environmental Research Institute, P.O. Box 470 86, 402 58 Göteborg, Sweden; <sup>2</sup> GKSS-Research Centre, Institute of Hydrophysics, Model Systems Unit (GMS), Max-Planck-Strasse 1, D-21502 Geesthacht, Germany; <sup>3</sup> Norwegian Institute for Air Pollution Research (NILU), P.O. Box 100, N-2007 Kjeller, Norway

(\* author for correspondence, e-mail: john.munthe@ivl.se)

(Received 29 March 1999; accepted 14 September 2000)

**Abstract.** The atmosphere remains the major source of mercury in Swedish ecosystems. Since the late eighties, atmospheric emissions of mercury have drastically decreased in Europe. Wet deposition of mercury has decreased over the last decade but still exhibits a clear south-to-north gradient, greatly influenced by source areas in northern and central Europe. The decreases in emissions can be attributed to both direct measures to close known point sources and a declining economy and energy consumption in many East European countries. Further reductions of mercury emissions will require that other source categories such as indirect emissions from mercury-containing products and crematories are be considered.

**Keywords:** deposition, emissions, mercury, methylmercury, modelling, products

## 1. Introduction

Mercury (Hg) is a pollutant mainly introduced into the environment via the atmosphere. Anthropogenic Hg emissions to air have increased the levels in all compartments of the environment including air, water and biota during the twentieth century. The negative effects associated with Hg are mainly related to increased levels of methylmercury (MeHg) in fish. In thousands of remote freshwater lakes in Sweden and elsewhere in the Boreal forest belt, atmospheric transport and deposition of Hg has led to increased MeHg levels in fish, making them unsuitable for human consumption. Although no cases of adverse human health effects due to consumption of freshwater fish have been identified in Sweden, documented effects from human tragedies in Minamata, Japan, and Iraq (WHO, 1990) have led to serious concern specifically focused on prenatal exposure.



## 2. Emissions of Mercury

### 2.1. EMISSIONS OF MERCURY

Mercury is emitted from a wide variety of industrial sources. Major source categories include coal combustion, waste incineration, chlor-alkali industries and secondary metal smelters (Pacyna, 1989). Available emission inventories indicate total European emissions varying between 740 tons per year in 1988/89 (Axenfeld *et al.*, 1991), 440 tons in 1990 (Berdowski *et al.*, 1997) and 800, 802, 697 and 634 tons per year for 1988, 1989, 1990 and 1992, respectively (Pirrone *et al.*, 1996). Recently, an estimate for 1995 was published indicating further reductions to 342 tons (Pacyna and Pacyna, 2000). For the years before 1988, emission estimates are not available for Europe but Swedish estimates indicate that a maximum occurred around 1960 (Lindqvist *et al.*, 1991). In 1990, the political and economical changes in eastern Europe directly led to a decreased load of atmospheric Hg in Sweden. When Germany was unified in 1991, many redundant industrial operations and coal combustion plants were shut down. This led to drastic cuts in Hg emissions, which clearly could be observed in air concentrations (Iverfeldt *et al.*, 1995) and wet deposition in Southern Scandinavia (see further discussion in Section 5 and 6).

Swedish emissions of Hg to air have decreased drastically during the last decade from around 5.2 tons in 1985 to below 1 ton in 1995 (SCB, 1998). The major source categories at present are presented in Table I.

The present European emission levels still represent a significant anthropogenic contribution to the atmospheric deposition of Hg in Sweden. After closing of major sources, further measures will require that other source categories be considered. One such category is crematories, which is the largest individual source category in Sweden today. Although consisting of a large number of small sources, measures to control Hg emissions from crematories are today required by authorities in Sweden.

In addition to the major point source categories, diffuse emissions also contribute sizeable amounts of Hg to the atmosphere. A specific source category of interest is Hg in products. Hg is contained in a large number of household products. This Hg can be directly emitted to air during use, after breakage or if incinerated with household waste. Scrap metal re-cycling can also contribute to Hg emissions to air, if Hg-containing scrap is used in metal production. Diffuse emissions will also occur after uncontrolled disposal or disposal in landfills. The life cycle of products containing Hg is in some cases several decades. Even though restrictions on Hg use are in effect, a large store of Hg in society still exists. This accumulated Hg will eventually be discarded, contributing to Hg emissions if not disposed of safely.

In a study of the possible contribution of Hg-containing products (batteries, light sources, electrical equipment, measuring and control instruments) to the overall European emissions, it was concluded that around 18% of the total anthropogenic Hg emissions in Europe could be attributed to this source category (Munthe and

TABLE I  
Major point source categories of Hg in  
Sweden, 1995 (SCB, 1998)

Source category	Emissions of Hg kg yr <sup>-1</sup>
Mining	10
Chlor-alkali plants	120
Iron and steel industry	110
Metal works	74
Waste incineration	90
Crematories	280
District heating	97
Energy production	
Industry	72
Private	39
Other	4
Total	896

Kindbom, 1997). The largest proportion, ca 10% was estimated to originate from light sources and electrical equipment. This estimate was based on an evaluation of the life cycle of Hg-containing products with emissions arising during use and after the product was discarded. Both contributions to emissions from point sources (e.g. incineration of waste containing Hg from products and scrap metal smelters) and diffuse emissions during use and from disposal in landfills were considered.

The contribution of Hg in products to the deposition of Hg in Scandinavia were also estimated, based on model calculations of the GKSS Hg-model (see Section 6.1) (Petersen, *et al.*, 1995; Munthe *et al.*, 1997). Emissions of Hg contained in products were assumed as percentages of emissions from other source categories (waste incineration, scrap smelters etc.). Estimates were made for both southern and northern Scandinavia, representing transport distances of roughly 300 to 1 500 km from the major source regions in central Europe. The calculated relative deposition fluxes attributable to Hg in products are presented in Table II. The results indicate that emissions of Hg caused by products contribute 10–14% to the wet deposition input in Scandinavia. The influence is lower in northern Scandinavia but is still significant. These results, although associated with considerable uncertainties, indicate that product-related Hg emissions can significantly contribute to the transboundary transport of this pollutant over the whole European region and that measures to limit the use of Hg in consumer products will lead to reduced atmospheric emissions and deposition.

TABLE II  
Relative contribution of Hg emitted from products to wet deposition in Scandinavia

Product group	Percentage of total anthropogenic emissions in Europe	Percentage of wet deposition in southern Scandinavia	Percentage of wet deposition in northern Scandinavia
Batteries	4	3	2
Measuring and control instruments	3	2	2
Light sources and electrical equipment	11	9	6
Total	18	14	10

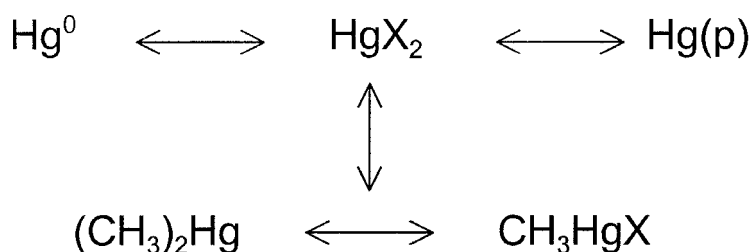


Figure 1. Schematic description of the chemical behaviour of atmospheric Hg. X= Cl, OH etc., Hg(p) = particulate mercury.

### 3. Chemical Transformations and Removal Mechanisms

Schroeder and Munthe (1998) have recently reviewed the atmospheric behaviour of Hg including chemical transformations, air-surface exchange processes and deposition. Only a brief summary is given here.

#### 3.1. CHEMICAL TRANSFORMATIONS

The chemistry of atmospheric Hg involves a number of processes where the chemical and physical properties are changed. A schematical description of major transformations is shown in Figure 1.

The processes described in Figure 1 include oxidation of  $\text{Hg}^0$  and formation of particulate phase species as well as formation/degradation of the methylated Hg compounds. Ozone is capable of oxidising  $\text{Hg}^0$  in both the gas (Hall, 1995) and aqueous (Munthe, 1992) phases as is OH radicals (Lin and Pehkonen, 1997). Reduction of Hg(II) can occur in the aqueous phase via a reaction with dissolved  $\text{SO}_2$  (Munthe *et al.*, 1991) and  $\text{HO}_2$  (Pehkonen and Lin, 1998). Reduction processes in the gas phase are not known.

The chemical degradation of dimethylmercury (DMHg) is of interest due to its potential occurrence as a precursor to monomethylmercury (MMHg) which is commonly found in precipitation. DMHg is volatile and will be emitted to the atmosphere if produced in aquatic or terrestrial environments. DMHg reacts with the radicals OH and Cl (Niki *et al.*, 1983a,b) oxygen atoms ( $O(^3P)$ ) (Lund Thomsen and Egsgaard, 1986) and  $NO_3$  (Sommar *et al.*, 1996). Detailed product studies have not been performed in these investigations but MMHg is a likely product. Reactions where MMHg is formed from inorganic Hg species are not known.

### 3.2. REMOVAL PROCESSES

Mercury is removed from the atmosphere both by dry and wet processes. Direct measurements of dry deposition are not available but evaluation of data from forest monitoring has shown that dry deposition to forest canopies is the major removal process for both Hg and MeHg in forested ecosystems (Lindberg *et al.*, 1991; Iverfeldt *et al.*, 1991; Hultberg *et al.* 1994; Munthe *et al.*, 1995a). Swedish investigations indicate that the total deposition (throughfall and litterfall) in forested areas is 2–3 times higher than the open field deposition. Further information on dry deposition fluxes can be found in these references and in Schroeder and Munthe (1998).

For wet deposition, the main governing factor is the presence of water-soluble and particulate phase forms of Hg. These forms are released directly from many point sources and can also be formed via atmospheric transformations as described in Section 4.1.

## 4. Geographical and Temporal Patterns of Mercury Deposition in Sweden

Mercury concentrations in air, in wet deposition and other environmental matrices have been monitored at the Swedish west coast for more than a decade. The results of these measurements have been summarised in Iverfeldt *et al.* (1995) and Munthe *et al.* (1995). One of the major conclusions from these studies is that the atmospheric input of total Hg at this location has decreased by at least a factor of 2 over a period of a few years from the late eighties to the present date. This decrease is evident in air concentrations, wet deposition fluxes as well as in lake sediment profiles. Southwesterly winds are prevailing at the west coast of Sweden which indicates that the observed decrease can only be attributed to decreases in European emissions of Hg.

In Figure 2, the wet deposition of Hg at 4 Swedish stations is presented. The geographical pattern is clear with higher deposition fluxes at the southern and southwestern stations (Vavihill and Rörvik, respectively) and lower at the eastern and northern stations Aspvreten and Bredkålen. Data from before 1992 is only available from Rörvik and Aspvreten but indicate a decline around 1990–91. The

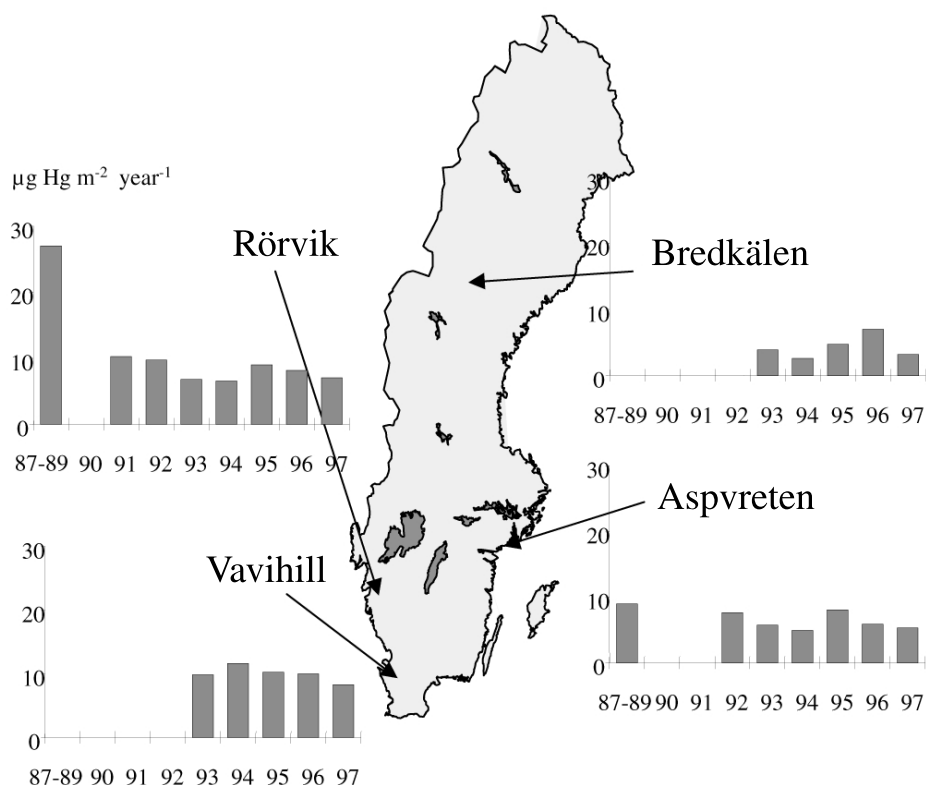


Figure 2. Wet deposition of Hg at 4 stations in Sweden.

decline is most evident at the Rörvik site, which is mainly influenced by emissions from continental Europe due to the prevailing southwesterly winds. During this time, the concentrations of gaseous Hg in air at Rörvik decreased drastically (Iverfeldt *et al.*, 1995) and this trend has also been observed in lake sediment records sampled close to the Swedish west coast (Munthe *et al.*, 1995) indicating a decrease in total Hg deposition by about 40%.

For wet deposition of MMHg, the temporal and geographical patterns are more difficult to interpret. In Figure 3, annual wet deposition fluxes of MMHg at 4 Swedish stations are presented. All annual values are within the range 0.05 to 0.1  $\mu\text{g}/\text{m}^2$  except for 1997 at Aspvreten. The levels at the northernmost station (Bredkälén) are similar to the other 3, which are located in the southern part of Sweden.

The geographical pattern of MMHg indicates that the major source areas and atmospheric behaviour are not the same as for total Hg. The pattern can possibly be explained by emissions from point source followed by a non-linear atmospheric behaviour with formation/degradation processes occurring during transport. Emissions from natural surfaces (i.e. production of MMHg or DMHg in aquatic or

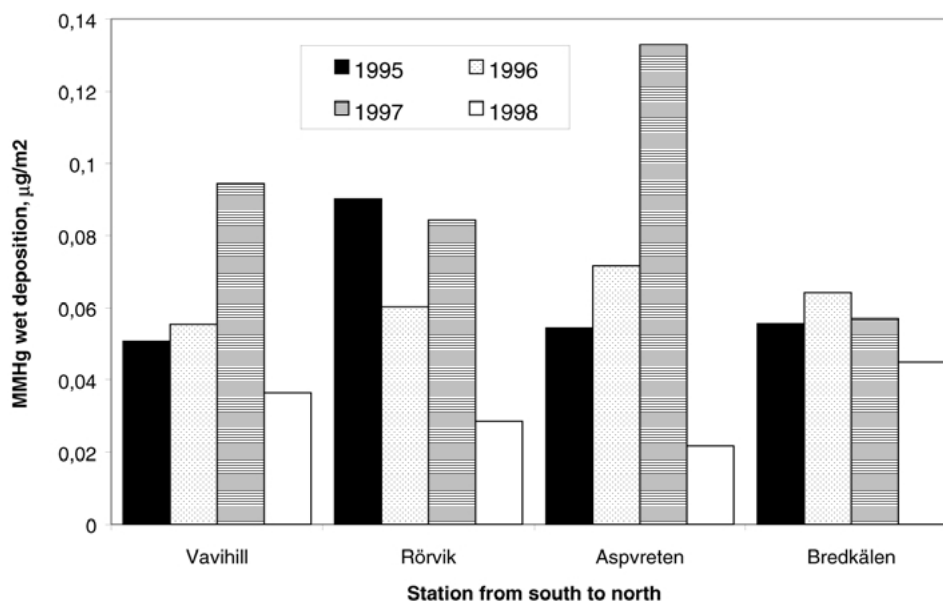


Figure 3. Wet deposition of MMHg at 4 Swedish stations.

terrestrial systems) may also be relevant. Further research into this topic is clearly warranted.

## 5. Relations Between Emission Control, Long Range Transport and Deposition

Transboundary transport of Hg in Europe is a well-known phenomenon and attempts to develop models describing this transport have been made during the last decades (Petersen *et al.*, 1995; 1998). Models are useful tools to assess the contribution of source areas to the deposition of Hg in Sweden and to evaluate the results of emission control measures. A detailed evaluation of the GKSS – Hg model has been presented in Petersen *et al.* (1995) including a comparison of modelled and measured air and precipitation concentrations of Hg.

### 5.1. EFFECTS OF REDUCING HG EMISSIONS

The GKSS-Hg model was run using the emission inventory presented by Axenfeld *et al.* (1991) and with the emissions reduced by 50% for all European countries. The inventory contains emissions for 3 Hg species (elemental Hg, oxidised gaseous Hg and particulate Hg). Emissions of all species were reduced by 50% in the model calculations. The simulated results for Hg<sup>0</sup> concentrations was then used to calculate the resulting wet deposition flux at the different sites using the parameterisation

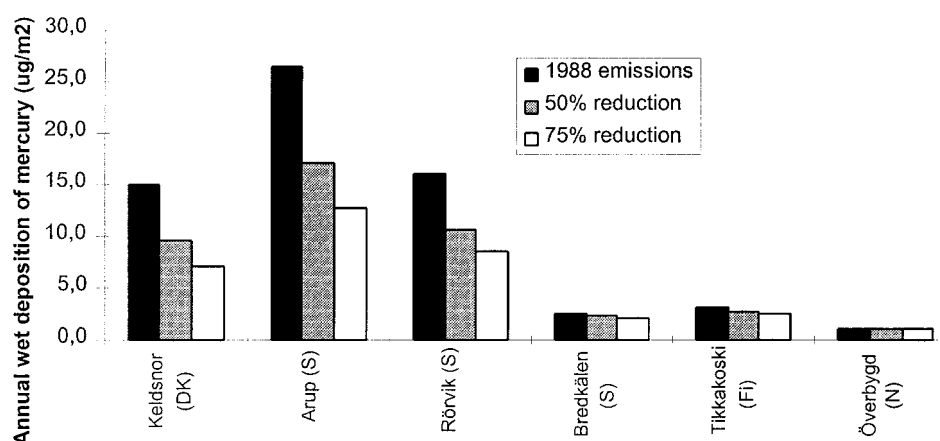


Figure 4. Modelled wet deposition fluxes of Hg at 6 Nordic sites. The columns represent the 3 scenarios; emissions according to the 1987/88 emissions inventory, 50% reduction of the emissions and 75% reduction of emissions.

described in Petersen *et al.*, (1995). Monthly averages of ozone and soot particles and precipitation amounts were taken from monitoring reports from EMEP and the Swedish National Monitoring Program (PMK) and used as model input. Details of model assumptions can be found in Petersen *et al.*, (1995).

Based on these results, the effect of a further reduction by 75% of the 1987/88 emissions was estimated by assuming the same relative changes in Hg<sup>0</sup> concentrations. The results of these scenario calculations are presented in Figure 4.

The model results clearly show that reducing emissions of Hg will lead to significant decreases in wet deposition fluxes in the southern regions of the Nordic countries. At the northern and eastern sites of Bredkålen, Tikkakoski and Överbygd the effects are smaller. The relative decreases for a 50% reduction in emissions range from about 35% at the southern sites to less than 10% at the northernmost site. For the 75% reductions scenario the estimated decrease ranges from over 50% in the south to about 10% in the north.

## 5.2. RELATIONS BETWEEN MERCURY AND SULPHUR EMISSIONS

The decreasing trend of Hg levels in the atmospheric deposition in Scandinavia during the last few years can be related to possible decline of Hg emissions, particularly in Central and Eastern Europe. Unfortunately, only very limited information exists on atmospheric Hg emissions in Europe at the beginning of the 1990's (Pacyna, 1994). National and regional emission inventories indicate that combustion of fuels, particularly coal emits more than half of the anthropogenic atmospheric Hg in Europe (Pacyna, 1994). In some countries where combustion of coal is the predominant way to produce heat and electricity, the contribution of Hg emissions from fuel combustion is even bigger. A recent emission report from Poland

concludes that fuel combustion generates more than 75 % of the atmospheric Hg in the country (Hlawiczka, 1994). Therefore, in the absence of complete information on the changes of Hg emissions to the atmosphere, trends of emissions of other pollutants from fuel combustion, such as sulphur dioxide, can be related to the decrease of Hg levels in the atmosphere.

Annual emissions of sulphur dioxide in Europe, as well as in some individual Eastern European countries, have decreased by at least 25% during the period 1988 to 1992. Substantial changes in sulphur dioxide emissions were also observed in the former German Democratic Republic before reunification of Germany in 1991.

Decline of the economical growth in the Eastern European countries at the beginning of the 1990's, related to the transition of the centrally planned economies in these countries to the market oriented ones, is the major reason for the sulphur dioxide emission changes. Electricity consumption by industry and large consumers in Poland went down by almost 30% during the period from 1988 to 1992 leading to a decrease of emissions from utility and industrial combustion plants. The consumption of brown coal in former German Democratic Republic, by far the main source of electricity and heat in the country, decreased by more than 12% only during the course of 1989. Several combustion units in major Czech power plants, including Tisova II, Prunerov, and Tisimice I were shut down in 1991 and 1992.

While the production of various industrial goods, electricity and heat has declined in Eastern Europe during the last decade, no major improvements of emission control installations have been made to reduce the amount of generated pollution to the air. Implementation of the recommendations from the so-called second sulphur protocol, to be prepared and accepted by the UN Economic Commission for Europe (ECE) countries will be an important factor in the reduction of sulphur dioxide emissions in the years to come. The installation of desulphurisation systems will inevitably result in emission reductions of Hg emissions. Depending on the type and efficiency of the desulphurisation systems, these installations may remove between 20 and 60% of Hg present in the exhaust gases (e.g. Pacyna, 1994).

No doubt, the lower consumption of fuels in Eastern Europe during recent years has caused the decrease of Hg emissions. However, there were also decreases of production in other industrial sectors, some of them known as Hg polluters. For example, a few chloralkali plants using the production technology based on Hg as an electrode, were closed down in the studied period because of economical reasons. In western Europe, likely reasons for decrease of Hg emissions to the air in Western Europe are different and related mostly to the installation of control equipment removing sulphur and nitrogen compounds from exhaust gases in various industries. The Hg method of chloralkali production in Western Europe is being gradually phased-out.

Since Hg and sulphur to some extent have the same major emission sources, it is of interest to compare the temporal trends in environmental loading. In Figure 5, the wet deposition of non-marine sulphate (NM SO<sub>4</sub>-S), corresponding to the

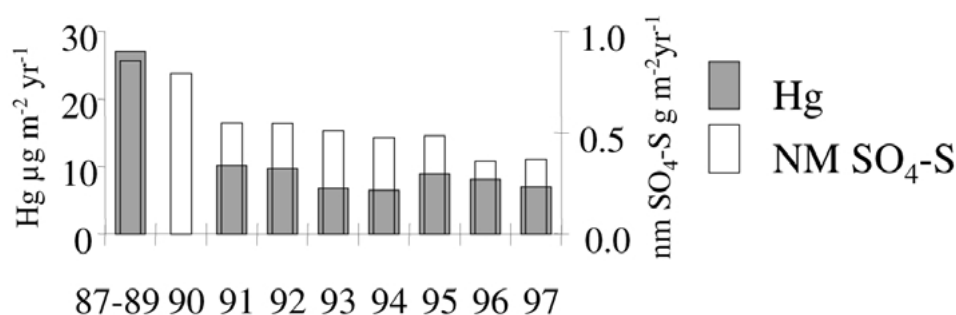


Figure 5. Wet deposition of Hg and NM  $\text{SO}_4\text{-S}$  at Rörvik, Sweden.

anthropogenic contribution to the total sulphate, and Hg at Rörvik on the Swedish west-coast is presented. At this site, the trends in Hg and NM  $\text{SO}_4\text{-S}$  are very similar in pattern indicating that the major sources indeed are the same. The decrease in Hg is more pronounced than the decrease in NM  $\text{SO}_4\text{-S}$ , which is in line with the additional closing down of sources emitting Hg but not sulphur (e.g. Chlor-alkali plants), as discussed above.

An interesting question is whether the decline of Hg emissions into the air is a permanent process or whether we can expect emission increase in the near future. The industrial decline in Eastern Europe, and consequently lower electricity and heat demand, is most likely only a temporary process. With its growing population and expectations of better quality of life, Eastern Europe is open for investments, some of them directed on restructuring of the present industrial status in the region. It is very crucial that the investment in various industrial plants is in parallel with the investment in technologies resulting in lesser emissions of various pollutants, including Hg, to the environment in the region. Although an international activity is now in force aiming at agreements on emission reductions of various toxic pollutants, with Hg as a priority compound, it is still not certain that the process of privatisation of industries in Eastern Europe will result in lowering fluxes of these pollutants into the environment.

## 6. Conclusions and Knowledge Gaps

Atmospheric transport and deposition is the major source of Hg to ecosystems in Sweden. The geographical pattern clearly demonstrates the existence of source regions in central and northern Europe with higher wet deposition in the south than in the north. Emissions of Hg have decreased in both Sweden and the rest of Europe since 1990. This has led to drastically lowered wet deposition fluxes mainly in southern Scandinavia. Despite this, anthropogenic emissions still represent the major source of atmospheric Hg in Sweden and further measures to control emissions are needed to reach pre-industrial levels.

Future agreements to control emissions of Hg will be based on detailed source-receptor calculations for Hg. This increases the requirements on our understanding of the emissions and atmospheric cycling of Hg. Major questions to be answered during the coming years are:

- What is the speciation of Hg emitted from different source categories?
- What is the source of methylated Hg forms found in the atmosphere?
- To what extent is Hg in the atmosphere over Europe influenced by emissions on a global scale?
- Will industrial and/or economical re-structuring of Eastern Europe lead to changes in Hg emissions?

### Acknowledgements

Data for this evaluation originates from the Swedish National Monitoring Program of the Swedish Environmental Protection Agency (NV). The investigation of Hg in products was funded by the Swedish National Chemicals Inspectorate and the scenario calculations by the Nordic Council of Ministers (NMR).

### References

- Axenfeldt, F., Munch, J. and Pacyna, J.: 1991, Europäische Test-Emissionsdatenbasis von Quecksilberkomponenten für Modellrechnungen. In: Umweltforschungsplan des Bundesministers für Umwelt, Naturschutz und Reaktorsicherheit. Forschungsvorhaben 104 02 726. Umweltbundesamt, Berlin (See also Petersen *et al.*, 1995).
- Berdowski, J. J. M., Baas, J., Bloos, J. P. J., Visschedijk, A. J. H. and Zandvelt, P. Y. J.: 1997, The European Emission Inventory of Heavy Metals and Persistent Organic Pollutants. Forschungsbericht 104 02 672/03, Umweltbundesamt and the TNO Institute of Environmental Sciences, Apeldoorn, The Netherlands, June 1997.
- Hall, B.: 1995, *Water, Air, Soil Pollut.* **80**, 301–315.
- Hlawiczka, S.: 1994, Report on heavy metals emission in Poland. A report to the UN ECE Task Force on Heavy Metals Emissions, Institute for Ecology of Industrial Areas, Katowice, Poland.
- Iverfeldt, Å.: 1991, *Water, Air, Soil, Pollut.* **56**, 553–542.
- Iverfeldt, Å., Munthe, J., Brosset, C. and Pacyna, J.: 1995, *Water, Air, Soil Pollution* **80**, 227–233.
- Lin, C. J. and Pehkonen, S. O.: 1997, *Atm. Environ.* **31**, 4125–4137.
- Lindberg, S. E., Turner, R. R., Meyers, T. P., Taylor G. E., Jr. and Schroeder, W. H.: 1991, *Water, Air, Soil Pollut.* **56**, 577–594.
- Lindqvist, O., Johansson, K., Aastrup, M., Andersson, A., Bringmark, L., Hovsenius, G., Hakanson, L., Iverfeldt, Å., Meili, M. and Timm, B.: 1991, *Water Air Soil Pollut.* **55**, 23–32.
- Lund Thomsen, E. and Egsgaard, H.: 1986, *Chem. Phys. Letters* **125**, 378–382.
- Munthe, J. and Kindbom, K.: 1997, Mercury in Mercury in products – a source of transboundary pollutant transport. Report to the National Chemicals Inspectorate (KemI).
- Munthe, J., Pleijel, K., Iverfeldt, Å., Kruger, O. and Petersen, G.: 1997, Atmospheric deposition of mercury in the Nordic countries at different scenarios of reduced anthropogenic emissions in Europe. Report to the Nordic Council of Ministers March 1998, IVL-Report B1292, Swedish Environmental Research Institute, P.O. Box 210 60, S-100 31 Stockholm, Sweden.

- Munthe, J., Hultberg, H. and Iverfeldt, Å.: 1995, *Water, Air, Soil Pollution* **80**, 363–371.
- Munthe, J., Hultberg, H., Lee, Y.-H., Parkman, H., Iverfeldt, Å. and Renberg, I.: 1995, *Water, Air, Soil Pollution* **85(2)**, 743–748.
- Munthe, J., Xiao, Z. F. and Lindqvist, O.: 1991, *Water, Air, and Soil Pollution* **56**, 621–630.
- Munthe, J.: 1992, *Atm. Environ.* **26A**, 1461–1468.
- Niki H., Maker P. S., Savage C. M. and Breitenbach, L. P.: 1983a, *J. Phys. Chem.* **87**, 3722–3724.
- Niki H., Maker P. S., Savage C. M. and Breitenbach, L. P.: 1983b, *J. Phys. Chem.* **87**, 4978–4981.
- Pacyna, J. M.: 1994, Atmospheric emissions of anthropogenic mercury in Europe in 1990. NILU Technical Report prepared for the Dutch TNO, Norwegian Institute for Air Research, Kjeller, Norway.
- Pacyna, J.M. and Pacyna, E. G.: 2000, Assessment of emissions/discharges of mercury reaching the Arctic environment. Norwegian Institute for Air Research, NILU OR Report 7/2000, Kjeller, Norway.
- Pehkonen, S. O. and Lin, C. J.: 1998, *J. A&WMA* **48**, 144–150.
- Petersen, G., Iverfeldt, Å. and Munthe, J.: 1995, *Atm. Environ.* **29**, 47–67.
- Petersen, G., Munthe, J., Pleijel, K., Bloxam, R., and Vinod Kumar, A.: 1998, *Atm. Environ.* **29**, 829–843.
- Pirrone, N., Keeler, G. J. and Nriagu, J.: 1996, *Atm. Environ.* **17**, 2981–2987.
- Pleijel, K. and Munthe, J.: 1995, *Atm. Environ.* **29**, 1441–1457.
- SCB: 1995, Statistiska Centralbyrån (Statistics Sweden). Data from the web site [www.scb.se](http://www.scb.se)
- Schroeder, W. H. and Munthe, J.: 1998, *Atm. Environ.* **29**, 809–822.
- Sommar, J., Hallqvist, M. and Ljungström, E.: 1996, *Chem. Phys. Letters* **257**, 434–438.
- WHO: 1990, International Programme on Chemical Safety (IPCS), Environmental Health Criteria 101, Methylmercury. World Health Organization, Geneva.



